Ghent University

Faculty of Pharmaceutical Sciences

NANOPOROUS MICROPARTICLES: TOWARDS A GENERIC VACCINE FORMULATION PLATFORM

MARIJKE DIERENDONCK

Pharmacist

Thesis submitted to obtain the degree of doctor in Pharmaceutical Sciences

2014

Promoters:

Prof. Dr. Ir. B. De Geest

Dr. Ir. S. De Koker

Laboratory of Pharmaceutical Technology

Ghent University

The Promoters

Prof. Dr. Ir. Bruno De Geest

Dr. Ir. Stefaan De Koker

The Author

Marijke Dierendonck

DANKWOORD

4 jaar, 500 keer sproeidrogen, 127 liter koffie, 322 paar handschoenen, 107.000 km autosnelweg maar ontelbare leuke momenten op dit labo. Dit waren de ingrediënten, het resultaat hierna neergepend.

Het is ondertussen 10 jaar geleden dat ik voor het eerst een voet zette in deze faculteit, maar nu is het voor mij tijd om de universiteitspoorten achter me te laten en van de gelegenheid gebruik te maken om de personen te bedanken voor hun bijdrage aan dit doctoraatswerk.

Allereerst wil ik graag mijn promotor Prof. Dr. De Geest bedanken om mij de kans te geven om te doctoreren. Bruno, bij jou kon ik steeds terecht voor grote en kleine problemen. Naast het bespreken van mijn data, het nalezen en verbeteren van artikels, posters, abstracts, het 'pimpen' van figuren… was er ook plaats voor sport en culinaire discussies. Je enthousiasme tijdens het vinden van het perfecte confocale microscopiebeeldje werkte aanstekelijk en zullen me nog lang bijblijven.

Daarnaast wil ik Prof. Jean Paul Remon en Prof. Chris Vervaet bedanken om mij welkom te heten binnen hun labo. Hierbij wil ik hen ook bedanken voor de ondersteuning en de mogelijkheid om mijn onderzoeksresultaten te presenteren op binnen- en buitenlandse congressen.

Een bijzonder woord van dank ook voor mijn co-promotor Dr. Ir. De Koker. Stefaan, alhoewel ik soms wat ruimte moest creëren op je werkplaats, stond je altijd klaar om me te helpen met de *in vivo* experimenten en het aanleren van ELISA's tot het maken van vries- en paraffinecoupes.

Eveneens wil ik Katharine, Ilse, Christine en Marc bedanken voor de hulp bij de administratieve taken en de ontspannende babbels van trouwvoorbereidingen tot de meest belangrijke bijzaak in het leven: voetbal.

Verder mogen mijn bureaucollega's in dit lijstje niet ontbreken. Wesley, vanaf dag één zaten we opgescheept aan hetzelfde bureau maar een goed glas bubbels en lekker eten bleek al snel een gezamenlijke interesse waar we over konden discussiëren. Nane, jij zorgde mee voor de female touch, Benoit mede West-Vlaming en culinair genieter, en sinds kort ook Ruben, de 'Lokerenboy', jullie allen zorgden samen voor de ontspannende, soms hilarische momenten in de 'verste' bureau.

De rest van alle (sommige ondertussen ex-)collega's: Lien D, Jurgen, Liesbeth P, Valérie, Bernd, Anouk, Lien L, Bart, Zhiyue, Hui, Kaat, Joke, Maxim, Ann-Katrien, Lieselotte, Liesbeth DC, Ana en de mensen van PAT wil ik bedanken voor de aangename werksfeer, deugddoende middag- en koffiepauzes, traktaties allerhande en de fantastische teambuildings.

Ook dank aan mijn thesisstudenten, Frederik, Stefanie en Jolien voor hun inzet, interesse en praktische hulp.

Niet te vergeten zijn de vrienden die er steeds waren voor de plezante etentjes, toffe feestjes,… Frederik & Kim, Daphne & Gilles, Delphine & Willem, Evelien & Steven, Lien en Oli, Liesbeth, Magalie & Wouter wil ik bedanken voor de ontspanning.

Tenslotte wil ik mijn familie en in het bijzonder mijn ouders en broer bedanken voor jullie steun tijdens de afgelopen jaren en omdat ik altijd op jullie kan rekenen. Jullie hebben me geleerd dat door hard te werken je wel je doel zult halen. Ook mijn schoonouders en schoonbroer wil ik bedanken omdat ik altijd welkom ben bij jullie.

Als allerlaatste, maar zeker niet als minste wil ik graag mijn man Ivo bedanken. Ivo, bedankt voor je geduld en eindeloze liefde. Jij kent me beter dan wie ook, kortom you're my true companion.

Nunc est bibendum!

TABLE OF CONTENTS

LIST OF ABBREVATIONS AND

SYMBOLS

ABTS	2,2'- Azinobis(3-ethylbenzothiazoline6-sulfonic acid)diammonium salt
ACK	Ammonium-Chloride-Potassium
AFM	Atomic force microscopy
AIBN	Azobisisobutyronitrile
Alum	Aluminium trihydroxide
APC	Antigen presenting cell
BCR	B cell receptor
$CaCO_3^{NP}$	Calcium carbonate nanoparticles
CD	Cluster of differentation
CFSE	Carboxyfluorescein diacetate succinimidyl ester
CpG	Cytosine –phosphate- guanine
CTA	Chain transfer agent
CTL	Cytoxic T lymphocyte
Đ	Dispersity
DAD	Diode array detector
DC	Dendritic cell
Δf	Change in resonance frequency
DIC	Differential interference contrast
DMA	Dimethylacetamide
DMF	Dimethylformamide
DMSO	Dimethylsulfoxide
DNA	Deoxyribonucleic acid
DP	Degree of polymerization
DS	Dextran sulfate
dsRNA	Double stranded Ribonucleic acid
DTT	Dithiotreitol
DQ-OVA	Dequenching-ovalbumin
EDTA	Ethylenediaminetetraacetic acid
EDX	Energy dispersive X-ray
ER	Endoplasmatic reticulum
FCS	Fetal calf serum
FACS	Fluorescence-activated cell sorting
FITC	Fluorescein isothiocyanate
GC	Gas chromatography
GM-CSF	Granulocyte macrophage colonial stimulating factor
HA	Hyaluronic acid
HF	Hydrofluoric acid
HIV	Human Immunodeficiency virus
HRP	Horseradish peroxidase
IFN-γ	Interferon-gamma
Ig	Immunoglobulin
IL	Interleukin
LbL	Layer-by-layer
LCST	Lower critical solution temperature

LPS	Lipopolysaccharide
MADIX	Macromolecular design via the interchange of xanthates
MHC	Major histocompatibility complex
Mn	Number average molecular weight
MPL	Monophosphoryl lipid A
MTT	3-(4,5-dimethylthiazol-2-yl)-2,5-diphenyltetrazolium bromide
Mw	Weight average molecular weight
NVP	N-vinylpyrrolidone
OVA	Ovalbumin
SPS	Poly (sodium 4-styrene sulfonate)
PAH	Poly(allylamine hydrochloride)
PAMAM	Poly (amido amine)
PAMPS	Pathogen associated molecular patterns
PBS	Phosphate buffered saline
PDAC	Poly (dimethyldiallylammoniumchloride)
PEI	Poly(ethylene imine)
PEtOx	Poly (2-ethyl-2-oxazoline)
P_LARG	Poly-L-arginine
PLGA	Poly (DL-Lactide-co-glycolide)
PMA	Poly(methacrylic acid)
PMA^{SH}	Thiolated poly(methacrylic acid)
PMeOx	Poly (2-mehtyl-2-oxazoline)
PMLC	Polymeric multilayer capsules
PMMA	Polymethylmethacrylate
PnPropOx	Poly(2-(n-propyl)-2-oxazoline)
PRRs	Pattern recognition receptors
PSS	Poly(styrene sulfonate)
PVA	Poly(vinyl alcohol)
PVP	Poly (N-vinylpyrrolidone)
PVP^{alkyne}	Alkyne functionalized poly (N-vinylpyrrolidone)
QCM	Quartz crystal microbalance
RAFT	Reversible addition-fragmentation chain transfer
RID	Refractive index detector
RPMI	Roswell Park Memorial Institute
SEC	Size exclusion chromatography
SEM	Scanning electron microscopy
SNARF	Seminaphthorhodafluor
TA	Tannic acid
TAP	Transporter associated with antigen processing
T_{CP}	cloud point temperature
TEM	Transmission electron microscopy
TCR	T cell receptor
T_{FH}	Follicular helper T cell
Th	T helper
TLR	Toll like receptor
TNF-α	Tumor necrosis factor alpha
UV	Ultraviolet
XRPD	X-ray powder diffraction
ζ	Zeta

PART I

OUTLINE AND AIMS OF THIS THESIS

OUTLINE AND AIMS OF THIS

THESIS

Vaccination, which is based on the principle of eliciting an immune response and immunological memory, is one of the major breakthroughs in medicine. Notwithstanding numerous infectious diseases can be prevented, there are still many diseases like HIV, malaria and tuberculosis where no effective vaccine is available at the moment. The reason for this failure is that current vaccination strategies against intracellular pathogens are not capable of inducing strong cellular immune responses. The crucial cells in initiating T cell responses are dendritic cells (DCs), which are specialized in internalizing antigen, processing them into peptide fragments and presenting these by respectively MHCII to CD4 T cells and MHCI to CD8 T cells. The way in which antigen is internalized by a DC, strongly affects how the antigen is processed and presented by a DC, and consequently the type and strength of immune response induced. Soluble antigens formulated with current approved adjuvants, such as aluminum hydroxide salts and MF59, induce predominantly antigen presentation to CD4 T cells and therefore fail to induce potent cellular immune responses. By contrast, particulate antigens are not only far more efficiently taken up by DCs, but are also presented by MHCI to CD8 T cells, thus enabling the induction of CTL responses.

In recent years, new particulate strategies like liposomes and PLGA microspheres to enhance antigen immunogenicity have been developed. They suffer from several drawbacks such as low antigen encapsulation efficiency, use of chemical solvents, physical stress that negatively affects their antigen stability and complex and multistep assembly procedures. In this thesis we aimed to develop a generic microparticulate antigen formulation technology that is straightforward and scalable.

CHAPTER 1 provides a general introduction to the immune system describing the different cells involved, the crucial role of cross-presentation by the dendritic cells and the shortcomings of current vaccination strategies. In **CHAPTER 2** the potential of polymeric multilayer capsules (PMLC) for vaccine delivery are reviewed. These PMLC are fabricated by layer-by-layer coating of interacting species onto a sacrificial template followed by the decomposition of this template, yielding hollow capsules. However, the multistep assembly procedure is time consuming and thus a major setback toward industrial applications. These limitations have prompted us at developing novel strategies to formulate vaccine antigens in polymeric particles. To provide an introduction to the scalable methods

to produce microparticles, **CHAPTER 3** describes automatization and simplification strategies and, more specifically, spray-based approaches.

In **CHAPTER 4** we aimed at developing a method to produce porous antigen loaded degradable polyelectrolyte microspheres by atomization into a hot air stream of a diluted aqueous mixture of oppositely charged polyelectrolytes, and calcium carbonate nanoparticles as a pore-forming component. Upon evaporation of the water phase, solid microparticles are obtained that do not aggregate or disassemble when redispersed in water. Subsequent extraction of the calcium carbonate yielded highly porous microparticles. This high porosity is expected to enhance intracellular processing of encapsulated antigen upon uptake by antigen presenting cells. We then further evaluated the physicochemical properties of these particles and their *in vitro* interaction with dendritic cells. **CHAPTER 5** elaborates further on the design of porous polyelectrolyte microparticles and presents a single-step method to encapsulate proteins into microspheres. Herein, mannitol was used as a sacrificial component instead of calcium carbonate nanoparticles. Mannitol has the advantage that it is a fully biocompatible water soluble sacrificial component, while in case of the calcium carbonate nanoparticles an additional step is needed to remove the core template. Furthermore, we demonstrated that the biological activity of encapsulated proteins is preserved, and investigated the intracellular behavior of the microparticles after uptake by dendritic cells and assessed the ability to promote cross-presentation.

In **CHAPTER 6** we aimed to investigate the *in vivo* behavior in mice of the porous microparticles produced in **CHAPTER 5**. Tissue response and the induction of cellular and humoral immune responses was investigated.

As an alternative to electrostatic interaction, also hydrogen bonding can act as a driving force to form stable complexes. In **CHAPTER 7** the aim was to explore hydrogen bonding between tannic acid as hydrogen donor and neutral charged polymers as hydrogen bond acceptors to assemble multilayer films. The obtained know how was then used in **CHAPTER 8** to design porous microparticles based on hydrogen bonding. *In vitro* studies were performed to assess their interaction with dendritic cells in terms of cytotoxicity, particle uptake and their potential to promote antigen cross-presentation.

In addition we also compared head-to-head the polyelectrolyte-based and hydrogen bonding based systems and attempted to relate the differences in immuno-biological behavior to their physicochemical properties.

PART II

GENERAL INTRODUCTION

CHAPTER 1

THE IMMUNE SYSTEM

CHAPTER 1

THE IMMUNE SYSTEM

1. HISTORIC BACKGROUND

The term vaccination is derived from the Latin word for cow (vacca). Edward Jenner discovered at the end of the 18th century that the fatal disease smallpox could be prevented by inoculation with the cowpox virus. These basics were later on expanded by Koch, Lister and Louis Pasteur. The latter discovered the possibility to modify the virulence of an infectious agent and to induce protection with it.[1, 2] Since then, our knowledge about vaccinology and more in general, the immune system has been vastly extended.

2. INNATE AND ADAPTIVE IMMUNE SYSTEM

Our immune system can be divided into innate and adaptive immune responses. Innate immunity represents the first line defense against pathogens that have invaded the host. It's characterized by a rapid recruitment of phagocytic cells to the site of infection, antigen non-specific and a lack of memory. However, recently the term "trained immunity" has been proposed to describe enhanced and sustained innate immune responses against infections after previous exposure to certain infectious agents.[3] Cells of the innate immune system rely on a limited number of receptors (PRRs: Pattern Recognition Receptors) that recognize conserved molecular structures (PAMPs: Pathogen Associated Molecular Patterns) expressed by a wide variety of infectious agents. [4]

The adaptive immune system can be further divided into humoral (B lymphocytes) and cellular immune (T lymphocytes) responses. When naive B lymphocytes or B cells recognize antigen (in presence of adequate auxiliary cells and signals) bound onto their B cell receptor (BCR), they become activated and differentiate into antibody-secreting plasma cells and memory B cells (**Figure 1**).[5-7]
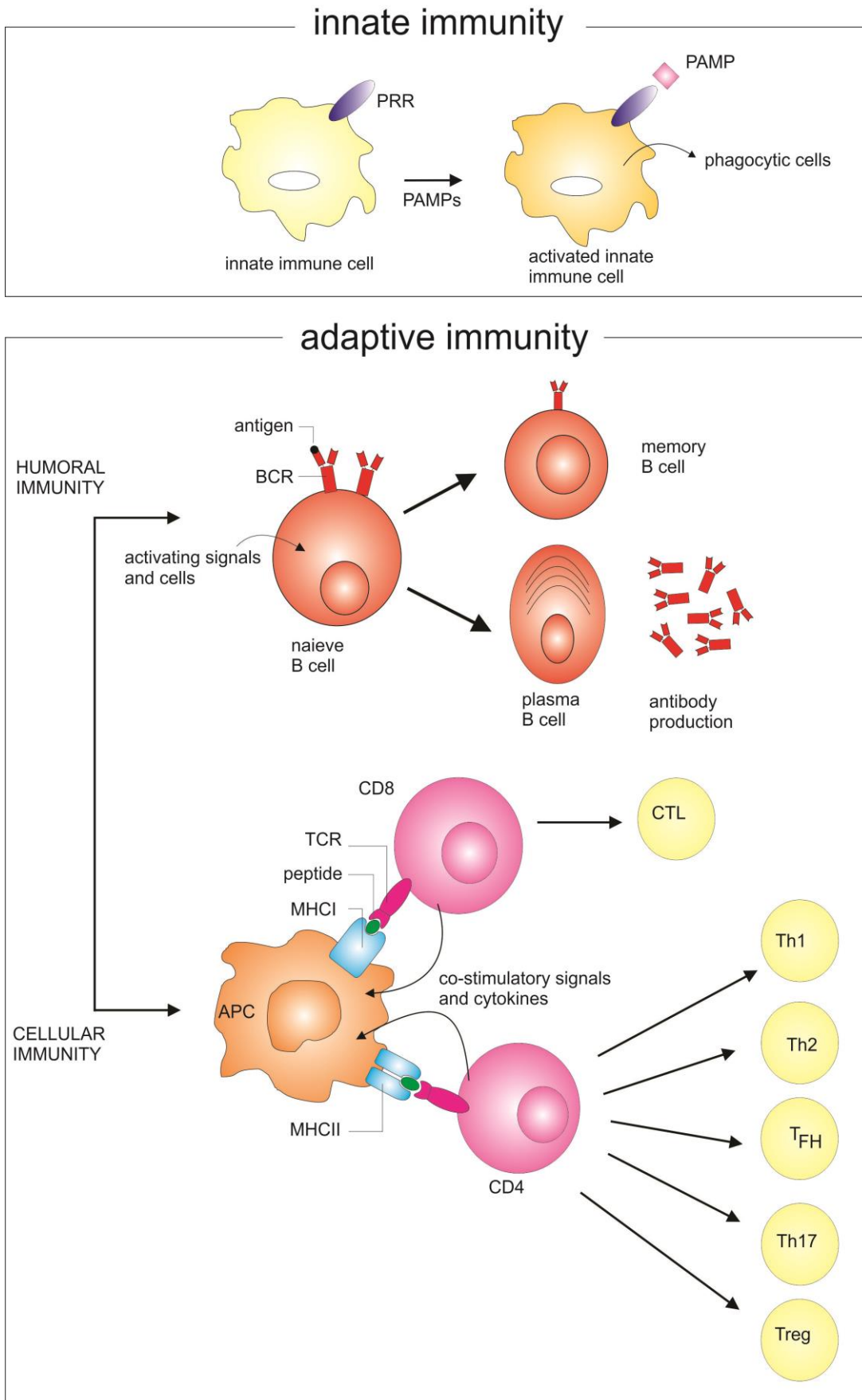
Figure 1. Schematic overview of the immune system.

Two main classes of naive T cells can be distinguished by the cell-surface protein CD4 or CD8 respectively, on their surface. Upon activation, naive CD4 or CD8 T cells differentiate into different effector T cells, each specialized in a specific function. CD8 T cells differentiate into cytotoxic T cells (CTLs) and can kill infected or malignant cells.[8] Different subsets of CD4 T cells help other cells in their function and, hence, are called helper T cells. They regulate the activity of other immune cells through the secretion of cytokines. Th1 cells secrete mainly IFN-γ and activate macrophages to destruct intracellular pathogens and aid B cells in producing opsonizing antibodies. Cytokines produced by Th2 cells, IL-4, IL-5 and IL-13, activate eosinophils, mast cells, to control parasite infections and induce the IgE isotype switching by B cells.[8, 9] A third subset are the follicular helper T cells (T_{FH}). They stimulate the antibody production by B cells and can produce cytokines characteristic for either Th1 or Th2 cells.[10] The last identified subset of CD4 T cells, Th17 cells are characterized by secreting the cytokines IL-17 and IL-22, that stimulate the neutrophil response and help to protect against extracellular bacteria and fungi (**Figure 1**).[11, 12] Besides these T helper cells, also regulatory T (Treg) exist that are able to suppress an immune response, by secreting the cytokines TGFß and IL-10. [13]

In contrast to B lymphocytes, T lymphocytes cannot recognize antigens by their T cell receptor (TCR), instead a naive T cell reacts to a specific antigen when it is presented as a peptide-MHC complex.[14] Two classes of MHC or major histocompatibility complex, MHCI and MHCII, can be distinguished and the function of these specialized glycoproteins is to deliver pathogen-derived peptides to the cell surface. They differ in structure, in the way of obtaining peptides, and cellular localization. Cytosolic proteins are processed and transported in the endoplasmatic reticulum (ER), where they are placed onto MHCI molecules. These class I molecules are expressed by virtually all nucleated cells and bind to CD8 T cells. Extracellular proteins taken up and processed into intracellular vesicles are bound to MHCII molecules, are only expressed by antigen presenting cells of the immune system (macrophages, B cells, dendritic cell and thymic epithelial cells) and bind to CD4 T cells.[15] Since dendritic cells are the most efficient in presenting antigens, they are discussed into more detail below.

3. DENDRITIC CELLS

3.1. From antigen uptake to antigen presenting

Dendritic cells were first described by Steinman in 1972[16] and since then it has become clear that DCs play a key role in the immune system. Different subsets, each with their localization and function have been described.[17-19] One division can be made between plasmacytoid DCs (pDC) and

conventional DCs (cDC). The latter can be further divided into migratory DCs and lymphoid-tissue resident DCs. Migratory DCs sample antigens in the peripheral tissues and migrate through the lymphatics to the lymph nodes, while lymphoid-tissue resident DCs collect antigens in the lymphoid organ. Both can be further divided into specialized subsets.[20, 21]

To sample antigens, DCs have to be in an immature state. They are efficient in taking up antigens, but not in stimulating T cells. Mechanisms of how DC take up particles include phagocytosis, macropinocytosis and can proceed through various receptors such as C-type lectin receptors as well Fcγ and Fcε receptors.[22, 23] Once DCs have captured antigen, they undergo a maturation process, where peptide fragments of the antigen are loaded onto MHC molecules and transported to the cell surface while in the meantime DCs migrate to the lymphoid tissues. These mature DCs are capable of activating T cells which requires 3 signals: as mentioned before the antigen needs to be presented as a peptide-MHC complex (signal 1), a costimulatory signal from the DC (signal 2) and cytokines that direct T cell differentiation into the different subsets of effector T cells (signal 3).[24-26] Thus, the activation of naive T cells by dendritic cells occurs in three steps, 1) antigen uptake and processing, 2) maturation of DC and migration to the lymph nodes and 3) activation of naive T cells.[8]

3.2. Maturation of DCs

Maturation defined as the differentiation of DCs triggered by environmental stimuli plays a pivotal role in immunogenicity.[27, 28] These signals include microbial products, proinflammatory cytokines, lymphocytes, immune complexes and endogenous ligands.[29] Microbial products such as LPS, CpG DNA, dsRNA act via Toll-like receptors (TLRs) that are part of the pattern recognition receptors (previously described in the paragraph on the innate immune system). The involvement of PRRs such as TLRs in maturation features DCs as a link between innate and adaptive immunity.[30] After the receipt of the maturation signal, functional changes occur such as translocation of peptide-MHC complexes from lysosomes inside the cell to the cell surface, activation of the processing machinery in the late endosomes or lysosomes, remodelling the surface with loss of endocytic/phagocytic receptors and upregulation of costimulatory molecules. The maturation pathway then helps to address which lymphocyte functions will be induced. [18, 27, 29, 30]

A difference has to be made between phenotypically matured dendritic cells and functionally matured or immunogenic DCs. Sometimes dendritic cells may express maturation/activation markers but are unable to prime T cell responses and even instead induce tolerance.[24, 31-33] The understanding of functional maturation on the molecular level is still incomplete.[32, 33]

As described before, cytosolic proteins are degraded and their peptides are presented to CD8 T cells in complex with MHCI molecules and extracellular proteins are presented on MHCII molecules to CD4 T cells. However extracellular proteins can also be presented on MHCI molecules, a process called cross-presentation, which is explained into detail in the next paragraph.

3.3. Cross-presentation

The classical MHCI pathway ubiquitinates proteins in the cytoplasm (i.e. proteins are conjugated with ubiquitin molecules, which marks them for fast degradation) and are further degraded by the proteasome into peptides. The majority of these peptides are further hydrolyzed, but a fraction of them are transported into the lumen of the endoplasmatic reticulum (ER) by a transporter associated with antigen processing (TAP). In the ER, the peptides are further cleaved, loaded onto MHCI molecules and transported through the Golgi cisternae to the cell surface. Thus, it is obvious that external proteins, which are not produced by the cell, cannot be presented on MHCI molecules since they cannot pass the plasma membrane to enter the cytosol. [15, 34] But how do DCs present exogenous proteins onto MHCI molecules?

The phenomenon of cross-presentation was discovered by Bevan in 1976.[35] It wasn't until 1990s that antigen presenting cells (APCs) such as dendritic cells and macrophages were identified as the cross-presenting cells.[36] Subsequently, it became clear that cross-presentation was most efficiently carried out by dendritic cells, and more specifically by certain DC subsets (CD8+DC lineage).[37, 38] Particulate proteins, taken up by phagocytosis, are more effective in cross-presentation than soluble proteins. Dendritic cells cross-present the internalized antigens by at least two pathways (**Figure 2**), the cytosolic or the vacuolar pathway.[34, 39, 40]

In the cytosolic pathway (**Figure 2**) the proteasome and TAP are required for cross-presentation.[41] Since proteasomes are only present in the cytosol and not in endocytic compartments, this means that the internalized antigens needs to be transferred from the phagosome (i.e. the organelle where the internalized antigens end up after uptake by the DC) into the cytosol, where they are degraded by the proteasome and the obtained peptides can then be transported into the ER by TAP and loaded on MHCI molecules.[34, 39, 40]

The mechanism of antigen export from phagosome to cytosol is not yet completely understood, but phagosomes contain also proteins that are normally present in the ER. More in particular these proteins are the components involved in the MHCI pathway, thus concluding that phagosomes and ER fuses together and exchange molecules for cross-presentation.[42-45] Moreover, instead of peptides

transported into the ER, they can be taken up again by phagosomes and loaded onto MHCI molecules.[34, 39, 40]

The vacuolar pathway (**Figure** 2) on the other hand, does not require the proteasome and TAP, but instead the antigen processing and loading onto MHCI molecules takes place in the vacuole, where cathepsin S, a lysosomal protease is important in producing the peptides.[46]

 The peptide-MHCI complex on the DC, together with the co-stimulatory molecules and cytokines, is able to prime naive CD8 T cells into cytoxic T cells.
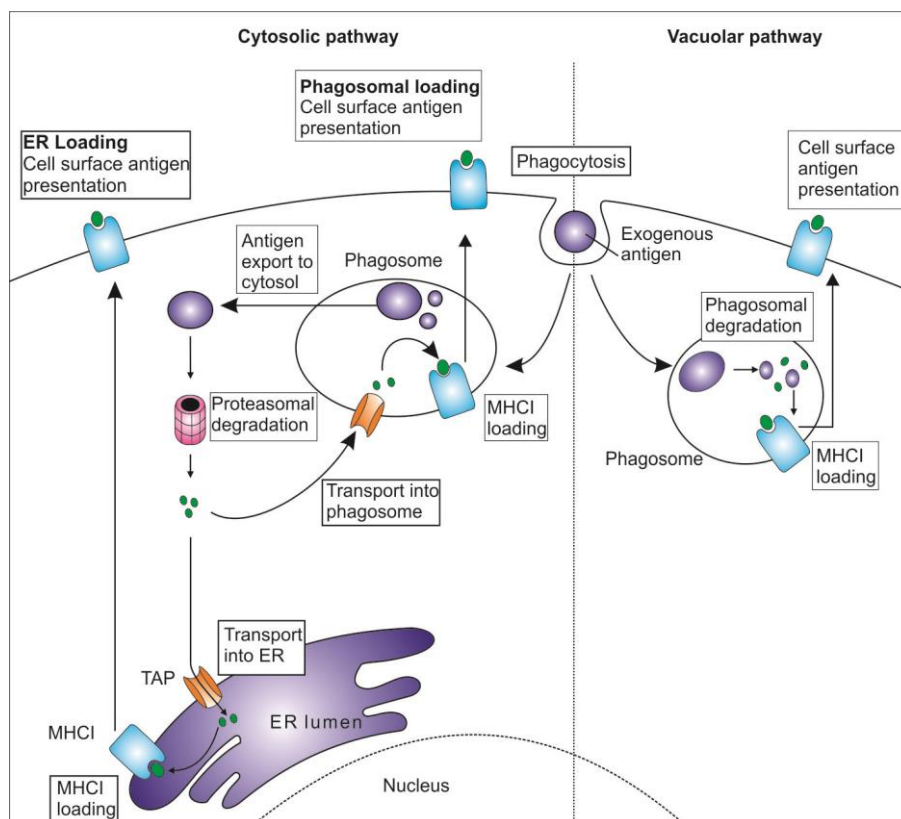

Figure 2. Intracellular pathway for cross-presentation in dendritic cells. (adapted from[39])

4. DCs AS A TARGET FOR THE DEVELOPMENT OF NEW VACCINES

Since DCs play a central role in immunity, they are logically a target for the development of new vaccines. Vaccination is based on the principle of eliciting an immune response and immunological memory.[47, 48] It plays an essential role in controlling infectious diseases, by saving yearly 2 to 3 million lives worldwide.[49] In Belgium, children receive vaccinations against bacterial (Diphteria, Tetanus, Pertussis, *Haemophilus influenza B, Streptococcus pneumonia* and *Meningococcus* group C) and viral

(Poliomyelitis, Hepatitis B, Rotavirus, Measles, Mumps and Rubella) diseases before the age of two. Although only the vaccine against polio is obliged, the others are also strongly recommended.[50]

Despite of the success, there are still diseases like HIV, malaria and tuberculosis that cannot yet be prevented by vaccination. Conventional vaccines are based on live attenuated pathogens which prevent infections by antibodies.[51] They are often associated with safety concerns such as reversion to virulence or insufficient attenuation and severe adverse effects due to the use of complete pathogens.[52, 53] As a consequence of these safety issues, killed/inactivated and subunit vaccines composed of purified parts of the pathogen such as toxins, proteins and polysaccharides have been investigated. The most recently licensed vaccines are developed through genetic engineering creating recombinant subunit products.[54, 55] These vaccines are safer compared to live pathogens but are as well unable to evoke strong cellular immune responses.[51] Therefore, adjuvants need to be added to increase the immunogenicity and to become effective vaccines.[56] Very few adjuvants have been approved for human use. Alum (aluminium salts) and AS04 (combination of aluminium hydroxide and monophosphoryl lipid A (MPL)) are the only adjuvants approved in the United States. In Europe, also oil in water emulsions (MF59, AS03) and virosomes are licensed for influenza vaccines.[57] Adjuvants can be divided into two categories, immunopotentiators and delivery systems, according to their working mechanisms. Although this might be too simplistic since delivery systems can also act as immunopotentiators.[58, 59] In recent years, adjuvants systems that can induce CD8 T cell responses have been developed.[40, 60] An overview of different adjuvant systems is given in **Table 1**. Among them, polymer-based particulate antigen delivery systems are a promising approach.[61-63] Their interaction with immune cells is discussed into detail in the following **CHAPTER 2**.

Table 1. An overview of adjuvant systems

Class	Example	Advantages	Disadvantages
Mineral salts	Alum[57, 64-66]	-Licensed -Increased stability and immunogenicity of antigens -Used extensively -Low cost	-Mode of action not completely understood -Little effect on Th1 immune response
O/W emulsion	MF59[40, 57]	-Licensed (EU) -Immunostimulating activity -Enhance antigen uptake by DCs	-Do not induce CD8 T cell responses
W/O emulsion	CFA[40], IFA[40]	-/	-Restricted to animals (toxicity)
	Montanide[40]	-Induce cytotoxic T cell responses	-Restricted to severe conditions (toxicity) -Severe adverse events -Terminated studies
Lipid vesicles	Liposomes[40, 64, 65, 67]	-Versatile delivery systems -Natural constituent of lipid bilayer membranes -Entrap a wide range of components -Tailoring possible -Basis for virosomes/VLP	-Not active per se -Stability issues -Chemical degradation (unsaturated lipids)
	Virosomes[40, 64]	-Licensed (EU): f.e. Epaxal® -Functional viral envelope glycoproteins aid in cell uptake and membrane fusion to deliver the antigen to the target cell	-Not always an improved immunogenicity profile (compared to unadjuvanted seasonal influenza vaccines) -Unknown mode of action, acts more as a delivery system
	VLP[40, 68]	-Licensed: f.e. Gardasil® -Function as PAMPs -Strong B and T cell responses	-Practical utility -Only small sized vaccine antigens
Saponin	QS21[64, 65, 67]	-Derived from plant *Quillaja saponaria* -Purified fraction of QuilA -Enhancing antigen presentation to APCs -Inducing CTL responses	-First studies in human showed some residual lytic activity at the injection site -Toxic in a variety of experimental animals => modify structure at molecular level
Polymeric particles	PLGA[40, 60, 61]	-Tailoring possible -Offering maturation stimuli that act directly on APCs	-Not approved for human use
Toll-like receptor agonist	PolyI:C (TLR3)[69]	-Facilitates antigen cross-presentation	-Degradation by serum nucleases (in primates) -High doses cause severe safety problems => derivatives
	MPL (TLR4)[64, 69]	-Chemically detoxified form of LPS -Acts on the innate immune cells -Stimulate expression of co-stimulatory molecules and cytokine release	-More mild-moderate adverse events compared to Alum

	Flagellin (TLR5)[69]	-Fused with a recombinant vaccine antigen -Induces DC maturation -No injection site inflammation or severe adverse effects detected in mice/non-human primates	-No information on immunogenicity/ safety in humans
	Imidazoquinolines (TLR7, TLR8)[64, 69]	- Augment T cell responses against viral infections -Inducer of pro-inflammatory cytokines -Licensed for topical use (Imiquimod)	-Only preclinical studies in mice -Ability of mice to respond to TLR8 ligand being questioned -Severe adverse effects after oral/systemic use in humans
	ISS of microbial DNA (Cpg, TLR9)[64]	-Ability to induce Th1 immunity and cytotoxic T cells -Strong anti-viral activity -Accelerate, increase magnitude and prolong the duration of vaccine specific antibody responses	-Currently only used in cancer therapy
Combination adjuvants	Class		
ISCOMs[40, 64, 65]	Saponins Cholesterol Phopholipids	-Protein antigen entrapped by hydrophobic interactions -Taken up by APC by endocytosis -Promote a broad immune response	-Failed to induce T cell responses in cancer patients with advance tumors -High and multidose administrations required -Antigen must be amphiphilic
AS01[70]	MPL Liposomes QS21	-Improve cell-mediated immunity	-Only preclinical studies -Reactogenicity profile unknown
AS02[64]	MPL O/W emulsion QS21	-Stronger humoral response compared to AS01	-Need to combine with right antigen in order to elicit the proper immune response
AS03[65, 69]	O/W emulsion α-tocopherol (vitamin)	-Licensed (EU) -Enhances antigen load in macrophages and granulocyte recruitment in lymph nodes	-Higher incidence of local and systemic reactions compared to nonadjuvant vaccine -occurrence of narcolepsy?
AS04[57, 64]	Alum MPL	-Licensed (EU) f.e. Cervarix® -Local activation of NF-KB activity and cytokine production	-Predominantly Th1 based immune responses -Spatial and temporal colocalisation of AS04 and the required antigen

IFA: incomplete freund adjuvant, CFA: complete freund adjuvant, VLP: virus like particle, ISCOM: immune stimulating complexes, MPL: monophosphoryl lipid A, AS: adjuvant systems.

REFERENCES

1. Hilleman, M. R. Vaccines in historic evolution and perspective: a narrative of vaccine discoveries. Vaccine 2000, 18, 1436-1447.
2. Bazin, H. A brief history of the prevention of infectious diseases by immunisations. Comparative Immunology Microbiology and Infectious Diseases 2003, 26, 293-308.
3. Netea, M. G.; Quintin, J.; van der Meer, J. W. M. Trained Immunity: A Memory for Innate Host Defense. Cell Host & Microbe 2011, 9, 355-361.
4. Turvey, S. E.; Broide, D. H. Innate immunity. Journal of Allergy and Clinical Immunology 2010, 125, S24-S32.
5. Chu, V. T.; Berek, C. The establishment of the plasma cell survival niche in the bone marrow. Immunological Reviews 2013, 251, 177-188.
6. Yuseff, M.-I.; Pierobon, P.; Reversat, A.; Lennon-Dumenil, A.-M. How B cells capture, process and present antigens: a crucial role for cell polarity. Nature Reviews Immunology 2013, 13, 475-486.
7. Batista, F. D.; Harwood, N. E. The who, how and where of antigen presentation to B cells. Nature Reviews Immunology 2009, 9, 15-27.
8. Moser, M.; Leo, O. Key concepts in immunology. Vaccine 2010, 28, C2-C13.
9. Mosmann, T. R.; Sad, S. The expanding universe of T-cell subsets: Th1, Th2 and more. Immunology Today 1996, 17, 138-146.
10. Tangye, S. G.; Ma, C. S.; Brink, R.; Deenick, E. K. The good, the bad and the ugly - T-FH cells in human health and disease. Nature Reviews Immunology 2013, 13, 412-426.
11. Harrington, L. E.; Hatton, R. D.; Mangan, P. R.; Turner, H.; Murphy, T. L.; Murphy, K. M.; Weaver, C. T. Interleukin 17-producing CD4(+) effector T cells develop via a lineage distinct from the T helper type 1 and 2 lineages. Nature Immunology 2005, 6, 1123-1132.
12. Harrington, L. E.; Mangan, P. R.; Weaver, C. T. Expanding the effector CD4 T-cell repertoire: the Th17 lineage. Current Opinion in Immunology 2006, 18, 349-356.
13. Josefowicz, S. Z.; Lu, L.-F.; Rudensky, A. Y. Regulatory T Cells: Mechanisms of Differentiation and Function. Annual Review of Immunology, Vol 30 2012, 30, 531-564.
14. Rudolph, M. G.; Stanfield, R. L.; Wilson, I. A. How TCRs bind MHCs, peptides, and coreceptors. In Annual Review of Immunology, 2006; Vol. 24, pp 419-466.
15. Jensen, P. E. Recent advances in antigen processing and presentation. Nature Immunology 2007, 8, 1041-1048.
16. Steinman, R. M.; Cohn, Z. A. Identification of a novel cell type in peripheral lymphoid organs of mice. Journal of Experimental Medicine 1973, 137, 1142-1162.
17. Shortman, K.; Liu, Y. J. Mouse and human dendritic cell subtypes. Nature Reviews Immunology 2002, 2, 151-161.
18. Ueno, H.; Klechevsky, E.; Morita, R.; Aspord, C.; Cao, T.; Matsui, T.; Di Pucchio, T.; Connolly, J.; Fay, J. W.; Pascual, V.; Palucka, A. K.; Banchereau, J. Dendritic cell subsets in health and disease. Immunological Reviews 2007, 219, 118-142.
19. Ueno, H.; Klechevsky, E.; Schmitt, N.; Ni, L.; Flamar, A.-L.; Zurawski, S.; Zurawski, G.; Palucka, K.; Banchereau, J.; Oh, S. Targeting human dendritic cell subsets for improved vaccines. Seminars in Immunology 2011, 23, 21-27.
20. Shortman, K.; Naik, S. H. Steady-state and inflammatory dendritic-cell development. Nature Reviews Immunology 2007, 7, 19-30.
21. Shortman, K.; Heath, W. R. The CD8+dendritic cell subset. Immunological Reviews 2010, 234, 18-31.
22. Banchereau, J.; Steinman, R. M. Dendritic cells and the control of immunity. Nature 1998, 392, 245-252.
23. Banchereau, J.; Briere, F.; Caux, C.; Davoust, J.; Lebecque, S.; Liu, Y. T.; Pulendran, B.; Palucka, K. Immunobiology of dendritic cells. Annual Review of Immunology 2000, 18, 767-+.

24. Joffre, O.; Nolte, M. A.; Spoerri, R.; Reis e Sousa, C. Inflammatory signals in dendritic cell activation and the induction of adaptive immunity. Immunological Reviews 2009, 227, 234-247.

25. Kapsenberg, M. L. Dendritic-cell control of pathogen-driven T-cell polarization. Nature Reviews Immunology 2003, 3, 984-993.

26. Reis e Sousa, C. 2011 ESCI Award for Excellence in Basic/Translational Research: innate regulation of adaptive immunity by dendritic cells. European Journal of Clinical Investigation 2011, 41, 907-916.

27. Steinman, R. M.; Banchereau, J. Taking dendritic cells into medicine. Nature 2007, 449, 419-426.

28. Trombetta, E. S.; Mellman, I. Cell biology of antigen processing in vitro and in vivo. In Annual Review of Immunology, 2005; Vol. 23, pp 975-1028.

29. Steinman, R. M. Dendritic cells: Understanding immunogenicity. European Journal of Immunology 2007, 37, S53-S60.

30. Mellman, I.; Steinman, R. M. Dendritic cells: Specialized and regulated antigen processing machines. Cell 2001, 106, 255-258.

31. Reis e Sousa, C. Essay - Dendritic cells in a mature age. Nature Reviews Immunology 2006, 6, 476-483.

32. Steinman, R. M. Decisions About Dendritic Cells: Past, Present, and Future. Annual Review of Immunology, Vol 30 2012, 30, 1-22.

33. Burchill, M. A.; Tamburini, B. A.; Pennock, N. D.; White, J. T.; Kurche, J. S.; Kedl, R. M. T cell vaccinology: Exploring the known unknowns. Vaccine 2013, 31, 297-305.

34. Rock, K. L.; Shen, L. Cross-presentation: underlying mechanisms and role in immune surveillance. Immunological Reviews 2005, 207, 166-183.

35. Bevan, M. J. Cross-priming for a secondary cytotoxic response to minor H-antigens with H-2 congenic cells which do not cross-react in cytotoxic assay. Journal of Experimental Medicine 1976, 143, 1283-1288.

36. Rock, K. L.; Gamble, S.; Rothstein, L. Presentation of exogenous antigen with class-I major histocompatibility complex-molecules. Science 1990, 249, 918-921.

37. Dresch, C.; Leverrier, Y.; Marvel, J.; Shortman, K. Development of antigen cross-presentation capacity in dendritic cells. Trends in Immunology 2012, 33, 381-388.

38. Heath, W. R.; Belz, G. T.; Behrens, G. M. N.; Smith, C. M.; Forehan, S. P.; Parish, I. A.; Davey, G. M.; Wilson, N. S.; Carbone, F. R.; Villadangos, J. A. Cross-presentation, dendritic cell subsets, and the generation of immunity to cellular antigens. Immunological Reviews 2004, 199, 9-26.

39. Joffre, O. P.; Segura, E.; Savina, A.; Amigorena, S. Cross-presentation by dendritic cells. Nature Reviews Immunology 2012, 12, 557-569.

40. Foged, C.; Hansen, J.; Agger, E. M. License to kill: Formulation requirements for optimal priming of CD8(+) CTL responses with particulate vaccine delivery systems. European Journal of Pharmaceutical Sciences 2012, 45, 482-491.

41. Kovacsovicsbankowski, M.; Rock, K. L. A phagosome-to-cytosol pathway for exogneous antigens presented on MHC class-I molecules. Science 1995, 267, 243- 246.

42. Houde, M.; Bertholet, S.; Gagnon, E.; Brunet, S.; Goyette, G.; Laplante, A.; Princiotta, M. F.; Thibault, P.; Sacks, D.; Desjardins, M. Phagosomes are competent organelles for antigen cross-presentation. Nature 2003, 425, 402-406.

43. Guermonprez, P.; Saveanu, L.; Kleijmeer, M.; Davoust, J.; van Endert, P.; Amigorena, S. ER-phagosome fusion defines an MHC class I cross-presentation compartment in dendritic cells. Nature 2003, 425, 397-402.

44. Ackerman, A. L.; Cresswell, P. Cellular mechanisms governing cross-presentation of exogenous antigens. Nature Immunology 2004, 5, 678-684.

45.   Ackerman, A. L.; Giodini, A.; Cresswell, P. A role for the endoplasmic reticulum protein retrotranslocation machinery during crosspresentation by dendritic cells. Immunity 2006, 25, 607-617.

46.   Shen, L. J.; Sigal, L. J.; Boes, M.; Rock, K. L. Important role of cathepsin S in generating peptides for TAP-independent MHC class I crosspresentation in vivo. Immunity 2004, 21, 155-165.

47.   Sallusto, F.; Lanzavecchia, A.; Araki, K.; Ahmed, R. From Vaccines to Memory and Back. Immunity 2010, 33, 451-463.

48.   Plotkin, S. A. Vaccines: past, present and future. Nature Medicine 2005, 11, S5-S11.

49.   WHO. http://www.who.int/topics/immunization/en/ (accessed March, 26).

50.   Gezin, K. e. http://www.kindengezin.be/gezondheid-en-vaccineren/vaccinaties/verplichte-en-vrije-vaccins/ (accessed March, 26).

51.   De Gregorio, E.; Rappuoli, R. Vaccines for the future: learning from human immunology. Microbial Biotechnology 2012, 5, 149-155.

52.   Rappuoli, R. Twenty-first century vaccines. Philosophical Transactions of the Royal Society B-Biological Sciences 2011, 366, 2756-2758.

53.   O'Hagan, D. T.; Rappluoli, R. The safety of vaccines. Drug Discovery Today 2004, 9, 846-854.

54.   Bachmann, M. F.; Jennings, G. T. Vaccine delivery: a matter of size, geometry, kinetics and molecular patterns. Nature Reviews Immunology 2010, 10, 787-796.

55.   Plotkin, S. A.; Plotkin, S. L. The development of vaccines: how the past led to the future. Nature Reviews Microbiology 2011, 9, 889-893.

56.   Guy, B. The perfect mix: recent progress in adjuvant research. Nature Reviews Microbiology 2007, 5, 505-517.

57.   Mbow, M. L.; De Gregorio, E.; Valiante, N. M.; Rappuoli, R. New adjuvants for human vaccines. Current Opinion in Immunology 2010, 22, 411-416.

58.   O'Hagan, D. T.; De Gregorio, E. The path to a successful vaccine adjuvant - 'The long and winding road'. Drug Discovery Today 2009, 14, 541-551.

59.   McKee, A. S.; Munks, M. W.; Marrack, P. How do adjuvants work? Important considerations for new generation adjuvants. Immunity 2007, 27, 687-690.

60.   O'Hagan, D. T.; Singh, M.; Ulmer, J. B. Microparticle-based technologies for vaccines. Methods 2006, 40, 10-19.

61.   Reddy, S. T.; Swartz, M. A.; Hubbell, J. A. Targeting dendritic cells with biomaterials: developing the next generation of vaccines. Trends in Immunology 2006, 27, 573-579.

62.   Moon, J. J.; Suh, H.; Bershteyn, A.; Stephan, M. T.; Liu, H.; Huang, B.; Sohail, M.; Luo, S.; Um, S. H.; Khant, H.; Goodwin, J. T.; Ramos, J.; Chiu, W.; Irvine, D. J. Interbilayer-crosslinked multilamellar vesicles as synthetic vaccines for potent humoral and cellular immune responses. Nature Materials 2011, 10, 243-251.

63.   Leleux, J.; Roy, K. Micro and Nanoparticle-Based Delivery Systems for Vaccine Immunotherapy: An Immunological and Materials Perspective. Advanced Healthcare Materials 2013, 2, 72-94.

64.   Leroux-Roels, G. Unmet needs in modern vaccinology Adjuvants to improve the immune response. Vaccine 2010, 28, C25-C36.

65.   Garcia, A.; De Sanctis, J. B. An overview of adjuvant formulations and delivery. Apmis 2014, 122, 257-267.

66.   Kool, M.; Fierens, K.; Lambrecht, B. N. Alum adjuvant: some of the tricks of the oldest adjuvant. Journal of Medical Microbiology 2012, 61, 927-934.

67.   Copland, M. J.; Rades, T.; Davies, N. M.; Baird, M. A. Lipid based particulate formulations for the delivery of antigen. Immunology and Cell Biology 2005, 83, 97-105.

68.   Grgacic, E. V. L.; Anderson, D. A. Virus-like particles: Passport to immune recognition. Methods 2006, 40, 60-65.

69.   Steinhagen, F.; Kinjo, T.; Bode, C.; Klinman, D. M. TLR-based immune adjuvants. Vaccine 2011, 29, 3341-3355.

70.   Garcon, N.; Chomez, P.; Van Mechelen, M. GlaxoSmithKline Adjuvant systems in vaccines: concepts, achievements and perspectives. Expert Review of Vaccines 2007, 6, 723-739.

24

CHAPTER 2

INTERACTION BETWEEN POLYMERIC MULTILAYER CAPSULES AND IMMUNE CELLS

CHAPTER 2

INTERACTION BETWEEN

POLYMERIC MULTILAYER

CAPSULES AND IMMUNE CELLS

1. INTRODUCTION

Polymeric multilayer capsules (PMLC) have been introduced in the late nineties by the group of Helmuth Möhwald and are based on sequential adsorption (i.e. layer-by-layer or LbL assembly)[1] of interacting species onto a sacrificial template followed by the decomposition of this template.[2, 3] Typical interactions allowing the assembly of PMLC are electrostatics, H-bonding and covalent chemistry. **Figure 1** schematically represents the process of capsule assembly. Based on the pioneering work of Gero Decher in the early nineties, this approach witnessed increased popularity due to its conceptual simplicity. Indeed, the LbL technique allows the relatively easy assembly of ultrathin layered capsules using commercially available polymers and common lab equipment while avoiding toxic solvents. In addition, due to its high versatility, the capsules' properties can be tailored onto the nanoscale, e.g. by varying the number of layers deposited, polymer composition and physicochemical properties, or even by endowing the capsules' surface with additional components such as nanoparticles,[4] lipids,[5] viruses[6] etc.
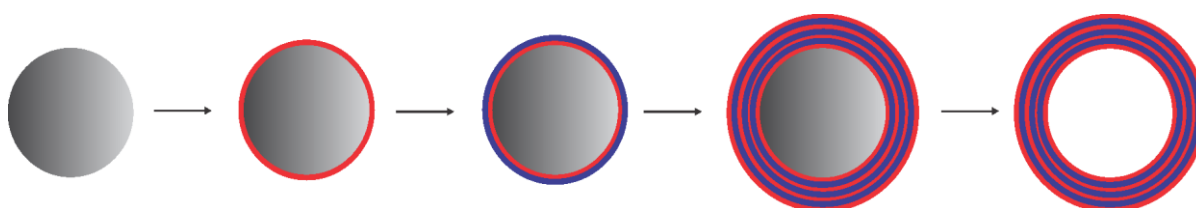

Figure 1. Schematic representation of LbL coating of a sacrificial microtemplate followed by the decomposition of this template, yielding hollow polymeric multilayer capsules.

Drawn by these appealing properties, material scientists have started designing and evaluating new drug delivery systems based on LbL assembly.[7-11] Taking into consideration the long (i.e. more than 30 years) time it took before liposomal drug formulations reached the market,[12] it is evident that

PMLC are still in an early stage of development. Nevertheless, several groups have been evaluating PMLC intensively as carriers for drug molecules both *in vitro* and *in vivo*.[13-17] Currently, one of the best-studied fields of application is the delivery of vaccine antigens to immune cells. Thereby, we focus in this chapter on the recent progress that has been made in designing PMLC intended for microparticulate vaccine delivery. This field is only in an early stage and PMLC are currently merely used to encapsulate vaccine antigens or peptides in their hollow void or within the capsule wall. However, the concept of LbL assembly holds the potential to fabricate well defined vaccines carriers with specific immune-stimulatory and or targeting ligands, by incorporating these during capsule fabrication. Such an approach would pave the road toward a rational and modular design of antigen/adjuvant systems.
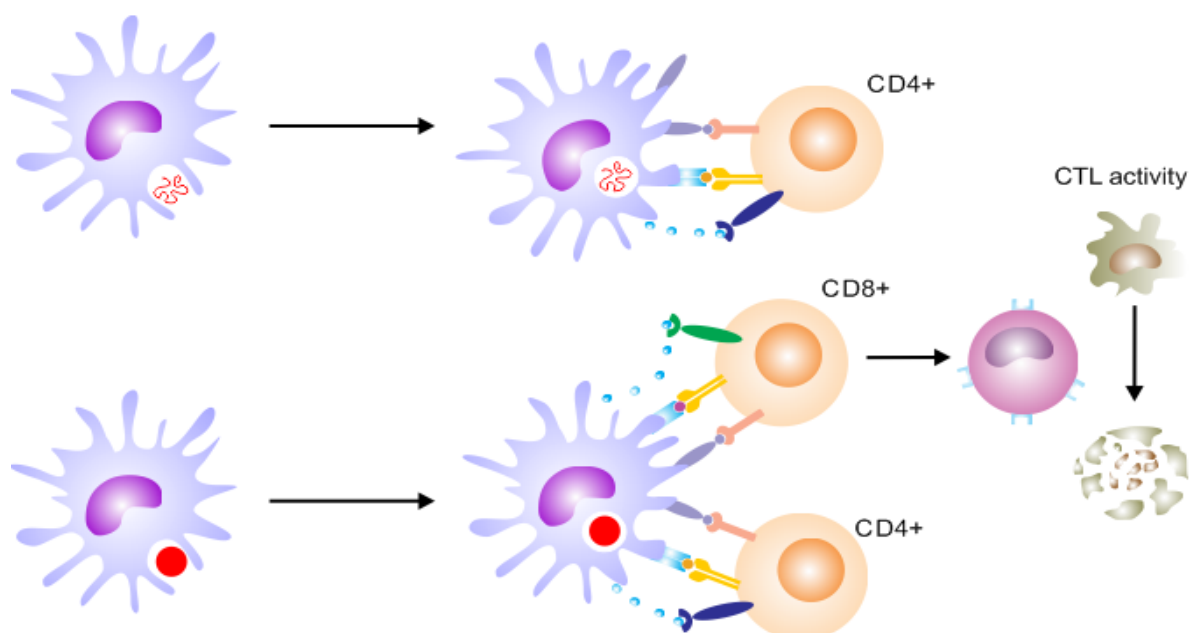

Figure 2. Schematic representation of antigen presentation by dendritic cells (DCs) to T cells. Soluble antigen is predominantly presented to CD4 T cells. Particulate antigen is presented to both CD4 and CD8 T cells (i.e. cross-presentation) and depending on the cytokine environment, CD8 T cells can differentiate to cytotoxic T cells (CTLs) that can recognize and eliminate infected or malignant cells.

Microparticulate antigen delivery – i.e. encapsulation of vaccine antigens in polymeric nano- and microparticles – has emerged to promote adaptive immune response to recombinant antigens by enhancing antigen presentation by dendritic cells (DCs).[18-21] Dendritic cells (DCs) continuously sample antigens in peripheral tissues, process them and transport them to the draining lymph nodes for presentation to T cells. While soluble antigens are mainly presented via MHCII to CD4 T cells, particulate antigens are also presented via MHCI to CD8 T cells (**Figure 2**). This is of paramount importance, as CD8 T cells can differentiate into cytotoxic T cells capable of killing not only pathogen

infected cells but also malignant cells. As a consequence, formulating antigens in polymeric particles is considered to be highly promising for the development of effective vaccines against insidious pathogens including HIV, tuberculosis, and malaria. In addition, particulate antigen carriers might also become valuable tools to develop therapeutic cancer vaccines.

2. CELLULAR INTERACTION WITH POLYMERIC MULTILAYER CAPSULES

Recently, a series of publications have emerged, addressing the potential of polyelectrolyte multilayer capsules for vaccine delivery.[7, 9, 22] In our opinion, an ideal microparticulate antigen delivery vehicle should at least two requirements. First, antigen should be encapsulated highly efficiently, preferably under non-denaturing conditions, in order to avoid extensive loss of expensive recombinant antigens. Second, while the antigen should remain stably entrapped in the capsules before uptake by professional APCs, once internalized, the antigen should become readily available for enzymatic processing and loading onto MHC molecules.

To tackle the first challenge, the use of inorganic particles as templates for the LbL assembly has turned out to be extremely well suited. Due to their porous structure, calcium carbonate and mesoporous silica particles exhibit an extremely large surface to volume ratio, allowing proteins to adsorb and to become efficiently encapsulated following deposition of the LbL layers.[23, 24] Subsequently, these inorganic templates can be readily dissolved under aqueous conditions yielding hollow capsules entrapping the antigen. Dissolution of mesoporous silica is typically achieved using diluted HF buffers, while calcium carbonate particles can be dissolved either at acidic pH or by adding EDTA to complex the Ca^{2+} ions.

Designing capsules that selectively release their payload upon cellular internalization represents a major challenge. A profound knowledge is required on the characteristics of the intracellular compartments where the capsules end up following internalization by APCs. Such insights should allow a more rational choice of the capsules' building blocks enabling the generation of capsules capable of responding to specific physicochemical stimuli present in these organelles. The issue of capsule internalization and fate and its repercussions on capsule design have been addressed by various groups. A first question concerns the route of internalization of PMLC. Confocal and transmission electron microscopy was used to investigate DCs that were incubated with PMLC. DCs formed large, actin-rich, cytoplasmic protrusions that engulfed the capsules, leading to cellular uptake. Using inhibitors of different cellular uptake pathways (**Figure 3A**), it was demonstrated that by blocking actin polymerization or macropinocytosis, capsule uptake was completely abolished. In

addition, a role for lipid raft formation in capsule uptake was suggested as blocking of caveolae mediated endocytosis prevented capsule uptake, which was not observed when blocking clathrin mediated uptake.[25]

A simple but informative way to investigate the intracellular fate of the capsules is to incubate cells with PMLC followed by co-staining of either the cytosol or the intracellular acidic vesicles (endosomes, lysosome, phagosomes). As shown in **Figure 3B**, by confocal microscopy images recorded from DCs that were incubated overnight with PMLC, capsules clearly co-localize with acidic vesicles, while no co-localization with the cytosolic stain CellTracker was observed. To further assess whether these organelles are able to acidify the whole capsule volume – which is considerable larger that the volume of empty (endo/lyso/phago)somes – the pH-sensitive dye SNARF-dextran was encapsulated. SNARF-dextran changes its excitation and emission spectrum as function of the pH of the medium. At alkaline pH, SNARF emits red fluorescence whereas at acidic pH, green fluorescence is emitted. **Figure 3C** shows a confocal microscopy image of MDA-MB435S breast cancer cells that were incubated with SNARF-dextran loaded capsules.[26] The pH of the medium was slightly increased to enhance the contrast between free capsules and internalized capsules. From the strong increase in green fluorescence intensity, it was confirmed that PMLC indeed end up in acidic compartments upon cellular internalization.

Taken together, these initial studies have shown that PMLC experience a shift to a more acidic pH following cellular uptake, a feature that might be exploited to trigger capsule disassembly. Indeed, pH decrease is commonly used in the field of intracellular drug delivery, e.g. gene or cancer therapy, to trigger the release of drug molecules in the endosomes or in acidified tumour tissue.[27] Moreover, several polyelectrolytes as well as lipids have been reported to release drugs in the cytosol by destabilizing endosomal membranes.
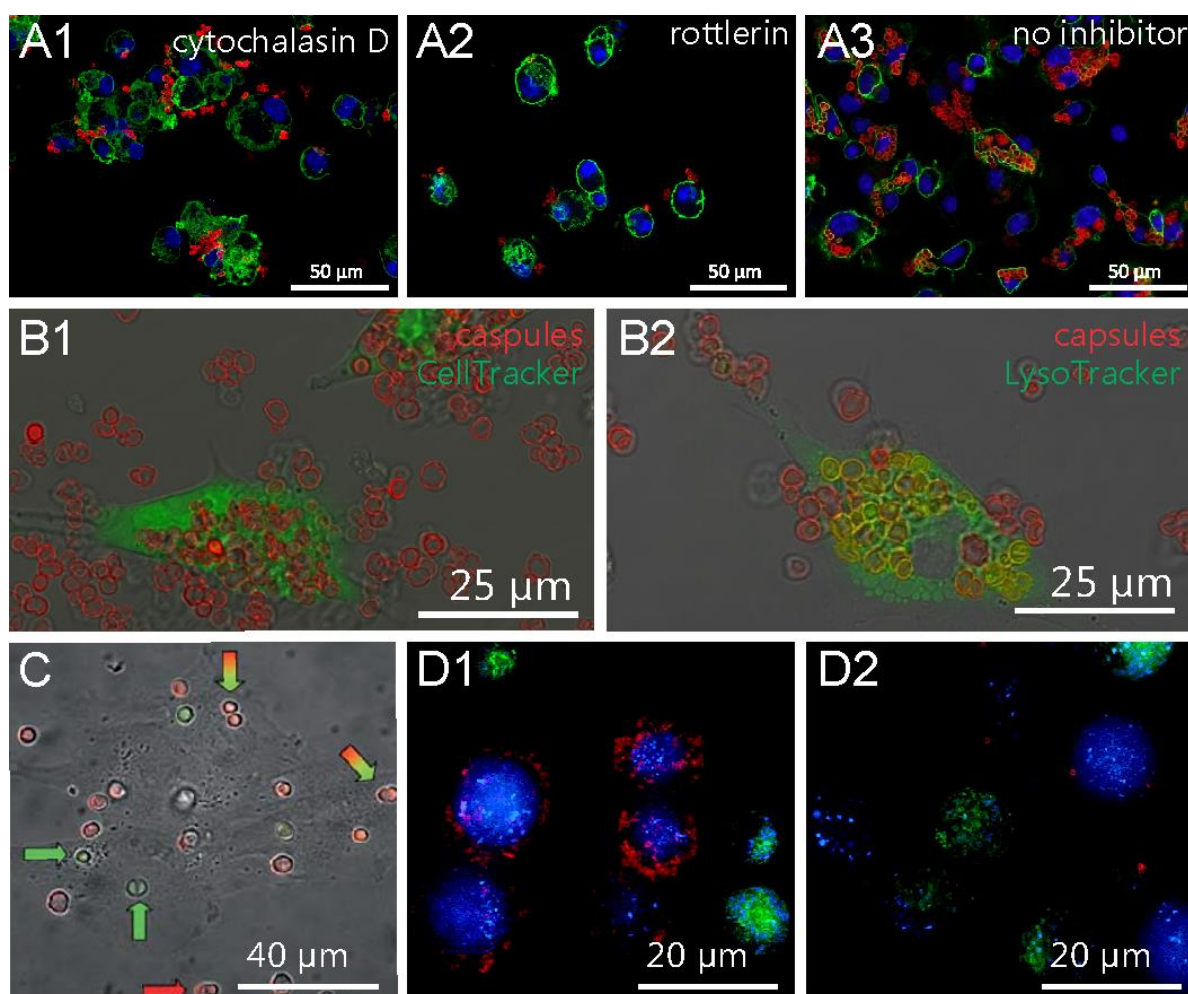
Figure 3. **(A)** Confocal images of the effects of cytochalasin D **(A1)** and rottlerin **(A2)**, on microcapsule uptake by DCs. PMLC based on (dextran sulfate/poly-L-arginine) were labeled fluorescent red in their shell using rhodamine-conjugated poly-L-arginine. The cell membrane was stained fluorescent green using Alexa Fluor 488 conjugated cholera toxin subunit B. Cell nuclei were stained fluorescent blue with DAPI. **(B)** Confocal microscopy images of DCs incubated with (dextran sulfate/poly-L-arginine) capsules (fluorescent red). In panel **B1**, DCs were stained with CellTrackerGreen to visualize the cytoplasm and in panel **B2** with LysotrackerGreen to visualize acidic cellular compartments. **(C)** Confocal microscopy image of SNARF-loaded capsules that change from fluorescent red to green upon internalization by MDA-MB435S breast cancer cells. **(D)** Fluorescence microscopy images of LIM cancer cells that expressed the huA33 antigen (blue cells) and control LIM cancer cells that did not expressed the huA33 antigen (green cells), incubated with capsules (fluorescent red) functionalized with **(D1)** the huA33 monoclonal antibody and **(D2)** IgG as control.[25,26,40]

Also in the field of PMLC, the effect of pH on capsule behaviour and drug release has been studied extensively.[28] Polyelectrolytes containing primary amine or carboxylic acid groups exhibit a strong pH dependent swelling and shrinking. Unfortunately, compared to drug delivery systems based on single polymers, the pH regions in which drug release is triggered from polyelectrolyte based PMLC are extremely basic or acidic. This is due to the fact that upon complexation, the apparent pKa of the inter-polyelectrolyte complexes shifts, rendering the complexes stable in pH regions where based on the pKa of the single polyelectrolytes, the complexes are expected to disassemble.[29] As a

consequence, a wide variety of polymers available from the field of non-viral gene delivery have failed to construct PMLC that disassemble upon uptake in intracellular acidic vesicles. Thanks to the advent of single-component capsules, obtained by removal of one of the interacting polymer layers or by covalent LbL assembly, this failure might be resolved soon.

In this context, PMLC composed of poly(2-(diisopropylamino)ethyl methacrylate), a polymer which exhibits a strong shift from hydrophobic to hydrophilic behaviour around pH 6.5, making this polymer responsive to an intracellular pH switch, were assembled.[30] By assembling alternating layers of azide-, respectively alkyne-modified poly(2-(diisopropylamino)ethyl methacrylate) via Cu^{I} catalysed cycloaddition – i.e. 'click' chemistry – single component capsules responsive in the expected pH region were obtained. Drug delivery applications of this system have not been shown so far but are highly anticipated. As an interesting alternative to exploit the pH dependent ionization of polyelectrolytes, Hammond and co-workers took advantage of the pH dependent recognition between iminobiotin and neutravidin. These molecules form a stable affinity bond at neutral to alkaline pH, but disassemble as soon as the pH becomes slightly acidic. Ultra small capsules assembled on quantum dots were shown to disassemble in acidic hypoxic regions of solid tumours in mice models.[15]

Intracellular organelles such as endosomes, lysosomes and phagosomes contain high concentrations of proteases. Thereby, a convenient way to engineer multilayer capsules to release their payload upon cellular uptake involves the use of polypeptides prone to enzymatic degradation as building blocks (**Figure 4A**).

In this context capsules composed of dextran sulfate (DS) and poly-L-arginine (P$_L$ARG) were assembled.[31] **Figure 4B** shows a series of confocal microscopy images of these capsules incubated in an aqueous pronase solution. Pronase is a mixture of non-specific proteases that are capable of cleaving virtually any peptide bond. As evidenced by these images, the (DS/P$_L$ARG) capsules gradually degrade as a function of time and dissolve into the surrounding medium. When incubated *in vitro* with phagocyting cancer cells, these capsules became internalized and gradually lost their integrity until only debris of broken capsules was visible within the cells. By contrast, control capsules composed of non-degradable polyelectrolytes such as poly(styrene sulfonate) (PSS) and poly(allylamine hydrochloride) (PAH) retained their structural integrity even several days after cellular uptake.

An in depth investigation of the *in vitro* interaction between enzyme-degradable DS/P$_L$ARG capsules and dendritic cells was performed using transmission electron microscopy (**Figure 4C**).[25] Upon cellular uptake these capsules initially retained their spherical shape and became surrounded by a lipid bilayer membrane, supporting the earlier observation that these capsules are located in macropinosomal or phagosomal vesicles. Over a 24 h time period, the capsules' shell however severely deformed and finally ruptured, followed by invagination of cytoplasmic content into the capsules' hollow void, which remained however separated from the cytoplasm by a lipid bilayer membrane.

Besides a drop in pH and a proteolytic environment, also a shift from an oxidative to a reductive environment is sensed when crossing the cellular membrane. This reductive environment is predominantly present in the cellular cytosol but not in the acidic phagolysosomal vesicles where PMLC are typically located upon cellular entry. Nevertheless in the last few years, the use of disulfide linkages, that render polymeric constructs reduction-sensitive, has received considerable attention by the drug delivery community.[27] Reduction-sensitive PMLC have been explored by a number of groups, either using ferrocenes[32] or disulfides.[33, 34]

Haynie and co-workers designed polypeptides, containing cysteine residues, with an overall anionic, respectively cationic charge that could be assembled through electrostatic interaction.[33] By crosslinking of these cysteine residues via oxidative disulphide formation, these capsules where rendered stable over a wide pH range while non-crosslinked capsules were unstable at physiological pH.

The Caruso group reported in an extensive series of papers on single-component PMLC that are stabilized through reduction-sensitive disulfide linkages.[34, 35] These capsules were assembled either through H-bonding or covalent assembly of sequential layers. Both these approaches avoided the use of polycations, which are often associated with cytotoxicity, although this remains a controversial issue as will be discussed further in this chapter.
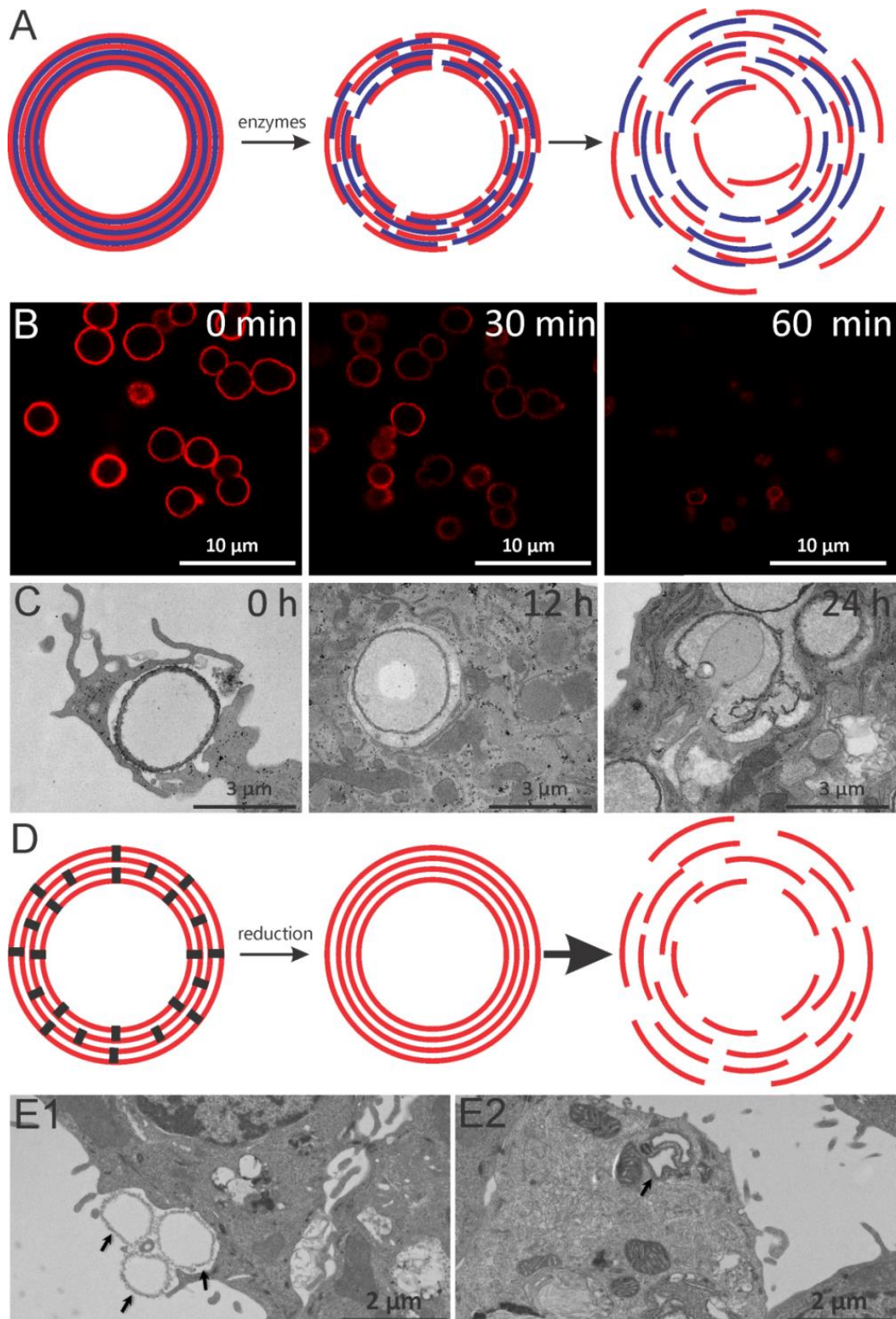
Figure 4. **(A)** Schematic representation of enzyme-responsive multilayer capsules. **(B)** Confocal microscopy images of (DS/P$_L$ARG) capsules (fluorescent red) incubated in aqueous pronase solution. **(C)** Transmission electron microscopy images at different time intervals of dendritic cells that have internalized (dextran sulfate/poly-L-arginine) capsules. **(D)** Schematic representation of disulphide cross-linked single-component capsules and their reduction triggered disassembly. **(E)** Transmission electron microscopy images of LIM1899 cells that have internalized PMA^{SH} capsules. The arrows in panel **(E1)** show cellular protrusions involved in capsules uptake, the arrows in panel **(E2)** indicate internalized and deformed capsules.[25,31,41]

H-bonded capsules are typically assembled using poly(methacrylic acid) (PMA) as hydrogen bond donor and poly(N-vinylpyrrolidone) (PVP) as hydrogen bond acceptor. At acidic pH, below the pKa of PMA at which the carboxylic acid groups are protonated and the polymer is non-charged, PMA readily allows multilayer film assembly by consecutive coating steps with PVP. When transferred to physiological pH, the PMAs' carboxylic acid groups become deprotonated and electrostatic repulsion between successive PMA layers leads to capsule deconstruction. To stabilize these capsules at physiological pH, PMA was substituted with thiol moieties (i.e. PMA^{SH}), allowing cross-linking of the capsules via disulfide bridge formation prior to core dissolution. After core-dissolution and adjusting the medium to the physiological pH of 7.4, the PVP is leached out as protonation of the PMA^{SH}s' carboxylic acid groups no longer favors H-bonding with the PVP. In this way, single component capsules are obtained. Incubation in reductive medium, containing glutathione, leads to capsule disassembly due to cleavage of the disulfide bonds as schematically shown in **Figure 4D**.

Alternative to crosslinking PMA layers in H-bonded capsules, click chemistry (i.e. Cu^{I} catalyzed cycloaddition of azides to alkynes, forming a triazole linkage) was explored to stabilize PMLC capsules through reduction-sensitive linkers.[36-38] For this purpose, capsules were assembled from alternating layers of PMA and PVP^{alkyne}, i.e. a copolymer of vinylpyrrolidone and an alkyne functionalized monomer. After assembly, the multilayers are infiltrated with a bisazide crosslinker bearing a disulfide bond. Using standard conditions for aqueous click chemistry (i.e copper sulfate and ascorbic acid to reduce the cupper to its Cu^{I} state) the PVP layers are covalently bound through reduction-sensitive disulfide bridges. The use of this type of click chemistry suffers from the significant drawback of requiring cupper, which is potentially toxic. However, recent progress (ref) in organic and polymer chemistry is paving the way for cupper-free click chemistry that circumvents the above-mentioned issue. Moreover, the increasing popularity of the click chemistry approach for bio-conjugation is owed to its orthogonality, meaning that this reaction commonly does not interfere with other function groups such as primary amines, thiols and carboxylic acids abundantly present in biological systems.[39] This feature enables to construct and post-functionalize PMLC with antibodies that allowed receptor mediated capsule association with extremely high (i.e. +99%) specificity (**Figure 3D**).[40]

The intracellular fate of H-bonded PMA^{SH} capsules was assessed by Caruso and co-workers in several papers. PMA^{SH} capsules were found to strongly deform upon internalization by cells (**Figure 4E**) and were located in intracellular acidic vesicles.[41] These vesicles were identified by immunohistochemical staining as being predominantly late endosomes and lysosomes. This is in analogy with the findings reported by other groups on polypeptide and polysaccharide based capsules that degrade through

enzymatic action. Interestingly, when these capsules carried a lipophilic payload, this payload was released after cellular uptake and distributed throughout the cellular cytoplasm. In contrast, high molecular weight hydrophilic compounds remained within acidic vesicles. A recent study focused on the influence on drug released exerted disulfide reduction within the capsule wall during cellular uptake.[42] Test-tube results involving addition of reductive species such as DTT and glutathione clearly demonstrated that PMA[SH] capsules could disassemble and release their payload upon reduction of the disulfide crosslinks.

However, as mentioned earlier in this chapter, reduction is performed in the cytosol rather than in endosomal compartments. Nevertheless, it was demonstrated that capsules with non-degradable cross-links where unable to release their drug payload, while capsules bearing disulfide crosslinks readily enabled intracellular drug release (**Figure 5A-B**).[42] To clarify this contradictory situation, the role of thiols associated with cell surface proteins was investigated. These so-called exofacial thiols were found to catalyze redox-activated release from the capsules. Blocking of these thiol groups did not affect capsule internalization, but completely abolished intracellular release.

Finally, even more important to the fate of the capsules themselves is the intracellular localization of the encapsulated drug molecules. As mentioned above, hydrophobic low molecular weights species could be released from reduction-sensitive capsules upon cellular uptake.[42] The intracellular fate of hydrophilic high molecular weights species, such as proteins, has been investigated.[43] For this purpose, dequenching-ovalbumin (DQ-OVA) was encapsulated in degradable (DS/P$_L$ARG) and non-degradable (PSS/PAH) capsules and incubated *in vitro* with a 3T3 fibroblast cell line or with DCs derived from murine bone marrow (**Figure 5 C-D).**[43]

DQ-OVA is a fluorogenic substrate for proteases, comprised of OVA that is excessively substituted with BODIPY dyes. In its native state, DQ-OVA is subjected to strong fluorescence quenching due to its excessive labeling. However, upon enzymatic degradation of DQ-OVA into single dye-labeled peptides, quenching is alleviated and bright green fluorescence emerges. Whereas in the extracellular medium, DQ-OVA loaded degradable capsules did not emit significant fluorescence, upon cellular internalization by either 3T3 fibroblasts (**Figure 5C**) or DCs, green fluorescence emerged within 22 h for 3T3 fibroblasts and as soon as 2 h for DCs. These observations indicate a significant effect of cell type on capsules uptake and processing.
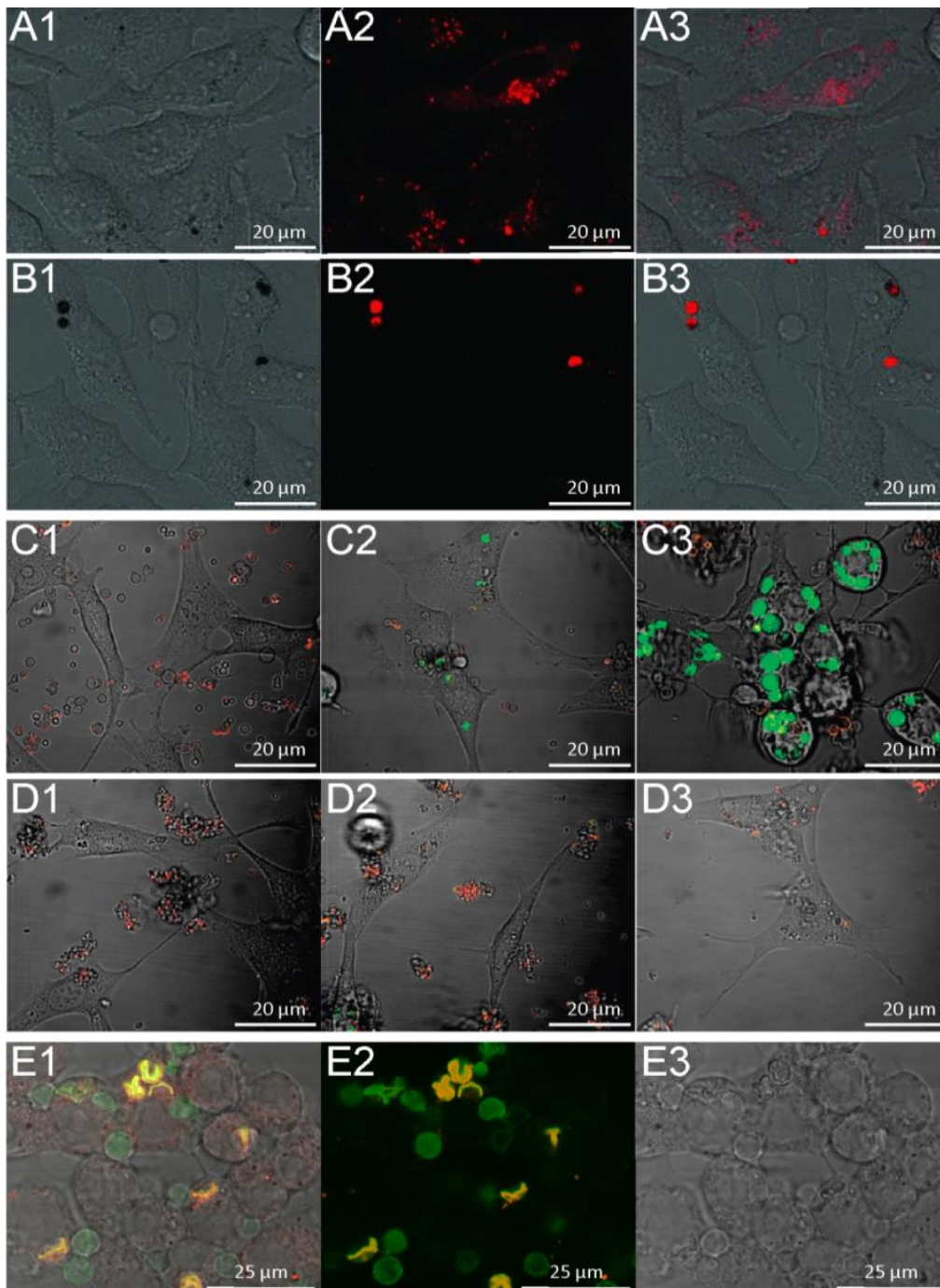
Figure 5. **(A-B)** Confocal microscopy images of HeLa cells incubated with **(A)** reduction-sensitive PMA$^{SH(disulfide)}$ and **(B)** reduction-insensitive PMA$^{SH(thioether)}$ capsules. Both types of capsules were loaded with the hydrophobic dye DiI. **(C-D)** Confocal microscopy images of 3T3 fibroblasts incubated with respectively **(C)** degradable (DS/P$_L$ARG) capsules and **(D)** non-degredable (PSS/PAH) capsules. Both types of capsule were loaded with the fluorogenic DQ-OVA. This probes emits red fluorescence due to excimer formation and starts to emit green fluorescence upon proteolytic cleavage of the OVA. Images were recorded **(C1-D1)** immediately after addition of the capsule to the cells, **(C2-D2)** after 30 h of incubation and **(C3-D3)** after 60 h of incubation. **(E)** Confocal microscopy images of cross-linked HA/PAH after 2 h co-incubation with RAW mouse macrophages. Capsules are stained green fluorescent using HA^{FITC}, while the cellular lysosomes are stained using LysoTracker Red. Co-localization between the green and red channel is observed as a yellow/orange color. [42,43,46]

Similarly, major differences between cell lines regarding the uptake of PMA[SH] capsules were observed.[41] Importantly, when encapsulating DQ-OVA in non-degradable capsules (**Figure 5D**), intracellular processing was not detected at all, thereby highlighting the importance of capsule design on the ability of PMLC to allow intracellular drug release. Additionally, when comparing data obtained from transmission electron microscopy and confocal microscopy, it is worthwhile to note that although visual rupturing of the shell of (DS/P$_L$ARG) capsules took over 12 h to occur inside DCs, processing of encapsulated DQ-OVA by the same DCs took off as soon as after 2h of co-incubation.[25] Therefore, it can be assumed that intracellular proteases can readily traverse the (DS/P$_L$ARG) capsule wall, whereas this seems not to be the case for (PSS/PAH) capsules. The underlying reason for this is likely an interplay between different factors including higher permeability of the (DS/P$_L$ARG) membrane and the appearance of nanopores by enzymatic processing and mechanical stress exerted inside cells.

The effect of mechanical stress on capsules' morphology has been addressed by demonstrating that non-degradable capsules are less prone to intracellular deformation when these are reinforced with metal nanoparticles.[44] From the pioneering work of the Kotov group on planar multilayer films, it is known that organic/inorganic hybrid films exhibit a dramatic increase in mechanical strength compared to solely organic multlilayers.[45] The effect of mechanical strength on intracellular capsule deformation was further highlighted using capsules containing hyaluronic acid (HA) as polyanion, which is known from the literature on planar multilayers to yield very soft structures. Indeed, as shown in **Figure 5E**, these capsules deformed immediately after uptake by RAW macrophages.[46]

3. *IN VITRO* AND *IN VIVO* INTERACTION WITH IMMUNE CELLS

A first important issue when evaluating biomedical materials *in vivo* is how these materials interact with complex living tissues. In view of using PMLC as carrier for mucosal drug delivery, De Cock et al. investigated the interactions between mucosal tissue and polyanions, polycations and their respective inter-polyelectrolyte complexes and multilayered capsules.[47]

To circumvent ethical issues regarding the use of higher mammalian species such as rabbits – which are currently used to evaluate mucosal irritation of e.g. cosmetic products – Arion lustanicus (a type of slugs) was used as test species.[48] The surface of these species consists of an outer single epithelium layer as well as mucus, overlying connective tissue. In steady-state conditions, these slugs produce a limited amount of mucus. However, when exposed to an irritating component, mucus secretion is induced as a protective mechanism. As shown in **Figure 6A**, both polyanions and

polycations, irrespective of their degradability, induced mucus secretion which was more pronounced for cationic than for anionic species. However, upon complexation, either as by simply mixing oppositely charged polyelectrolytes in water or by assembling the polyelectrolytes in a multilayered fashion onto sacrificial $CaCO_3$ templates, no mucosal irritation could be detected at all.[47] These observations suggest a dramatic lowering in toxicity of complexed polyelectrolytes relative to their soluble counterparts. Most likely, this effect is due to the solid and charge-screened state of complexed polyelectrolytes.

The mucosal immune response *in vivo* in murine models upon pulmonary delivery of (DS/P$_L$ARG) capsules was further assessed by instillation of capsules.[14] This resulted in a mild and transient inflammatory response involving the recruitment of monocytes and granulocytes. Capsule uptake and transportation to the draining lymph nodes occurred by both macrophages and dendritic cells. Encapsulating FITC-dextran allowed monitoring the *in vivo* fate of the capsules over time. Two days after administration in the lungs, intact capsules could still be observed by confocal microscopy on cytospins taken from lungs fluid (**Figure 6B**) as well as on tissue sections (**Figure 6C**) taken from the lungs. However, one week after administration barely any intact capsules were still visible whereas after 2 weeks only debris of broken capsules that released their fluorescent payload was observed.
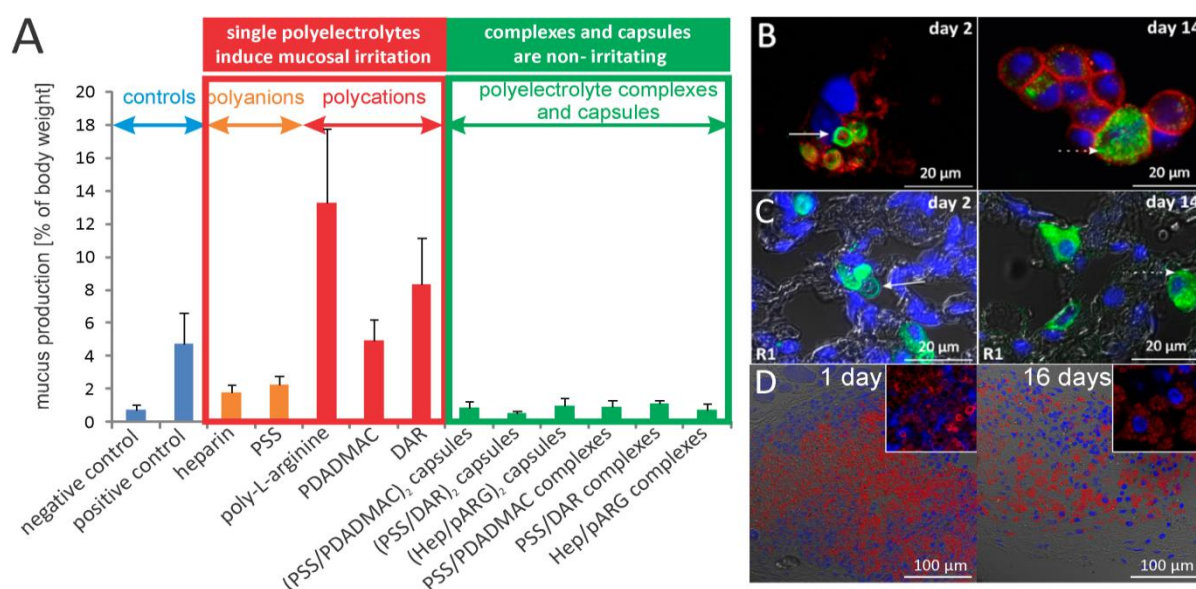

Figure 6. **(A)** Mucosal irritation induced by soluble polyelectrolytes, polyelectrolyte multilayer capsules and the corresponding complex coacervates. **(B-C)** Confocal microscopy images recorded at different time points of **(B)** alveolar macrophages and DCs collected from the bronchi and **(C)** lung tissue sections of mice that received degradable (DS/P$_L$ARG) capsules via pulmonary administration. **(D)** Confocal microscopy images of skin tissue sections of mice that received capsules via subcutaneous injection.[13,14,47]

The *in vivo* fate of DS/P$_L$ARG capsules after subcutaneous injection was also addressed. This route of administration resulted in the formation of a porous structure consisting of jammed capsules at the injection spot. Granulocytes and monocytes readily infiltrated the injected capsule mass starting from the periphery and gradually proceeding towards the centre. Over time, capsules became internalized by infiltrating macrophages and lost their integrity. Preceding cellular internalization, capsules retained their structural integrity, as shown on the confocal image taken 1 day post injection. Sixteen days post injection, the majority of the capsules were internalized by macrophages and had undergone substantial deformation (**Figure 6D**). One month after injection, capsules had further been degraded and solely capsules debris inside cells was still noticeable. Importantly, *in vivo* capsule deformation was found to be strongly dependent on the shell thickness with capsules consisting of 4 polyelectrolytes bilayers exhibiting slower deformation kinetics when compared to capsules composed of 2 bilayers. Capsules with only one bilayer appeared to be very thin, resulting in their swift deformation upon *in vivo* administration. [13]

The most crucial cells in the initiation of adaptive immune responses are the DCs, which process internalized antigens and transport them to the lymph nodes for presentation to T cells. Thereby, the capacity of respectively PMA^{SH} and (DS/P$_L$ARG) capsules to promote presentation of encapsulated antigens by DCs to T cells both *in vitro* and *in vivo* was evaluated. KP9, the CD8 epitope of a model HIV antigen, was covalently attached to PMA^{SH} capsules assembled through hydrogen bonding.[49] Subsequently, these peptide vaccine capsules were incubated with blood of HIV-infected macaques, containing antigen presenting cells as well as KP9 specific CD8 T cells. Relative to bare control capsules, KP9-conjugated capsules induced the secretion of the inflammatory cytokines TNF-α and IFN-γ, indicating that covalent linkage of peptide vaccines to PMLC still allows processing and presentation of the peptide to T cells.[49]

Using ovalbumin (OVA; chicken egg albumin) as a model antigen offers a more quantitative read-out of antigen presentation by measuring the proliferation of OT-I and OT-II transgenic T cells. OT-I cells are transgenic CD8 T cells with a T cell receptor that specifically recognizes the OVA-CD8 epitope presented via MHCI, whereas OT-II cells are transgenic CD4 T cells that specifically recognize the OVA-CD4 epitope presented via MHC-II. Encapsulation of OVA in PMA^{SH} capsules still allowed OVA to be presented to CD4 and CD8 T cells but not with a greater potency than soluble OVA. In contrast, antigen presentation was strongly increased when applying the capsules *in vivo*.[17] This effect was most pronounced on the level of CD4 T cells, which witnessed a 100 fold increase in proliferation while proliferation of CD8 T cells merely increased 4 fold (**Figure 7A**). The discrepancy between *in*

vitro and *in vivo* effects is intriguing and might be due to increased targeting of antigen presenting cells *in vivo* or to yet unknown immune activating properties of this type of capsules.[17]
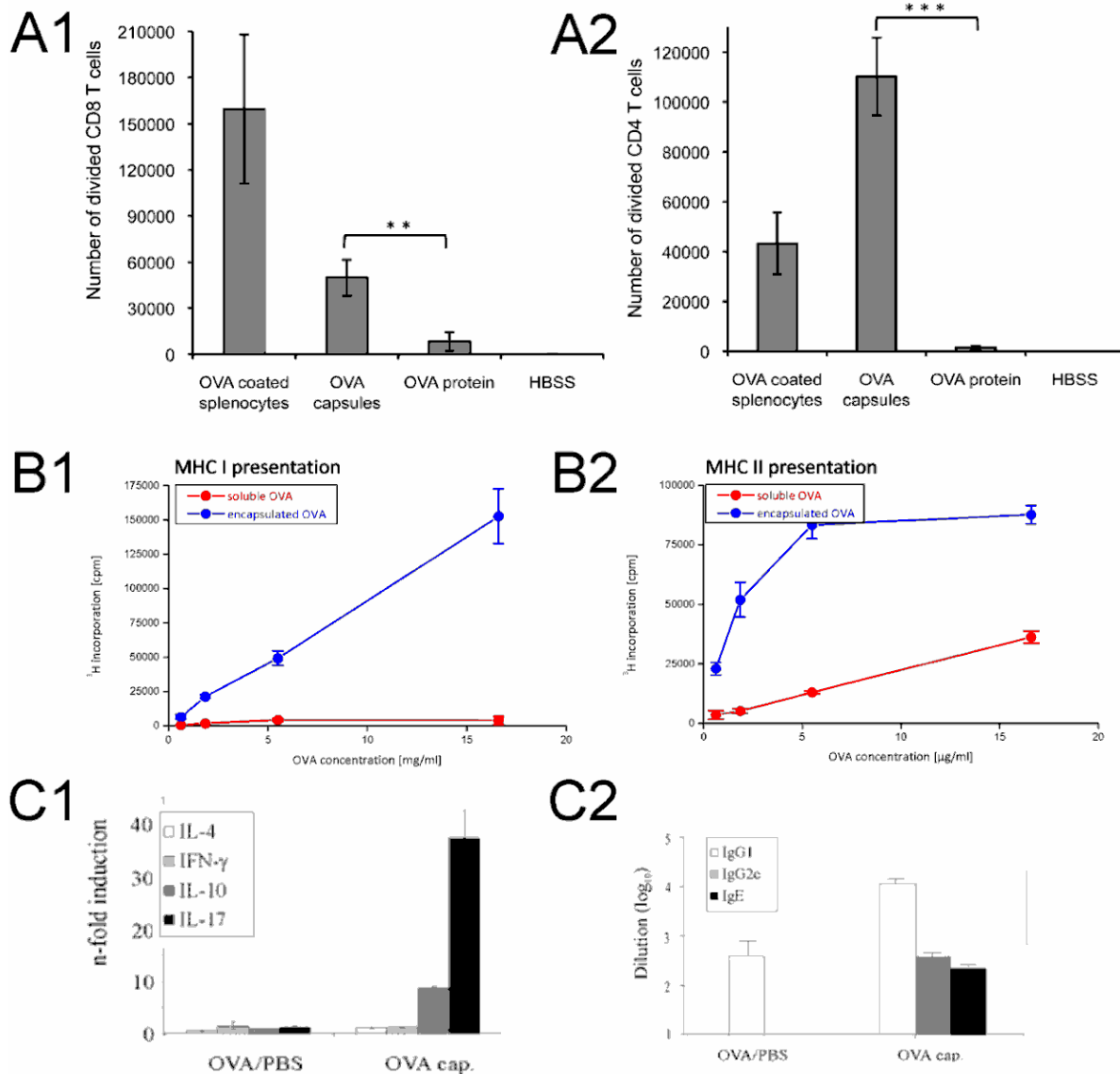

Figure 7. **(A)** Comparison of CD8 (OT-I; A1) and CD4 (OT-II; A2) T cell proliferation *in vivo* after vaccinating with OVA-loaded PMA[SH] capsules or soluble OVA. CFSE labeled OT-I CD8 and OT-II CD4 T cells were adoptively transferred into mice 24 h prior to intravenous vaccination. **(B)** Antigen presentation by DCs after uptake of soluble and (DS/P$_L$ARG) encapsulated OVA. Proliferation of OT-I cells was used as a measure for MHC-I-mediated cross-presentation of OVA **(B1)**, proliferation of OT-II cells as a measure for MHC-II mediated presentation **(B2)**. **(C1)** Expression of cytokine profiles expressed by pulmonary CD4 T cells in response to vaccination with either soluble or (DS/P$_L$ARG) encapsulated OVA. **(C2)** Serum OVA-specific antibody titers elicited following vaccination with either soluble or (DS/P$_L$ARG) encapsulated OVA.[14,17,25]

Electrostatically assembled (DS/P$_L$ARG) capsules were found to increase *in vitro* and *in vivo* presentation to both CD4 and CD8 T cells (**Figure 7B**).[25, 50] This effect was more dramatic for CD8 presentation and moderate for CD4 presentation. The immune response of mice immunized

pulmonary with either (DS/P$_L$ARG) encapsulated OVA or soluble OVA was also investigated. By analyzing the T cell cytokine secretion profile, it was observed that this type of capsules induced a Th17 skewed immune response after pulmonary administration (**Figure 7C1**).[14] This type of immune response is considered to compose a crucial part of the mucosal immune defence against fungi and extracellular bacteria. Importantly, when compared to a mixture of soluble antigen and empty capsules, antigen encapsulation inside the PMLC strongly augmented the strength of this local mucosal immune response, clearly demonstrating the necessity of antigen encapsulation for optimal induction of immunity by PMLC. On the level of the humoral immune response, capsule mediated vaccination (**Figure 7C2**) evoked strongly elevated antibody titers and isotype switching to opsonizing IgG2c antibodies, further establishing the potential of these capsules as vaccine carriers.

4. CONCLUSIONS

In this chapter, we have reviewed the recent advances in the field of polymeric multilayer capsules in view of potential applications as vaccine carrier. *In vitro* results have highlighted the potential of these carrier systems as they are efficiently internalized by antigen presenting cells and allow fast processing of encapsulated antigen. This might offer an advantage over other, more established, matrix particles that gradually release their payload via diffusion or by erosion controlled degradation mechanisms over time periods of days or even weeks. *In vivo* studies on multilayer capsules have pointed out that these capsules are relatively well tolerated by mucosal tissue as well as upon subcutaneous injection. Immunization via these routes of administration has shown to induce potent cellular immune responses, opening perspectives for the delivery of clinically relevant antigens. However, a major concern remains the elaborate and cost-inefficient assembly procedure, inherent to a multilayer approach.

Without doubt, the different approaches reviewed in this chapter show potential as vaccine carriers. However, major efforts are still required to elucidate in detail the *in vivo* interaction between these materials and immune cells as well as their long-term effects. In addition, as the major advantage of the LbL assembly lays in its high versatility, this tremendous benefit should be further exploited. Furthermore, these carrier systems will have to compete with engineered liposomal[21] and matrix particles[20, 51] to truly realize their potential as vaccine carrier.

REFERENCES

1. Decher, G., Fuzzy nanoassemblies: Toward layered polymeric multicomposites. Science 1997, 277, 1232-1237.
2. Caruso, F.; Caruso, R. A.; Mohwald, H., Nanoengineering of inorganic and hybrid hollow spheres by colloidal templating. Science 1998, 282, 1111-1114.
3. Donath, E.; Sukhorukov, G. B.; Caruso, F.; Davis, S. A.; Mohwald, H., Novel hollow polymer shells by colloid-templated assembly of polyelectrolytes. Angew. Chem.-Int. Edit. 1998, 37, 2202-2205.
4. Shchukin, D. G.; Sukhorukov, G. B.; Mohwald, H., Smart inorganic/organic nanocomposite hollow microcapsules. Angew. Chem.-Int. Edit. 2003, 42, 4472-4475.
5. Moya, S.; Donath, E.; Sukhorukov, G. B.; Auch, M.; Baumler, H.; Lichtenfeld, H.; Mohwald, H., Lipid coating on polyelectrolyte surface modified colloidal particles and polyelectrolyte capsules. Macromolecules 2000, 33, 4538-4544.
6. Fischlechner, M.; Zschornig, O.; Hofmann, J.; Donath, E., Engineering virus functionalities on colloidal polyelectrolyte lipid composites. Angew. Chem.-Int. Edit. 2005, 44, 2892-2895.
7. Becker, A. L.; Johnston, A. P. R.; Caruso, F., Layer-By-Layer-Assembled Capsules and Films for Therapeutic Delivery. Small 2010, 6, 1836-1852.
8. De Geest, B. G.; Sanders, N. N.; Sukhorukov, G. B.; Demeester, J.; De Smedt, S. C., Release mechanisms for polyelectrolyte capsules. Chem. Soc. Rev. 2007, 36, 636-649.
9. De Koker, S.; De Cock, L. J.; Rivera-Gil, P.; Parak, W. J.; Velty, R. A.; Vervaet, C.; Remon, J. P.; Grooten, J.; De Geest, B. G., Polymeric multilayer capsules delivering biotherapeutics. Adv. Drug Deliv. Rev. 2011, 63, 748-761.
10. Johnston, A. P. R.; Zelikin, A. N.; Caruso, F., Assembling DNA into advanced materials: From nanostructured films to Biosensing and delivery systems. Adv. Mater. 2007, 19, 3727-3730.
11. Yan, Y.; Such, G. K.; Johnston, A. P. R.; Lomas, H.; Caruso, F., Toward Therapeutic Delivery with Layer-by-Layer Engineered Particles. ACS Nano 2011, 5, 4252-4257.
12. Torchilin, V. P., Recent advances with liposomes as pharmaceutical carriers. Nat. Rev. Drug Discov. 2005, 4, 145-160.
13. De Koker, S.; De Geest, B. G.; Cuvelier, C.; Ferdinande, L.; Deckers, W.; Hennink, W. E.; De Smedt, S.; Mertens, N., In vivo cellular uptake, degradation, and biocompatibility of polyelectrolyte microcapsules. Adv. Funct. Mater. 2007, 17, 3754-3763.
14. De Koker, S.; Naessens, T.; De Geest, B. G.; Bogaert, P.; Demeester, J.; De Smedt, S.; Grooten, J., Biodegradable Polyelectrolyte Microcapsules: Antigen Delivery Tools with Th17 Skewing Activity after Pulmonary Delivery. J. Immunol. 2010, 184, 203-211.
15. Poon, Z.; Chang, D.; Zhao, X. Y.; Hammond, P. T., Layer-by-Layer Nanoparticles with a pH-Sheddable Layer for in Vivo Targeting of Tumor Hypoxia. ACS Nano 2011, 5, 4284-4292.
16. Poon, Z.; Lee, J. B.; Morton, S. W.; Hammond, P. T., Controlling in Vivo Stability and Biodistribution in Electrostatically Assembled Nanoparticles for Systemic Delivery. Nano Lett. 2011, 11, 2096-2103.
17. Sexton, A.; Whitney, P. G.; Chong, S. F.; Zelikin, A. N.; Johnston, A. P. R.; De Rose, R.; Brooks, A. G.; Caruso, F.; Kent, S. J., A Protective Vaccine Delivery System for In Vivo T Cell Stimulation Using Nanoengineered Polymer Hydrogel Capsules. ACS Nano 2009, 3, 3391-3400.
18. Hubbell, J. A.; Thomas, S. N.; Swartz, M. A., Materials engineering for immunomodulation. Nature 2009, 462, 449-460.
19. De Koker, S.; Lambrecht, B. N.; Willart, M. A.; van Kooyk, Y.; Grooten, J.; Vervaet, C.; Remon, J. P.; De Geest, B. G., Designing polymeric particles for antigen delivery. Chem. Soc. Rev. 2011, 40, 320-339.

20. Kwon, Y. J.; James, E.; Shastri, N.; Frechet, J. M. J., In vivo targeting of dendritic cells for activation of cellular immunity using vaccine carriers based on pH-responsive microparticles. Proc. Natl. Acad. Sci. U. S. A. 2005, 102, 18264-18268.

21. Moon, J. J.; Suh, H.; Bershteyn, A.; Stephan, M. T.; Liu, H.; Huang, B.; Sohail, M.; Luo, S.; Um, S. H.; Khant, H.; Goodwin, J. T.; Ramos, J.; Chiu, W.; Irvine, D. J., Interbilayer-crosslinked multilamellar vesicles as synthetic vaccines for potent humoral and cellular immune responses. Nature Materials 2011, 10, 243-251.

22. De Cock, L. J.; De Koker, S.; De Geest, B. G.; Grooten, J.; Vervaet, C.; Remon, J. P.; Sukhorukov, G. B.; Antipina, M. N., Polymeric Multilayer Capsules in Drug Delivery. Angew. Chem.-Int. Edit. 2010, 49, 6954-6973.

23. Volodkin, D. V.; Larionova, N. I.; Sukhorukov, G. B., Protein encapsulation via porous CaCO3 microparticles templating. Biomacromolecules 2004, 5, 1962-1972.

24. Wang, Y. J.; Yu, A. M.; Caruso, F., Nanoporous polyelectrolyte spheres prepared by sequentially coating sacrificial mesoporous silica spheres. Angew. Chem.-Int. Edit. 2005, 44, 2888-2892.

25. De Koker, S.; De Geest, B. G.; Singh, S. K.; De Rycke, R.; Naessens, T.; Van Kooyk, Y.; Demeester, J.; De Smedt, S. C.; Grooten, J., Polyelectrolyte Microcapsules as Antigen Delivery Vehicles To Dendritic Cells: Uptake, Processing, and Cross-Presentation of Encapsulated Antigens. Angew. Chem.-Int. Edit. 2009, 48, 8485-8489.

26. Kreft, O.; Javier, A. M.; Sukhorukov, G. B.; Parak, W. J., Polymer microcapsules as mobile local pH-sensors. J. Mater. Chem. 2007, 17, 4471-4476.

27. Yoo, J. W.; Irvine, D. J.; Discher, D. E.; Mitragotri, S., Bio-inspired, bioengineered and biomimetic drug delivery carriers. Nat. Rev. Drug Discov. 2011, 10, 521-535.

28. Sukhorukov, G. B.; Antipov, A. A.; Voigt, A.; Donath, E.; Mohwald, H., pH-controlled macromolecule encapsulation in and release from polyelectrolyte multilayer nanocapsules. Macromol. Rapid Commun. 2001, 22, 44-46.

29. Petrov, A. I.; Antipov, A. A.; Sukhorukov, G. B., Base-acid equilibria in polyelectrolyte systems: From weak polvelectrolytes to interpolyelectrolyte complexes and multilayered polyelectrolyte shells. Macromolecules 2003, 36, 10079-10086.

30. Liang, K.; Such, G. K.; Zhu, Z. Y.; Yan, Y.; Lomas, H.; Caruso, F., Charge-Shifting Click Capsules with Dual-Responsive Cargo Release Mechanisms. Adv. Mater. 2011, 23, H273-+.

31. De Geest, B. G.; Vandenbroucke, R. E.; Guenther, A. M.; Sukhorukov, G. B.; Hennink, W. E.; Sanders, N. N.; Demeester, J.; De Smedt, S. C., Intracellularly degradable polyelectrolyte microcapsules. Adv. Mater. 2006, 18, 1005-+.

32. Ma, Y. J.; Dong, W. F.; Hempenius, M. A.; Mohwald, H.; Vancso, G. J., Redox-controlled molecular permeability of composite-wall microcapsules. Nature Materials 2006, 5, 724-729.

33. Haynie, D. T.; Palath, N.; Liu, Y.; Li, B. Y.; Pargaonkar, N., Biomimetic nanostructured materials: Inherent reversible stabilization of polypeptide microcapsules. Langmuir 2005, 21, 1136-1138.

34. Zelikin, A. N.; Quinn, J. F.; Caruso, F., Disulfide cross-linked polymer capsules: En route to biodeconstructible systems. Biomacromolecules 2006, 7, 27-30.

35. Zelikin, A. N.; Li, Q.; Caruso, F., Disulfide-stabilized poly(methacrylic acid) capsules: Formation, cross-linking, and degradation behavior. Chem. Mat. 2008, 20, 2655-2661.

36. Leung, M. K. M.; Such, G. K.; Johnston, A. P. R.; Biswas, D. P.; Zhu, Z. Y.; Yan, Y.; Lutz, J. F.; Caruso, F., Assembly and Degradation of Low-Fouling Click-Functionalized Poly(ethylene glycol)-Based Multilayer Films and Capsules. Small 2011, 7, 1075-1085.

37. Ochs, C. J.; Such, G. K.; Yan, Y.; van Koeverden, M. P.; Caruso, F., Biodegradable Click Capsules with Engineered Drug-Loaded Multilayers. ACS Nano 2010, 4, 1653-1663.

38. Yap, H. P.; Johnston, A. P. R.; Such, G. K.; Yan, Y.; Caruso, F., Click-Engineered, Bioresponsive, Drug-Loaded PEG Spheres. Adv. Mater. 2009, 21, 4348-+.

39. Kolb, H. C.; Finn, M. G.; Sharpless, K. B., Click chemistry: Diverse chemical function from a few good reactions. Angew. Chem.-Int. Edit. 2001, 40, 2004-+.

40.   Kamphuis, M. M. J.; Johnston, A. P. R.; Such, G. K.; Dam, H. H.; Evans, R. A.; Scott, A. M.; Nice, E. C.; Heath, J. K.; Caruso, F., Targeting of Cancer Cells Using Click-Functionalized Polymer Capsules. J. Am. Chem. Soc. 2010, 132, 15881-15883.

41.   Yan, Y.; Johnston, A. P. R.; Dodds, S. J.; Kamphuis, M. M. J.; Ferguson, C.; Parton, R. G.; Nice, E. C.; Heath, J. K.; Caruso, F., Uptake and Intracellular Fate of Disulfide-Bonded Polymer Hydrogel Capsules for Doxorubicin Delivery to Colorectal Cancer Cells. ACS Nano 2010, 4, 2928-2936.

42.   Yan, Y.; Wang, Y. J.; Heath, J. K.; Nice, E. C.; Caruso, F., Cellular Association and Cargo Release of Redox-Responsive Polymer Capsules Mediated by Exofacial Thiols. Adv. Mater. 2011, 23, 3916-+.

43.   Rivera-Gil, P.; De Koker, S.; De Geest, B. G.; Parak, W. J., Intracellular Processing of Proteins Mediated by Biodegradable Polyelectrolyte Capsules. Nano Lett. 2009, 9, 4398-4402.

44.   Bedard, M. F.; Munoz-Javier, A.; Mueller, R.; del Pino, P.; Fery, A.; Parak, W. J.; Skirtach, A. G.; Sukhorukov, G. B., On the mechanical stability of polymeric microcontainers functionalized with nanoparticles. Soft Matter 2009, 5, 148-155.

45.   Mamedov, A. A.; Kotov, N. A.; Prato, M.; Guldi, D. M.; Wicksted, J. P.; Hirsch, A., Molecular design of strong single-wall carbon nanotube/polyelectrolyte multilayer composites. Nature Materials 2002, 1, 190-194.

46.   Szarpak, A.; Cui, D.; Dubreuil, F.; De Geest, B. G.; De Cock, L. J.; Picart, C.; Auzely-Velty, R., Designing Hyaluronic Acid-Based Layer-by-Layer Capsules as a Carrier for Intracellular Drug Delivery. Biomacromolecules 2010, 11, 713-720.

47.   De Cock, L. J.; Lenoir, J.; De Koker, S.; Vermeersch, V.; Skirtach, A. G.; Dubruel, P.; Adriaens, E.; Vervaet, C.; Remon, J. P.; De Geest, B. G., Mucosal irritation potential of polyelectrolyte multilayer capsules. Biomaterials 2011, 32, 1967-1977.

48.   Adriaens, E.; Remon, J. P., Gastropods as an evaluation tool for screening the irritating potency of absorption enhancers and drugs. Pharm. Res. 1999, 16, 1240-1244.

49.   De Rose, R.; Zelikin, A. N.; Johnston, A. P. R.; Sexton, A.; Chong, S. F.; Cortez, C.; Mulholland, W.; Caruso, F.; Kent, S. J., Binding, Internalization, and Antigen Presentation of Vaccine-Loaded Nanoengineered Capsules in Blood. Adv. Mater. 2008, 20, 4698-+.

50.   De Geest, B. G.; Willart, M. A.; Hammad, H.; Lambrecht, B. N.; Pollard, C.; Bogaert, P.; De Filette, M.; Saelens, X.; Vervaet, C.; Remon, J. P.; Grooten, J.; De Koker, S., Polymeric Multilayer Capsule-Mediated Vaccination Induces Protective Immunity Against Cancer and Viral Infection. ACS Nano 2012, 6, 2136-2149.

51.   Kasturi, S. P.; Skountzou, I.; Albrecht, R. A.; Koutsonanos, D.; Hua, T.; Nakaya, H. I.; Ravindran, R.; Stewart, S.; Alam, M.; Kwissa, M.; Villinger, F.; Murthy, N.; Steel, J.; Jacob, J.; Hogan, R. J.; Garcia-Sastre, A.; Compans, R.; Pulendran, B., Programming the magnitude and persistence of antibody responses with innate immunity. Nature 2011, 470, 543-U136.

CHAPTER 3

JUST SPRAY IT- LBL ASSEMBLY ENTERS A NEW AGE

CHAPTER 3

JUST SPRAY IT – LBL ASSEMBLY

ENTERS A NEW AGE

1. DRAWBACKS OF LBL ASSEMBLY

As described in the previous chapter, PMLC have first been introduced in the late nineties by the pioneering work of Gero Decher and Rubner.[1, 2] Taking into account the exponential profile of the citation curve of this review in 1997 in Science[3], it is evident that during the past two decades this technique has gathered major attention by scientists in the academic field. Inherent to its conceptual simplicity, the LbL approach offers the possibility to construct ultrathin films by simple immersion into an aqueous solution.

Whereas in the first decade of LbL research work was mostly focused on planar substrates and electrostatic interaction as the driving force for multilayer build-up, in the late nineties, non planar substrates were introduced to produce hollow capsules after LbL coating and subsequent dissolution of spherical microparticles.[4] All these developments have found applications in diverse fields such as anti-fog and anti-reflection coatings, drug delivery, tissue engineering scaffolds etc.[5-9]

However, most of these applications remained within an academic environment and were not embraced by industry. This can be attributed to 2 reasons: (1) the limited stability of these films and (2) the multistep assembly procedure. Especially this multistep procedure is a serious constraint toward industrial applications as it is time consuming, i.e. deposition of a film consisting of dozens of bilayers takes more than 10 h using a robotic dipping-apparatus (**Figure 1A**). Moreover, dipping and rinsing of the substrates from one recipient to another involves the risk of cross-contamination of the polyelectrolytes. Furthermore, dipping can only be carried out on substrates with limited dimensions and cannot be integrated in a continuous manufacturing line to coat large surfaces.

2. AUTOMATIZATION AND SIMPLIFICATION OF LBL ASSEMBLY

To cope with these issues, a lot of effort has been put into simplifying the assembly procedure while attempting to retain the conceptual versatility of the LbL approach as far as possible. Automatization

strategies using filtration based set-ups or microfluidic chips have been proposed to speed-up LbL assembly and to limit human intervention during each deposition step.[10, 11]

Schlenoff and co-workers were the first to report on spraying (**Figure 1B**) instead of dipping as an attractive alternative to construct multilayer films.[12] Over the last decade this approach has witnessed a strong growth and can be considered as an important step towards a broad applicability of LbL coating technology.[13]
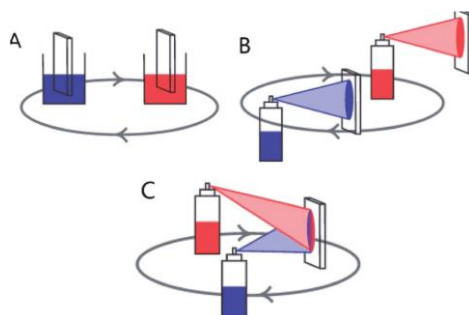

Figure 1. Schematic representation of 'dipping' and 'spraying' procedures applied for deposition of multilayer films. For simplicity we did not depict the rinsing steps. Panel **(A)** represent alternate dipping of a substrate into solutions of interacting species. Panel **(B)** and **(C)** represents alternate **(B)**, respectively simultaneous **(C)** spraying of a substrate with solutions of interacting species.[12]

Five years later, in 2005, the groups of Decher, Voegel and Schaaf (further referred to as the 'Strasbourg groups') confirmed the observations by Schlenoff and went deeper into this topic and elucidated some fundamental differences between dipping and spraying using PSS and PAH as polyelectrolytes.[14] Film deposition by spraying appeared to be regular even in the absence of rinsing steps, although films constructed with rinsing after each layer deposition are thicker. This was suggested to be due to film rearrangement (and not merely removal of unadsorbed or weakly bound polyelectrolyte) taking place during rinsing that allows a better anchoring of the subsequent layer. Furthermore, although film deposition by spraying does not allow the newly adsorbed layer to reach equilibrium, the quality of the films, as measured by atomic force microscopy (AFM), was found to be excellent. Importantly, this is not the case when films are produced by dipping using short (in the order of seconds) dipping times. This was attributed to the fast and thorough mixing of the newly incoming polyelectrolyte solution with the underlying film by spraying while this process is much slower when dipping. As a consequence, film build-up by spraying does not reach saturation coverage rendering film thickness dependent on polyelectrolyte concentration and spraying time.

In a subsequent study the same group investigated the possibility to produce films by continuous and simultaneous spraying (**Figure 1C**) of polyelectrolytes of opposite charges (i.e. PAH and poly(glutamic acid)).[15] The authors found that spraying of polyelectrolytes at a 1:1 ratio of the spraying rate allowed to produce films with a film thickness that grows linearly over time as measured by ellipsometry. AFM showed that a sufficient spraying time (±50 s) was required to obtain smooth and uniform films. In a series of follow-up papers by the same group of authors the scope of the approach was further broadened by demonstrating the ability to incorporate intact liposomes[16] within the films as well as by constructing films solely based on inorganic species.[17, 18]
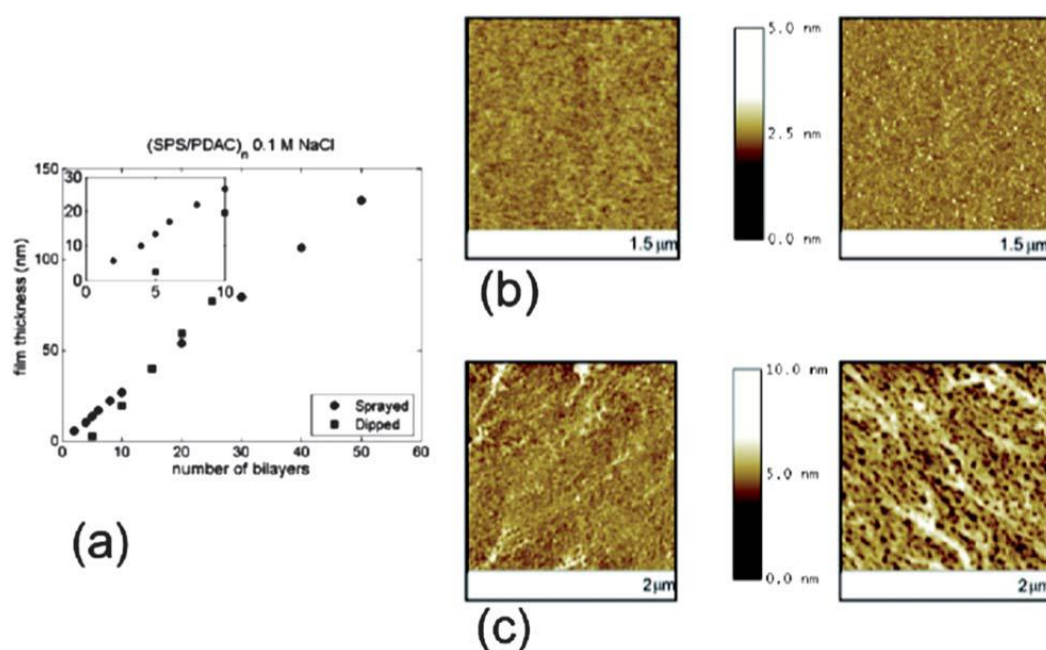
Figure 2. (A) Correlation of total film thickness with layer pair number for the (SPS/PDAC)n system both by spray deposition and dipping. Thickness was evaluated using ellipsometry and checked using profilometry. Reported values are averages taken from several data points on a silicon wafer and vary by less than ±2 nm. Both dipped and sprayed films exhibit linear growth rates above 5 layer pairs, but the sprayed films have no initial nonlinear growth regime. **(B)** AFM height images of a sprayed (SPS/PDAC)n (i) 0.5 layer pair, PDAC surface and (ii) 1.0 layer pair, SPS surface. Coverage is thin but uniform. **(C)** AFM height images of a dipped (SPS/PDAC)n (i) 0.5 layer pair and (ii) 1.0 layer pair. Initially, 'islands' form on the silicon substrate. (Reproduced from reference[19])

The Hammond group further elaborated on automatization of the spraying LbL approach by developing a computer controlled spraying apparatus with 3 s polyelectrolyte spraying times followed by dripping and rinsing steps.[19] This set-up allowed to elucidate why LbL build-up of strong polyelectrolytes by spraying follows a linear growth regime whereas dipped multilayers exhibit an initial exponential growth at low bilayers numbers followed by a linear growth (**Figure 2A**). As shown in the AFM images in **Figures 2B and C,** dipping leads, due to diffusion of the chains and

complexation, to regions of higher charge density. 'Globular islands' are formed on the substrate surface which gradually fill the surface. Once a smooth film is obtained the total film thickness grows linearly upon deposition of additional polyelectrolyte bilayers. In contrast, spraying creates an ultrafine mist of droplets which cover the entire surface homogeneously and simultaneously. Furthermore, the liquid is quickly removed by dripping which kinetically traps the polyelectrolyte chains in their confirmation when they reached the surface, immediately leading to a uniform growth regime.

The same authors also broadened the applicability of the spray LbL approach to the use of inorganic nanoparticles and weakly bound polyelectrolyte pairs such as poly(acrylic acid) and PAMAM dendrimers.[20-22] Such films could find applications for surface mediated release of one or multiple drug molecules in a controlled fashion. Titanium dioxide nanoparticle containing films proved to be capable of photocatalytic processing of toxic volatile organic components upon UV-irradiation. Besides planar substrates, the spraying approach also proved viable to coat 3D substrates such as electrospun scaffolds, which allows introduction of anisotropy into the films, a feature unmet by the traditional dipping-based assembly approach.[23] Additionally, also films based on hydrogen bonding as driving force could be assembled by sequential spraying.[20]

3. SPRAY DRYING

The above described approach of LbL spraying is performed by spraying an excess of polymer solution which is removed via dripping. Due to this constraint, applying spray drying could be used as a technique to produce spherical particles thereby mimicking the hollow LbL capsules. The following paragraph will elucidate further the general principles of spray drying.

3.1. The spray drying process

Spray drying is defined as the conversion of a liquid feed formulation (solution, suspension, emulsion) into a dry powder in a single step process. Four different stages can be distinguished as depicted in **Figure 3**. In a first step, the feed is atomized into a spray of droplets. Next the droplets come in contact with the heated drying medium (usually air or nitrogen), resulting in evaporation of the solvent and the formation of particles. Finally, the dried product is separated from the drying medium (**Figure 3**). These stages, together with the physical and chemical properties of the feed influence the powder characteristics such as particle size, morphology, fine or coarse particle powders and moisture content.[24]
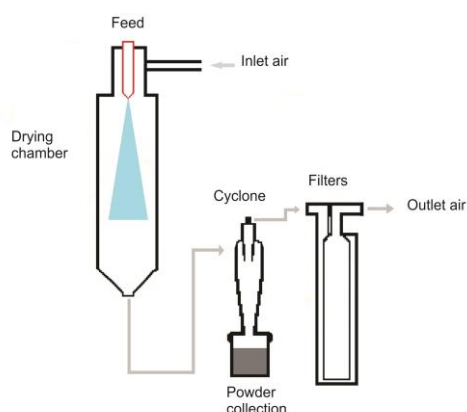
Figure 3. A schematic overview of a spray dryer.

The formation of the spray or atomization is the key parameter since this must create conditions for optimum evaporation when in contact with drying medium. This in turn leads to a dry wall operation, and discharging a dried product of required properties from the drying chamber and associated dry particulate collectors. The different atomizers can be classified according to the source of energy used in the droplet formation: centrifugal energy in rotary atomizers, pressure energy in pressure nozzles, kinetic energy in pneumatic nozzles and acoustic/pulsation energy in sonic nozzles. The selection on the atomizer type depends mainly on the desired droplet size (**Table 1**).

Table 1: Mean droplet size of different atomizer devices.

Type of atomizer	Mean droplet size (μm)
Rotary atomizer	20-200
Pressure nozzle	50-400
Pneumatic nozzle	5-75
Sonic nozzle	10-50

A second stage is the spray-air contact, mixing and droplet/particle flow. The spray-air contact is determined by the position of the atomizer in relation to the drying medium inlet. In a co-current flow mode (**Figure 4A**), the atomized product and heated drying medium pass through the drying chamber in the same direction. This is preferable for heat-sensitive materials since spray evaporation is rapid, the drying medium cools accordingly and the dried product comes then in contact with much cooler drying medium. Alternatively, a counter-current flow mode (**Figure 4B**) means that the sprayed product and the heated drying medium enters at opposite ends of the drying chamber. This formation offers dryer performance with excellent heat utilization for non-heat sensitive products. Spray dryer designs that combine both co-current and counter-current flow are classified as mixed-

flow spray dryers (**Figure 4C**). In this fountain-type system partially dried particles enter the hottest regions in the drying chamber (near the entrance of the drying medium) and thus the powder is subjected to higher particle temperatures.
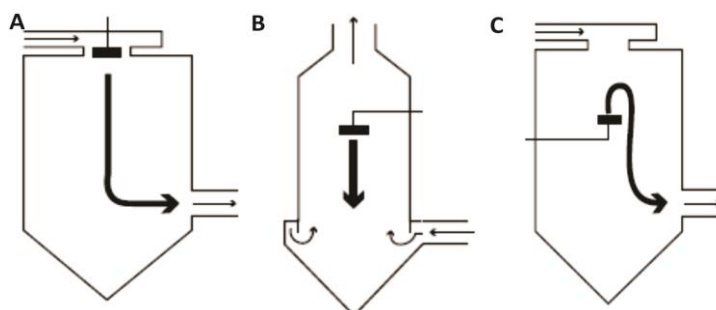

Figure 4. Schematic overview of the different spray-air contact flow modes: (A) co-current, (B) counter-current and (C) mixed flow. (adapted from[25])

The next stage combines drying and particle formation. The moisture migrates from within the droplet to the droplet/air surface by diffusional or capillary mechanisms and evaporates as long as saturated surface conditions are maintained. When the critical point is reached – saturated surface conditions can no longer be maintained because of the fact that the moisture content is too low- a dry layer starts to form at the droplet surface, hence developing the particle.

Finally, separation between the particles and the drying medium and dried product discharge takes place in the base of the drying chamber and in the particulate collection system. Dry collection equipment consists of cyclone, scrubbers, bag filters or electrostatic precipitators.

The previous described flow modes of the drying chambers (co-current, counter-current and mixed-flow) can be implemented into different spray drying systems: open cycle, closed cycle and semi-closed cycle systems. The open cycle layouts are applied to aqueous feeds and the most widely used in the industry. Hereby is the drying gas, air, being drawn from the atmosphere and the emitted air is first cleaned by a combination of cyclones, scrubbers, bag filters and electrostatic precipitators and then discharged into the atmosphere. Closed cycle systems are based on recycling and reusing the drying medium, which usually is an inert gas, such as nitrogen. This system enables the spray drying of organic/flammable solvents, oxygen sensitive products and toxic products and completely recovers the evaporated solvent. Semi-closed cycle systems are, as the name indicates, a combination of the open and closed cycle system. From a pharmaceutical point of view it's interesting to point out that aseptic systems are available to produce sterile powders.[24]

3.2. Applications in pharmaceutical industry

Spray drying has been widely used in pharmaceutical industry. It has been applied to improve the compression properties from excipients such as lactose or drugs like acetozalamide.[26, 27] Also it has been used for encapsulation in order to obtain controlled drug release formulations (i.e. risedronate, corticosteroids, buspirone, pain killers[28-33]) or taste masking (i.e. acetaminophen, sumatriptan, antibiotics[34-36]). Spray drying is furthermore a method to enhance the solubility and dissolution rate of poorly soluble drugs (i.e. spironolactone[37], fenofibrate[38]). Additionally, dry powders for inhalation in the treatment of lung diseases (i.e. theophylline, antibiotics, NSAIDs or corticosteroids [39-41]) as well as dry powder vaccines[42-44] can also be produced by spray drying.

Nonetheless, spray drying heat sensitive biopharmaceutics such as vaccine antigens is, as mentioned before, preferable carried out in a co-current flow modes and requires the addition of stabilizing excipients to preserve their integrity during the process and storage afterwards. These stabilizing components can be sugar compounds like trehalose, sucrose or mannitol. Furthermore biodegradable polymers or proteins can also be used.[45, 46]

REFERENCES

1.   Decher, G.; Hong, J. D.; Schmitt, J. Buildup of ultrathin multilayer films by a self-assembly process. 3. consecutive alternating adsorption of anionic and cationic polyelectrolytes on charged surfaces. Thin Solid Films 1992, 210, 831-835.
2.   Ferreira, M.; Cheung, J. H.; Rubner, M. F. Molecular self-assembly of conjugated polyions- a new process for fabricating multilayer thin-film heterostructures. Thin Solid Films 1994, 244, 806-809.
3.   Decher, G. Fuzzy nanoassemblies: Toward layered polymeric multicomposites. Science 1997, 277, 1232-1237.
4.   Quinn, J. F.; Johnston, A. P. R.; Such, G. K.; Zelikin, A. N.; Caruso, F. Next generation, sequentially assembled ultrathin films: beyond electrostatics. Chem. Soc. Rev. 2007, 36, 707-718.
5.   Such, G. K.; Johnston, A. P. R.; Caruso, F. Engineered hydrogen-bonded polymer multilayers: from assembly to biomedical applications. Chem. Soc. Rev. 2011, 40, 19-29.
6.   Lavalle, P.; Voegel, J. C.; Vautier, D.; Senger, B.; Schaaf, P.; Ball, V. Dynamic Aspects of Films Prepared by a Sequential Deposition of Species: Perspectives for Smart and Responsive Materials. Adv. Mater. 2011, 23, 1191-1221.
7.   Wang, Y.; Angelatos, A. S.; Caruso, F. Template synthesis of nanostructured materials via layer-by-layer assembly. Chem. Mat. 2008, 20, 848-858.
8.   Hiller, J.; Mendelsohn, J. D.; Rubner, M. F. Reversibly erasable nanoporous anti-reflection coatings from polyelectrolyte multilayers. Nature Materials 2002, 1, 59-63.
9.   Nuraje, N.; Asmatulu, R.; Cohen, R. E.; Rubner, M. F. Durable Antifog Films from Layer-by-Layer Molecularly Blended Hydrophilic Polysaccharides. Langmuir 2011, 27, 782-791.
10. Voigt, A.; Lichtenfeld, H.; Sukhorukov, G. B.; Zastrow, H.; Donath, E.; Baumler, H.; Mohwald, H. Membrane filtration for microencapsulation and microcapsules fabrication by layer-by-layer polyelectrolyte adsorption. Ind. Eng. Chem. Res. 1999, 38, 4037-4043.
11. Priest, C.; Quinn, A.; Postma, A.; Zelikin, A. N.; Ralston, J.; Caruso, F. Microfluidic polymer multilayer adsorption on liquid crystal droplets for microcapsule synthesis. Lab Chip 2008, 8, 2182-2187.
12. Schlenoff, J. B.; Dubas, S. T.; Farhat, T. Sprayed polyelectrolyte multilayers. Langmuir 2000, 16, 9968-9969.
13. Schaaf, P.; Voegel, J. C.; Jierry, L.; Boulmedais, F. Spray-Assisted Polyelectrolyte Multilayer Buildup: from Step-by-Step to Single-Step Polyelectrolyte Film Constructions. Adv. Mater. 2012, 24, 1001-1016.
14. Izquierdo, A.; Ono, S. S.; Voegel, J. C.; Schaaf, P.; Decher, G. Dipping versus spraying: Exploring the deposition conditions for speeding up layer-by-layer assembly. Langmuir 2005, 21, 7558-7567.
15. Porcel, C. H.; Izquierdo, A.; Ball, V.; Decher, G.; Voegel, J. C.; Schaaf, P. Ultrathin coatings and (poly(glutamic acid)/polyallylamine) films deposited by continuous and simultaneous spraying. Langmuir 2005, 21, 800-802.
16. Michel, A.; Izquierdo, A.; Decher, G.; Voegel, J. C.; Schaaf, P.; Ball, V. Layer by layer self-assembled polyelectrolyte multilayers with embedded phospholipid vesicles obtained by spraying: Integrity of the vesicles. Langmuir 2005, 21, 7854-7859.
17. Popa, G.; Boulmedais, F.; Zhao, P.; Hemmerle, J.; Vidal, L.; Mathieu, E.; Felix, O.; Schaaf, P.; Decher, G.; Voegel, J. C. Nanoscale Precipitation Coating: The Deposition of Inorganic Films through Step-by-Step Spray-Assembly. ACS Nano 2010, 4, 4792-4798.
18. Lefort, M.; Popa, G.; Seyrek, E.; Szamocki, R.; Felix, O.; Hemmerle, J.; Vidal, L.; Voegel, J. C.; Boulmedais, F.; Decher, G.; Schaaf, P. Spray-On Organic/Inorganic Films: A General Method for the Formation of Functional Nano- to Microscale Coatings. Angew. Chem.-Int. Edit. 2010, 49, 10110-10113.

19. Krogman, K. C.; Zacharia, N. S.; Schroeder, S.; Hammond, P. T. Automated process for improved uniformity and versatility of layer-by-layer deposition. Langmuir 2007, 23, 3137-3141.

20. Kim, B.-S.; Park, S. W.; Hammond, P. T. Hydrogen-bonding layer-by-layer assembled biodegradable polymeric micelles as drug delivery vehicles from surfaces. ACS Nano 2008, 2, 386-392.

21. Kim, B. S.; Smith, R. C.; Poon, Z.; Hammond, P. T. MAD (Multiagent Delivery) Nanolayer: Delivering Multiple Therapeutics from Hierarchically Assembled Surface Coatings. Langmuir 2009, 25, 14086-14092.

22. Krogman, K. C.; Zacharia, N. S.; Grillo, D. M.; Hammond, P. T. Photocatalytic layer-by-layer coatings for degradation of acutely toxic agents. Chem. Mat. 2008, 20, 1924-1930.

23. Krogman, K. C.; Lowery, J. L.; Zacharia, N. S.; Rutledge, G. C.; Hammond, P. T. Spraying asymmetry into functional membranes layer-by-layer. Nature Materials 2009, 8, 512-518.

24. Masters, K. Spray drying in practice. SprayDryConsult Internationl ApS: Charlottenlund, Denmark, 2002.

25. Buchi. http://www.buchi.com/en (accessed 25 April 2014).

26. Broadhead, J.; Rouan, S. K. E.; Rhodes, C. T. The spray drying of pharmaceuticals. Drug Development and Industrial Pharmacy 1992, 18, 1169-1206.

27. Di Martino, P.; Scoppa, M.; Joiris, E.; Palmieri, G. F.; Andres, C.; Pourcelot, Y.; Martelli, S. The spray drying of acetazolamide as method to modify crystal properties and to improve compression behaviour. International Journal of Pharmaceutics 2001, 213, 209-221.

28. Velasquez, A. A.; Mattiazzi, J.; Ferreira, L. M.; Pohlmann, L.; Silva, C. B.; Rolim, C. M. B.; Cruz, L. Risedronate-loaded Eudragit S100 microparticles formulated into tablets. Pharmaceutical Development and Technology 2014, 19, 263-268.

29. Tobar-Grande, B.; Godoy, R.; Bustos, P.; von Plessing, C.; Fattal, E.; Tsapis, N.; Olave, C.; Gomez-Gaete, C. Development of biodegradable methylprednisolone microparticles for treatment of articular pathology using a spray-drying technique. International Journal of Nanomedicine 2013, 8, 2065-2076.

30. Chaw, C. S.; Yang, Y. Y.; Lim, I. J.; Phan, T. T. Water-soluble betamethasone-loaded poly(lactide-co-glycolide) hollow microparticles as a sustained release dosage form. Journal of Microencapsulation 2003, 20, 349-359.

31. Al-Zoubi, N.; AlKhatib, H. S.; Bustanji, Y.; Aiedeh, K.; Malamataris, S. Sustained-release of buspirone HCl by co spray-drying with aqueous polymeric dispersions. European Journal of Pharmaceutics and Biopharmaceutics 2008, 69, 735-742.

32. Palmieri, G. F.; Bonacucina, G.; Di Martino, P.; Martelli, S. Spray-drying as a method for microparticulate controlled release systems preparation: Advantages and limits. I. Water-soluble drugs. Drug Development and Industrial Pharmacy 2001, 27, 195-204.

33. Palmieri, G. F.; Bonacucina, G.; Di Martino, P.; Martelli, S. Gastro-resistant microspheres containing ketoprofen. Journal of Microencapsulation 2002, 19, 111-119.

34. Thanh Huong Hoang, T.; Lemdani, M.; Flament, M.-P. Optimizing the taste-masked formulation of acetaminophen using sodium caseinate and lecithin by experimental design. International Journal of Pharmaceutics 2013, 453, 408-415.

35. Sheshala, R.; Khan, N.; Darwis, Y. Formulation and Optimization of Orally Disintegrating Tablets of Sumatriptan Succinate. Chemical & Pharmaceutical Bulletin 2011, 59, 920-928.

36. Zgoulli, S.; Grek, V.; Barre, G.; Goffinet, G.; Thonart, P.; Zinner, S. Microencapsulation of erythromycin and clarithromycin using a spray-drying technique. Journal of Microencapsulation 1999, 16, 565-571.

37. Yassin, A. E. B.; Alanazi, F. K.; El-Badry, M.; Alsarra, I. A.; Barakat, N. S.; Alanazi, F. K. Preparation and Characterization of Spironolactone-Loaded Gelucire Microparticles Using Spray-Drying Technique. Drug Development and Industrial Pharmacy 2009, 35, 297-304.

38. Kim, G. G.; Poudel, B. K.; Marasini, N.; Lee, D. W.; Tran Tuan, H.; Yang, K. Y.; Kim, J. O.; Yong, C. S.; Choi, H.-G. Enhancement of oral bioavailability of fenofibrate by solid self-

microemulsifying drug delivery systems. Drug Development and Industrial Pharmacy 2013, 39, 1431-1438.

39.   Pilcer, G.; De Bueger, V.; Traina, K.; Traore, H.; Sebti, T.; Vanderbist, F.; Amighi, K. Carrier-free combination for dry powder inhalation of antibiotics in the treatment of lung infections in cystic fibrosis. International Journal of Pharmaceutics 2013, 451, 112-120.

40.   Stigliani, M.; Aquino, R. P.; Del Gaudio, P.; Mencherini, T.; Sansone, F.; Russo, P. Non-steroidal anti-inflammatory drug for pulmonary administration: Design and investigation of ketoprofen lysinate fine dry powders. International Journal of Pharmaceutics 2013, 448, 198-204.

41.   Boraey, M. A.; Hoe, S.; Sharif, H.; Miller, D. P.; Lechuga-Ballesteros, D.; Vehring, R. Improvement of the dispersibility of spray-dried budesonide powders using leucine in an ethanol-water cosolvent system. Powder Technology 2013, 236, 171-178.

42.   Shastri, P. N.; Kim, M.-C.; Quan, F.-S.; D'Souza, M. J.; Kang, S.-M. Immunogenicity and protection of oral influenza vaccines formulated into microparticles. Journal of Pharmaceutical Sciences 2012, 101, 3623-3635.

43.   Ohtake, S.; Martin, R. A.; Yee, L.; Chen, D.; Kristensen, D. D.; Lechuga-Ballesteros, D.; Truong-Le, V. Heat-stable measles vaccine produced by spray drying. Vaccine 2010, 28, 1275-1284.

44.   Amorij, J. P.; Huckriede, A.; Wischut, J.; Frijlink, H. W.; Hinrichs, W. L. J. Development of stable influenza vaccine powder formulations: Challenges and possibilities. Pharm. Res. 2008, 25, 1256-1273.

45.   McAdams, D.; Chen, D.; Kristensen, D. Spray drying and vaccine stabilization. Expert Review of Vaccines 2012, 11, 1211-1219.

46.   Schuele, S.; Schulz-Fademrecht, T.; Garidel, P.; Bechtold-Peters, K.; Friess, W. Stabilization of IgG1 in spray-dried powders for inhalation. European Journal of Pharmaceutics and Biopharmaceutics 2008, 69, 793-807.

PART III

RESULTS

CHAPTER 4

FACILE TWO STEP SYNTHESIS OF POROUS ANTIGEN LOADED DEGRADABLE POLYELECTROLYTE MICROSPHERES

CHAPTER 4

FACILE TWO STEP SYNTHESIS

OF POROUS ANTIGEN LOADED

DEGRADABLE

POLYELECTROLYTE

MICROSPHERES

1. INTRODUCTION

Without doubt, the development of vaccines constitutes one of the major breakthroughs of human medicine, allowing us to prevent numerous infectious diseases.[1] Nevertheless, for major killers such as HIV, malaria and tuberculosis no effective vaccines are available today. The failure of current vaccination strategies to elicit cellular immune responses, especially CD8 cytotoxic T cells (CTLs) that can recognize and eliminate infected cells, is considered to be one of the major reasons for this failure.[2-4] Consequently, there is an urgent need to develop new vaccine formulations that can induce such CTL responses. One of the most promising approaches to achieve this goal is encapsulation of antigens in particulate carriers with dimensions between 0.1-10 µm.[5]

A plethora of studies has now demonstrated that such carriers can strongly enhance antigen presentation by dendritic cells (DCs), the most potent antigen presenting cells capable of priming effector T cell responses, not only quantitatively but also qualitatively. Antigen being presented by a DC as a MHC/peptide complex to the T cell receptor indeed constitutes the first step in the initiation of T cell responses. Two different pathways occur for antigen presentation by MHCI and MHCII to CD8 and CD4 T cells, respectively. MHCI presentation is responsible for the processing and presentation of cytosolic proteins, which are cleaved by the proteasome, transported to the endoplasmatic reticulum, and subsequently loaded onto MHCI molecules. By contrast, MHCII presentation occurs for endocytosed proteins, which are degraded in endolysosomal compartments,

loaded onto MHCII molecules and subsequently presented at the cell surface. The way in which antigen is internalized by a DC however strongly affects how the antigen is processed and presented by a DC, and consequently also the type and strength of immune response induced. Although soluble antigens are almost exclusively presented by MHCII to CD4 T cells, particulate antigens not only are far more efficiently taken up by DCs, but are also presented by MHCI to CD8 T cells,[6] thus enabling the induction of CTL responses. Although particulate carriers have the capacity to evoke potent cellular immunity, their clinical application has been impeded largely by practical problems involving their generation including a low antigen encapsulation efficiency, the use of chemical solvents and physical stresses that negatively affect antigen stability and the involvement of complex and labor-intensive multistep processes to generate them.

Polymeric multilayer capsules[7-13] have emerged as promising microscopic carriers for the delivery of antigens to DCs, overcoming some of the problems described above.[14-17] These capsules are based on alternate deposition of polymers (so-called layer-by-layer technology),[18, 19] either through electrostatic interaction[20-22] or hydrogen bonding,[23] onto a sacrificial template followed by the decomposition of the template resulting in hollow capsules and allowing efficient antigen encapsulation under non-denaturing conditions. Several papers have now demonstrated the potential of these capsules to target antigens to APCs both *in vitro* and *in vivo*, resulting in strongly enhanced antigen presentation to CD4 and CD8 T cells and the induction of broad and strong immune responses.[14-17, 24-26] The major advantage for their success is presumably threefold: 1) They protect the antigen from degradation before reaching DCs; 2) Because of their size (1-10 μm) they are preferably targeted to DCs; and 3) Because of their soft thin shell, which is prone to the reductive conditions or endosomal proteases depending on the nature of the capsule shell, they allow the antigen to be readily processed upon internalization by DCs.[14, 27] Moreover, these capsules have been shown to be biocompatible and degradable, both *in vitro* and *in vivo*.

Notwithstanding their excellent performance, polymeric multilayer capsules are fabricated in a multiple steps, which is a rather cost-inefficient fashion involving the use of a large excess of polymer and several centrifugation steps during deposition of each single layer. Therefore, a simple and versatile strategy involving a minimum of process steps that mimics polymeric multilayer capsules would be of uttermost importance to allow this type of antigen carriers to reach the clinical stage.
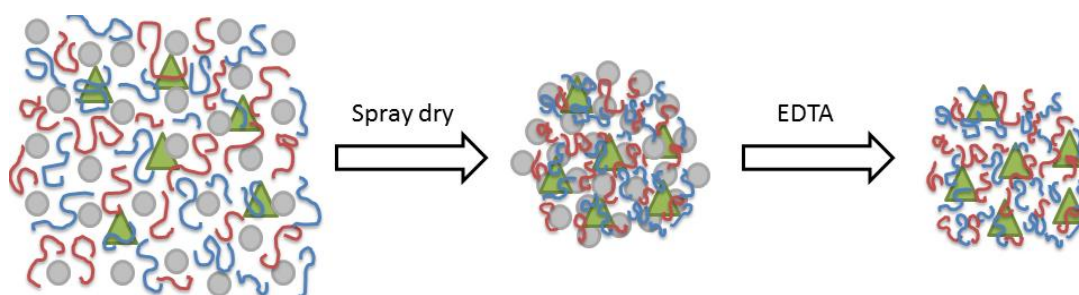
Figure 1. Schematic illustration of the encapsulation of antigen (green triangles) into porous polyelectrolyte (red and blue curves) microspheres by spray drying a mixture of antigen, polyelectrolytes and calcium carbonate nanoparticles ($CaCO_3^{NP}$; gray disc) followed by extraction of the $CaCO_3^{NP}$ by treatment with EDTA.

2. MATERIALS AND METHODS

2.1. Materials

Calcium carbonate nanoparticles ($CaCO_3^{NP}$) were obtained from Plasmachem. Dextran sulfate (DS; 10 kDa), poly-L-arginine(P_LARG, 100 kDa), ovalbumin (OVA; grade VII) and Hoechst 33258 were obtained from Sigma-Aldrich. OVA-Alexa Fluor488, Cy5 conjugated cholera toxin B, LysoTracker Red and CellTracker Red were obtained from Invitrogen. All water used in the experiments was of Milli-Q grade.

2.2. Synthesis of (porous) microspheres

$CaCO_3^{NP}$, DS, OVA and P_LARG were mixed in water in a 40/4/1/5 ratio at a total solid concentration of 1 %. In detail, 200 mg $CaCO_3^{NP}$, 20 mg DS and 5 mg OVA were dissolved in 20 ml water. Subsequently, 25mg P_LARG was dissolved in 5 ml water and added dropwise to the stirring $CaCO_3^{NP}$/DS/OVA dispersion. Spray drying of this mixture was performed in a lab-scale Büchi B290 spray dryer. The mixture was fed to a two-fluid nozzle (diameter 0.7 mm) at the top of the spray dryer. In addition, the spray dryer operated in co-current air flow at 35 m³/h with an inlet drying air temperature of 130 °C and an outlet drying air temperature of 65°C. Owing to evaporation of the liquid, the temperature in the droplet itself is significantly lower than that in the air stream.[28]

2.3. Particle characterization

Laser diffraction was performed on a Malvern Mastersizer equipped with an RF300 objective. ζ-potential measurements were performed on a Malvern Nanosize ZS. Confocal microscopy images were recorded on a Leica SP5 AOBS confocal microscope. Scanning electron microscopy images and EDX-spectra were recorded on a quanta FEG FEI 200 apparatus. Samples were dried on a silicon

wafer and sputtered with an ultrathin layer of palladium/gold. Transmission electron microscopy images of ultrathin microtomed sections were recorded on a JEOL 1010 electron microscope.

2.4. DC uptake assessment.

Female C57BL/6 mice were purchased from Janvier and housed in a specified pathogen-free facility in micro-isolator units. Dendritic cells were generated using a modified Inaba protocol. Two to six months C57BL/6 mice were sacrificed and bone marrow was flushed from their femurs and tibias. After lysis of red blood cells with ACK lysis buffer (BioWhittaker), granulocytes and B cells were depleted using Gr-1 (Pharmingen) and B220 (Pharmingen) antibodies respectively, and low-toxicity rabbit complement (Cedarlane Laboratories Ltd.). Cells were seeded at a density of 2×10^5 cells/ml in 175 cm^2 Falcon tubes (Becton Dickinson) in DC medium (RPMI 1640 medium containing 5% LPS-free FCS, 1% penicillin/streptomycin, 1% L-glutamine and 50 µM β-mercaptoethanol) containing 10 ng/ml IL-4 and 10 ng/ml GM-CSF (both from Peprotech). After two days and again after four days of culture, the nonadherent cells were centrifuged, resuspended in fresh medium and replated to the same falcons. On the sixth day, nonadherent cells were removed and fresh medium containing 10 ng/ml GM-CSF and 5 ng/ml IL-4 was added. On day 8 of culture, nonadherent cells were harvested and seeded in Lab-Tek (Nunc, Thermo Scientific) eight-chambered cover glasses. The porous microspheres were suspended in PBS at a concentration corresponding to 0.5 mg/ml OVA, and 10 µl of this suspension was added to the DCs. After 2 h incubation, the cells were fixed in an aqueous 4% formaldehyde solution overnight. Subsequently, the cells were washed three times with PBS and stained with Cy5-conjugated cholera toxin subunit B (5µg/mL) and Hoechst 33258 (2µg/mL). For the assessment of the intracellular localization of the porous microspheres, cells were not fixed with formaldehyde, and the cellular cytoplasm and acidic vesicles were stained by CellTracker Red (1µg/mL) and LysoTracker Red (1µg/mL), respectively, and visualized directly by confocal microscopy.

3. RESULTS AND DISCUSSION

Herein we report on the synthesis of porous antigen loaded degradable polyelectrolyte microspheres using spray drying as simple, yet efficient and scalable production technique. **Figure 1** shows a schematic illustration of the formation of these porous microspheres. Key in our present work is the use as a sacrificial component of calcium carbonate nanoparticles, which are directly spray dried in combination with antigen and oppositely charged polyelectrolytes to form a polyelectrolyte framework that entraps the antigen and the calcium carbonate nanoparticles. Extraction of the calcium carbonate subsequently leads to porous microspheres. We reasoned that a porous system exhibits a much higher surface to volume ratio, which, upon internalization by DCs, will enhance the

access of proteases to the encapsulated antigen followed by antigen processing and initiation of the immune response.

Calcium carbonate nanoparticles ($CaCO_3^{NP}$) with an average diameter of 90 nm and a ζ-potential of 6.8 ± 0.4 mV were mixed with dextran sulfate (DS) and ovalbumin (OVA; used as model antigen in this work) under stirring. The slightly cationic surface charge of $CaCO_3^{NP}$ means that anionic DS and OVA will at least partly associate with the $CaCO_3^{NP}$ through electrostatic interaction and presumably also by physical adsorption. Subsequently poly-L-arginine (P_LARG) was added dropwise to allow further electrostatic complexation between P_LARG and DS or OVA. Hollow polyelectrolyte multilayer capsules based on $CaCO_3$ microparticle templates coated with DS and P_LARG have been shown by our group to be non-toxic and degradable upon cellular uptake, both *in vitro* and *in vivo*.[29, 30] In this work, the ratio of $CaCO_3$ to OVA, DS and P_LARG was 40/1/4/5, respectively, which tends to mimic the conditions used for the encapsulation of OVA into hollow DS/P_LARG multilayer capsules templated on OVA co-precipitated $CaCO_3$ microparticles, reported in our previous work[14, 15] and by others.[31] Subsequently, the mixture was spray dried using a Büchi B290 bench top spray drier and collected as a dry powder compromising 80% $CaCO_3$. These particles are referred to as solid microspheres further in this chapter. Porous microspheres were obtained by resuspending the dry powder in an aqueous 0.2 M solution of ethylene diamine tetra acetic acid (EDTA), which is a potent complexing agent for calcium ions[32, 33] and serves to extract the $CaCO_3^{NP}$ from the solid microspheres.[31] The characteristics of these spray dried microspheres before (solid) and after (porous) $CaCO_3$ dissolution are summarized in **Table 1**.

Table 1: Overview of the microsphere characteristics (n=3)

	ζ-potential	Size	OVA encapsulation
Solid microspheres	-6.8 ± 0.4 mV	6.0 ± 0.4 µm	94 ± 1 %
Porous microspheres	-18 ± 0.7 mV	5.8 ± 0.1 µm	86 ± 1%

The morphologies of the $CaCO_3$ nanoparticles, the solid microspheres and the porous microspheres were visualized by scanning electron microscopy (SEM; **Figure 2A**). $CaCO_3^{NP}$ exhibited a primary particle size of roughly 90 nm (**Figure 2A1**) and upon spray drying are grouped into spherical clusters (**Figure 2A2**) with an average size of 6 µm (**Figure 2B**; note that some polydispersity is inherent to spray drying[28]) and a ζ-potential of -6.8 mV, as determined by laser diffraction (**Figure 2B**) and dynamic light scattering respectively, upon resuspension in aqueous medium. Most importantly, as is addressed below in more detail by confocal microscopy, the spray dried microspheres remain stable upon resuspension in aqueous medium and do not disassemble into the initial starting components.

As a control we also spray dried a mixture of $CaCO_3^{NP}$ and OVA and no cluster formation could be observed (data not shown), indicating the requirement of the DS/P_LARG polyelectrolyte complex framework to obtain stable microspheres. Extraction of the $CaCO_3^{NP}$ by an aqueous EDTA solution leads to the formation of porous microspheres (**Figure 2A3,4**), which have a ζ-potential of -18 mV and are most likely stabilized through a combination of electrostatic and hydrophobic interactions together with physical entanglements of the polymer and protein chains. Short-range hydrophobic forces play a major role in the formation of polyelectrolyte complexes. These originate from contact between hydrophobic parts of the polyelectrolyte chains, excluding hydration molecules.[34] The highly porous state of the microspheres is highlighted in the transmission electron microscopy of **Figure 2A4** and complete removal of the $CaCO_3^{NP}$ by treatment with EDTA was confirmed by energy dispersive X-ray (EDX) analysis. The EDX spectrum shown in **Figure 2C** of the solid (**C1**) microspheres clearly exhibits two calcium peaks which are lacking in the EDX spectrum of the porous (**C2**) microspheres. **Figure 2C2** exhibits a predominant silicon peak. This silicon peak is most likely due to the porous structure of the microspheres, which allows the electron beam to reach the underlying silicon wafer on which the microspheres were deposited upon sample preparation. Laser diffraction (**Figure 2B**) did not show any significant change in mean diameter of the porous microspheres compared to the solid ones, indicating that upon $CaCO_3^{NP}$ removal not substantial shrinkage or swelling of the polyelectrolyte framework occurs.

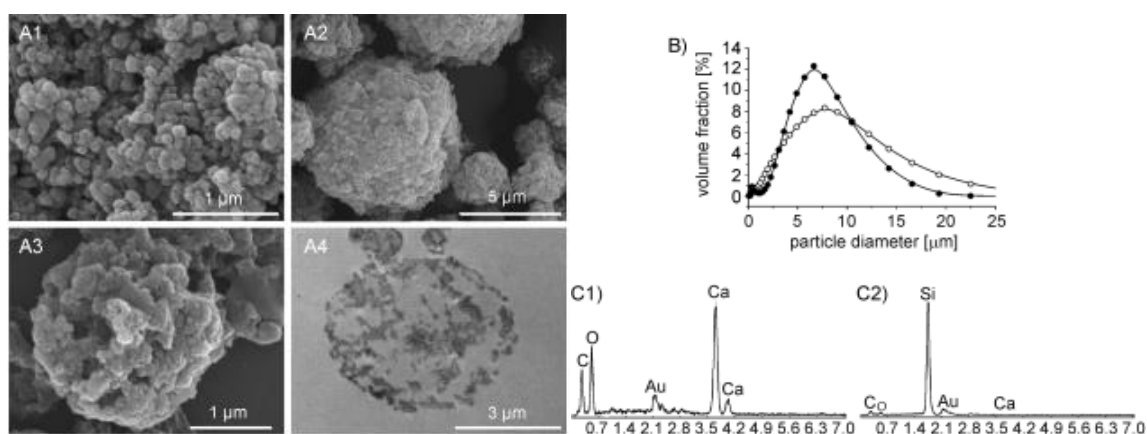**Figure 2**. **(A)** Scanning electron microscopy images of **(A1)** $CaCO_3^{NP}$ (note that the aggregation is due to drying of the sample prior to SEM imaging), **(A2)** spray dried $CaCO_3^{NP}$ /$DS/OVA/P_LARG$ microspheres, and **(A3)** porous $DS/OVA/P_LARG$ microspheres after treatment with EDTA. **(A4)** Transmission electron microscopy image of porous $DS/OVA/P_LARG$ microspheres after treatment with EDTA. **(B)** Size distribution of solid spray dried $CaCO_3^{NP}$/$DS/OVA/P_LARG$ microspheres (●) and porous $DS/OVA/P_LARG$ microspheres obtained after EDTA treatment (o). **(C)** Energy-dispersive X-ray (EDX) spectra of **(C1)** solid spray dried $CaCO_3^{NP}$/$DS/OVA/P_LARG$ microspheres and **(C2)** porous DS/OVA/PLARG microspheres obtained after EDTA treatment.

Confocal microscopy was used to visualize the microspheres in a hydrated state. For visualization purpose, green fluorescent OVA-Alexa Fluor488 was mixed with native OVA in a 1:50 ratio. The confocal micrographs in **Figure 3A** confirm that the microspheres remain stable in aqueous medium. When the microspheres are resuspended in a 0.2 M EDTA solution, the dark shine in the transmission channel (**Figure 3A2**) vanished and transparent (**Figure 3B2**) 'sponge-like' porous microspheres were obtained (**Figure 3B**). Importantly, the green fluorescent OVA-Alexa Fluor488 was retained within the polyelectrolyte framework of the porous microspheres rather than being spontaneous released into the surrounding aqueous medium.
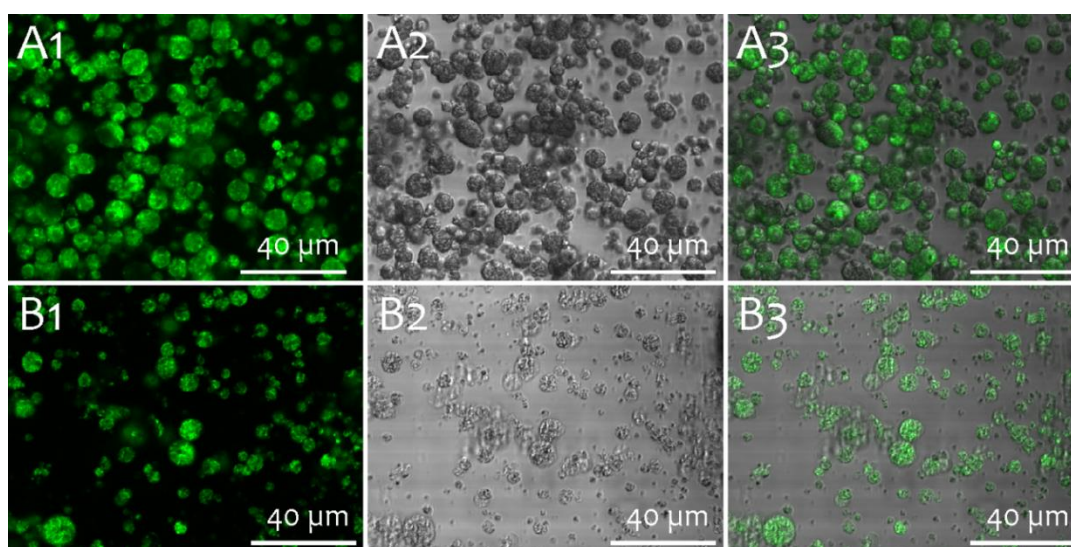
Figure 3. Confocal microscopy images of **(A)** spray dried solid $CaCO_3^{NP}$ /DS/OVA/P$_L$ARG microspheres and **(B)** porous DS/OVA/P$_L$ARG microspheres obtained after treatment with EDTA. The green fluorescence is due to OVA-Alexa Fluor488.

Quantification of the encapsulation efficiency was determined by resuspending dry solid microspheres in phosphate buffered saline (PBS; pH 7.4) and in an aqueous 0.2 M EDTA solution. Subsequently, the microspheres were centrifuged and the OVA concentration in the supernatant was determined. An encapsulation efficiency (defined as the amount of protein that is retained within the microspheres upon resuspension relative to the amount of protein in the dry microspheres) of 94 ± 1 % upon resuspension in PBS and 85 ± 1 % upon resuspension in an aqueous 0.2 M EDTA solution was observed. These results show that upon resuspension in PBS only 6 ± 1 % of the OVA is released from the solid microspheres whereas 15 ± 1 % of the OVA is released upon extraction of the $CaCO_3^{NP}$ from the microspheres. The higher amount of released OVA from the porous microspheres relative to that from the solid microspheres is attributed to the higher surface area of the porous ones, allowing OVA that is weakly bound to the surface to be released. However, an encapsulation

efficiency of 85 % into the porous polyelectrolyte spheres is considerable higher than the approximately 50 % that was reported earlier for encapsulation of OVA into hollow polyelectrolyte multilayer capsules. In that case, OVA was co-precipitated into calcium carbonate microparticles by mixing it with calcium chloride and sodium carbonate. After alternate coating of these microparticles with DS and P$_L$ARG and subsequent dissolution of the CaCO$_3$ microparticles approximately 50 % of the OVA was lost due to diffusion through the polyelectrolyte membrane.

As it is our aim to use the porous polyelectrolyte microspheres as antigen carriers for vaccination purpose, it is important to assess whether these porous microspheres are able to deliver their payload to DCs. Murine DCs were differentiated from bone marrow and incubated with OVA-Alexa Fluor488 loaded porous microspheres followed by confocal microscopy imaging. To discriminate whether the microspheres were internalized by DCs, we counterstained the cell nuclei blue fluorescent with Hoechst and the cell membrane red fluorescent with Cy5 conjugated cholera toxin B (**Figures 4A,B**). As the green fluorescent microspheres, cell nuclei and cell membrane were visible in the same confocal plane and the microspheres were clearly situated within the boundaries of the cell membrane we could unambiguously conclude that the microspheres were effectively internalized by the DCs. In a subsequent series of experiments to assess the intracellular localization of the porous microspheres we counterstained with red fluorescence the cellular cytoplasm (CellTracker Red; **Figure 4C**) and the intracellular acidic vesicles, such as endosomes and lysosomes (LysoTracker Red; **Figure 4D**). Colocalization between green and red fluorescence, yielding a yellow/orange signal indicated by orange arrows in **Figure 4D1**, shows the presence of the porous microspheres in that specific compartment. Porous microspheres that do not colocalize with the endosomes only yield a green signal and were indicated in **Figure 4D1** with a green arrow. When comparing the images in **Figure 4C** and **4D**, one can unambiguously conclude that the porous microspheres are located in intracellular acidic vesicles. This result is in agreement with literature data on microparticles with similar sizes and composition.[29, 35, 36]
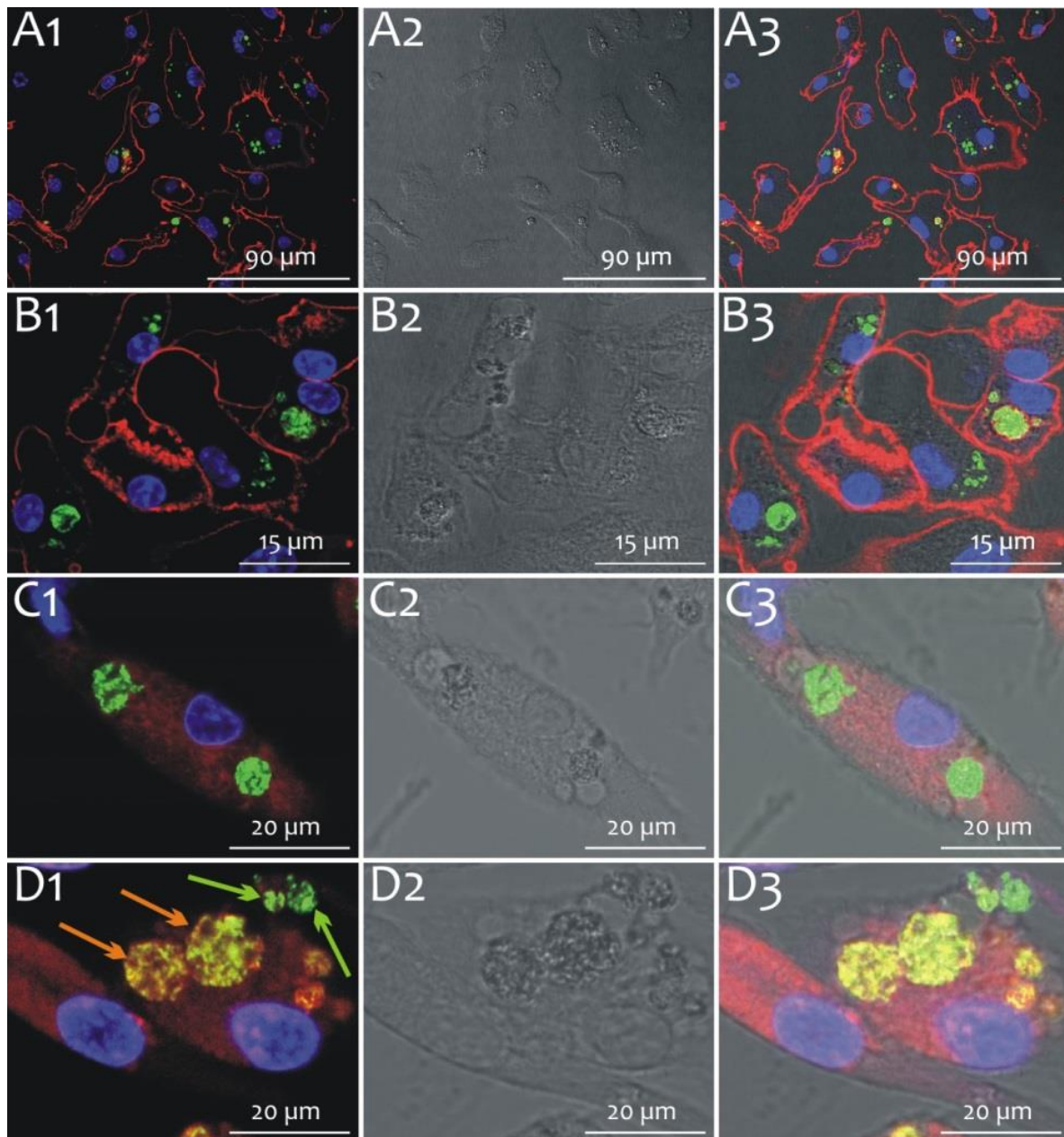
Figure 4. Confocal microscopy images of bone marrow dendritic cells incubated with green fluorescent OVA-Alexa Fluor488 loaded porous microspheres. The cell nuclei in all panels were stained blue fluorescent with Hoechst. Panels **(A)** and **(B)**, taken at different zoom levels, show images were Cy5-conjugated cholera toxin B was used to stain the cell membrane. Panels **(C)** show images in which CellTracker Red (red fluorescence) was used to stain the cellular cytoplasm and the panels **(D)** show images in which LysoTracker Red (red fluorescence) was used to stain intracellular acid vesicles. In panel **(D1)**, colocalization between red and green fluorescence (a yellow/orange signal indicates cellular uptake of the porous microspheres) is annotated with an orange arrow. Porous microspheres that are not yet taken up only exhibit a green signal and are annotated in panel **(D1)** with a green arrow. Panels (1) show the overlay of blue, green and red fluorescence channels, panels (2) show the differential interference contrast (DIC) channel, and panels (3) show the overlay of blue, green, red and DIC channels.

4. CONCLUSION

In conclusion, we have demonstrated a facile method to encapsulate antigen into porous degradable polyelectrolyte microspheres. The major advantage of this approach is the possibility to produce these microspheres on a large scale involving a minimum of process steps combined with a high encapsulation efficiency that minimizes the waste of expensive antigen and polyelectrolytes. The conceptual simplicity of the porous microspheres makes it possible to further tailor the microsphere surface with specific ligands with immune-potentiating properties such as oligonucleotides containing unmethylated CpG motifs.[6] Furthermore, we have demonstrated that the porous microspheres are efficiently taken up by DCs, which are the most potent antigen presenting cells. These types of microspheres could be promising vaccine delivery systems and the presented approach for polyelectrolyte microsphere formation is not only restricted to antigen encapsulation/ delivery, but could find the same broad applications as multilayer capsules such as enzymatic microreactors,[37, 38] gene delivery[39, 40] and low molecular weight drug delivery.[41]

REFERENCES

1.   O'Hagan, D. T.; Valiante, N. M., Recent advances in the discovery and delivery of vaccine adjuvants. Nat. Rev. Drug Discov. 2003, 2, 727-735.

2.   Rappuoli, R., Bridging the knowledge gaps in vaccine design. Nat. Biotechnol. 2007, 25, 1361-1366.

3.   Ulmer, J. B.; Valley, U.; Rappuoli, R., Vaccine manufacturing: challenges and solutions. Nat. Biotechnol. 2006, 24, 1377-1383.

4.   Rosenberg, S. A.; Yang, J. C.; Restifo, N. P., Cancer immunotherapy: moving beyond current vaccines. Nature Medicine 2004, 10, 909-915.

5.   Singh, M.; O'Hagan, D., Advances in vaccine adjuvants. Nat. Biotechnol. 1999, 17, 1075-1081.

6.   Jain, S.; Yap, W. T.; Irvine, D. J., Synthesis of protein-loaded hydrogel particles in an aqueous two-phase system for coincident antigen and CpG oligonucleotide delivery to antigen-presenting cells. Biomacromolecules 2005, 6, 2590-2600.

7.   Caruso, F.; Caruso, R. A.; Mohwald, H., Nanoengineering of inorganic and hybrid hollow spheres by colloidal templating. Science 1998, 282, 1111-1114.

8.   Donath, E.; Sukhorukov, G. B.; Caruso, F.; Davis, S. A.; Mohwald, H., Novel hollow polymer shells by colloid-templated assembly of polyelectrolytes. Angew. Chem.-Int. Edit. 1998, 37, 2202-2205.

9.   Sukhorukov, G. B.; Donath, E.; Davis, S.; Lichtenfeld, H.; Caruso, F.; Popov, V. I.; Mohwald, H., Stepwise polyelectrolyte assembly on particle surfaces: a novel approach to colloid design. Polym. Adv. Technol. 1998, 9, 759-767.

10. Sukhorukov, G. B.; Mohwald, H., Multifunctional cargo systems for biotechnology. Trends Biotechnol. 2007, 25, 93-98.

11. Peyratout, C. S.; Dahne, L., Tailor-made polyelectrolyte microcapsules: From multilayers to smart containers. Angew. Chem.-Int. Edit. 2004, 43, 3762-3783.

12. Skirtach, A. G.; Javier, A. M.; Kreft, O.; Kohler, K.; Alberola, A. P.; Mohwald, H.; Parak, W. J.; Sukhorukov, G. B., Laser-induced release of encapsulated materials inside living cells. Angew. Chem.-Int. Edit. 2006, 45, 4612-4617.

13. De Cock, L. J.; De Koker, S.; De Geest, B. G.; Grooten, J.; Vervaet, C.; Remon, J. P.; Sukhorukov, G. B.; Antipina, M. N., Polymeric Multilayer Capsules in Drug Delivery. Angew. Chem.-Int. Edit. 2010, 49, 6954-6973.

14. De Koker, S.; De Geest, B. G.; Singh, S. K.; De Rycke, R.; Naessens, T.; Van Kooyk, Y.; Demeester, J.; De Smedt, S. C.; Grooten, J., Polyelectrolyte Microcapsules as Antigen Delivery Vehicles To Dendritic Cells: Uptake, Processing, and Cross-Presentation of Encapsulated Antigens. Angew. Chem.-Int. Edit. 2009, 48, 8485-8489.

15. De Koker, S.; Naessens, T.; De Geest, B. G.; Bogaert, P.; Demeester, J.; De Smedt, S.; Grooten, J., Biodegradable Polyelectrolyte Microcapsules: Antigen Delivery Tools with Th17 Skewing Activity after Pulmonary Delivery. J. Immunol. 2010, 184, 203-211.

16. De Rose, R.; Zelikin, A. N.; Johnston, A. P. R.; Sexton, A.; Chong, S. F.; Cortez, C.; Mulholland, W.; Caruso, F.; Kent, S. J., Binding, Internalization, and Antigen Presentation of Vaccine-Loaded Nanoengineered Capsules in Blood. Adv. Mater. 2008, 20, 4698-+.

17. Palankar, R.; Skirtach, A. G.; Kreft, O.; Bedard, M.; Garstka, M.; Gould, K.; Mohwald, H.; Sukhorukov, G. B.; Winterhalter, M.; Springer, S., Controlled Intracellular Release of Peptides from Microcapsules Enhances Antigen Presentation on MHC Class I Molecules. Small 2009, 5, 2168-2176.

18. Decher, G., Fuzzy nanoassemblies: Toward layered polymeric multicomposites. Science 1997, 277, 1232-1237.

19. Boudou, T.; Crouzier, T.; Ren, K. F.; Blin, G.; Picart, C., Multiple Functionalities of Polyelectrolyte Multilayer Films: New Biomedical Applications. Adv. Mater. 2010, 22, 441-467.

20. De Geest, B. G.; De Koker, S.; Sukhorukov, G. B.; Kreft, O.; Parak, W. J.; Skirtach, A. G.; Demeester, J.; De Smedt, S. C.; Hennink, W. E., Polyelectrolyte microcapsules for biomedical applications. Soft Matter 2009, 5, 282-291.

21. De Geest, B. G.; Sanders, N. N.; Sukhorukov, G. B.; Demeester, J.; De Smedt, S. C., Release mechanisms for polyelectrolyte capsules. Chem. Soc. Rev. 2007, 36, 636-649.

22. De Geest, B. G.; Sukhorukov, G. B.; Mohwald, H., The pros and cons of polyelectrolyte capsules in drug delivery. Expert Opin. Drug Deliv. 2009, 6, 613-624.

23. Quinn, J. F.; Johnston, A. P. R.; Such, G. K.; Zelikin, A. N.; Caruso, F., Next generation, sequentially assembled ultrathin films: beyond electrostatics. Chem. Soc. Rev. 2007, 36, 707-718.

24. Sexton, A.; Whitney, P. G.; Chong, S. F.; Zelikin, A. N.; Johnston, A. P. R.; De Rose, R.; Brooks, A. G.; Caruso, F.; Kent, S. J., A Protective Vaccine Delivery System for In Vivo T Cell Stimulation Using Nanoengineered Polymer Hydrogel Capsules. ACS Nano 2009, 3, 3391-3400.

25. Chong, S. F.; Sexton, A.; De Rose, R.; Kent, S. J.; Zelikin, A. N.; Caruso, F., A paradigm for peptide vaccine delivery using viral epitopes encapsulated in degradable polymer hydrogel capsules. Biomaterials 2009, 30, 5178-5186.

26. Selina, O. E.; Belov, S. Y.; Vlasova, N. N.; Balysheva, V. I.; Churin, A. I.; Bartkoviak, A.; Sukhorukov, G. B.; Markvicheva, E. A., Biodegradable microcapsules with entrapped DNA for development of new DNA vaccines. Russ. J. Bioorg. Chem. 2009, 35, 103-110.

27. Rivera-Gil, P.; De Koker, S.; De Geest, B. G.; Parak, W. J., Intracellular Processing of Proteins Mediated by Biodegradable Polyelectrolyte Capsules. Nano Lett. 2009, 9, 4398-4402.

28. Masters, K., Spray drying in practice. SprayDryConsult Internationl ApS: Charlottenlund, Denmark, 2002.

29. De Geest, B. G.; Vandenbroucke, R. E.; Guenther, A. M.; Sukhorukov, G. B.; Hennink, W. E.; Sanders, N. N.; Demeester, J.; De Smedt, S. C., Intracellularly degradable polyelectrolyte microcapsules. Adv. Mater. 2006, 18, 1005-+.

30. De Koker, S.; De Geest, B. G.; Cuvelier, C.; Ferdinande, L.; Deckers, W.; Hennink, W. E.; De Smedt, S.; Mertens, N., In vivo cellular uptake, degradation, and biocompatibility of polyelectrolyte microcapsules. Adv. Funct. Mater. 2007, 17, 3754-3763.

31. Petrov, A. I.; Volodkin, D. V.; Sukhorukov, G. B., Protein-calcium carbonate coprecipitation: A tool for protein encapsulation. Biotechnol. Prog. 2005, 21, 918-925.

32. Volodkin, D. V.; Larionova, N. I.; Sukhorukov, G. B., Protein encapsulation via porous CaCO3 microparticles templating. Biomacromolecules 2004, 5, 1962-1972.

33. Volodkin, D. V.; Petrov, A. I.; Prevot, M.; Sukhorukov, G. B., Matrix polyelectrolyte microcapsules: New system for macromolecule encapsulation. Langmuir 2004, 20, 3398-3406.

34. Kotov, N. A., Layer-by-layer self-assembly: The contribution of hydrophobic interactions. Nanostructured Materials 1999, 12, 789-796.

35. Kreft, O.; Javier, A. M.; Sukhorukov, G. B.; Parak, W. J., Polymer microcapsules as mobile local pH-sensors. J. Mater. Chem. 2007, 17, 4471-4476.

36. Javier, A. M.; Kreft, O.; Semmling, M.; Kempter, S.; Skirtach, A. G.; Bruns, O. T.; del Pino, P.; Bedard, M. F.; Raedler, J.; Kaes, J.; Plank, C.; Sukhorukov, G. B.; Parak, W. J., Uptake of Colloidal Polyelectrolyte-Coated Particles and Polyelectrolyte Multilayer Capsules by Living Cells. Adv. Mater. 2008, 20, 4281-4287.

37. Wang, Y. J.; Caruso, F., Nanoporous protein particles through templating mesoporous silica spheres. Adv. Mater. 2006, 18, 795-+.

38. Wang, Y. J.; Yu, A. M.; Caruso, F., Nanoporous polyelectrolyte spheres prepared by sequentially coating sacrificial mesoporous silica spheres. Angew. Chem.-Int. Edit. 2005, 44, 2888-2892.

39. Zelikin, A. N.; Becker, A. L.; Johnston, A. P. R.; Wark, K. L.; Turatti, F.; Caruso, F., A general approach for DNA encapsulation in degradable polymer Microcapsules. ACS Nano 2007, 1, 63-69.

40. Zelikin, A. N.; Li, Q.; Caruso, F., Degradable polyelectrolyte capsules filled with oligonucleotide sequences. Angew. Chem.-Int. Edit. 2006, 45, 7743-7745.

41. Wang, Y. J.; Bansal, V.; Zelikin, A. N.; Caruso, F., Templated synthesis of single-component polymer capsules and their application in drug delivery. Nano Lett. 2008, 8, 1741-1745.

CHAPTER 5

SINGLE-STEP FORMATION OF DEGRADABLE INTRACELLULAR BIOMOLECULE MICROREACTORS

CHAPTER 5

SINGLE-STEP FORMATION OF

DEGRADABLE INTRACELLULAR

BIOMOLECULE

MICROREACTORS

1. INTRODUCTION

Microparticulate encapsulation strategies have gained increased interest for the encapsulation of biomolecules for drug delivery or to serve as a microreactor. We hypothesize that fully hydrated microparticles should exhibit superior properties for applications such as intracellular protein delivery and as an enzyme microreactor where one desires to separate the enzyme physically from the surrounding medium. Our hypothesis is supported by the fact that fully hydrated microparticles allow in- and outwards diffusion of water as well as reactants and reaction products. Moreover, microparticles with additionally a porous interconnected structure should allow an even faster and more efficient intraparticle processing as the presence of pores along with a higher surface to volume ratio which allows efficient access, especially of macromolecular reactants such as proteins which would encounter serious diffusion limitation to enter densely structured microparticles.[1]

A wide spectrum of synthetic methods to produce porous microparticles has been described in literature and was recently reviewed.[2] Generally, the synthesis involves the use of organic solvents as well as reactive chemistries such as radical polymerization or condensation reactions. In our research group we are developing polyelectrolyte-based microparticles using merely water-based solutions of oppositely charged polyelectrolytes that self-assemble through electrostatic interaction. An intriguing class of polyelectrolyte-based microparticles are polyelectrolyte multi-layered[3] microcapsules.[4, 5] These microparticles are made by sequential deposition of oppositely charged species onto a charged template followed by the decomposition of this template. By depositing typically 2 – 5 polyelectrolyte bilayers onto microparticles with sizes typically between 500 nm and 10 μm, hollow capsules can be designed. A striking feature of these microparticles is that they are

perm-selective, meaning that low molecular weight species such as solvents, ions and metabolites can freely diffuse in- and outwards.[6] However, high molecular weight species such as proteins remain entrapped within the capsules.

In our group we are particularly interested in developing microparticulate vaccines that specifically target their payload to antigen presenting cells, such as dendritic cells[7-12] the working horses of our immune system. Both our group[8, 10] and the Caruso group[13, 14] reported that such multilayered capsules, based on degradable polymers, were efficiently taken up by dendritic cells both *in vitro* and *in vivo* and are excellent inducers of T-cell responses. Several other groups have described the use of such capsules as enzyme microreactor comprising enzymes that are stably encapsulated either inside the hollow void of the capsules or into the shell.[15-18]

Despite numerous advantages, the major drawback of LbL capsules is their multi-step fabrication involving several centrifugation-redispersion steps per deposited polyelectrolyte layer. Moreover, in a typical LbL procedure, polyelectrolytes are deposited from solutions containing approximately a 100-fold excess of polyelectrolyte while the non-adsorbed polyelectrolytes are usually wasted. Therefore, we envisioned to develop simplified procedures to produce polyelectrolyte microparticles while maintaining as much as possible their versatile properties. In the previous chapter we reported on the use of spray drying to produce porous polyelectrolyte microparticles by co-spray drying oppositely charged polyelectrolytes with calcium carbonate nanoparticles as sacrificial component followed by extraction of the calcium carbonate nanoparticles with an EDTA solution.[19] This two-step procedure allowed the efficient incorporation of ovalbumin as a model antigen into porous microparticles that were efficiently taken up by dendritic cells, envisioning application in microparticulate vaccine delivery.

In this chapter we demonstrate that by co-spray drying polyelectrolytes with mannitol – a water soluble well-established pharmaceutical excipient – nanoporous polyelectrolyte microparticles can be produced that allow protein encapsulation with nearly 100 % efficiency with excellent preservation of biological activity. Moreover, a dry powder formulation is obtained which offers additional benefits for long time storage (essential for vaccine applications), only requiring reconstitution in aqueous medium at the time of use. Spray drying is widely used in the pharmaceutical industry and is commonly used to convert water soluble species into a water soluble dry powder. By contrast, the novelty of our method involves a nanodispersion of polyelectrolyte complexes with proteins that are subsequently formulated through spray drying into spherical microparticles that remain stable upon rehydration in aqueous medium. Key in this work is the use of

a fully biocompatible (i.e. mannitol) water soluble sacrificial component that readily dissolves upon redispersion of the spray dried microparticles in water. In this way additional steps to remove and purification steps to dissolve organic (e.g. polystyrene or melamine formaldehyde latexes) or inorganic (e.g. calcium carbonate or silica particles) core templates are avoided.

Using horseradish peroxidase (HRP) as the model enzyme, we demonstrate that enzymatic activity is retained within the microparticles, indicating the potential of the system as enzymatic microreactor. Furthermore, in an *in vitro* model for vaccine delivery using ovalbumin (OVA) as the model antigen we demonstrated that encapsulated OVA is readily processed by intracellular lysosomal proteases of dendritic cells, and subsequently, the CD8 epitope of OVA is presented on the cell surface as an MHCI complex. This process is termed cross-presentation, meaning that extracellular antigen becomes internalized and presented to CD8 T cells which is crucial to induce cellular immune responses to combat intracellular viral pathogens as well as cancer. In this sense, the microparticles act as intracellular protein microreactors.

2. MATERIALS AND METHODS

2.1. Materials

Mannitol was obtained from Cargill. Dextran sulfate (DS; Mw $\sim$ 9-20 kDa), poly-L-arginine (P$_L$ARG; Mw > 70 kDa), poly(DL-lactide-co-glycolide) PLGA (50:50, Mw $\sim$ 40-75 kDa), poly(vinyl alcohol) (PVA; 80% hydrolyzed, Mw $\sim$ 9-10 kDa), ovalbumin (OVA), horseradish peroxidase (HRP), 2,2'-Azinobis(3-ethylbenzothiazoline-6-Sulfonic Acid)diammonium salt (ABTS) and Ampliflu red (Amplex Red) were obtained from Sigma-Aldrich. Phosphate buffered saline (PBS), OVA-Alexa Fluor488, CellTracker red and LysoTracker Red were obtained from Invitrogen. H_2O_2 was obtained from Fagron. All water used in the experiments was of Milli Q-grade.

2.2. Synthesis of (porous) microspheres

Mannitol, DS, OVA and P$_L$ARG were mixed in water in a 40/4/1/5 ratio at a total solid concentration of 1%. In detail, 200 mg mannitol, 20 mg DS, and 5 mg OVA were dissolved in 20 mL water. Subsequently 25 mg P$_L$ARG was dissolved in 5 mL of water and added dropwise to the stirring mannitol/DS/OVA dispersion. This was carried out analogously for the HRP microspheres. Spray drying of these mixtures was performed in a lab-scale Büchi B290 spray dryer. The mixture was fed to a two-fluid nozzle (diameter 0.7 mm) at the top of the spray dryer. In addition, the spray dryer operated in co-current air flow at drying air temperature of 130 °C. Fluorescent microparticles were prepared using a mixture of OVA with green fluorescent OVA-Alexa Fluor488 in a 50:1 ratio.

2.3. Synthesis of PLGA microspheres.

OVA was encapsulated in PLGA microspheres according to a general procedure reported by Lynn and Langer.[20] An aqueous OVA solution (200 µl; 10 mg/ml) was emulsified by 10 s sonication in 4 ml of dichloromethane containing 200 mg PLGA. This primary emulsion was then emulsified in 50 ml of an aqueous 1 % PVA solution using a Silverson high shear homogenizer for 30 s at maximum power. Subsequently, the obtained secondary emulsion was diluted with 100 ml of an aqueous 0.5 % PVA solution and stirred for 3h under ambient conditions to allow evaporation of dichloromethane. Finally the hardened PLGA microspheres were collected by centrifugation (10 min at 4000 g) and washed three times with deionized water. The encapsulation efficiency of OVA was determined by encapsulating Alexa Fluor 488-conjugated OVA instead of blank OVA and subsequently measuring the OVA-Alexa Fluor488 concentration in the supernatant using a Perkin-Elmer Envision multilabel plate reader.

2.4. Particle characterization.

Confocal microscopy images were recorded on a Leica SP5 AOBS confocal microscope. Scanning electron microscopy images were recorded on a quanta FEG FEI 200 apparatus. Samples were dried on a silicon wafer and sputtered with an thin layer of palladium/gold. Transmission electron microscopy images of ultrathin microtomed sections were recorded on a JEOL 1010 electron microscope. Laser diffraction was performed on a Malvern Mastersizer equipped with an 300 RF objective. The ζ-potential measurements were performed on a Malvern Nanosizer ZS. X-ray powder diffractograms were performed on a PANalytical X'Pert PRO X-ray diffractometer (Siemens). XRPD patterns were obtained with Cu Kα radiation (45kV x 40 mA; λ = 1.5406A) at a scanning speed of 25° (2 θ)/ min and step size of 0.03° (2θ). Measurements were done in the reflection mode in the 2θ range of 5-40°. Analysis of the diffractograms was done by visual inspection. The encapsulation efficiency was determined by resuspending a known amount of OVA-Alexa Fluor488-loaded microparticles (thus containing a known amount of protein (protein conc$^{dry\ microparticles}$) in phosphate buffered saline followed by centrifugation and measuring the OVA-Alexa Fluor488 concentration (protein conc^{supernatant}) in the supernatant using a Perkin-Elmer Envision multilabel plate reader. The encapsulation efficiency is then calculated as follows:

$$Encapsulation\ efficiency = 100x \frac{protein\ conc^{dry\ microparticles} - protein\ conc^{supernatant}}{protein\ conc^{dry\ microparticles}}$$

2.5. Determination of enzymatic activity.

Enzymatic activity of encapsulated HRP was monitored by measuring the absorbance at 405 nm with a Perkin-Elmer Envision multilabel plate reader. In detail, 0.1 ml of an ABTS solution (0.01 mg/ml) and 0.1 ml of a HRP solution (0.00025 mg/ml) or 0.1 ml resuspended spray dried microparticles (0.0125 mg/ml in 0.1M phosphate buffer) or a aqueous dispersion of mannitol, DS, P_LARG and HRP (0.0125 mg/ml in 0.1M phosphate buffer) was mixed in the wells of a 96 well plate. Then 0.1 ml of a H_2O_2 solution (0.03%) was added. The absorbance was measured every 20 seconds at 405 nm, and the reaction was allowed to proceed for 5 min. Each reaction was carried out in six-fold. Visualization by confocal microscopy was performed using Amplex Red as a fluorogenic substrate. A 50 μl drop of microparticle suspension (5 mg/ml) was put on a microscopy coverslip followed by the addition of 2 μl of 0.05 mg/ml Amplex Red and 3 μl H_2O_2 (20 mM). Confocal images were recorded using a Leica SP5 AOBS confocal microscope by excitation with the 561 nm laser line and detection at 580 nm.

2.6. DC uptake assessment

Female C57BL/6 mice were purchased from Janvier and housed in a specified pathogen-free facility in micro-isolator units. Dendritic cells were generated using a modified Inaba protocol. Two to six months C57BL/6 mice were sacrificed and bone marrow was flushed from their femurs and tibias. After lysis of red blood cells with ACK lysis buffer (BioWhittaker), granulocytes and B cells were depleted using Gr-1 (Pharmingen) and B220 (Pharmingen) antibodies respectively, and low-toxicity rabbit complement (Cedarlane Laboratories Ltd.). Cells were seeded at a density of 2 x 10^5 cells/ml in 175 cm^2 Falcon tubes (Becton Dickinson) in DC medium (RPMI 1640 medium containing 5% LPS-free FCS, 1% penicillin/streptomycin, 1% L-glutamine and 50 μM β-mercaptoethanol) containing 10 ng/ml IL-4 and 10 ng/ml GM-CSF (both from Peprotech). After two days and again after four days of culture, the non-adherent cells were centrifuged, resuspended in fresh medium and replated to the same falcons. On the sixth day, non-adherent cells were removed and fresh medium containing 10 ng/ml GM-CSF and 5 ng/ml IL-4 was added. On day 8 of culture, non-adherent cells were harvested and seeded at a density of 50 x 10^3 in Lab-Tek (Nunc, Thermo Scientific) 8-chambered cover glasses. The spray dried microparticles were resuspended in PBS at a concentration corresponding to 0.5 mg/ml OVA, and 10 μl of this suspension was added to the DCs. After 2h incubation the cells were fixed in an aqueous 4 % formaldehyde solution overnight. Subsequently the cells were washed three times with PBS and stained with Hoechst 33258 (2 μg/ml). For the assessment of the intracellular localization of the porous microspheres, cells were not fixed with formaldehyde, and the cellular cytoplasm and acidic vesicles, were stained by CellTracker Red (1 μg/ml) and LysoTracker Red (1 μg/ml), respectively, and directly visualized by confocal microscopy.

2.7. Determination of MHCI presentation

To assess the capacity of spray dried particles to enhance antigen presentation of encapsulated antigen, bone marrow derived dendritic cells were isolated as described above and incubated with a dilution series of either soluble ovalbumin or the equivalent amount of ovalbumin encapsulated in spray dried particles. Forty-eight hours later, cells were stained with anti-CD11c-APC (BD biosciences) and 25D1.16-PE (ebioscience), which specifically recognizes the ovalbumin derived peptide SIINFEKL presented by MHCI at the cell surface. Cells were stained with aqua Live/Dead® stain (Molecular probes) to exclude dead cells from the analysis. Samples were analyzed by flow cytometry (Becton Dickinson, LSRII) with a minimum event account of 50.000 in the live CD11c+ gate. Specificity of the antibody staining was verified by pulsing DC with PBS, which showed a negligible SIINFEKL detection of 0.23%, while DC directly pulsed with SIINFEKL showed a detection of 91%. Statistical analysis was performed using an one-way ANOVA with Bonferroni post-hoc test ($p < 0.05$ = significant).

3. RESULTS AND DISCUSSION

An aqueous dispersion (1% w/w) was prepared by mixing mannitol, dextran sulfate (DS) and ovalbumin (OVA) under stirring followed by dropwise addition of poly-L-arginine (P_LARG) to allow electrostatic complexation between DS, OVA and P_LARG. The ratio (w/w) of mannitol to OVA, DS and P_LARG was chosen to be 40/1/4/5, respectively, which is based on our previous experience with hollow LbL capsules and porous polyelectrolyte microspheres based on calcium carbonate as the sacrificial template. Subsequently, the mixture was spray dried using a lab-scale Büchi B290 spray drier and collected as a dry powder (**Figure 1A1, A2**). Upon addition of water, the mannitol readily dissolves and stable microparticles consisting of a polyelectrolyte framework encapsulating the co-spray dried protein remains (**Figures 1B1, B2**). Laser diffraction (**Figure 1D**) measurements on these particles show a mean diameter of 7µm.
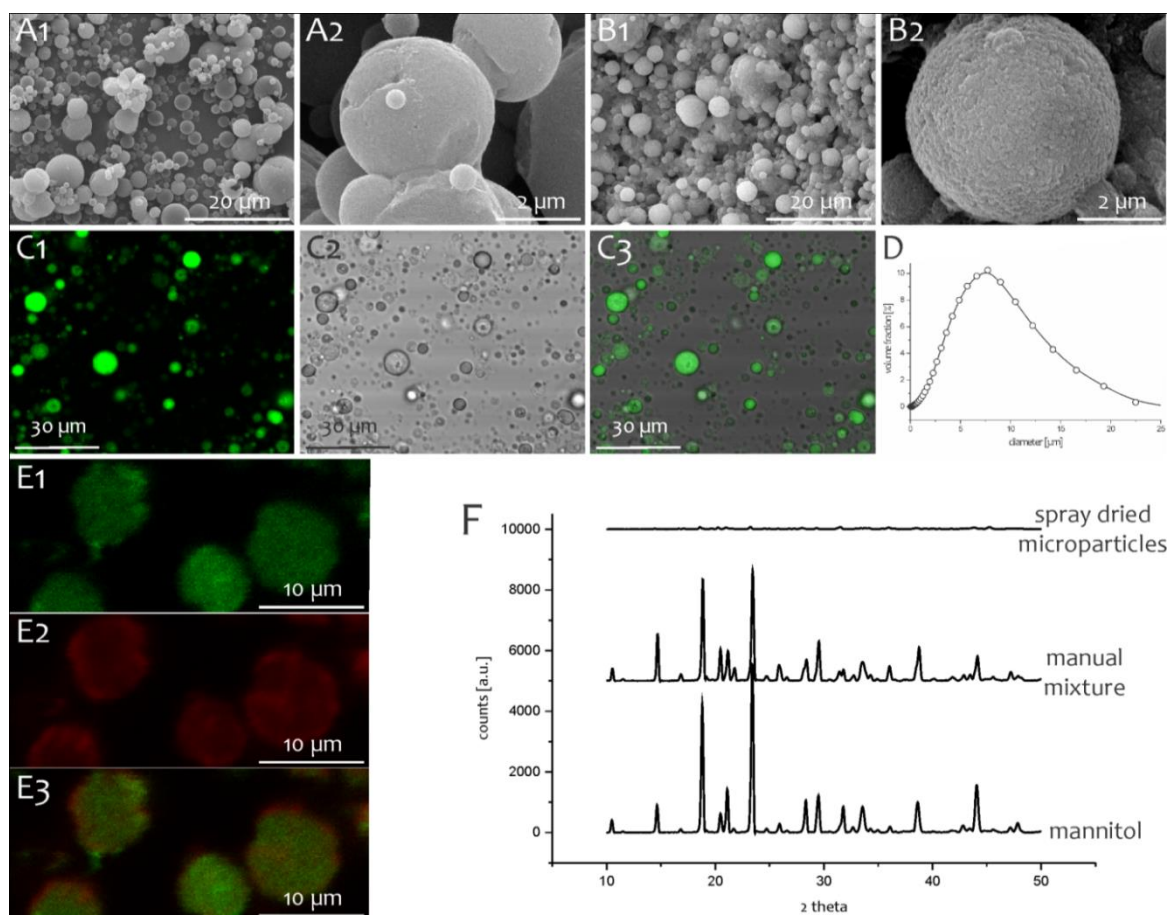
Figure 1. Physicochemical characterization of spray dried polyelectrolyte microspheres. **(A,B)** Scanning electron microscopy images of spray dried polyelectrolyte microspheres **(A)** before and **(B)** after removal of mannitol. **(C)** Confocal microscopy images of the spray dried polyelectrolyte microspheres dispersed in water. Alexa Fluor488 (green fluorescence)-conjugated ovalbumin was encapsulated as model antigen. **(D)** Size distribution of the spray dried polyelectrolyte microspheres obtained by laser diffraction. **(E)** Confocal microscopy images of double-labeled microspheres containing Alexa Fluor488-conjugated ovalbumin **(E1)**, rhodamine isothiocyanate-conjugated poly-L-arginine **(E2)**. **(E3)** Overlay of the green and red fluorescence channel. **(F)** X-ray powder diffractograms of pure mannitol, a mannitol/polyelectrolyte physical mixture and spray dried polyelectrolyte microspheres.

To allow visualization by fluorescence microscopy, green fluorescent OVA-Alexa Fluor488 was used and the confocal images in **Figures 1C1-1C3** confirm that the green fluorescent OVA-Alexa Fluor488 is retained within the porous microspheres rather than being released into the surrounding aqueous medium. To assess the spatial distribution of polyelectrolytes and mannitol, a batch of microspheres was produced with both the OVA (Alexa Fluor488) and the P_LARG fluorescently labeled. Confocal microscopy images of the microspheres upon rehydration (**Figure 1E**) demonstrate that the OVA is homogeneously distributed throughout the whole microsphere volume while the P_LARG shows a slightly higher concentration near the microsphere surface. Quantification of the encapsulation efficiency was done by resuspending the particles in phosphate buffered saline (PBS; pH= 7.4 and 150 mM NaCl). Subsequently, the microspheres were centrifuged and the amount of OVA in the

supernatant was measured. The encapsulation efficiency is defined as the amount of protein that is retained within the microparticles after resuspending relative to the amount of protein in the dry microparticles. After resuspension in PBS, an encapsulation efficiency of 99 ± 1% was calculated. This encapsulation efficiency is remarkably higher than previously reported, not only for OVA encapsulation within hollow LbL capsules (50% encapsulation efficiency for calcium carbonate templates capsules which offer the highest encapsulation efficiency of all types of LbL capsules)[8, 10] but also within porous antigen-loaded degradable polyelectrolyte microspheres with calcium carbonate as the sacrificial template (85% encapsulation efficiency).[19] In order to compare our spray dried microspheres with a 'golden standard' in drug delivery, we encapsulated OVA in poly(DL-lactide-co-glycolide (PLGA) microspheres using a general procedure reported by Lynn and Langer.[20]

Figure 2 shows microscopy images and size distribution of these microspheres that have a mean diameter of 0.5 μm as measured by laser diffraction. The encapsulation efficiency was determined by measuring the concentration of fluorescently labeled OVA-Alexa Fluor488 in the supernatant after centrifugation of the particles and found to be 63 ± 15%, which is again substantially lower than in case of the spray dried polyelectrolyte microspheres. Moreover, the OVA:polymer ratio is 1:100 in case of PLGA while it is 1:10 in case of the spray dried polyelectrolyte microspheres, indicating that much fewer polymers are required to keep the OVA stably encapsulated. Moreover, the synthesis of PLGA microspheres requires the use of organic solvents which involves safety as well as environmental risks.
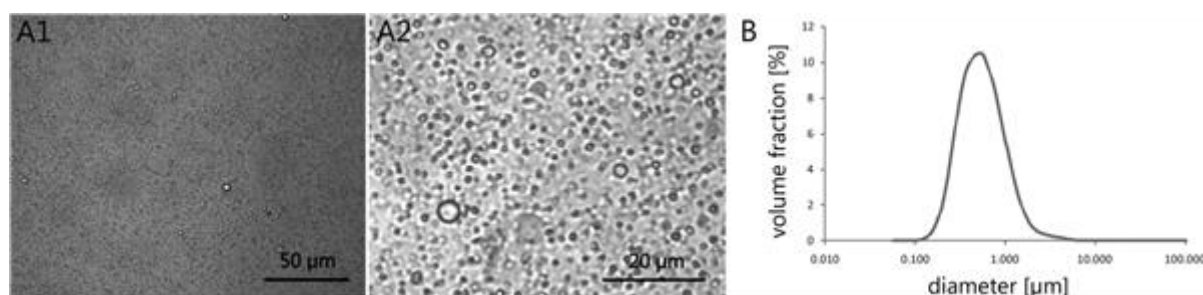

Figure 2. Optical microscopy images **(A)** and size distribution **(B)** of PLGA microspheres.

Further physicochemical characterization of the microspheres was done by X-ray powder diffraction (XRPD; **Figure 1F**). The crystallographic state of mannitol after spray drying is important because amorphous mannitol could provide enhanced protection of encapsulated proteins against denaturation. Several papers have indeed reported on the role of proteins in retaining mannitol in amorphous form after spray drying. The mannitol:protein ratio has been shown to influence the stabilization. A high protein concentration is required to obtain amorphous mannitol. However,in

that case, the amount of mannitol present in the formulation is no longer sufficient to stabilize the protein.[21, 22] **Figure 1F** shows the XRPD diffractograms of crude mannitol, physically dry mixed mannitol, DS, P$_L$ARG and OVA, and finally the spray dried microparticles. Crude mannitol is crystalline with characteristic peaks at 10.6 and 14.7°, and the XRPD spectrum of the physically dry mixture of mannitol, DS, P$_L$ARG and OVA showed crystallinity similar to that of pure mannitol, indicating that merely mixing of the substances did not lead to any change in their crystallographic state. By contrast, the diffractograms of the spray dried particles exhibit a dramatic reduction of crystallinity, indicating the formation of amorphous mannitol. Note that OVA spray dried with mannitol without polyelectrolytes yielded crystalline mannitol and that spray dried mannitol with polyelectrolytes also yielded amorphous mannitol in absence of OVA (data not shown).

For applications in drug delivery as well as to serve as microreactor for enzymatic processing, the preservation of the biological activity of the encapsulated protein within the polyelectrolyte framework is of paramount importance. Therefore we encapsulated an enzyme, horseradish peroxidase (HRP), instead of OVA and compared the enzymatic catalytic activity (i.e. rate of substrate conversion) by the free HRP enzyme in solution to the rates of conversion yielded by the aqueous mannitol/DS/HRP/P$_L$ARG dispersion and by the HRP-loaded spray dried microparticles. This was performed by following the increase in UV-VIS absorbance at 403 nm due to the conversion of the substrate ABTS (2,2'- azinobis(3-ethylbenzothiazoline-6-Sulfonic acid) diammonium salt) by HRP:

$$H_2O_2 + 2\ ABTS + 2H^+ \xrightarrow{HRP} 2\ radical\ cation^{\lambda=403nm} + 2H_2O$$
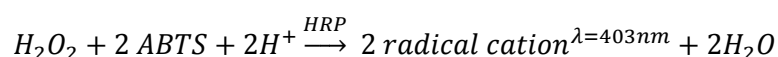
From the slope of the obtained kinetic curves, the enzymatic catalytic activity (**Figure 3A**) was derived. When the rate of conversion of ABTS by free HRP solution is equal to 100%, an activity of 87 ± 3% for the physical mixture and 84 ± 5% for the spray dried microparticles is calculated. This shows that upon mixing, a 13 ± 3% drop in enzymatic activity occurs which is likely due to electrostatic interaction with the DS/P$_L$ARG polyelectrolyte complexes.[15] As HRP has an isoelectric point of ~8.8, it is positively charged at neutral pH and is likely to undergo complexation with DS. Most strikingly, the spray drying process itself only induces a further activity decrease of merely 3 %.
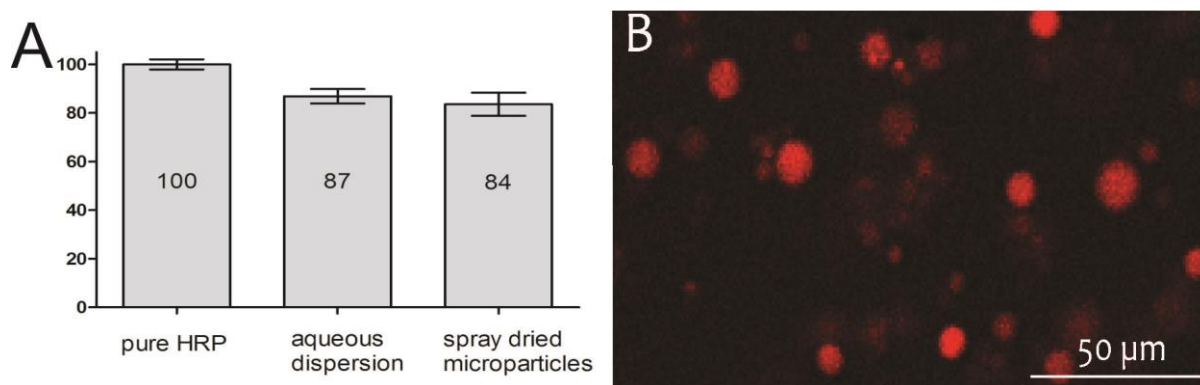
Figure 3. **(A)** Quantification of the relative enzymatic activity by conversion of 2,2'-azinobis(3-ethylbenzothiazoline-6-Sulfonic acid) diammonium salt (ABTS) by free horseradish peroxidase (HRP) in solution, an aqueous dispersion of mannitol, polyelectrolyte and HRP and spray dried microparticles after resuspension in phosphate buffered saline (PBS) (n=6, technical replicates). **(B)** Confocal microscopy image showing the conversion of Amplex Red to resorufin (red fluorescence) within the spray dried microspheres after addition of H_2O_2.

As a control, we also measured the enzymatic activity of HRP spray dried with DS/P_LARG but without mannitol and the enzymatic activity of HRP spray dried with mannitol but without the polyelectrolytes DS/P_LARG. Without mannitol, bumped dense microparticles were obtained (**Figure 4A** for SEM images), which could only be recovered at very low yields, most likely due to electrostatic interaction with the glass wall of the spray drying cylinder. The enzymatic activity of the encapsulated HRP was measured to be 50 ± 8 % which is significantly lower than in case of mannitol/DS/HRP/P_LARG microparticles.
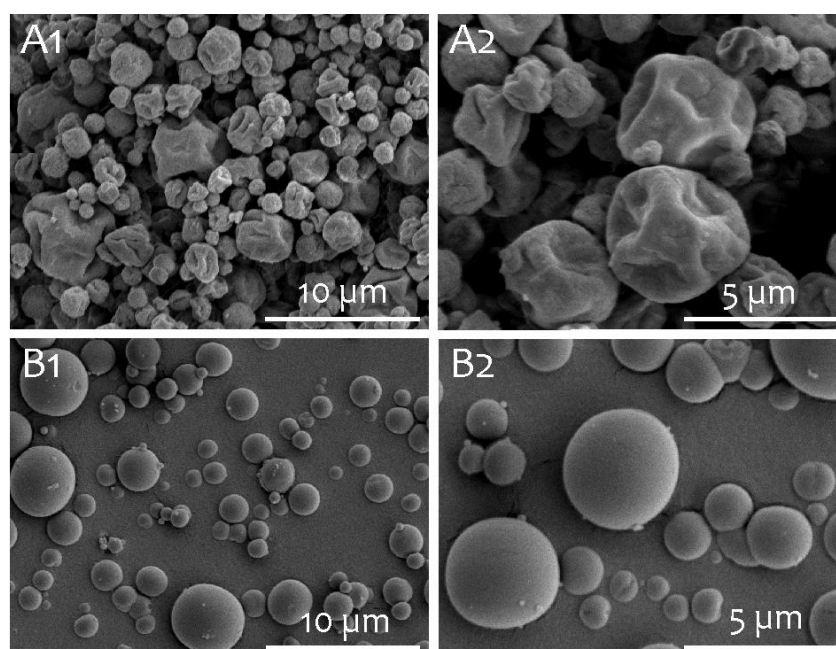

Figure 4. Scanning electron microscopy images of spray dried microparticles consisting of **(A)** HRP/DS/P_LARG, thus without mannitol and **(B)** HRP/mannitol, this without the polyelectrolytes DS/P_LARG.
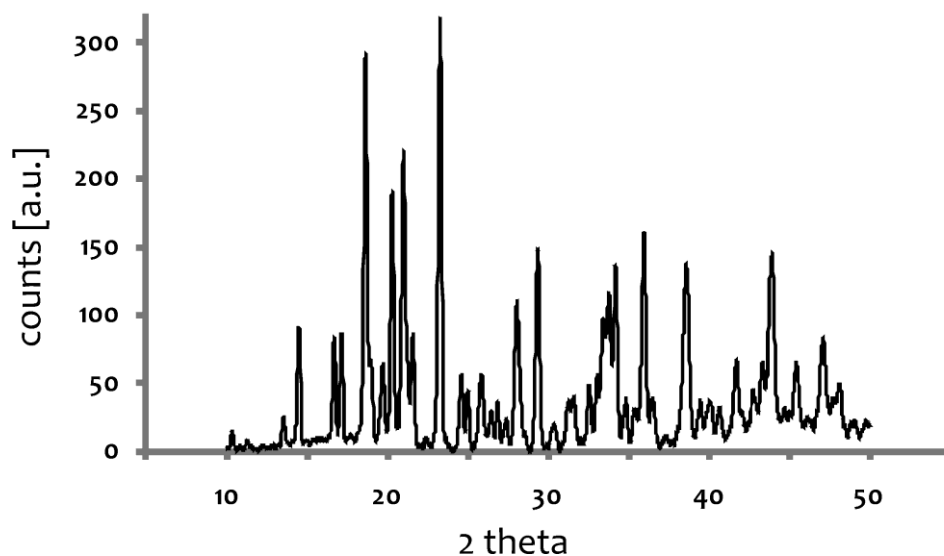
Figure 5. X-ray powder diffractograms of HRP co-spray dried with mannitol. Without polyelectrolytes DS/P_LARG, the mannitol clearly remains crystalline.

Microparticles consisting solely of HRP and mannitol, thus without polyelectrolytes were also obtained as a perfectly spherically shaped powder (**Figure 4B**). They dissolve readily upon addition of water, yielding a solution rather than a microparticle suspension obtained in the case of spray dried mannitol/DS/HRP/P_LARG microparticles. Moreover, the enzymatic activity of the encapsulated HRP was measured to be 61 ± 12 % which is again significantly lower than in the case of mannitol/DS/HRP/P_LARG microparticles. Taking into account that XRPD measurements on the mannitol/HRP microparticles (without polyelectrolytes) show the mannitol to be in a crystalline state (**Figure 5**) while the presence of polyelectrolytes yields amorphous mannitol, we hypothesize that the presence of amorphous mannitol strongly augments the preservation of the enzymatic activity of encapsulated HRP.

Thus the encapsulation approach demonstrated in this work allows a much higher preservation (i.e. 84 ± 5%) of HRP activity compared to LbL polyelectrolyte capsules (Dextran sulfate/protamine) or amphiphilic vesicles (PS-PIAT (polystyrene$_{40}$–b–poly(L isocyanoalanine (2-thiphen-3-yl-ethyl) amide)$_{50}$)) where typically a reduction of 50 - 85% of enzymatic activity upon encapsulation is observed.[15, 18, 23] Moreover, these other encapsulation strategies suffer from far lower encapsulation efficiencies compared to our spray drying approach. To demonstrate that enzymatic reaction occurs inside the spray dried microparticles, we used Amplex Red as fluorogenic substrate instead of ABTS. In the presence of H_2O_2, Amplex Red is converted by HRP to resorufin which is strongly fluorescent. **Figure 3B** shows a confocal microscopy image after addition of Amplex Red and H_2O_2 to a

mannitol/DS/HRP/P$_L$ARG microparticle suspension. The fluorescent microspheres indicate that reaction takes place inside the microspheres[24] followed by diffusion of the dye, coloring the medium.

In a next series of experiments, we investigated the interaction of the polyelectrolyte microspheres with dendritic cells (DCs), which are the primary target cell population for vaccine delivery. In this work, we used DCs derived from bone marrow of mice. **Figure 6A,B** shows confocal microscopy images of DCs incubated with spray dried microparticles loaded with OVA-Alexa Fluor488 (green fluorescence). In **Figure 6A**, the cellular cytoplasm was stained red fluorescent with CellTracker Red and in **Figure 6B**, the intracellular acidic vesicles (phagosomes, endosomes, lysosomes) were stained red fluorescent with LysoTracker Red. From the overlay between the fluorescence image and the DIC (differential interference contrast) channel in **Figure 6A2**, it is evident that the polyelectrolyte microparticles became internalized. In **Figure 6B1**, co-localization – expressed as a yellow/orange signal – between the green fluorescence of the polyelectrolyte microparticles and the red fluorescence of the intracellular vesicles is observed. For clarity of presentation, we have marked in **Figure 6B1** an internalized polyelectrolyte microparticle with an orange arrow and marked a non-internalized polyelectrolyte microparticle with a green arrow. These data indicate that upon internalization the polyelectrolyte microparticles end up in intracellular acidic vesicles, which is common for most types of microparticles so far reported in literature.[8, 25] More detail on the intracellular behavior of the internalized microparticles was obtained by imaging ultrathin sections of epoxy-embedded DCs by transmission electron microscopy (TEM). **Figure 6C** shows TEM images of DCs incubated for 4 h (**Figures 6C1, C2**) and 24h (**Figures 6C3, C4**). Following uptake, the particles were surrounded by a membrane (red arrow, **Figure 6C2**), which indicates that the particles end up in phagolysosomal compartments following uptake, as was also previously described for hollow LbL capsules. These data are also in accordance with the observed co-localization with Lysotracker Red, as shown in **Figure 6B1**. The TEM images in **Figures 6C3,C4** clearly demonstrate that after 1 day incubation the polyelectrolyte microparticles become deformed, and the zoomed image in **Figure 6C4** shows the recruitment of different intracellular organelles such as ER (blue arrow), mitochondria (green arrow) and lysosomes (yellow arrow) towards the deformed polyelectrolyte microparticle. These TEM data indicate an active intracellular processing of the internalized polyelectrolyte microparticles and puts them en route towards potential application in vaccine delivery.
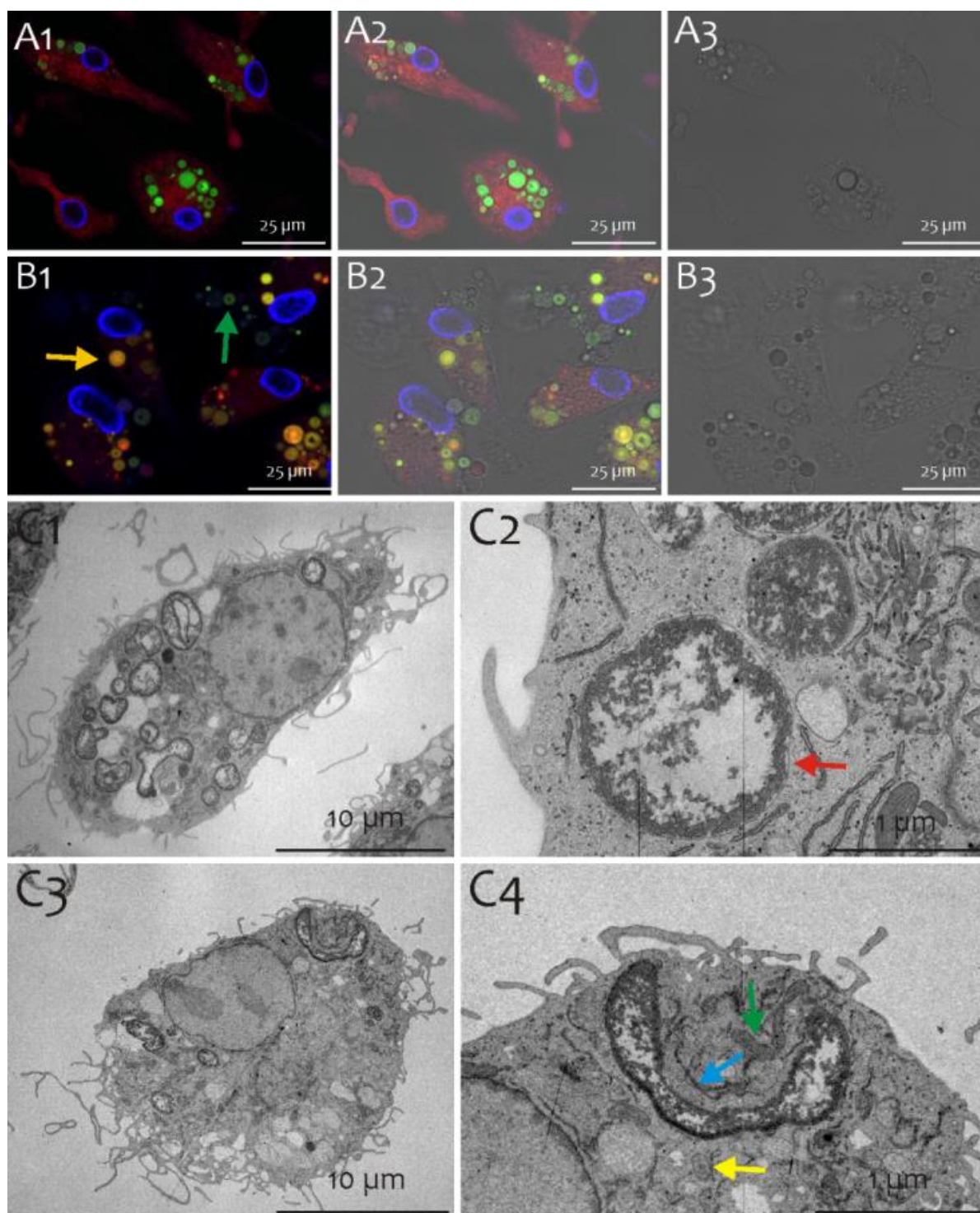
Figure 6. Assessment of cellular uptake of the spray dried polyelectrolyte microspheres by dendritic cells. **(A,B)** Confocal microscopy images of dendritic cells incubated with spray dried polyelectrolyte microspheres loaded with Alexa Fluor488-conjugated ovalbumin (green fluorescence). In row **A** the cellular cytoplasm was stained with CellTracker red (red fluorescence). In row **B**, the intracellular acidic vesicles (phagosomes, endosomes, lysosomes) were stained with LysoTracker Red (red fluorescene). In both cases the cell nuclei were stained with Hoechst (blue fluorescence). Column 1 shows the overlay between the blue, green and red channels, column 2 shows the overlay between the blue, green, red and DIC (differential interference contrast) channels, and column 3 shows the DIC channel. **(C)** Transmission electron microscopy images of spray dried polyelectrolyte microspheres internalized by dendritic cells after **(C1,C2)** 4 h and **(C3,C4)** 24 h of incubation.

Finally, we aimed to assess whether the encapsulated OVA is still available for processing upon internalization by DCs and, if so, whether the peptide fragments become cross-presented via a peptide-MHC class I complex. Following endocytosis, soluble exogenous antigens are generally cleaved by lysosomal proteases and presented via a peptide-MHC class II complex to CD4 T-cells. DCs also harbor the capacity to present exogenous antigens via MHCI, a feature called cross-presentation that is necessary to prime CD8 cytotoxic T cells capable of killing virally infected cells. However, cross-presentation of soluble antigens occurs extremely inefficiently but is dramatically augmented when the antigen is in a particulate form, as was found for several types of microparticulate antigen carriers.[8, 26, 27] To address whether this important feature also holds true for the spray dried polyelectrolyte microspheres, we incubated DCs with equivalent amounts of soluble OVA and OVA encapsulated in either hollow LbL capsules, PLGA microspheres or spray dried polyelectrolyte microspheres. After a 48 h incubation period, DCs were stained with the 25-D1.16 mAb which specifically recognizes the SIINFEKL OVA CD8 epitope complexed to MHC class I H-2Kb molecules.[28]

As shown in **Figure 7**, a dose-dependent increase in cross-presentation of encapsulated OVA was observed when compared to the soluble antigen. Spray dried particles were significantly more potent than PLGA and hollow capsules LbL in stimulating antigen cross-presentation. This is most likely due to the fact that the spray dried polyelectrolyte microspheres carry more antigen per particle compare to hollow LbL capsules and PLGA microspheres, thus delivering more antigen when a DC internalizes a particle. Moreover, the spray dried polyelectrolyte microspheres allow readily processing of the encapsulated antigen due to their fully hydrated structure, which is not the case for PLGA microspheres which gradually release their payload through surface-erosion-based degradation and therefore are incapable of inducing antigen cross-presentation within the experimental time frame of 48 h.
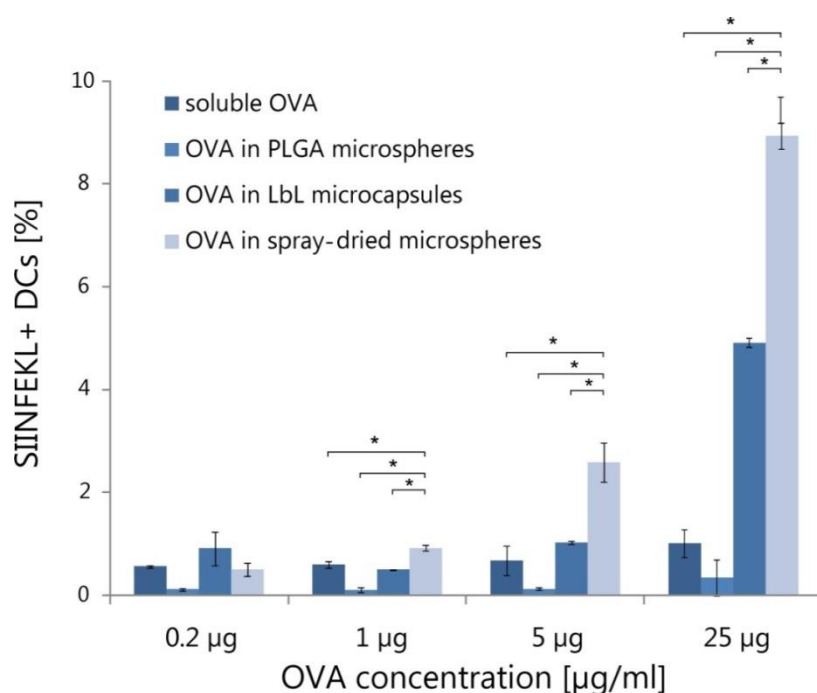
Figure 7. Cross-presentation of the SIINFEKL OVA CD8 peptide measured by FACS analysis on 25-D1.16 mAb stained DCs that were incubated with soluble OVA, OVA encapsulated in PLGA microspheres, OVA encapsulated in hollow LbL capsules and OVA encapsulated in spray dried polyelectrolyte microspheres. Experiments were run in triplicate (technical replicates). The polymers used for fabricating the LbL capsules were the same as those used for the spray-dried polyelectrolyte microspheres (i.e. DS/P$_L$ARG). An asterix "*" indicates the statistically significant groups.

4. CONCLUSION

In conclusion, we have demonstrated in this paper a one-step all-aqueous approach to encapsulate proteins into polyelectrolyte microspheres. The role of the polyelectrolytes is two-fold. The first is to form stable microspheres upon redispersion of the spray dried powder in water. Second, the polyelectrolyte framework suppresses the mannitol crystallization – used as additional excipient for spray drying – which is shown to be beneficial for both the bioactivity of encapsulated proteins as well as for the process yield. Furthermore, these data indicate that the spray drying process does not dramatically hamper intracellular proteases to enter the polyelectrolyte matrix and to subsequently process the antigen into peptide fragments allowing their presentation onto the DC surface. The observed cross-presentation paves the road to further develop this technology as vaccine delivery platform for insidious viral pathogens as well as cancer.

REFERENCES

1.   Jain, S.; Yap, W. T.; Irvine, D. J., Synthesis of protein-loaded hydrogel particles in an aqueous two-phase system for coincident antigen and CpG oligonucleotide delivery to antigen-presenting cells. Biomacromolecules 2005, 6, 2590-2600.

2.   Gokmen, M. T.; Du Prez, F. E., Porous polymer particles-A comprehensive guide to synthesis, characterization, functionalization and applications. Progress in Polymer Science 2012, 37, 365-405.

3.   Decher, G., Fuzzy nanoassemblies: Toward layered polymeric multicomposites. Science 1997, 277, 1232-1237.

4.   Caruso, F.; Caruso, R. A.; Mohwald, H., Nanoengineering of inorganic and hybrid hollow spheres by colloidal templating. Science 1998, 282, 1111-1114.

5.   Donath, E.; Sukhorukov, G. B.; Caruso, F.; Davis, S. A.; Mohwald, H., Novel hollow polymer shells by colloid-templated assembly of polyelectrolytes. Angew. Chem.-Int. Edit. 1998, 37, 2202-2205.

6.   Sukhorukov, G. B.; Brumen, M.; Donath, E.; Mohwald, H., Hollow polyelectrolyte shells: Exclusion of polymers and donnan equilibrium. J. Phys. Chem. B 1999, 103, 6434-6440.

7.   De Geest, B. G.; Vandenbroucke, R. E.; Guenther, A. M.; Sukhorukov, G. B.; Hennink, W. E.; Sanders, N. N.; Demeester, J.; De Smedt, S. C., Intracellularly degradable polyelectrolyte microcapsules. Adv. Mater. 2006, 18, 1005-+.

8.   De Koker, S.; De Geest, B. G.; Singh, S. K.; De Rycke, R.; Naessens, T.; Van Kooyk, Y.; Demeester, J.; De Smedt, S. C.; Grooten, J., Polyelectrolyte Microcapsules as Antigen Delivery Vehicles To Dendritic Cells: Uptake, Processing, and Cross-Presentation of Encapsulated Antigens. Angew. Chem.-Int. Edit. 2009, 48, 8485-8489.

9.   De Koker, S.; Lambrecht, B. N.; Willart, M. A.; van Kooyk, Y.; Grooten, J.; Vervaet, C.; Remon, J. P.; De Geest, B. G., Designing polymeric particles for antigen delivery. Chem. Soc. Rev. 2011, 40, 320-339.

10.   De Koker, S.; Naessens, T.; De Geest, B. G.; Bogaert, P.; Demeester, J.; De Smedt, S.; Grooten, J., Biodegradable Polyelectrolyte Microcapsules: Antigen Delivery Tools with Th17 Skewing Activity after Pulmonary Delivery. J. Immunol. 2010, 184, 203-211.

11.   De Cock, L. J.; Lenoir, J.; De Koker, S.; Vermeersch, V.; Skirtach, A. G.; Dubruel, P.; Adriaens, E.; Vervaet, C.; Remon, J. P.; De Geest, B. G., Mucosal irritation potential of polyelectrolyte multilayer capsules. Biomaterials 2011, 32, 1967-1977.

12.   De Geest, B. G.; De Koker, S.; Gonnissen, Y.; De Cock, L. J.; Grooten, J.; Remon, J. P.; Vervaet, C., A single step process for the synthesis of antigen laden thermosensitive microparticles. Soft Matter 2010, 6, 305-310.

13.   De Rose, R.; Zelikin, A. N.; Johnston, A. P. R.; Sexton, A.; Chong, S. F.; Cortez, C.; Mulholland, W.; Caruso, F.; Kent, S. J., Binding, Internalization, and Antigen Presentation of Vaccine-Loaded Nanoengineered Capsules in Blood. Adv. Mater. 2008, 20, 4698-+.

14.   Sexton, A.; Whitney, P. G.; Chong, S. F.; Zelikin, A. N.; Johnston, A. P. R.; De Rose, R.; Brooks, A. G.; Caruso, F.; Kent, S. J., A Protective Vaccine Delivery System for In Vivo T Cell Stimulation Using Nanoengineered Polymer Hydrogel Capsules. ACS Nano 2009, 3, 3391-3400.

15.   Balabushevich, N. G.; Sukhorukov, G. B.; Larionova, N. I., Polyelectrolyte multilayer microspheres as carriers for bienzyme system: Preparation and characterization. Macromol. Rapid Commun. 2005, 26, 1168-1172.

16.   Kreft, O.; Prevot, M.; Mohwald, H.; Sukhorukov, G. B., Shell-in-shell microcapsules: A novel tool for integrated, spatially confined enzymatic reactions. Angew. Chem.-Int. Edit. 2007, 46, 5605-5608.

17.   Wang, Y. J.; Caruso, F., Nanoporous protein particles through templating mesoporous silica spheres. Adv. Mater. 2006, 18, 795-+.

18. Stein, E. W.; Volodkin, D. V.; McShane, M. J.; Sukhorukov, G. B., Real-time assessment of spatial and temporal coupled catalysis within polyelectrolyte microcapsules containing coimmobilized mucose oxiase and peroxidase. Biomacromolecules 2006, 7, 710-719.

19. Dierendonck, M.; De Koker, S.; Cuvelier, C.; Grooten, J.; Vervaet, C.; Remon, J. P.; De Geest, B. G., Facile Two-Step Synthesis of Porous Antigen-Loaded Degradable Polyelectrolyte Microspheres. Angew. Chem.-Int. Edit. 2010, 49, 8620-8624.

20. Lynn, D. M.; Amiji, M. M.; Langer, R., pH-responsive polymer microspheres: Rapid release of encapsulated material within the range of intracellular pH. Angew. Chem.-Int. Edit. 2001, 40, 1707-1710.

21. Hulse, W. L.; Forbes, R. T.; Bonner, M. C.; Getrost, M., Influence of protein on mannitol polymorphic form produced during co-spray drying. International Journal of Pharmaceutics 2009, 382, 67-72.

22. Andya, J. D.; Maa, Y. F.; Costantino, H. R.; Nguyen, P. A.; Dasovich, N.; Sweeney, T. D.; Hsu, C. C.; Shire, S. J., The effect of formulation excipients on protein stability and aerosol performance of spray-dried powders of a recombinant humanized anti-IgE monoclonal antibody. Pharm. Res. 1999, 16, 350-358.

23. Vriezema, D. M.; Garcia, P. M. L.; Oltra, N. S.; Hatzakis, N. S.; Kuiper, S. M.; Nolte, R. J. M.; Rowan, A. E.; van Hest, J. C. M., Positional assembly of enzymes in polymersome nanoreactors for cascade reactions. Angew. Chem.-Int. Edit. 2007, 46, 7378-7382.

24. Yashchenok, A. M.; Delcea, M.; Videnova, K.; Jares-Erijman, E. A.; Jovin, T. M.; Konrad, M.; Mohwald, H.; Skirtach, A. G., Enzyme Reaction in the Pores of CaCO3 Particles upon Ultrasound Disruption of Attached Substrate-Filled Liposomes. Angew. Chem.-Int. Edit. 2010, 49, 8116-8120.

25. Javier, A. M.; Kreft, O.; Semmling, M.; Kempter, S.; Skirtach, A. G.; Bruns, O. T.; del Pino, P.; Bedard, M. F.; Raedler, J.; Kaes, J.; Plank, C.; Sukhorukov, G. B.; Parak, W. J., Uptake of Colloidal Polyelectrolyte-Coated Particles and Polyelectrolyte Multilayer Capsules by Living Cells. Adv. Mater. 2008, 20, 4281-4287.

26. Moon, J. J.; Suh, H.; Bershteyn, A.; Stephan, M. T.; Liu, H.; Huang, B.; Sohail, M.; Luo, S.; Um, S. H.; Khant, H.; Goodwin, J. T.; Ramos, J.; Chiu, W.; Irvine, D. J., Interbilayer-crosslinked multilamellar vesicles as synthetic vaccines for potent humoral and cellular immune responses. Nature Materials 2011, 10, 243-251.

27. Broaders, K. E.; Cohen, J. A.; Beaudette, T. T.; Bachelder, E. M.; Frechet, J. M. J., Acetalated dextran is a chemically and biologically tunable material for particulate immunotherapy. Proc. Natl. Acad. Sci. U. S. A. 2009, 106, 5497-5502.

28. Palankar, R.; Skirtach, A. G.; Kreft, O.; Bedard, M.; Garstka, M.; Gould, K.; Mohwald, H.; Sukhorukov, G. B.; Winterhalter, M.; Springer, S., Controlled Intracellular Release of Peptides from Microcapsules Enhances Antigen Presentation on MHC Class I Molecules. Small 2009, 5, 2168-2176.

CHAPTER 6

NANOPOROUS POLYELECTROLYTE VACCINE MICROCARRIERS – *IN VITRO* AND *IN VIVO* EVALUATION

CHAPTER 6

NANOPOROUS POLYELECTROLYTE VACCINE MICROCARRIERS – *IN VITRO* AND *IN VIVO* EVALUATION

1. INTRODUCTION

Formulating vaccine antigens into microcarriers has emerged as an attractive strategy to boost antigen-specific immune responses, in particular the cellular arm of the immune response.[1-3] Whereas soluble antigen is predominantly presented by dendritic cells (DCs; the most potent class of antigen presenting cells of our immune system) to CD4 T cells, antigen in the form of nano- and microparticles becomes presented to both CD4 and CD8 T cells, a process termed cross-presentation of exogenous antigen.[4] The reason for this is that particulate antigen is better recognized by DCs as being foreign, thereby altering the route of internalization and presentation of the antigen. The functional relevance of these processes lays in the fact that in presence of the correct cytokine stimuli, CD8 T cells can differentiate into cytotoxic T cells (CTLs) that can recognize and eliminate infected or malignant cells. The latter is of great importance for the development of vaccines against intracellular pathogens such as HIV, tuberculosis, malaria, … and for therapeutic anti-cancer vaccines.[5]

Many nano- and microparticulate vaccine formulation strategies have been reported in literature.[1-3] However, there remains a clear need for simple and scalable formulation strategies involving a minimal of batch operation and avoiding organic solvents and reactive chemistries. Additionally, when envisioning vaccines for the developing world and for pandemic vaccines, there is a particular interest for formulation that avoid the cold chain and do not require refrigerated conditions for transportation and long term storage.[6] In this regard, a dry powder formulation that can be reconstituted in aqueous medium only prior to administration would be highly beneficial.
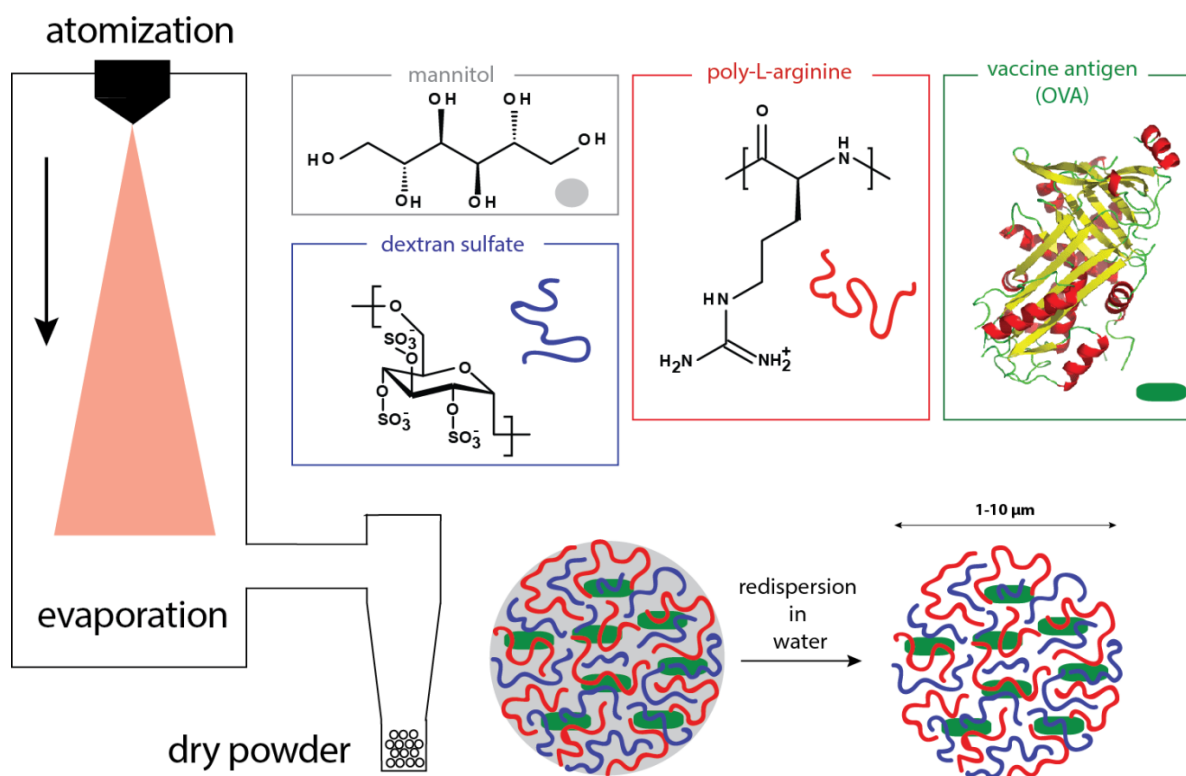
Figure 1. Schematic representation of the encapsulation of protein antigen in porous polyelectrolyte microparticles. As pore-former mannitol is used which instantaneously dissolves upon redisperion in aqueous medium, thereby creating a highly porous matrix.

Recently we have reported on a novel type of vaccine microcarriers based on oppositely charged polyelectrolytes that form stable microparticles via electrostatic interaction as schematically shown in **Figure 1**.[7-9] These microparticles were assembled by atomizing a diluted aqueous solution of the polyelectrolytes into a hot air stream. This spray drying process evaporates the water to yield solid microparticles. By adding protein antigen to the polyelectrolyte mixture prior to spray drying the antigen becomes encapsulated within the polyelectrolyte matrix and, interestingly, remains stably encapsulated upon redispersion of the microparticles in aqueous medium. Using dextran sulfate (DS) and poly-L-arginine (P$_L$ARG) as degradable polyanion/polycation we found it key to introduce a pore-former in our formulation. This is also illustrated in **Figure 1**. Mannitol is a hydrophilic component which is added in excess to the polyelectrolyte/protein mixture and becomes incorporated as well into the microparticles. Upon redispersion in aqueous medium the mannitol dissolved and leaches out, thereby creating a highly porous internal structure within the microparticles. For both the encapsulation of vaccine antigens and enzymes, the use of mannitol appeared crucial to preserve the bioactivity of these proteins *in vitro*. Indeed, mannitol is a known stabilizer in spray drying applications and the porous structure within the microparticles allows enzyme substrates or intracellular proteases to access encapsulated proteins much more efficiently.

In this chapter we aimed to explore the potential of the nanoporous polyelectrolyte microcarriers for vaccine delivery *in vitro* and *in vivo*. First we optimized the fabrication procedure by changing the spray dry parameters of gas flow and feed flow to obtain microspheres that are non-aggregated, with high particle recovery yield and size distribution below 10 µm to enhance cellular uptake while still assuring optimum encapsulation efficiency. Secondly we evaluated the potential of the microparticles to enhance antigen cross-presentation to CD8 T cells *in vitro*. Thirdly, we evaluated the microcarriers *in vivo* with respect to their tissue response and antigen specific immune response in mouse models.

2. MATERIALS AND METHODS

2.1. Materials

Mannitol was obtained from Cargill. Dextran sulfate (DS; MW: 9-20kDa), poly-L-arginine (P$_L$ARG; MW >70kDa), ovalbumin (OVA) were obtained from Sigma Aldrich. OVA-Alexa Fluor488 and phosphate buffered saline (PBS) were obtained from Invitrogen. All water used in the experiments was of Milli-Q grade.

2.2. Formulation optimization

The influence of spray drying parameters on the yield and shape of the particles was investigated by varying different process parameters. Spray drying was performed with a lab-scale Büchi B290 spray dryer equipped with a two-fluid nozzle (0.7 mm diameter). The setting of the inlet temperature was 120°C and gas flow varies between 0.23-0.75 bar. The mixtures were fed via a peristaltic feed pump at a feed flow of 1 ml/min to 10 ml/min. Dry powder was collected.

2.3. Preparation of the microparticles via spray drying

Mannitol, DS, OVA and P$_L$ARG were mixed in water in a 40/4/1/5 ratio at a total solid concentration of 1%. Two different adding sequences were compared. In the first case, 200 mg of mannitol, 20 mg of DS and 5 mg of OVA were dissolved in 20 ml water. Subsequently 25 mg of P$_L$ARG was dissolved in 5 ml water and was added in drops to the stirring mannitol/DS/OVA solution. Secondly, 200 mg mannitol and 20 mg DS was dissolved in 19 ml water, further P$_L$ARG was added analogously and finally 5 mg OVA was dissolved in 1ml water and added in drops. Fluorescent particles were prepared using a mixture of OVA with Alexa Fluor488 conjugated ovalbumin in a 50:1 ratio. Spray drying was performed with a lab-scale Büchi B290 spray dryer equipped with a two-fluid nozzle (0.7 mm diameter). The setting of the inlet temperature was 120°C and gas flow 0.75 bar. The mixtures were fed via a peristaltic feed pump at a feed flow of 1 ml/min. Dry powder was collected.

2.4. Particle characterization

Laser diffraction was performed on a Malvern Mastersizer equipped with an 300RF objective. Scanning Electron Microscopy (SEM) was conducted on a Quanta 200 FEG FEI scanning electron microscope. Samples were sputtered with a palladium-gold layer prior to imaging. Transmission electron microscopy was performed on a JEOL 1010 instrument. Confocal microscopy was conducted on a Leica SP5 microscope equipped with a 63X oil immersion objective.

2.5. *In vitro* and *in vivo* experiments

2.5.1. Cell lines and animals

C57BL/6 mice were obtained from Janvier. OT-I transgenic mice (C57BL/6) were purchased from Harlan. Mice were housed under specific-pathogen-free conditions. All animal experiments were approved by the Local Ethical Committee of Ghent University. The immortalized mouse dendritic cell line DC2.4 was a kind gift from Prof. Dr. Ken Rock (Dana-Farber Cancer Institute, Boston, MA, USA). Bone-marrow-derived DCs were generated by flushing tibia and femurs of 2–4 months old C57BL/6 mice. After red blood cell lysis, cells were cultured in complete RPMI (Roswell Park Memorial Institute) medium containing 20 ng/mL GM-CSF (granulocyte macrophage colony-stimulating factor) for 6–8 days.

2.5.2. Cell toxicity assay

The cytotoxicity of the spray dried particles was assessed according to De Koker et al.[10] DC2.4 cells were grown and seeded in a 96 well plate at a density of 5×10^3 cells/well and incubated with different concentrations of the respective samples for 24 hours. Afterwards, the medium was refreshed and cells were cultured for another 48 hours. Medium was removed and MTT (3-(4,5-dimethylthiazol-2-yl)-2,5-diphenyltetrazolium bromide) was added. MTT is reduced by mitochondrial dehydrogenases of living cells into an insoluble purple formazan dye. After 4 hours of incubation at 37°C, cells are solubilized by dimethylsulfoxide (DMSO) and the released, solubilized formazan is measured spectrophotometrically at 590 nm. The absorbance is a measure of the viability of the cells.

2.5.3. In vitro microparticle uptake

For confocal microscopy experiments, DC2.4 were seeded in 8 well microscopy chambers (Nunc) at a density of 50×10^3 cells per well and allowed to adhere overnight. Subsequently, OVA-Alexa Fluor488 loaded- microparticles were added and the cells were further cultured for 24 h. Finally, the cells were

washed with PBS and fixated with 4% paraformaldehyde. Prior to imaging the cells were stained with Hoechst and Alexa Fluor 647-conjugated cholera toxin subunit B.

For flow cytometry, DC2.4 cells were seeded in 24 well plates at a density of 10^5 cells per well and allowed to adhere overnight. Subsequently, OVA-Alexa Fluor488 loaded microparticles (10 µL of a 10 mg/ml suspension) were added and the wells were cultured for another 24 h. Finally, the cells were washed, detached from the wells and stained with Live/Dead® fixable red dead cell stain kit (Life technologies) for 30 min on ice to exclude dead cells from the analysis. Cells were acquired on a BD Accuri C6 flow cytometer and analyzed with FlowJo. As a negative control unpulsed DC2.4 cells were used. Doublets were discriminated by forward/side scatter gating.

2.5.4. In vitro antigen-presentation assay

Cell suspensions of OVA-specific CD8 T cells were prepared from spleen and lymph nodes from OT-I mice. Single cell suspensions were prepared, and CD8 T cells were isolated from the suspensions using Dynal mouse CD8 negative isolation kit (Invitrogen) according to the manufacturers' instructions and subsequently labeled with CFSE (carboxyfluorescein diacetate succinimidyl ester). DCs obtained from bone marrow of C57BL/6 mice were pulsed with serial dilutions of the respective samples (corresponding to 0.2, 2 and 5µg/ml OVA) for 24 h, washed, counted and subsequently co-cultured with OT-I T cells at different DC:T cell ratios (1:5; 1:10; 1:20 and 1:100) for 48 h in round bottomed well plates. After 48 h, the division of the OT-I T cells was measured by flow cytometry using a BD LSR II.

2.5.5. Readout of in vivo antibody response (ELISA)

Mice were subcutaneously vaccinated twice with a 3 week interval with 100 µL containing 20 µg of either soluble or encapsulated OVA. For the detection of anti-OVA antibodies, blood samples were collected from the ventral tail vein. Maxisorp (Nunc) plates were precoated with OVA (10 mg/ml) overnight. Wells were blocked with 200 µL PBS 1% (w/v) bovine serum albumin (BSA) (Sigma Aldrich) for 2 hours at room temperature. Serial dilutions of serum in PBS 1% BSA were added and incubated for 2 hours at room temperature. Subsequently goat anti-mouse IgG1-HRP (Southern Biotech; HRP= horseradish peroxidase) diluted in PBS (1/5000) was added for 1 hour at room temperature. Plates were washed 3 times between each step with PBS 0.1% Tween20 (Sigma Aldrich). Peroxidase activity was measured using 50 µL/well TMB substrate (BD Opteia™, BD biosciences) and optical densities were read at 450 nm after stopping the reaction by adding 25 µL/well 1M H_2SO_4. Data show antibody titers of individual mice.

2.5.6. Readout of in vivo cellular immune response (ELISA)

The amount of IFN-γ in the supernatant of splenocytes incubated with the MHCI or MHCII epitope of OVA was determined using the mouse IFN-γ Ready-Set-Go!® ELISA kit (eBioscience) according to the manufacturer's instructions. In detail, Maxisorp (Nunc) plates were precoated with capture antibody in coating buffer overnight at 4°C. Wells were blocked with 200 µL/well of 1x Assay diluent for 1 hour at room temperature. Serial dilutions of standard concentrations and samples (supernatants of splenocytes) were added and incubated at 4°C overnight. Then, biotin-conjugated detection antibody diluted in 1x Assay diluent was added and subsequently 100 µL/well of avidin-HRP diluted in 1x assay diluent was added and incubated for 30 minutes at room temperature. Plates were washed 3 times between each step with PBS 0.05% Tween20 (Sigma Aldrich). Peroxidase activity was measured using 100 µL/well TMB substrate (Substrate solution) and optical densities were read at 450 nm after stopping the reaction by adding 50 µL/well 2M H_2SO_4.

2.5.7. Readout of in vivo cellular response (ELISPOT)

Splenocytes were harvested three weeks after the booster immunization. Suspensions of 2×10^5 splenocytes were cultured onto IFN-γ ELISPOT plates (Diaclone) in triplicate and restimulated with 5 mg/mL of either the OVA MHCI epitope peptide SIINFEKL or the OVA MHCII epitope peptide ISQAVHAAHAEINEAGR (both Anaspec) and incubated for 24 hours at 37°C in a CO_2 incubator. Medium alone (100µL) or concanavolin A (100 µL, 2 µg/ml) were used as negative or positive controls, respectively. Then, biotinylated detection antibody was added and incubated at room temperature for 1 h 30 min and subsequently 100 µL/well of streptavidin-AP(Alkaline phosphatase) conjugate was added and incubated for 1 hour at room temperature. Plates were washed 3 times between each step with PBS 0.05% Tween20 (Sigma Aldrich). Alkaline phosphatase activity was determined using 100 µL/well BCIP/NBT (5-bromo-4-chloro-3-indolyl-phosphate/nitro blue tetrazolium) substrate and spots were developed after a 5-10 minutes incubation period. The frequency of the resulting coloured spots were counted using an Immunospot ELISPOT reader (AID).

2.5.8 In vivo tissue response

OVA-Alexa Fluor488 loaded microparticles were injected subcutaneously in the flanks of mice. At different time intervals mice were sacrificed and the injection site was dissected. Tissue samples were fixed in 4% paraformaldehyde in PBS, dehydrated in ethanol, embedded in paraffin and 5 µm sections were cut with a microtome. After deparaffinisation, sections were either mounted with DAPI-containing Vectashield mounting medium (VectorLabs) or stained with haematoxylin and eosin and then mounted with Vectashield.

3. RESULTS AND DISCUSSION

3.1. Formulation and process optimization

In a first series of experiments we aimed at exploring the effect of formulation and process conditions on the microparticulate vaccine formulations. As depicted in **Figure 1**, dextran sulfate (DS) was used as negatively charged polyelectrolyte (i.e. polyanion) and poly-L-arginine (P_LARG) was used as positively charged polyelectrolyte (i.e. polycation). Ovalbumin (OVA) was used as model vaccine antigen, it has a Mw ~ 43 kDa and an isoelectric point of 4.5 meaning that at neutral pH it will bear an overall negative charge. The three major parameters that reflect the quality of the microparticulate formulations are:

- ***Particle recovery***: The amount of dry microparticles that is collected in the recipient after the cyclone in the spray drier.

- ***Particle integrity***: The ability of the obtained dry power to be reconstituted in aqueous medium into a monomodal suspension of individual non-aggregating and non-disintegrating microparticles.

- ***Encapsulation efficiency***: The fraction of protein antigen that is, upon redispersion in aqueous medium, retained within the microparticles and is not released into the outer medium.

First, we varied the relative amount of mannitol that was added to the solution prior to spray drying. **Table 1** summarizes the ratios that were used and the outcome of the spray drying experiments. The lower mannitol to antigen ratios, or absence of mannitol lead to poor recovery due to sticking of the powder to the wall of the spray drying equipment. This is in analogy with the common use of mannitol in pharmaceutical technology to enhance the yield of spray drying,[11] owing to its excellent flowing capability. However, too high mannitol to antigen ratios yielded particles that did not retain their spherical morphology upon redispersion in water and disassembled into smaller polyelectrolyte coacervates and released a significant amount of antigen into the external medium. These findings prompted us at using a mannitol/DS/P_LARG/OVA ratio of 200/20/25/5 for further experiments. Interestingly, this approximate ratio of the respective compounds is similar to our previous work on hollow Layer-by-Layer capsules where porous calcium carbonate microparticles were loaded with OVA and subsequently coated with alternating layers of DS and P_LARG followed by dissolution of the calcium carbonate core templates.[10, 12-16] Evidently, in the present work the single calcium carbonate pore former (which creates capsules with a hollow void) is replaced by mannitol that creates a nanoporous internal structure as described earlier in **CHAPTER 5**.

Table 1. Influence of the mannitol to antigen ratio[1] on the quality of the spray dried microparticulate formulations.

Mannitol:Antigen ratio	Particle Recovery	Particle integrity	Encapsulation efficiency
0:5	-	++	++
50:5	+	++	++
200:5	++	++	++
500:5	++	-	-

[1]Formulations were spray dried on a 25 mL scale composed of respectively 20/25/5 mg of DS/P$_L$ARG/OVA. The ratio is expressed as wt %.

Secondly, we aimed at investigating the effect of processing conditions on particle recovery. Using the above-mentioned composition of the formulation, spray drying was performed a different values of the flow rate (i.e. the flow at which the liquid is fed to the nozzle) and pressure of the atomizing air stream. The graph in **Figure 2A** depicts particle recovery as function of the different processing parameters. Increasing the flow rate leads to a decrease in particle recovery. This can be explained by the higher the feed pump rate, as for a higher throughput, more energy is needed to evaporate the water to form solid particles. When the pump rate is too high, wet and sticky particles are obtained that adhere to the glass wall of the spray drier, thereby decreasing the yield. When the feed flow was kept constant (1ml/min), a higher yield was obtained with a higher gas flow. Based on these findings, experiments were continued using a flow rate of 1 mL/min and an air pressure of 0.75 bar. To verify that these formulation and processing conditions afforded the proper production of microparticles scanning electron microscopy (SEM) was used to characterize the microparticles after spray drying. As shown in **Figure 2B**, perfectly spherical shaped microparticles are obtained with a size below 10 μm. After redispersion in water, the size distribution (**Figure 2C**), as determined by laserdiffraction remained below 10 μm and transmission electron microscopy (TEM; **Figure 2D**), recorded from epoxy-embedded and ultramicrotomed microparticles, revealed a highly porous internal structure of the particles that is created upon dissolution of the mannitol into aqueous medium.
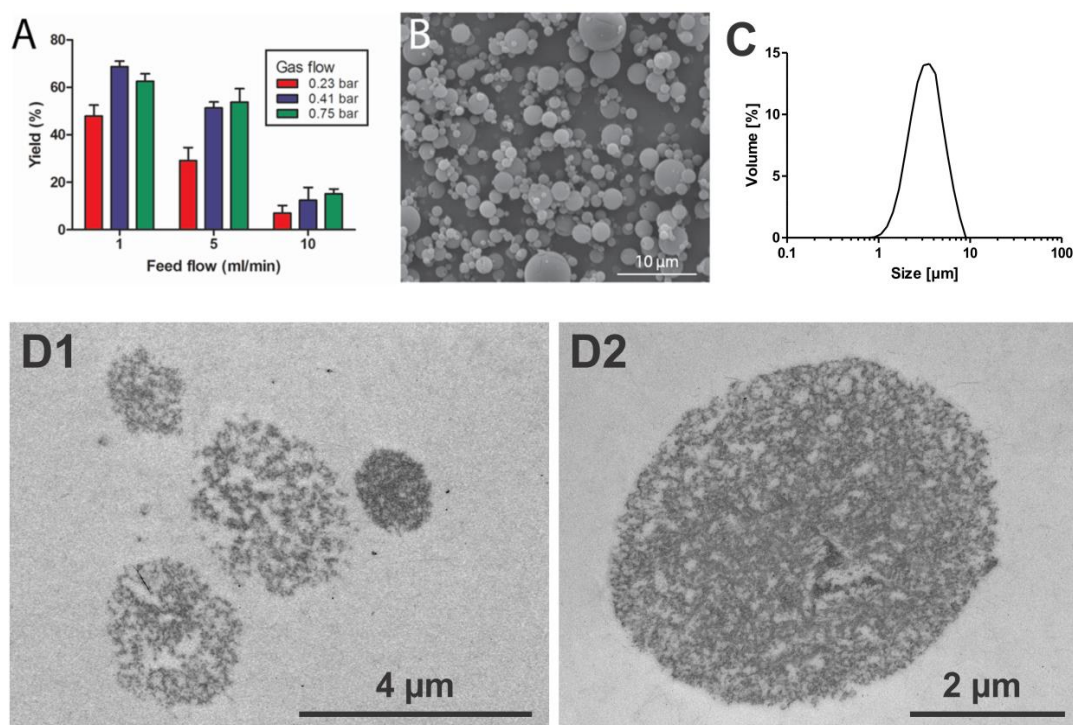
Figure 2. (A) Microparticle recovery expressed as the weight percentage of the microparticles collected in the recipient after the cyclone to the original dry weight of the formulation prior to spray drying. **(B)** Scanning electron microscopy image of the spray dried microparticles before resuspension in aqueous medium. **(C)** Size distribution measured by laser diffraction of the microparticles redispersed in water. **(B)** and **(C)** were recorded from microparticles produced at optimal formulation and processing conditions. **(D)** Transmission electron microscopy images of epoxy-embedded and ultramicrotomed porous microparticles obtained after resuspension in aqueous medium.

3.2. Exploring the influence of the sequence of addition

Here we aimed to investigate whether the sequence of addition of the respective components prior to spray during can affect the overall charge, encapsulation efficiency, spatial ordering of the antigen and further, on in this work, immuno-biological properties. To do so, we prepared microparticles as listed in **Table 2**. Besides OVA loaded microparticles we also prepared empty microparticles where we used different dextran sulfate to poly-L-arginine ratios, to test whether the surface charge of the microparticles can be modulated. We observed that changing the ratio of dextran sulfate to poly-L-arginine allowed to shift the zeta-potential from positive to negative depending on whether the polyanion (i.e. dextran sulfate) or the polycation (i.e. poly-L-arginine) is in excess. These latter two microparticles without OVA will be used further on in this work in control experiments where soluble OVA is added to these empty particles.

Table 2. Influence of the sequence of addition on the formulation properties[1]

Formulation	Sequence	ratio (wt.%)	ζ-potential	Encapsulation efficiency
1	mannitol/DS/OVA/P$_L$ARG	200/20/5/25	42 ± 3 mV	110 ± 11 %
2	mannitol/DS/P$_L$ARG/OVA	200/20/25/5	-30 ± 4 mV	110 ± 10 %
3	mannitol/DS/P$_L$ARG[2]	200/20/25	40 ± 1 mV[3]	99 ± 0.1 %
			26 ± 1 mV[4]	
4	mannitol/DS/P$_L$ARG[2]	200/25/20	-43 ± 1 mV[3]	100 ± 0.2 %
			-43 ± 1 mV[4]	

[1] Formulations were spray dried on a 25 mL scale. (n=3)

[2] Soluble OVA was added after spray drying.

[3] ζ-potential measured before soluble OVA was added.

[4] ζ-potential measured after soluble OVA was added.

The ζ-potential of the OVA-loaded microparticles also strongly depended on the sequence in which the respective components are added prior to spray drying. Indeed, when OVA is added last, a negative ζ-potential value of -30 mV was measured whereas an outspoken positive value of 42 mV was measured when P$_L$ARG was added last. These findings suggest that the component that was added last would be distributed more at the surface of the particles. To confirm this hypothesis, microparticles were spray dried using green fluorescent (i.e. Alexa Fluor488) labelled OVA, and subsequently imaged by fluorescence microscopy. These images, shown in **Figure 3**, confirm that when OVA is added before P$_L$ARG (i.e. DS/OVA/P$_L$ARG(+)), microparticles are obtained with OVA homogenously distributed within the volume of the microparticles. This is in agreement with our previous findings in chapter 5. However, when OVA is added after P$_L$ARG (i.e. DS/P$_L$ARG/OVA(-)), it is preferentially located at the periphery of the particles. Additionally, the OVA distribution does not appear to be homogenous and bright spots of complexed OVA appear on the surface of the particles.

As empty particles will be used further on in this work for control experiments, we also wanted to investigate the interaction between these empty microparticles and soluble OVA. Therefore, we incubated both the positively and the negatively charged microparticles with soluble Alexa Fluor488 –conjugated OVA (i.e. sOVA-AF). Subsequently, the microparticles were imaged by fluorescence microscopy and the amount of unbound OVA was measured in the supernatant after centrifugation of the microparticles. In addition, also the ζ-potential after incubation with OVA was measured. As listed in **Table 2** and confirmed in **Figure 3**, both negatively and positively charged microparticles are capable of binding soluble OVA. However, in both cases aggregation was observed. This was most severe in case of positively charged microparticles that were likely subjected to bridging flocculation

upon addition of negatively charged OVA. Additionally, in both cases OVA was predominantly located at the periphery of the microparticles.
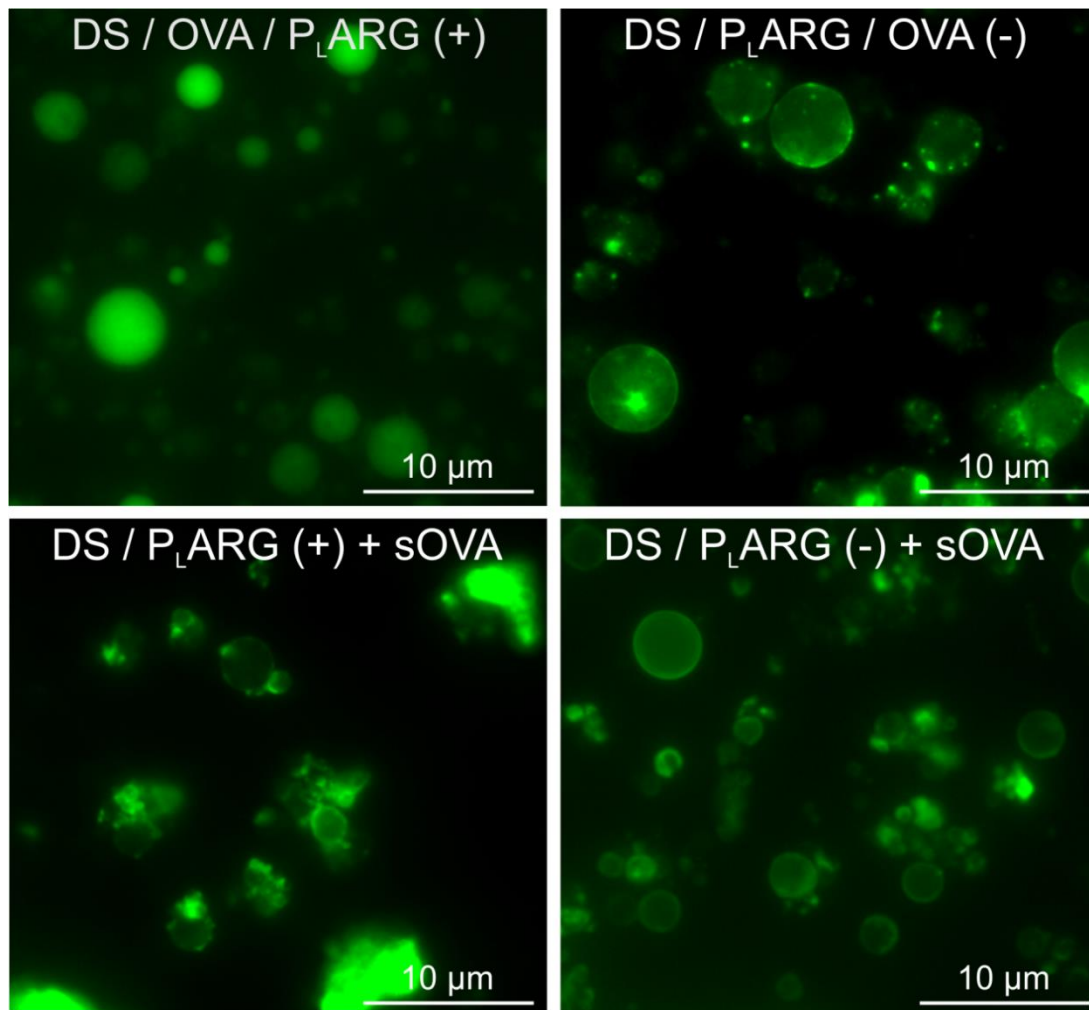

Figure 3. Fluorescence microscopy images of the different spray dried microparticle formulation either encapsulating OVA-Alexa Fluor488 or with OVA-Alexa Fluor488 added in solube form (i.e. sOVA-AF) to empty microparticles.

3.3. *In vitro* interaction with dendritic cells

In a first series of *in vitro* cell culture experiments we assessed whether the ζ-potential of the particles influences uptake by dendritic cells and possible cytotoxic effects. For these experiments we have chosen to use the immortalized mouse dendritic cell line DC2.4 as this is an excellent model to study cell uptake and have a prolonged lifetime than the primary DCs that will be used later on this work for investigating immuno-biological aspects. Cells were incubated overnight with microparticles, stained with a live/dead reagent and cells were analyzed by flow cytometry. Doublets and multiplets (i.e. clusters of multiple cells/particles instead of single cells) were discriminated by forward/side scatter gating and the live/dead reagent was used to select the living cells. The final

step in the gating strategy is plotting the fluorescence channel used for the detection of the microparticles (labelled fluorescent with OVA-Alexa Fluor488). Unpulsed DC2.4 cells were used as a negative control. As shown in **Figure 4B**, both positively and negatively charged microparticles were associated with DCs without any significant differences depending on the surface charge of the microparticles. Confocal microscopy (**Figure 4A)** was used to confirm that indeed the microparticles were taken up by the cells and not just adhered to the cell surface.
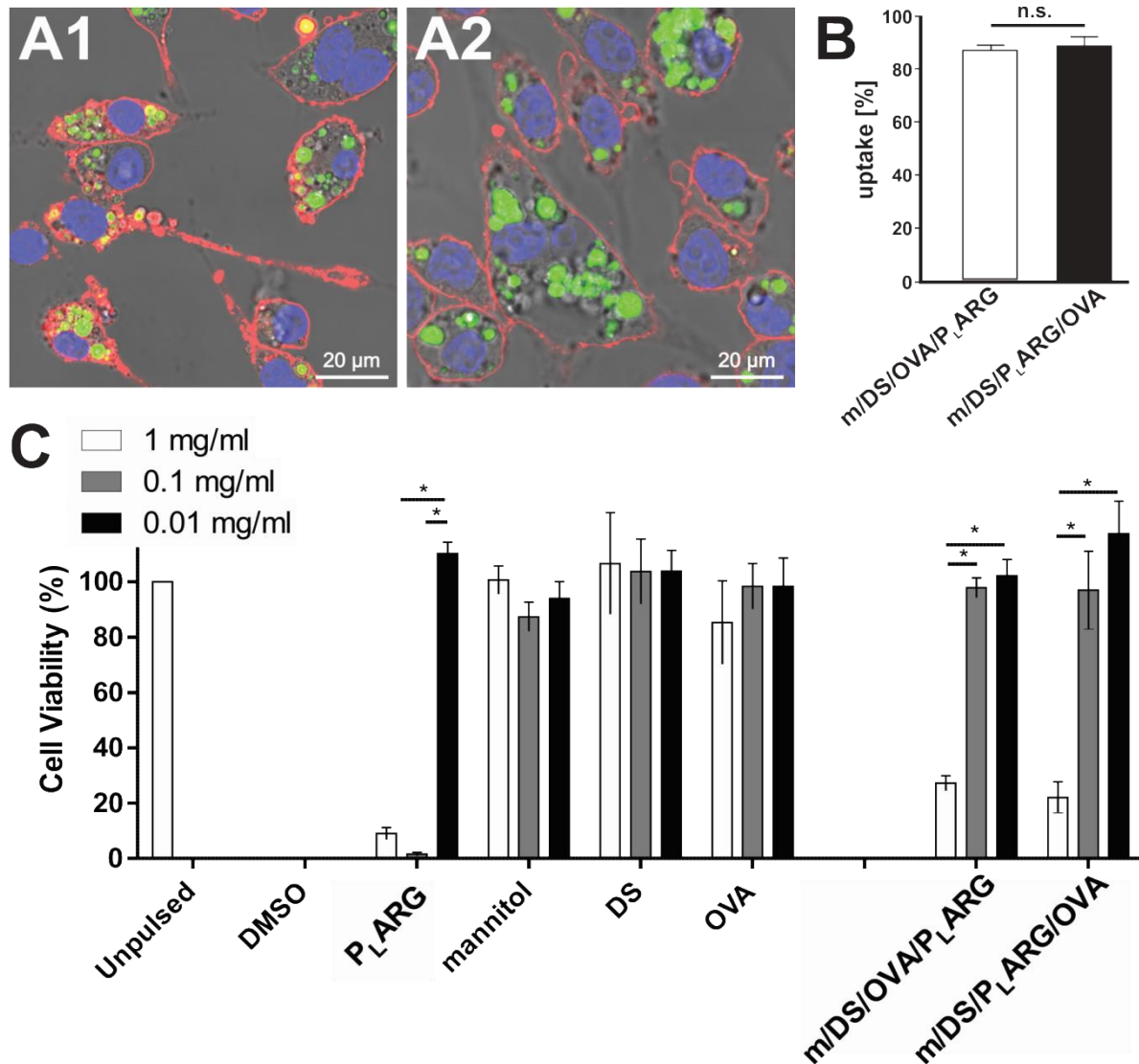
Figure 4. (A) Confocal microscopy images of DC2.4 cells incubated with OVA-Alexa Fluor488 loaded microparticles. **(A1)**: DS/OVA/P$_L$ARG and **(A2)**: DS/P$_L$ARG/OVA. The cell membrane was stained with Alexa Fluor647-conjugated cholera toxin subunit B and cell nuclei were stained with Hoechst. The images show an overlay with the DIC channel. **(B)** Quantification of *in vitro* uptake of microparticles by DC2.4 cells, measured by flow cytometry. **(C)** Cell toxicity, measured by MTT assay, of the microparticles and their respective components. (n=6, *: p<0.05).

Subsequently, MTT assay was used to investigate *in vitro* cytotoxic effects of the microparticles and their components on DCs. As shown in **Figure 4C**, DS, mannitol and ovalbumin are non-toxic. Contrary, P$_L$ARG significantly reduces cell viability over a broad concentration range. However, the electrostatic complexed microparticles only induce cell toxicity at elevated (i.e. 1mg/mL) concentrations. This is in accordance to recent observations by our research group on the effect of complexation on the *in vivo* mucosal irritation potential of polyelectrolytes. Indeed, whereas soluble polyelectrolytes, both polyanions and even more severely polycations, do induce mucosal irritation, this was fully suppressed in case of polyelectrolyte complexes. [17]

3.4. *In vitro* T cell presentation and T cell expansion

To assess the potential of the microparticles to enhance cross-presentation of antigen we performed an *in vitro* CD8 T cell presentation assay. For these experiments we used primary mouse DCs derived from bone marrow. As model antigen ovalbumin (OVA) was used. DCs were pulsed with either soluble OVA or encapsulated OVA. Both positively and negatively charged particles were evaluated. Subsequently, the DCs were co-cultured with OT-I cells, which are CD8 T cells that express the transgenic T cell receptor for MHCI complexed to the OVA CD8 peptide SIINFEKL. Prior to co-culturing the OT-I cells were stained with CFSE to allow for assessing subsequent cell division by flow cytometry.

A dose-response experiment was performed by pulsing DCs with different concentrations of soluble and encapsulated OVA. Also multiple DC to T cell ratios were evaluated. The gating strategy for flow cytometry analysis of the CD8 T cell proliferation is shown in **Figure 5A**. As shown by the flow cytometry histograms in **Figure 5B**, soluble OVA only marginally induces T cell proliferation. Contrary, encapsulated OVA strongly promotes antigen cross-presentation. For OVA concentrations of 2 and 5 μg/mL, DS/OVA/P$_L$ARG and DS/P$_L$ARG/OVA microparticles are equally potent in inducing T cell division. However, at a low OVA dose of 0.2 μg/mL only DS/P$_L$ARG/OVA microparticles are able to promote T cell proliferation (**Figure 5B and C**). In addition to measuring T cell expansion also cytokine (i.e. IFNγ, IL2, IL13, IL17) secretion in the supernatant of the DC – T cell co-cultures was measured. As shown in **Figure 5D**, the microparticles elicit the secretion of the cytokines IFNγ, IL-13 and IL-17, cytokines produced by Th1, Th2 and Th17 cells respectively. In the induction of an adaptive immune response IL-2 is produced by activated CD4 and CD8 T cells and is responsible for their proliferation.[18] The measured cytokines are indicative for a broad immune response. These findings firmly underline the ability of microparticulate formulation of antigen to dramatically enhance antigen presentation. The observation that microparticles with OVA situated at their periphery performed slightly better

than microparticles with OVA more embedded in their interior might be due to a higher availability of the OVA for processing upon cellular uptake within the timeframe of our experimental *in vitro* set-up.
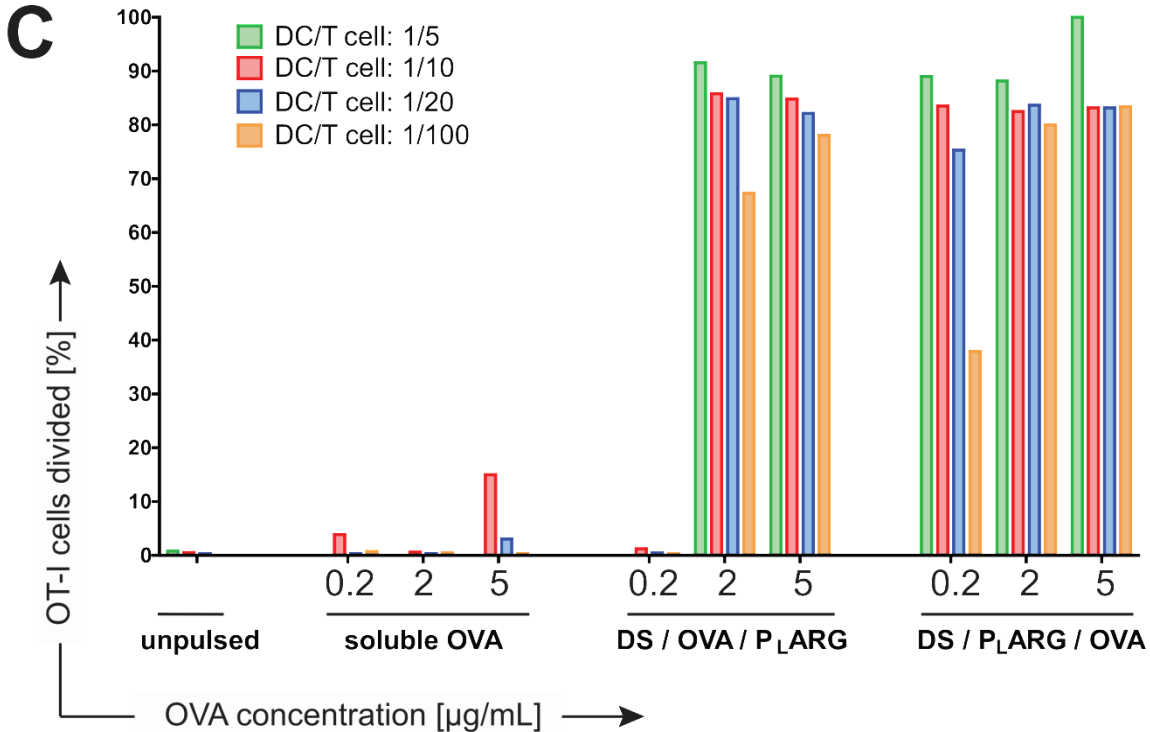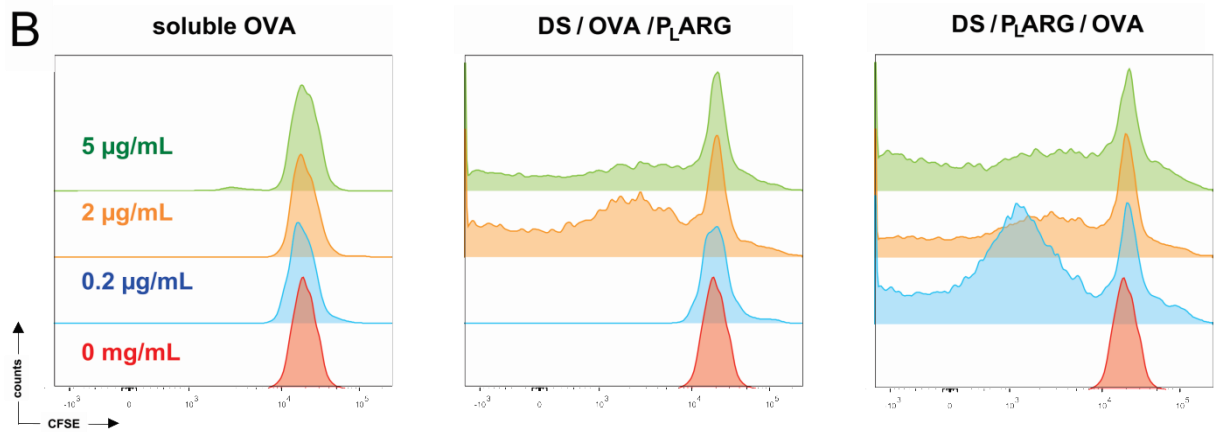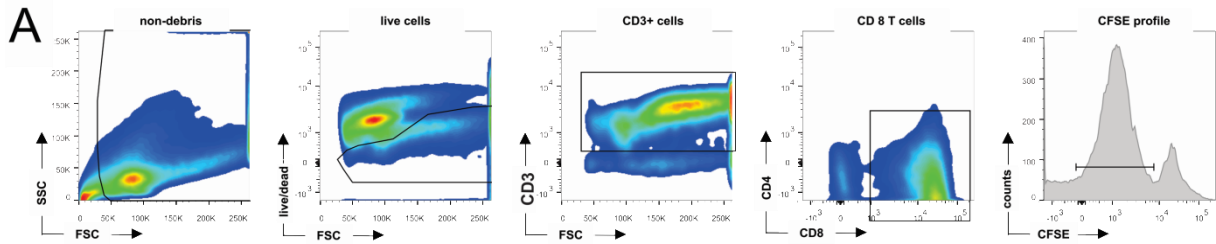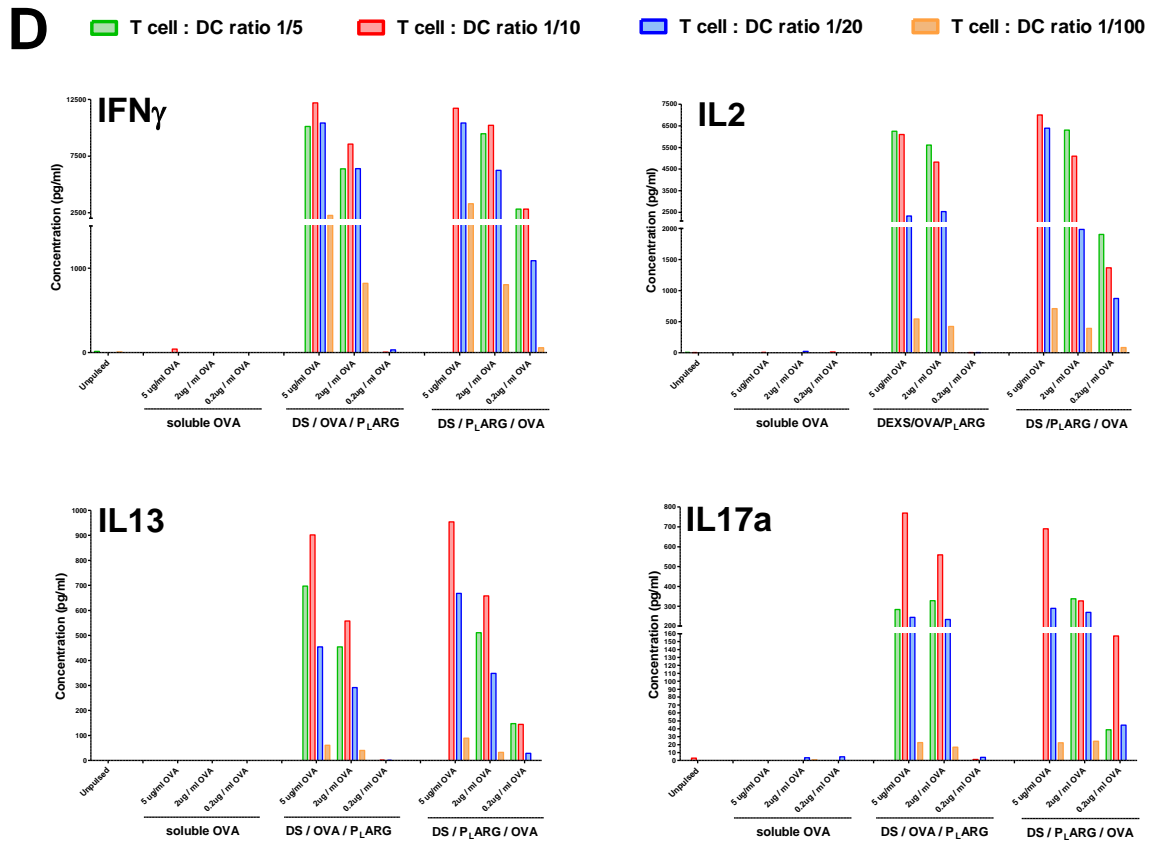
Figure 5. (A) Flow cytometry gating strategy to assess OT-I cell proliferation. **(B)** Flow cytometry histograms of OT-I proliferation in response to co-culturing with DCs pulsed with soluble OVA or encapsulated OVA at different OVA concentration. The OT-I cell to DC ratio was 1:20. In **(C)** Quantitative representation of OT-I cells division as shown in the gating strategy in panel **(A)**. **(D)** Cytokine secretion measured by ELISA in the supernatant of the DC – T cell co-cultures.

3.5. *In vivo* evaluation – tissue response

In a first series of *in vivo* experiments we screened the tissue response upon subcutaneous injection of the microparticles. Mice were subcutaneously injected with DS/OVA/P$_L$ARG microparticles and at different time intervals animals were sacrificed and the injection spot was dissected and analysed by haematoxylin and eosin (H&E) staining and confocal fluorescence microscopy. For the latter microparticles loaded with (green fluorescent) OVA-Alexa Fluor488 were used. **Figure 6** shows the corresponding micrographs. All series of images show a gradual cellular influx into the injected volume of microspheres. Importantly, no pronounced inflammation is observed and neovascularization and tissue necrosis remained absent. This suggest that injection of these microspheres does not induce a strong inflammatory response and are fairly well tolerated *in vivo*. Importantly, as indicated by the dashed contours in the panel corresponding to the 14 day time point, microparticles also become internalized by cells *in vivo*.
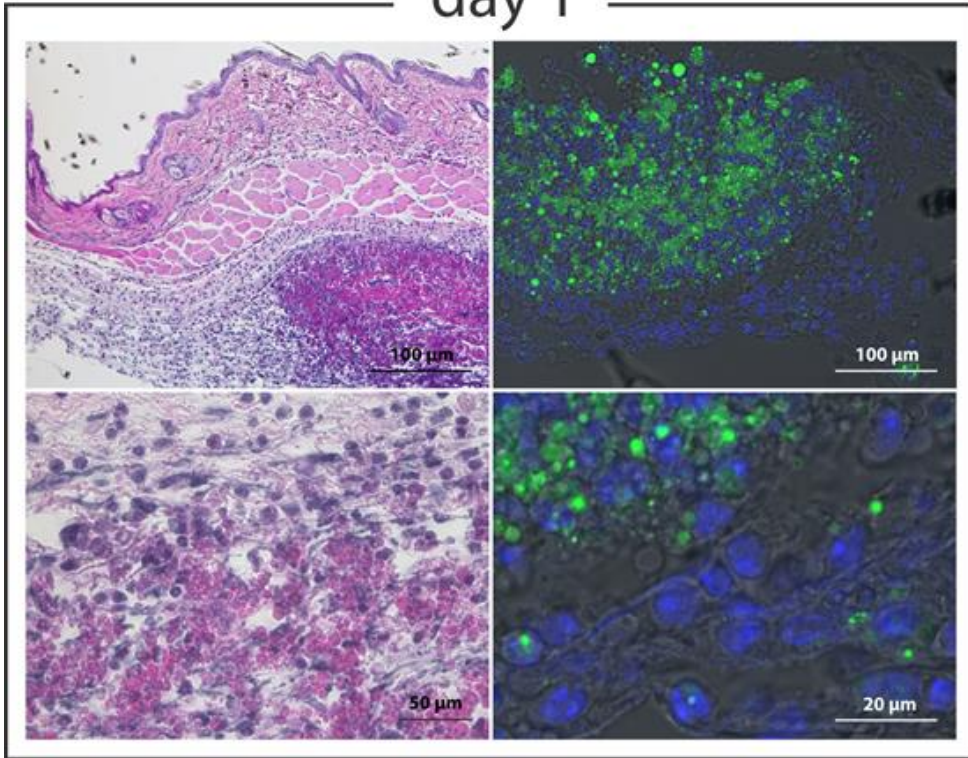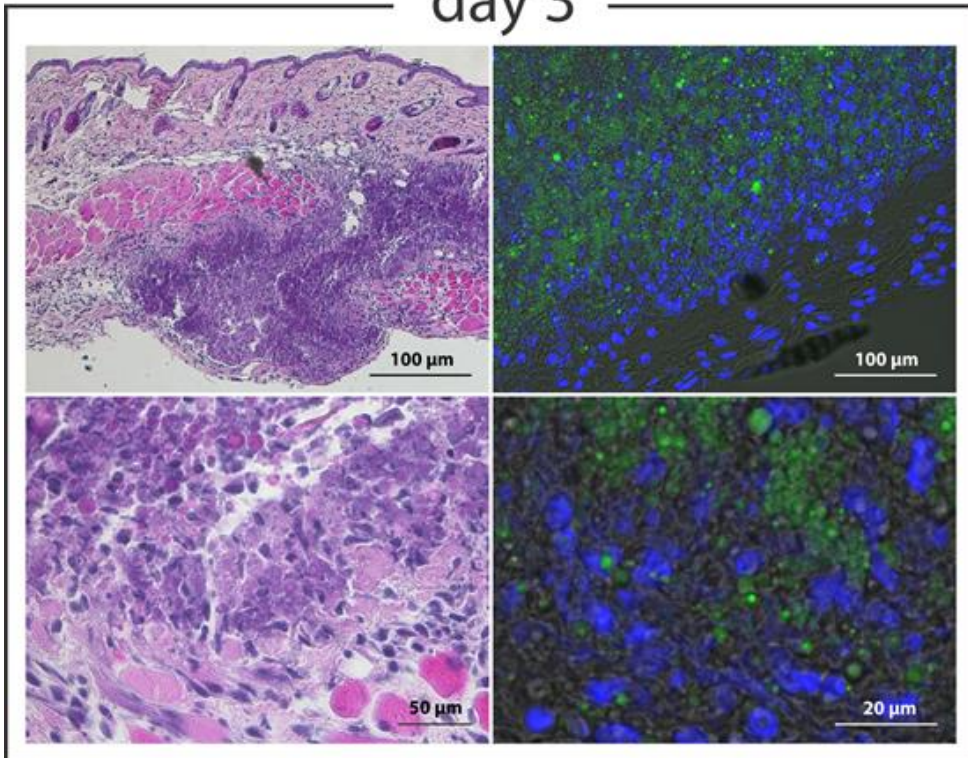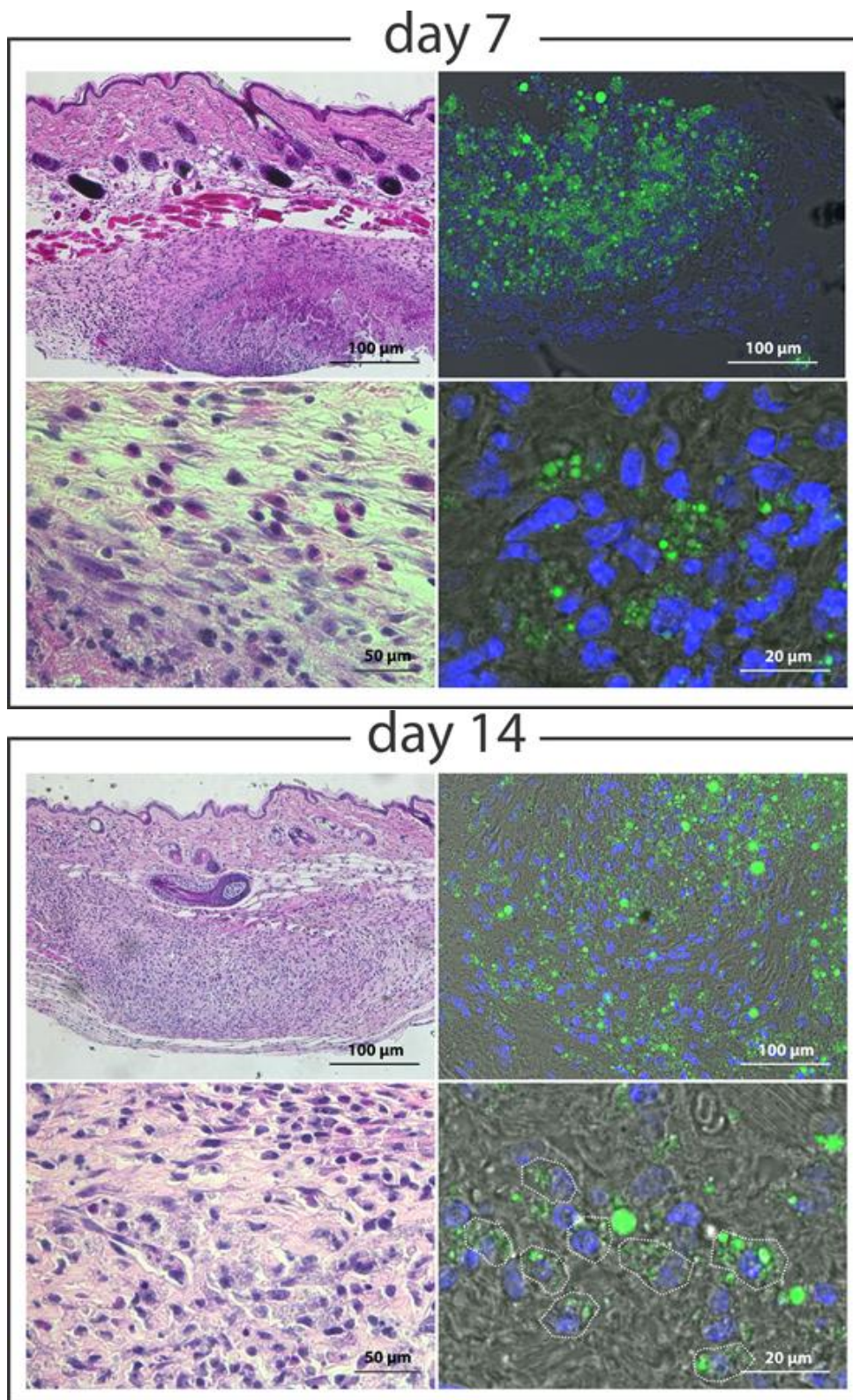
Figure 6. H&E staining (left panels) and confocal fluorescence (right panels) microscopy images recorded from tissue sections collected from the injection spot. Confocal images were stained with Hoechst to visualize the cell nuclei in blue. Green fluorescence originates from OVA-Alexa Fluor488 that was encapsulated within the microparticles. The confocal images also include the overlay with the DIC channel. The dashed contours in the day 14 pannel indicate cells that have internalized microparticles.

3.6. *In vivo* evaluation – antigen specific immune response

The previous paragraph confirmed that antigen encapsulated in porous polyelectrolyte microparticles is highly efficiently cross-presented by DCs to CD8 T cells *in vitro*. Additionally, *in vivo* low inflammatory responses were observed upon injection of the microparticles. These encouraging findings prompted us at further investigating the potential of the porous polyelectrolyte microparticles at enhancing antigen-specific immune responses *in vivo*.

Mice (in cohort of 5) were immunised with either soluble OVA or encapsulated OVA following a prime-boost scheme with a 3 week interval. The microparticle formulations used for these experiments were those listed in **Table 2**, i.e.

1) *(+) DS/OVA/P$_L$ARG*: positively charged microparticles OVA-encapsulating microparticles having the OVA embedded within the microparticles.

2) *(-) DS/P$_L$ARG/OVA*: negatively charged microparticles OVA-encapsulating microparticles having the OVA situated at the periphery of the microparticles.

3) *(+) DS/P$_L$ARG + sOVA*: empty positively charged microparticles to which soluble OVA was added

4) *(-) DS/P$_L$ARG + sOVA*: empty negatively charged microparticles to which soluble OVA was added

Additionally soluble OVA and OVA formulated with alum were used as control.

Figure 7 summarizes the immunological readout of the experiments. Three weeks after the booster immunization, the cellular immune response was quantified by measuring IFN-γ cytokine secretion by splenic CD4 and CD8 T cells (measured by ELISA) and the number of these T cells (measured by ELISPOT). The ELISA assay gives information about the ability of the cells to secrete cytokine when exposed to an antigen stimulus, and detects the total amount released from all cells. The ELISPOT assay measures release of cytokines from single cells. Both are carried out to discriminate between the number of secreting cells and the amount of cytokine secreted.[19] The discrepancy between the high IFN-γ production and low amount of IFN-γ producing T cells in the case of the (+)DS/PLARG + sOVA particles can be explained in view of antigen to DC ratio. When the antigen to DC ratio is low (i.e. small amount of antigen relative to a large number of DCs), a large number of secreting T cells are stimulated, however they secrete low levels of the cytokine. The opposite is true as well: when the antigen to DC ratio is high (i.e. large amount of antigen relative to a small number of DCs), a relative low number of T cells secrete high levels of cytokine. From these data it is clear that relative to soluble OVA encapsulated OVA dramatically enhances cellular immunity. Also a strong enhancement relative to soluble OVA formulated with alum is observed. The humoral immune

response was quantified by measuring anti-OVA IgG1 titers in serum via ELISA. Also here encapsulated antigen outperforms soluble antigen and performs equally well (or in case of (+) DS/OVA/PLARG microparticles slightly better) than soluble antigen formulated with alum.

Between the different microparticles formulations the differences are less outspoken. Positively charged empty microparticles with OVA added afterwards in soluble form appears to be less potent while positively charged OVA-loaded microparticles with OVA embedded, appear to be the most potent throughout the assays. At this point it is rather speculative to explain these observations. However, a major difference between the best performing formulation (i.e DS/OVA/P$_L$ARG) and the others is that the OVA is embedded within the interior of the microparticles while in case of the other formulations, the OVA is more situated at the periphery of the microparticles. The latter might be beneficial to enhance *in vitro* antigen presentation, as in this case the antigen is readily available upon phagocytosis of the microparticles. However, it might be less beneficial *in vivo* as antigen situated at the periphery of the microparticles might be more prone to leaching out before cellular uptake. Such phenomenon can especially be expected to take place in a complex physiological environment such as the extracellular medium. Furthermore, as depicted in **Figure 3**, empty particles mixed with soluble OVA are also prone to aggregation, which might reduce their uptake by antigen presenting cells *in vivo* and thereby decrease the amplitude of the evoked antigen-specific immune-response.
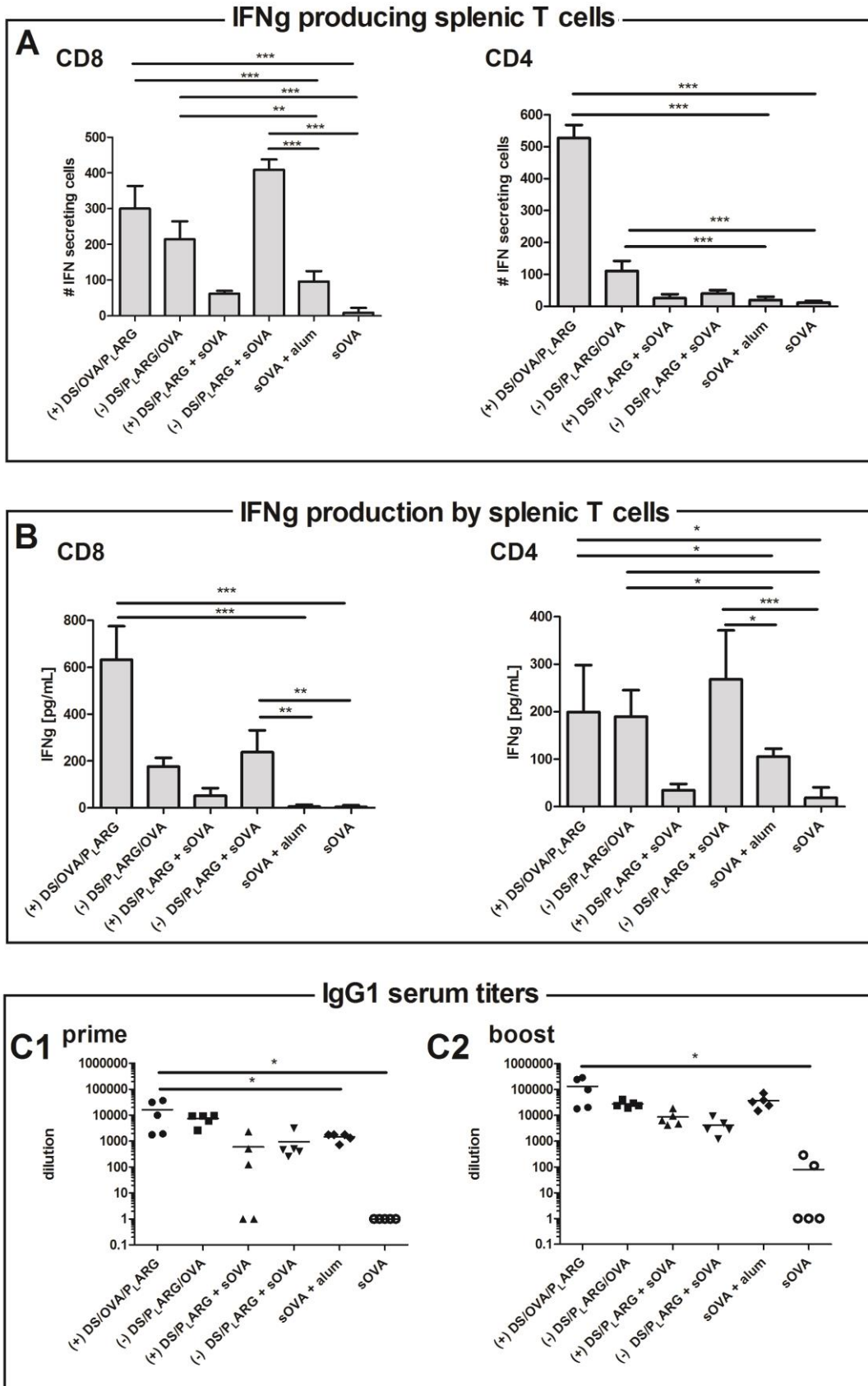
Figure 7. (A) IFN-γ secreting CD8 and CD4 T cells in the spleen. **(B)** IFN-γ cytokine secretions by splenic CD4 and CD8 T cells. **(C)** IgG1 titers after prime **(C1)** and boost **(C2)** injection. (n=5, *: p<0.05)

4. CONCLUSIONS

Summarizing, we have demonstrated in this work that porous polyelectrolyte microparticles are efficient in delivering antigen to dendritic cells and thereby promoting antigen cross presentation to CD8 T cells *in vitro*. *In vivo* in mice we have demonstrated that upon subcutaneous injection a mild tissue response is observed. Finally, we analyzed the antigen specific cellular and humoral immune response against a model vaccine antigen. These experiments demonstrated that encapsulating antigen into microporous microparticles strongly enhanced serum antibody titers and splenic T cell responses. Taken together our findings have demonstrated the potential of this formulation technology for vaccine delivery. This technology is a simple one-step method that yields a dry powder that could be attractive for application where long-term storage under non-refrigerated conditions is important, e.g. for pandemic vaccines and vaccines intended for the developing world.

REFERENCES

1. De Koker, S.; Lambrecht, B. N.; Willart, M. A.; van Kooyk, Y.; Grooten, J.; Vervaet, C.; Remon, J. P.; De Geest, B. G. Designing polymeric particles for antigen delivery. Chem. Soc. Rev. 2011, 40, 320-339.
2. Hubbell, J. A.; Thomas, S. N.; Swartz, M. A. Materials engineering for immunomodulation. Nature 2009, 462, 449-460.
3. Moon, J. J.; Huang, B.; Irvine, D. J. Engineering Nano- and Microparticles to Tune Immunity. Adv. Mater. 2012, 24, 3724-3746.
4. Banchereau, J.; Briere, F.; Caux, C.; Davoust, J.; Lebecque, S.; Liu, Y. T.; Pulendran, B.; Palucka, K. Immunobiology of dendritic cells. Annual Review of Immunology 2000, 18, 767-+.
5. Rappuoli, R. Bridging the knowledge gaps in vaccine design. Nat. Biotechnol. 2007, 25, 1361-1366.
6. Setia, S.; Mainzer, H.; Washington, M. L.; Coil, G.; Synder, R.; Weniger, B. G. Frequency and causes of vaccine wastage. Vaccine 2002, 20, 1148-1156.
7. Devriendt, B.; Baert, K.; Dierendonck, M.; Favoreel, H.; De Koker, S.; Remon, J. P.; De Geest, B. G.; Cox, E. One-step spray-dried polyelectrolyte microparticles enhance the antigen cross-presentation capacity of porcine dendritic cells. European Journal of Pharmaceutics and Biopharmaceutics 2013, 84, 421-429.
8. Dierendonck, M.; De Koker, S.; Cuvelier, C.; Grooten, J.; Vervaet, C.; Remon, J. P.; De Geest, B. G. Facile Two-Step Synthesis of Porous Antigen-Loaded Degradable Polyelectrolyte Microspheres. Angew. Chem.-Int. Edit. 2010, 49, 8620-8624.
9. Dierendonck, M.; De Koker, S.; De Rycke, R.; Bogaert, P.; Grooten, J.; Vervaet, C.; Remon, J. P.; De Geest, B. G. Single-Step Formation of Degradable Intracellular Biomolecule Microreactors. ACS Nano 2011, 5, 6886-6893.
10. De Koker, S.; De Geest, B. G.; Cuvelier, C.; Ferdinande, L.; Deckers, W.; Hennink, W. E.; De Smedt, S.; Mertens, N. In vivo cellular uptake, degradation, and biocompatibility of polyelectrolyte microcapsules. Adv. Funct. Mater. 2007, 17, 3754-3763.
11. Gonnissen, Y.; Remon, J. P.; Vervaet, C. Development of directly compressible powders via co-spray drying. European Journal of Pharmaceutics and Biopharmaceutics 2007, 67, 220-226.
12. De Geest, B. G.; Vandenbroucke, R. E.; Guenther, A. M.; Sukhorukov, G. B.; Hennink, W. E.; Sanders, N. N.; Demeester, J.; De Smedt, S. C. Intracellularly degradable polyelectrolyte microcapsules. Adv. Mater. 2006, 18, 1005-+.
13. De Geest, B. G.; Willart, M. A.; Hammad, H.; Lambrecht, B. N.; Pollard, C.; Bogaert, P.; De Filette, M.; Saelens, X.; Vervaet, C.; Remon, J. P.; Grooten, J.; De Koker, S. Polymeric Multilayer Capsule-Mediated Vaccination Induces Protective Immunity Against Cancer and Viral Infection. ACS Nano 2012, 6, 2136-2149.
14. De Geest, B. G.; Willart, M. A.; Lambrecht, B. N.; Pollard, C.; Vervaet, C.; Remon, J. P.; Grooten, J.; De Koker, S. Surface-Engineered Polyelectrolyte Multilayer Capsules: Synthetic Vaccines Mimicking Microbial Structure and Function. Angew. Chem.-Int. Edit. 2012, 51, 3862-3866.
15. De Koker, S.; De Geest, B. G.; Singh, S. K.; De Rycke, R.; Naessens, T.; Van Kooyk, Y.; Demeester, J.; De Smedt, S. C.; Grooten, J. Polyelectrolyte Microcapsules as Antigen Delivery Vehicles To Dendritic Cells: Uptake, Processing, and Cross-Presentation of Encapsulated Antigens. Angew. Chem.-Int. Edit. 2009, 48, 8485-8489.
16. De Koker, S.; Naessens, T.; De Geest, B. G.; Bogaert, P.; Demeester, J.; De Smedt, S.; Grooten, J. Biodegradable Polyelectrolyte Microcapsules: Antigen Delivery Tools with Th17 Skewing Activity after Pulmonary Delivery. J. Immunol. 2010, 184, 203-211.

17. De Cock, L. J.; Lenoir, J.; De Koker, S.; Vermeersch, V.; Skirtach, A. G.; Dubruel, P.; Adriaens, E.; Vervaet, C.; Remon, J. P.; De Geest, B. G. Mucosal irritation potential of polyelectrolyte multilayer capsules. Biomaterials 2011, 32, 1967-1977.

18. Boyman, O.; Sprent, J. The role of interleukin-2 during homeostasis and activation of the immune system. Nature Reviews Immunology 2012, 12, 180-190.

19. Clay, T. M.; Hobeika, A. C.; Mosca, P. J.; Lyerly, H. K.; Morse, M. A. Assays for monitoring cellular immune responses to active immunotherapy of cancer. Clinical Cancer Research 2001, 7, 1127-1135.

CHAPTER 7

HYDROGEN BONDED POLYMERIC MULTILAYER FILMS ASSEMBLED BELOW AND ABOVE THE CLOUD POINT TEMPERATURE

CHAPTER 7

HYDROGEN BONDED POLYMERIC MULTILAYER FILMS ASSEMBLED BELOW AND ABOVE THE CLOUD POINT TEMPERATURE

1. INTRODUCTION

Polymeric multilayer thin films, assembled via layer-by-layer (LbL) deposition of interacting species, have since their advent in the early nineties attracted major attention by scientist active in different fields of research.[1] Whereas initially LbL assembly involved the use of oppositely charged polyelectrolytes there is a steady increase of reports focusing on interactions other than electrostatics.[2] Amongst these, hydrogen bonding has become very popular.[3] Hydrogen bonded multilayer thin films rely on complex formation between electron-donor and electron-acceptor molecules and have been widely studied for drug delivery applications.[4-6] Often, hydrogen bonded multilayers are composed of a weak polyacid (such as poly((meth)acrylic acid)) and a neutral polymer bearing ether, ester or amide bonds. In protonated form the carboxylic acids form hydrogen bonds with the ether, ester or amide moieties of the other polymer, thereby serving as driving force for multilayer assembly. Due to the use of the weak polyacid, such multilayers are highly susceptible to pH and require cross-linking to be stable at physiological pH where the carboxylic acids are deprotonated and do not longer complex through hydrogen bonding. This ability has been explored by a number of groups to design intelligent materials via the use of environmentally sensitive crosslinks.[7, 8] Contrary to the use of weak polyacids, hydrogen bonded multilayer films based on tannic acid (TA), a naturally occurring polyphenol, are stable over a wide pH range (i.e. pH 2-11), while the multitude of phenolic groups on the TA form strong complexes with neutral polymers bearing ether, ester or amide bonds.[9-12] The ability to form stable assemblies under physiologically

relevant conditions, without the need for chemical crosslinking, is a major advantage of TA and has been explored by several groups for coating applications in the biomedical field. [13-15]

Poly(2-alkyl-2-oxazolines) are an attractive class of neutral hydrophilic polymers that are highly biocompatible and that can be engineered with tailored temperature-responsive properties by varying the nature of the alkyl side chains.[16, 17] Indeed, whereas poly(2-methyl-2-oxazoline) (PMeOx) does not exhibit lower critical solution (LCST) behavior, poly(2-ethyl-2-oxazoline) (PEtOx) has an cloud point temperature (T_{CP}) of 65 °C and poly(2-(n-propyl)-2-oxazoline) (PnPropOx) has a T_{CP} of 25 °C which is very appealing in view of biomedical applications.
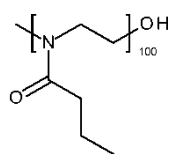

Figure 1. Molecular structure of poly(2-n-propyl-2-oxazoline) (PnPropOx).

In this chapter we report on multilayer thin film formation based on hydrogen bonding between TA and PnPropOx (**Figure 1**). In particular we demonstrate that both below the T_{CP}, with the polymer chains being in extended state, and above the T_{CP}, with the polymer chains being in collapsed aggregated state, multilayer formation with TA is possible. To the best of our knowledge, multilayer formation of the same polymer in such different states has not yet been reported for LbL deposition based on hydrogen bonding. However, we believe that such multilayers could find interesting applications for the design of functional coatings containing hydrophilic and hydrophobic payloads.

To allow for proper evaluation of the effect of the physicochemical state of the polymers on their self-assembly behavior with TA, we used in this study well defined PnPropOx with a DP of 100 (DP; degree of polymerization), produced via living cationic ring-opening polymerization of the respective 2-(n-propyl)-2-oxazoline.[18] Turbidity measurements confirmed the T_{CP} of the PnPropOx to be 25 °C. The amide group of the PnPropOx is capable of forming hydrogen bonds with tannic acid, as recently demonstrated by Demirel et al.[19]

2. MATERIALS AND METHODS

2.1. Materials

Mercaptosuccinic acid, branched PEI (25 kDa) and tannic acid (TA) were purchased from Sigma-Aldrich. Poly (2-(n-propyl)-2-oxazoline) with a DP of 100 was synthesized according to Hoogenboom et al.[18] SEC analysis against PMMA standards showed a Mn = 14 kDa and Đ = 1.14. Gold coated quartz chips with a nominal resonance frequency of 10 MHz were purchased from International Crystal Manufacturing Co (ICM). Silicon AFM cantilevers with a nominal resonance frequency of 75 kHz and a spring constant of 3N/m were obtained from Bruker. All water used in the experiments was of Milli-Q grade.

2.2. Quartz Crystal Microbalance (QCM)

QCM measurements were performed on a Gamry eQCM equipped with an ALS flow cell. Gold coated quartz chips were first coated by 1h immersion in an aqueous solution of mercaptosuccinic acid (2 mg/ml) followed by extensive rinsing with water. Secondly, the quartz chip was immersed into an aqueous PEI solution (2 mg/ml) for 1h and again extensively washed with water and dried under a gentle nitrogen stream. Next, the chip was mounted into the flow cell, water was injected and the measurement was continued until a flat baseline was obtained. Then the measurement was restarted and after 100 s 200 µL of tannic acid (TA; 2 mg/ml) was injected. 100 s later, 500 µL of water was injected to remove the non-adsorbed TA. 100 s later PnPropOx (2 mg/ml in water) was injected and after 100 s again 500 µL was injected. This procedure was repeated until a total of 10 TA/PnPropOx bilayers were deposited. Multilayer assembly below the T_{CP} of the PnPropOx was performed in a cold room thermostatted at 15°C while measurements at 45°C were performed by placing the equipment and all solutions in an oven thermostatted at 45°C

2.3 UV-VIS spectroscopy

Quartz slides rinsed with piranha solution to render them more hydrophilic were coated with PEI followed by dip coating with alternating TA (2 mg/ml in water) and PnPropOx (2 mg/ml in water). After deposition of each bilayer, the absorption spectrum was recorded with a Shimadzu spectrophotometer.

2.4. Atomic Force Microscopy (AFM)

Silicon wafers were manually cleaved into rectangular pieces, cleaned with piranha (3:1 H_2SO_4/H_2O_2). Similar to the quartz chips a precursor layer was applied by immersing the wafers for 1h in PEI (2

mg/ml in water), followed by extensive rinsing. Subsequently the silicon wafers were alternately dip-coated with TA (2 mg/ml in water) and PnPropOx (2 mg/ml in water), either at 15°C or 45°C. Between each step, the wafers were extensively rinsed with water (at the same temperature as the TA and PnPropOx solutions) to remove non-adsorbed material. After the desired number of bilayers was reached, the coated wafers were dried under a gentle stream of nitrogen.

3. RESULTS AND DISCUSSION

In a first series of experiments, we monitored the multilayer build-up of TA and PnPropOx using a quartz crystal microbalance (QCM) at 15 °C, i.e. below the T_{CP} of the PnPropOx. A gold-coated quartz chip (resonance frequency of 10 MHz) was preconditioned by adsorption of mercaptosuccinic acid via thiol-gold monolayer formation followed by the deposition of a poly(ethylene imine) precursor layer that facilitates the deposition of the first TA layer. This chip was then mounted onto a flow cell, water was injected and the QCM measurement was started. After a stable baseline was reached, multilayer assembly was initiated by injection of an aqueous TA solution (2 mg/ml in water). Immediately, the resonance frequency dropped and levelled off within 100 s after injection of the TA solution. Next, the flow cell was flushed with water to remove weakly bound and non-adsorbed TA. This was witnessed by a slight increase of the resonance frequency (also equilibrating within 100 s) indicating only minor desorption of the adsorbed TA. Subsequently a PnPropOx solution (2 mg/ml in water) was injected and again a drop in resonance frequency took place that levelled off within 100 s. After a washing step, the whole procedure was repeated until a total of 10 TA/PnPropOx bilayers were deposited, resulting in a repetitive pattern in the evolution of the resonance frequency thereby indicating a steady growth of the multilayer film, as exemplified by the blue curve in **Figure 2A**. In **Figure 2 C and D** the raw data of the QCM experiments are shown.

In a next series of experiments we assembled TA with PnPropOx above its T_{CP}. The evolution of Δf measured during TA/PnPropOx multilayer assembly above the T_{CP} is represented by the red curve in **Figure 2A**. Note that all steps in the assembly process, including the washing steps with water were performed at a constant temperature of 45 °C, well above the PnPropOx's T_{CP} of 25 °C. **Figure 2B** shows a representative expanded part of the QCM signal recorded from multilayer assembly of TA and PnPropOx below and above the T_{CP} of the PnPropOx. From these graphs it is clear that also above its T_{CP}, PnPropOx can be assembled in a layer-by-layer fashion with TA. Above the T_{CP}, PnPropOx is dehydrated and thus in the collapsed globular state. Therefore it is likely that hydrophobic interactions become important as well.[20, 21] Additionally, catechol-functional molecules such as TA are known to have a high affinity for a variety of substrates.[13, 22]
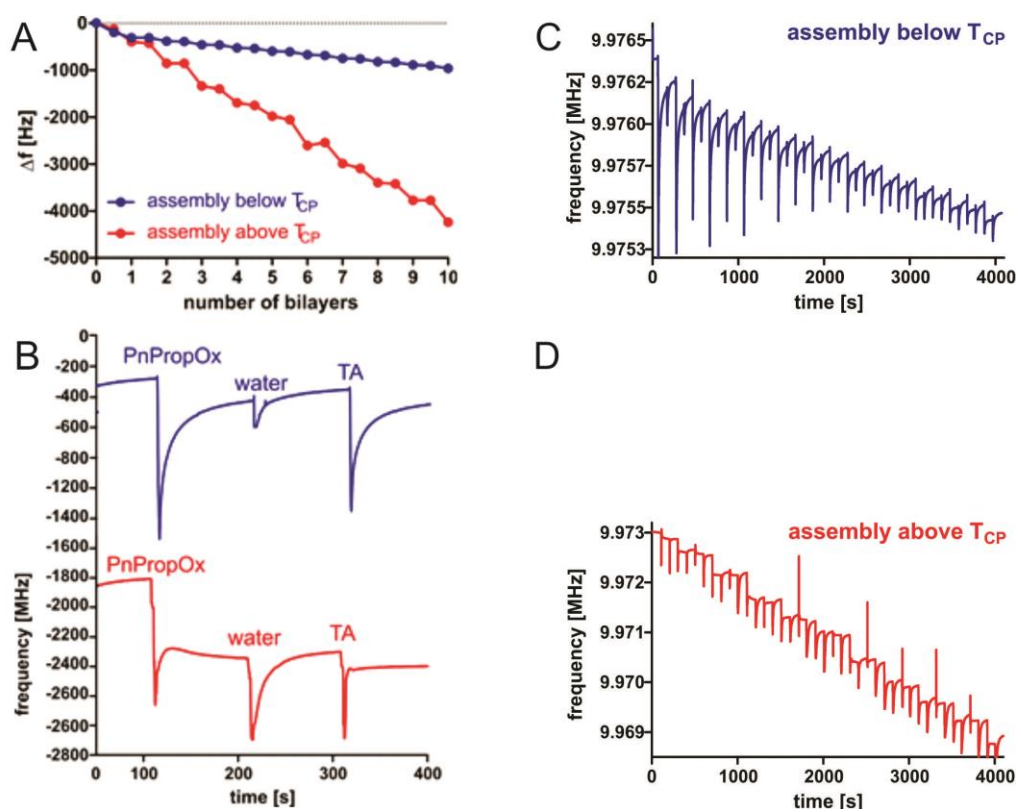
Figure 2. (A) Evolution of the change in resonance frequency (Δf) during multilayer assembly of TA and PnPropOx at 15 °C (below the T_{CP} of the PnPropOx; blue curve) and 45 °C (above the T_{CP} of the PnPropOx; red curve), respectively. **(B)** Representative section of the QCM signal measured during the assembly of a TA/PnPropOx bilayer below (blue curve) and above (red curve) the T_{CP} of PnPropOx. **(C,D)** The raw data of the QCM experiments.

Interestingly, the Δf that is measured upon adsorption of a PnPropOx layer above its LCST is significantly higher than the Δf measured upon adsorption below its T_{CP}. **Table 1** summarizes the mean Δf values for each of the respective adsorption steps (after washing) that are measured during TA/PnPropOx multilayer formation at the different assembly temperatures. This suggests that a higher mass of polymer is being deposited when the polymer chains adsorb onto the surface in the collapsed globular state (which is the case above their LCST), relative to the adsorption of polymers in a coiled state (which is the case below their T_{CP}). In contrast, no significant difference in Δf is observed for TA adsorption at 15 °C and 45 °C.

Table1. Mean frequency shift measured via QCM upon adsorption of TA and PnPropOx, either below or above the T_{CP} of PnPropOx.

	< T_{CP}	> T_{CP}
Δf (TA)	22 ± 60 Hz	42 ± 55 Hz
Δf (PnPropOx)	67 ± 15 Hz	382 ± 106 Hz

The QCM measurements were fully confirmed by UV-VIS measurements on quartz slides. These data (**Figure 3**) reveal that the absorbance at 210 nm and 280 nm, owing to TA, quasi linearly increases as function of the number of bilayers. In agreement with the QCM data, UV-VIS also shows a much higher increase in absorbance when the LbL assembly was performed above the T_{CP} of PnPropOx.
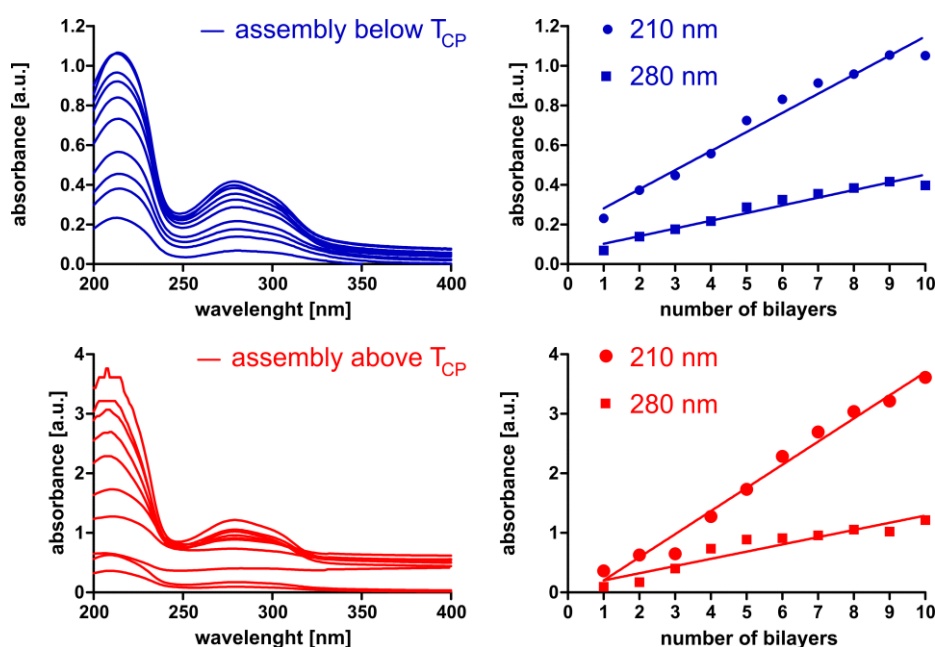

Figure 3. LbL assembly on quartz slides monitored by UV-VIS.

To further investigate the difference in multilayer assembly of TA/PnPropOx below and above the T_{CP} of PnPropOx, we used atomic force microscopy (AFM) to measure the topography of the films after respectively 1, 5 and 10 bilayers. Therefore, silicon substrates were pre-treated with piranha solution and dipcoated with a poly(ethylene imine) precursor layer followed by LbL deposition of TA/PnPropOx, either below or above the T_{CP}. **Figure 4** shows 5x5 μm scans (height channel) of TA/PnPropOx films below the T_{CP} and 5x5 μm and 50x50 μm scans of TA/PnPropOx films above the T_{CP}. All images were recorded in tapping mode in air (i.e. films were in dried state).

assembly below T$_{CP}$
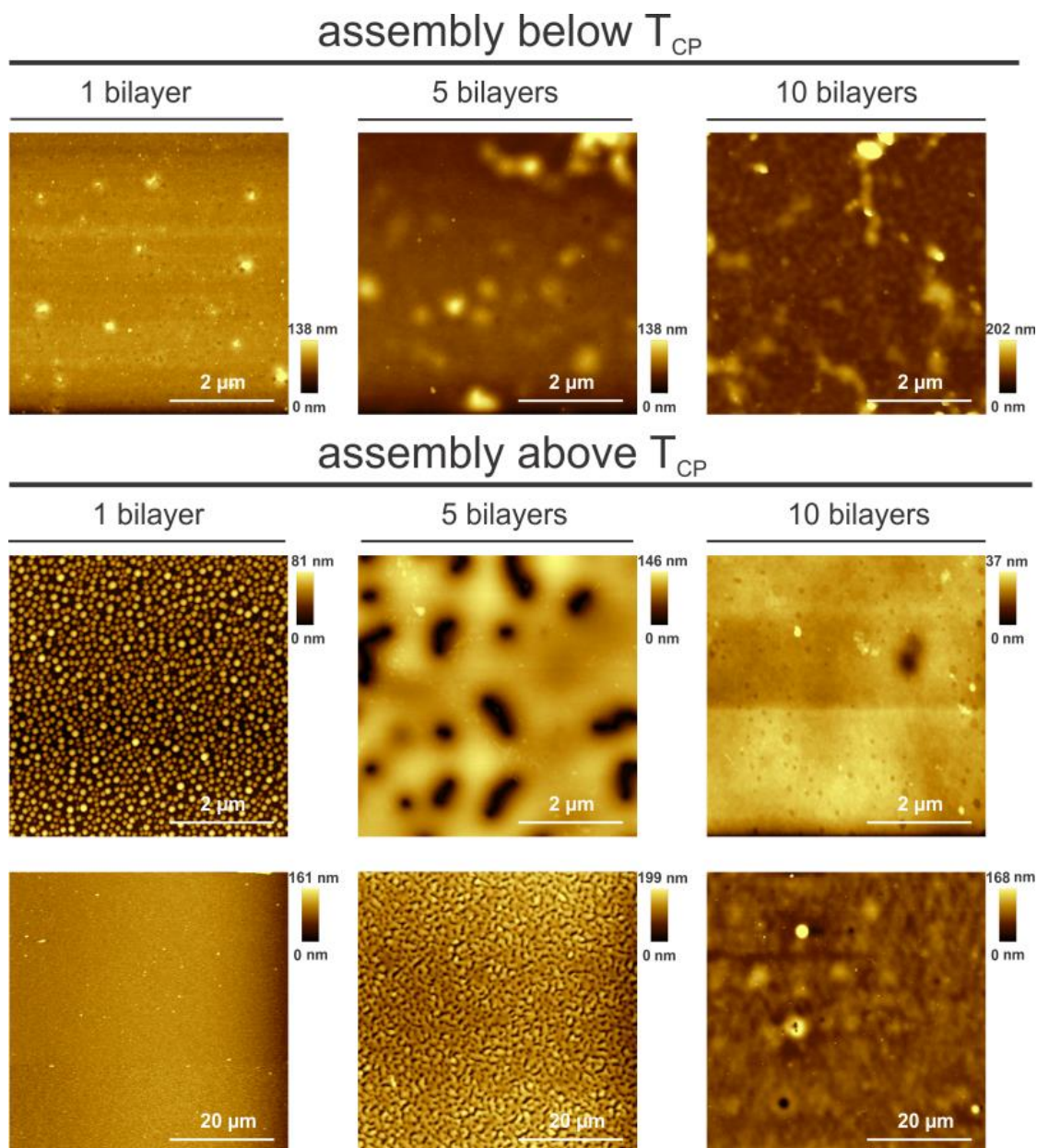

assembly above T$_{CP}$

Figure 4. AFM scans of TA/PnPropOx films below and above the LCST of PnPropOx.

Multilayer films assembled below the T$_{CP}$ of the PnPropOx exhibit a rather smooth granular morphology, starting with features of a few nanometers, gradually becoming larger with an increasing number of bilayers. In contrast, multilayer films assembled above the T$_{CP}$ of PnPropOx exhibit a dramatically different growth mechanism. During the deposition of the first TA/PnPropOx bilayer, granules with a height of 30-40 nm are deposited, likely corresponding to collapsed PnPropOx globules that adsorb onto the underlying TA layer. After 5 bilayers, the globules have merged into more continuous regions with a height ranging from 100-200 nm. Nonetheless, discrete regular holes are still present within the film. After 10 bilayers, the uncoated regions have disappeared and a smooth film surface remains. The height of the final 10 bilayer TA/PnPropOx film

assembled above the TCP of the PnPropOx was determined by measuring the step-height upon scratching the film and was measured to be 250 nm (data not shown).

These observation prompt us to assume that the multilayer growth of the TA/PnPropOx system above the T_{CP} of PnPropOx occurs through deposition of PnPropOx globules that first form discrete islands that steadily grow in lateral direction until a continuous film is formed. Such growth mechanism has earlier been reported for electrostatic self-assembly of so-called 'soft films' composed of highly hydrated polyelectrolytes such as hyaluronic acid and poly-L-lysine.[23] However, in the present case, the polymers (i.e. PnPropOx) are present in dehydrated globular state. It is worthwhile to note that the multilayer films assembled above the T_{CP} of the PnPropOx do not exhibit temperature-responsive behavior anymore. Indeed, exposure of the films to water of 15°C does not change their mass (as verified by QCM) nor their morphology (as verified by AFM). This rather surprising observation is likely to be attributed to the strong interaction between TA and the PnPropOx, hampering (partial) dissolution of the multilayer films, despite the presence of pure PnPropOx domains resulting from globule deposition.

4.CONCLUSION

Summarizing we have shown in this chapter the possibility to construct hydrogen bonded films of tannic acid and the temperature-responsive polymer poly(2-n-propyl-2-oxazoline). Multilayer growth was possible both below and above the T_{CP} of the polymer with distinctly different growth mechanisms.

REFERENCES

1. Decher, G., Fuzzy nanoassemblies: Toward layered polymeric multicomposites. Science 1997, 277, 1232-1237.
2. Quinn, J. F.; Johnston, A. P. R.; Such, G. K.; Zelikin, A. N.; Caruso, F., Next generation, sequentially assembled ultrathin films: beyond electrostatics. Chem. Soc. Rev. 2007, 36, 707-718.
3. Stockton, W. B.; Rubner, M. F., Molecular-level processing of conjugated polymers .4. Layer--layer manipulation of polyaniline via hydrogen-bonding interactions. Macromolecules 1997, 30, 2717-2725.
4. Such, G. K.; Johnston, A. P. R.; Caruso, F., Engineered hydrogen-bonded polymer multilayers: from assembly to biomedical applications. Chem. Soc. Rev. 2011, 40, 19-29.
5. De Cock, L. J.; De Koker, S.; De Geest, B. G.; Grooten, J.; Vervaet, C.; Remon, J. P.; Sukhorukov, G. B.; Antipina, M. N., Polymeric Multilayer Capsules in Drug Delivery. Angew. Chem.-Int. Edit. 2010, 49, 6954-6973.
6. De Koker, S.; Hoogenboom, R.; De Geest, B. G., Polymeric multilayer capsules for drug delivery. Chem. Soc. Rev. 2012, 41, 2867-2884.
7. Kozlovskaya, V.; Ok, S.; Sousa, A.; Libera, M.; Sukhishvili, S. A., Hydrogen-bonded polymer capsules formed by layer-by-layer self-assembly. Macromolecules 2003, 36, 8590-8592.
8. Zelikin, A. N.; Quinn, J. F.; Caruso, F., Disulfide cross-linked polymer capsules: En route to biodeconstructible systems. Biomacromolecules 2006, 7, 27-30.
9. Lomas, H.; Johnston, A. P. R.; Such, G. K.; Zhu, Z. Y.; Liang, K.; van Koeverden, M. P.; Alongkornchotikul, S.; Caruso, F., Polymersome-Loaded Capsules for Controlled Release of DNA. Small 2011, 7, 2109-2119.
10. Kozlovskaya, V.; Kharlampieva, E.; Drachuk, I.; Cheng, D.; Tsukruk, V. V., Responsive microcapsule reactors based on hydrogen-bonded tannic acid layer-by-layer assemblies. Soft Matter 2010, 6, 3596-3608.
11. Erel-Unal, I.; Sukhishvili, S. A., Hydrogen-bonded multilayers of a neutral polymer and a polyphenol. Macromolecules 2008, 41, 3962-3970.
12. Shutava, T.; Prouty, M.; Kommireddy, D.; Lvov, Y., pH responsive decomposable layer-by-layer nanofilms and capsules on the basis of tannic acid. Macromolecules 2005, 38, 2850-2858.
13. Ejima, H.; Richardson, J. J.; Liang, K.; Best, J. P.; van Koeverden, M. P.; Such, G. K.; Cui, J. W.; Caruso, F., One-Step Assembly of Coordination Complexes for Versatile Film and Particle Engineering. Science 2013, 341, 154-157.
14. Shukla, A.; Fang, J. C.; Puranam, S.; Jensen, F. R.; Hammond, P. T., Hemostatic Multilayer Coatings. Adv. Mater. 2012, 24, 492-+.
15. Kozlovskaya, V.; Harbaugh, S.; Drachuk, I.; Shchepelina, O.; Kelley-Loughnane, N.; Stone, M.; Tsukruk, V. V., Hydrogen-bonded LbL shells for living cell surface engineering. Soft Matter 2011, 7, 2364-2372.
16. Weber, C.; Hoogenboom, R.; Schubert, U. S., Temperature responsive bio-compatible polymers based on poly(ethylene oxide) and poly(2-oxazoline)s. Progress in Polymer Science 2012, 37, 686-714.
17. Hoogenboom, R., Poly(2-oxazoline)s: A Polymer Class with Numerous Potential Applications. Angew. Chem.-Int. Edit. 2009, 48, 7978-7994.
18. Hoogenboom, R.; Thijs, H. M. L.; Jochems, M.; van Lankvelt, B. M.; Fijten, M. W. M.; Schubert, U. S., Tuning the LCST of poly(2-oxazoline)s by varying composition and molecular weight: alternatives to poly(N-isopropylacrylamide)? Chem. Commun. 2008, 5758-5760.
19. Erel, I.; Schlaad, H.; Demirel, A. L., Effect of structural isomerism and polymer end group on the pH-stability of hydrogen-bonded multilayers. J. Colloid Interface Sci. 2011, 361, 477-482.

20.   Puddu, V.; Perry, C. C., Peptide Adsorption on Silica Nanoparticles: Evidence of Hydrophobic Interactions. ACS Nano 2012, 6, 6356-6363.

21.   Castelnovo, M.; Joanny, J. F., Formation of polyelectrolyte multilayers. Langmuir 2000, 16, 7524-7532.

22.   Lee, H.; Dellatore, S. M.; Miller, W. M.; Messersmith, P. B., Mussel-inspired surface chemistry for multifunctional coatings. Science 2007, 318, 426-430.

23.   Picart, C.; Lavalle, P.; Hubert, P.; Cuisinier, F. J. G.; Decher, G.; Schaaf, P.; Voegel, J. C., Buildup mechanism for poly(L-lysine)/hyaluronic acid films onto a solid surface. Langmuir 2001, 17, 7414-7424.

CHAPTER 8

NANOPOROUS HYDROGEN BONDED POLYMERIC MICROPARTICLES: FACILE AND ECONOMIC PRODUCTION OF CROSS-PRESENTATION PROMOTING VACCINE CARRIERS

CHAPTER 8

NANOPOROUS HYDROGEN BONDED POLYMERIC MICROPARTICLES: FACILE AND ECONOMIC PRODUCTION OF CROSS-PRESENTATION PROMOTING VACCINE CARRIERS

1. INTRODUCTION

Strategies that allow fast and efficient encapsulation of proteins into hydrophilic and fully hydrated microparticles are of great interest for a number of applications in biotechnology, diagnostics and biomedicine.[1-3] When envisioning intracellular delivery of vaccine antigens, such particles are particularly advantageous. Particles in the 0.1-10 μm size range mimic the dimensions of micro-organisms and are consequently readily recognized and internalized by dendritic cells, the main antigen presenting cells and inducers of adaptive immunity.[4-6] Once internalized, particulate antigens will be processed in the phagosomes and presented as MHC-peptide complexes to T cells. Particulate antigens are generally presented via MHCI and MHCII, enabling thereby the simultaneous induction of CD8 and CD4 T cell responses. In the appropriate inflammatory context, MHCI-peptide stimulated CD8 T cells will differentiate into cytotoxic T cells possessing the unique capacity to recognize and kill infected or transformed cells. This path of the immune response is termed cellular immunity and is thought to be crucial for effective vaccination against intracellular pathogens such as HIV, malaria, tuberculosis etc. and for anti-cancer immune therapy.[7] CD4 T cells stimulated by MHCII-peptide complexes can differentiate into distinct T helper subsets, which support B cells to produce antibodies that mobilize innate immune cells to combat pathogens. In contrast to particulate

antigens, presentation of extracellular soluble antigens is almost entirely restricted to the MHCII pathway. As a consequence, soluble antigens will largely fail to evoke CD8 T cell responses.
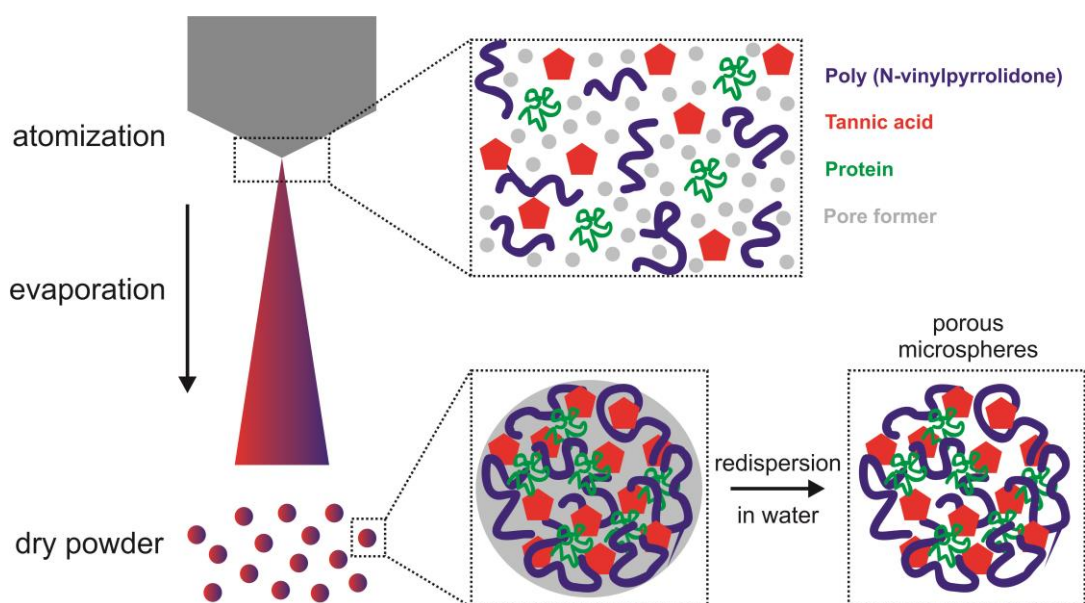

Scheme 1. Schematic representation of the encapsulation of protein antigen in porous microparticles based on H-bonding interacting species. As pore-former mannitol is used which instantaneously dissolves upon redisperion in aqueous medium, thereby creating a highly porous matrix.

Thus currently, there is major interest in the development of adjuvant systems that stimulate cellular immune responses via formulation in nano- and microparticles.[8-15] In this regard it is crucial to use materials and procedures that are biologically friendly and scalable from the laboratory to industry. Here we present an all aqueous one-step method to produce antigen loaded microparticles using hydrogen bonding as driving force for particle assembly. Based on our previous work[16-18] using oppositely charged polyelectrolytes that assemble via electrostatic interaction,[19-21] we apply atomization into air of diluted aqueous liquid containing antigen, H-bonding matrix-forming components, and mannitol as pore-forming component. This spray drying process yields solid microparticles with sub 10 μm dimension, to assure phagocytocis by DCs. Owing to its dry state, this formulation has particularly advantages for long time storage and transportation under non-refrigerated conditions, which is of major importance for pandemic vaccines and vaccines intended for the developing world.[22] The role of the pore-forming component in the formulation, is to create a nanoporous internal network within the microparticles upon redispersion of the particles in aqueous medium. As mannitol is highly water-soluble it will immediately dissolve, i.e. leach out of the particles, thereby creating porosity. The process to fabricate such microparticles is schematically depicted in **Scheme 1**. Our hypothesis is that microparticles with a nanoporous interior, unlike

monolithic particles, allow a more profound diffusion by intracellular proteases upon cellular uptake. This is expected to lead to a faster and more efficient processing and presentation of the full antigen payload.

As complementary H-bonding components we used tannic acid (TA; **Scheme 2A**) as hydrogen bond donor and poly(N-vinylpyrrolidone) (PVP; **Scheme 2B**) as hydrogen bond acceptor.[23] PVP is a neutral polymer that is available as pharma-grade and is allowed by the FDA as excipient for injectables. TA and PVP are known to form strong H-bonded complexes that remain stable over a wide pH range.[24-26] Whereas TA has been used for self-asembly,[27] including planar multilayer films and capsules via hydrogen bonding[28-31] and coordination complex formation,[32] the fabrication of microparticles by simply spraying species that interact via hydrogen bonding has, to the best of our knowledge, not yet been reported so far. Importantly, as polycations are generally regarded as cytotoxic, developing systems that can replace electrostatic interaction by hydrogen bonding are of strong interest for the biomedical field.[33, 34]
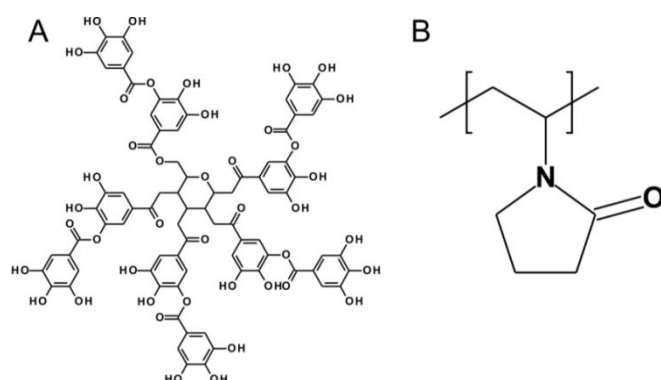
Scheme 2. Molecular structure of **(A)** tannic acid (TA), and **(B)** poly(N-vinylpyrrolidone) (PVP).

2. MATERIALS AND METHODS

2.1. Materials

Poly(N-vinylpyrrolidone) (Kollidon®12) was purchased from BASF. Tannic acid, N-vinylpyrrolidone (NVP), azobisisobutyronitrile (AIBN), fluorescein-o-acrylate, dimethylacetamide (DMA), dichloromethane and Hoechst were purchased from Sigma-Aldrich. Mannitol was purchased from Cargill. AlexaFluor488 conjugated ovalbumin (OVA-Alexa Fluor488), DQ-OVA and Alexa Fluor647 conjugated cholera toxin subunit B (CTB-Alexa Fluor647) were purchased from Life Technologies. The xanthate CTA [(S)-2-(ethyl propionate)-(O-ethyl xanthate)] was synthesized according to the literature procedure.[35]

2.2. Synthesis of fluorescent PVP (PVP-FITC)

NVP (2 g), xanthate CTA (26.7 mg) [(S)-2-(ethyl propionate)-(O-ethyl xanthate)] and AIBN (5.91 mg) and 6 mL anisole were added to a Schlenk flask at a molar ratio of monomer/CTA/AIBN of 150/1/0.3. After degassing by 3 freeze-pump-thaw cycles the Schlenk flask was placed in an oil bath set at 60°C for 24h. Subsequently, the reaction was quenched by immersion in an ice bath and exposure to air. The reaction mixture was then precipitated in hexane, dissolved in dichloromethane and re-precipitated in hexane for in total 3 times and recovered as a white powder. GC analysis indicated a $M_{n,th}$ of 11.4 kDa (based on conversion) while size exclusion chromatography (SEC) in DMA indicated a $M_{n,SEC}$ = 7.0 kDa and a dispersity (Đ) of 1.27. The reaction scheme is shown in **Scheme 3.** For fluorescent labeling, 50 mg of PVP and 10 mg of fluorescent-o-acrylate were dissolved in 2 mL and 1 mL of DMF, respectively, in Schlenk flasks. Prior to modification, the two solutions and propyl amine were degassed via 4 freeze-pump-thaw cycles. Subsequently, 1mL of degassed propyl amine was added to PVP solution under N_2 atmosphere and stirred for 2 h at room temperature to deprotect the thiol end-group of the PVP by aminolysis. Next, the excess of propylamine was removed by rotary evaporation. The reaction mixture was then again degassed and the fluorescein-o-acrylate solution was added by syringe under N_2 atmosphere and stirred overnight at room temperature. After dialysis against MilliQ water for 4 days and lyophilization, a fluffy orange colored powder was obtained.

SEC was performed on a Agilent 1260-series HPLC system equipped with a 1260 online degasser, a 1260 ISO-pump, a 1260 automatic liquid sampler, a thermostated column compartment, a 1260 diode array detector (DAD) and a 1260 refractive index detector (RID). Analyses were performed on a PSS Gram30 column in series with a PSS Gram1000 column at 50 °C. DMA containing 50 mM of LiCl was used as eluent at a flow rate of 0.593 mL/min. The spectra were analyzed using the Agilent Chemstation software with the GPC add on. Molar mass and dispersity (Đ) values were calculated against PMMA standards.

2.3. Quartz Crystal Microbalance

QCM measurements were performed on a Gamry eQCM equipped with an ALS flow cell. Gold coated quartz chips were first coated by 1h immersion in an aqueous solution of mercaptosuccinic acid (2 mg/mL) followed by extensive rinsing with water. Secondly, the quartz chip was immersed into an aqueous PEI solution (2 mg/mL) for 1h and again extensively washed with water and dried under a gentle nitrogen stream. Next, the chip was mounted into the flow cell, water was injected and the measurement was started and continued until a flat baseline was obtained. Then the measurement was restarted and after 100 sec 200 μL of tannic acid (TA; 2 mg/mL in water) was injected. 100 sec

later, 500 µL of water was injected to remove the non-adsorbed TA. 100 sec later PVP (2 mg/mL in water) was injected and after 100 sec again 500 µL of water was injected. This procedure was repeated until a total of 10 TA/PVP bilayers were deposited.

2.4. Preparation of TA/PVP microparticles via spray drying

Mannitol, PVP, OVA and TA were mixed in water in a 40/5/1/5 ratio and a total solid concentration of 0.5%. Three different adding sequences were evaluated. **First sequence**: 400 mg of mannitol, 10 mg of OVA and 50 mg of PVP were dissolved in 92 ml water. Subsequently 10 mL water containing 50 mg TA was added dropwise under stirring. **Second sequence**: 400 mg mannitol and 50 mg PVP were dissolved in 90 mL water, then 10 mL water containing 50 mg TA was added dropwise followed by the addition of 2 mL water containing 10 mg OVA. Both additions proceeded under stirring. **Third sequence**: 400 mg mannitol and 10 mg OVA were dissolved in 82 ml water. Next 10 mL water containing 50 mg of TA was added dropwise followed by the addition of 10 ml of water containing 50 mg of PVP. Both additions proceeded under stirring. Fluorescently labelled particles were prepared using either a mixture of OVA with Alexa Fluor488 conjugated ovalbumin or PVP with PVP-fluorescein, both in a 10:1 ratio. Spray drying was performed with a lab-scale Büchi B290 spray dryer equipped with a two fluid nozzle (0.7 mm diameter). The setting of the inlet temperature was 120°C and gas flow 0.55 bar. The mixtures were fed via a peristaltic feed pump at a feed flow of 2.4 ml/min. Dry powder was collected.

2.5. Encapsulation efficiency

The quantification of encapsulation efficiency was determined by resuspending a known amount of microspheres (OVA-Alexa Fluor488, PVP-fluorescein microspheres and non-labelled microspheres to measure respectively OVA, PVP and TA encapsulation) in phosphate buffered saline (PBS) followed by centrifugation and measuring the amount of non-encapsulated OVA-Alexa Fluor488, PVP-fluorescein or TA in the supernatant. For OVA-Alexa Fluor488 and PVP-fluorescein this was done via fluorescence spectrometry using a Perkin-Elmer Envision multilabel plate reader. TA concentration was measured via UV-VIS spectrophotometry at 280 nm.

2.6. Particle characterization

Laser diffraction was performed on a Malvern Mastersizer equipped with an 300RF objective. Scanning Electron Microscopy (SEM) was conducted on a Quanta 200 FEG FEI scanning electron microscope. Samples were sputtered with a palladium-gold layer prior to imaging. Transmission electron microscopy was performed on a JEOL 1010 instrument. Porosity of the particles was

assessed using ImageJ (NIH) by binarizing the TEM images followed by calculating the ratio of black to white pixels within a circular region of interest which comprises the microparticle section. Confocal microscopy was conducted on a Leica SP5 microscope equipped with a 63X oil immersion objective. DC2.4 cells were plated a density of 50 000 per well in 8 well Ibidi chambers and incubated overnight with 5 µL of a 25 mg/mL microparticle suspension. CTB-Alexa Fluor647 and Hoechst staining was performed according to the manufactures' instructions.

2.7. *In vitro* and *in vivo* experiments

2.7.1. Cell lines and animals

C57BL/6 mice were obtained from Janvier. OT-I transgenic mice (C57BL/6) were purchased from Harlan. Mice were housed under specific-pathogen-free conditions. All animal experiments were approved by the Local Ethical Committee of Ghent University. The immortalized mouse dendritic cell line DC2.4 was a kind gift from Prof. Dr. Ken Rock (Dana-Farber Cancer Institute, Boston, MA, USA). Bone-marrow-derived DCs were generated by flushing tibia and femurs of 2–4 months old C57BL/6 mice. After red blood cell lysis, cells were cultured in complete RPMI (Roswell Park Memorial Institute) medium containing 20 ng/mL GM-CSF (granulocyte macrophage colony-stimulating factor) for 6–8 days.

2.7.2. Cell toxicity assay

The cytotoxicity of the spray dried particles was assessed according to De Koker et al.[36] DC2.4 cells were grown and seeded in 96 well plate at a density of 5×10^3 cells/well and incubated with different concentrations of the respective samples for 6 hours. Afterwards, the medium was refreshed and cells were cultured for another 48 hours. Medium was removed and MTT (3-(4,5-dimethylthiazol-2-yl)-2,5-diphenyltetrazolium bromide) was added. MTT is reduced by mitochondrial dehydrogenases of living cells into an insoluble purple formazan dye. After 3 hours of incubation at 37°C, cells are solubilized by dimethylsulfoxide (DMSO) and the released, solubilized formazan is measured spectrophotometrically at 590 nm. The absorbance is a measure of the viability of the cells.

2.7.3. In vitro antigen-presentation assay

Cell suspensions of OVA-specific CD8 T cells were prepared from spleen and lymph nodes from OT-I mice. Single cell suspensions were prepared, and CD8 T cells were isolated from the suspensions using Dynal mouse CD8 negative isolation kit (Invitrogen) according to the manufacturers' instructions and subsequently labeled with CFSE (carboxyfluorescein diacetate succinimidyl ester). DCs obtained from bone marrow of C57BL/6 mice were pulsed with serial dilutions of the respective

samples (corresponding to 0.2, 2 and 5µg/ml OVA) for 24 h, washed, counted and subsequently co-cultured with OT-I T cells at different DC:T cell ratios (1:5; 1:10; 1:20 and 1:100) for 48 h in round bottomed well plates. After 48 h, the division of the OT-I T cells was measured by flow cytometry using a BD LSR II.

2.7.4. Readout of in vivo antibody response (ELISA)

Mice were subcutaneously vaccinated twice with a 3 week interval with 100 µL containing 20 µg of either soluble or encapsulated OVA. For the detection of anti-OVA antibodies, blood samples were collected from the ventral tail vein. Maxisorp (Nunc) plates were precoated with OVA (10 mg/ml) overnight. Wells were blocked with 200 µL PBS 1% (w/v) bovine serum albumin (BSA) (Sigma Aldrich) for 2 hours at room temperature. Serial dilutions of serum in PBS 1% BSA were added and incubated for 2 hours at room temperature. Subsequently goat anti-mouse IgG1-HRP (Southern Biotech; HRP= horseradish peroxidase) and goat anti-mouse IgG2c-HRP (Southern Biolabs) diluted in PBS (1/5000) was added for 1 hour at room temperature. Plates were washed 3 times between each step with PBS 0.1% Tween20 (Sigma Aldrich). Peroxidase activity was measured using 50 µL/well TMB substrate (BD Opteia^{TM}, BD biosciences) and optical densities were read at 450 nm after stopping the reaction by adding 25 µL/well 1M H_2SO_4. Data show antibody titers of individual mice.

2.7.5. Readout of in vivo cellular response (ELISPOT)

Splenocytes were harvested three weeks after the booster immunization. Suspensions of 2 x 10^5 splenocytes were cultured onto IFN-γ ELISPOT plates (Diaclone) in triplicate and restimulated with 5 mg/mL of either the OVA MHCI epitope peptide SIINFEKL or the OVA MHCII epitope peptide ISQAVHAAHAEINEAGR (both Anaspec) and incubated for 24 hours at 37°C in a CO_2 incubator. Medium alone (100µL) or concanavolin A (100 µL, 2 µg/ml) were used as negative or positive controls, respectively. Then, biotinylated detection antibody was added and incubated at room temperature for 1 h 30 min and subsequently 100 µL/well of streptavidin-AP(Alkaline phosphatase) conjugate was added and incubated for 1 hour at room temperature. Plates were washed 3 times between each step with PBS 0.05% Tween20 (Sigma Aldrich). Alkaline phosphatase activity was determined using 100 µL/well BCIP/NBT (5-bromo-4-chloro-3-indolyl-phosphate/nitro blue tetrazolium) substrate and spots were developed after a 5-10 minutes incubation period. The frequency of the resulting coloured spots were counted using an Immunospot ELISPOT reader (AID).

2.7.6. Tetramer staining

To determine the percentage of OVA-specific CD8 T cells post immunization, 200 µl blood of immunized mice was collected by tail bleeding. After lysis of red blood cells (ACK red blood cell lysis buffer), cells were stained with OVA-specific dextramers (Immudex) according to the manufacturer's instruction. Subsequently, cells were stained with Fc block, CD8 PerCP, CD3-Pacific blue and CD19-APC-Cy7 (all BD Biosciences) and analysed on a BD LSRII flow cytometer.

3. RESULTS AND DISCUSSION

3.1. Assembly of nanoporous hydrogen bonded microparticles

In this study, we used commercially available PVP, branded as Kollidon®12, which is available as endotoxin-free grade. As stated by the manufacturer, it has a molecular weight of 2-3 kDa, which was determined in our lab by SEC to be $M_{n,SEC}$ 1.8 kDa (Đ = 1.89), relative to PMMA standards, for that specific lot which was used during the whole study. As the molecular weight of the polymer is considerably lower compared to polymers that are commonly used in multilayer build up (i.e. typically around 50 kDa), we evaluated whether this PVP was capable to form stable assemblies with TA via Quartz Crystal Microbalance (QCM). Therefore, a gold coated quartz chip was pre-conditioned by adsorption of a monolayer of mercaptosuccinnic acid, inducing a negative surface charge, followed by a cationic poly(ethylene imine) (PEI) layer to promote further Layer-by-Layer (LbL) assembly. Subsequently, the multilayer build-up was started by injecting TA into the flow cell, followed by an adsorption time of 100 s to reach a stable value of the resonance frequency. A rinsing step with demi water was applied to remove non-adsorbed and weakly adsorbed TA from the flow cell and next PVP was injected. Immediately a drop in resonance frequency took place that levelled of within 100 s, then again followed by a washing step with demi water to remove unadsorbed and weakly adsorbed species. This procedure was repeated until a total of 10 TA/PVP bilayers was assembled. The raw data of the QCM signal shown in **Figure 1A**, depicts a steady decrease of the resonance frequency upon every adsorption step, with only a minor increase in resonance frequency upon each rinsing step. When plotting the evolution of resonance frequency as function of the number of deposited layers (**Figure 1B**), a linear decrease is observed indicating successful consecutive LbL build-up. These findings were confirmed by monitoring multilayer assembly (with intermittent drying) on quartz substrates with UV-VIS spectroscopy (data not shown). More general, this means that PVP with a relatively low molecular weight is able to form stable hydrogen bonded complexes with TA. These data are in accordance to earlier reports, albeit that PVP with a significantly higher molecular weight was used.[24]
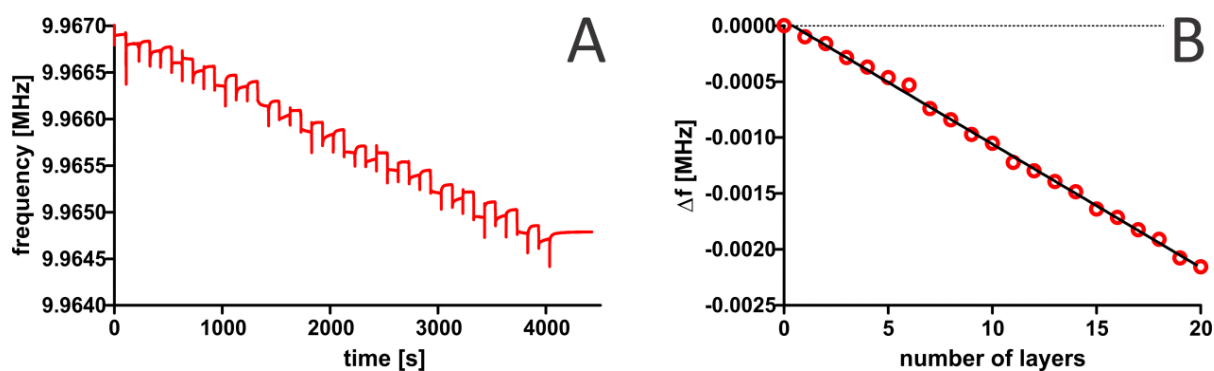
Figure 1. **(A)** QCM trace during assembly of a 10 TA/PVP bilayer film. **(B)** Decrease of the resonance frequency (Δf) as function of the deposition steps.

Encouraged by these findings, we proceeded with evaluating the formation of TA/PVP microparticles via an atomization-evaporation (i.e. spray drying) set up. Previously we have reported on the formation of porous particles composed of oppositely charged polyelectrolytes that form a stable complex via electrostatic interaction.[16-18] Proteins such as vaccine antigens and enzymes could, very efficiently, be entrapped within this polyelectrolyte network and key in assuring preservation of the biological activity of these proteins was the use of mannitol as pore-forming component mixed with the polyelectrolytes and proteins prior to spray drying.[17] Mannitol is FDA approved and highly water-soluble, thereby immediately dissolving and leaching from the particles upon redispersion in aqueous medium. Additionally, mannitol is often used in the pharmaceutical industry to enhance the overall yield of the spray drying process due to its excellent flow properties.[37] Therefore, in the current study, we prepared a diluted aqueous dispersion of mannitol, PVP and TA under constant stirring to avoid the formation of large precipitates. The ratios of these components were chosen based on our previous findings for polyelectrolyte based microparticles.[16, 17] The mixture was fed to the nozzle of the spray drier and atomized into a heated air stream. After evaporation of the water, the resulting solid particles were collected via a cyclone and stored for further studies.
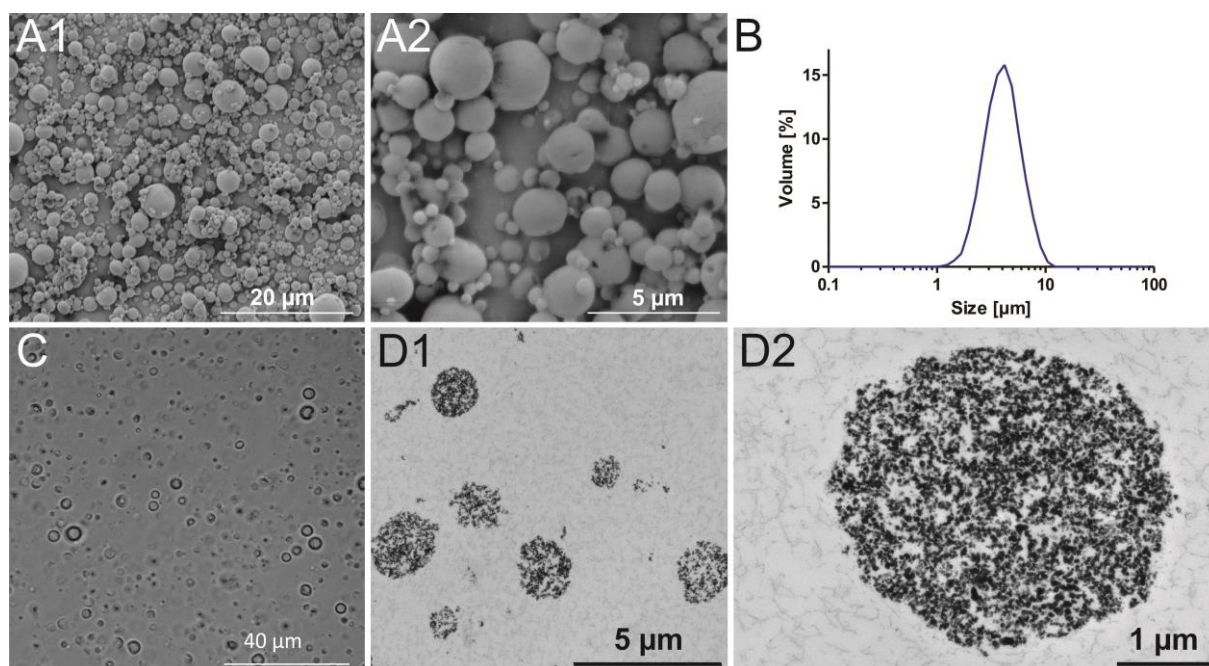
Figure 2. **(A)** Scanning electron microscopy images of the microparticles obtained in dry state after spray drying. **(B)** Size distribution of the microparticles measured by laser diffraction after redispersion in aqueous medium. **(C)** Optical microscopy image of TA/PVP microparticles upon redispersion of the solid spray dried powder in aqueous medium. **(D)** Transmission electron microscopy images (recorded from microtomed epoxy-embedded microparticles), depicting the high internal porosity of the microparticles after redispersion in water.

3.2. Particle characterization

The obtained microparticles were characterized in the dry state by scanning electron microscopy (SEM) and after rehydration in aqueous medium by laser diffraction and transmission electron microscopy (TEM). The SEM images in **Figure 2A** demonstrate that spherically shaped microparticles, with diameters in the dry state below 10 μm, are obtained via the spray drying process. Optical microscopy (**Figure 2C**) verifies that the microparticles remain stable upon redispersion in phosphate buffered saline (PBS) without agglomerating or disassembling, indicating that the hydrogen bonds between the TA and PVP are strong enough to form stable particles in water. This is further confirmed by laser diffraction in wet state, showing a monomodal particle size distribution between 1-10 μm and a volume mean particle diameter of 4.02 ± 0.25 μm (**Figure 2B**). Analysis of the SEM images by Image J yielded a number mean particle diameter of 1.04 ± 0.65 μm. This is markably lower than the size distribution obtained via laser diffraction. However it is important to consider the fact that laser diffraction was measured on particles in a swollen hydrated state whereas SEM was performed on dry particles. Additionally the volume mean diameter calculated by laser diffraction is strongly affected by larger particles, which thus accounts for the larger mean diameter measured by laser diffraction relative to the number mean diameter measured by SEM. These are important

findings in view of applying these particles as intracellular vaccine carriers where particle sizes below 10 μm are required for efficient phagocytosis by antigen presenting cells. To assess the internal structure of the TA/PVP microparticles, they were embedded in an epoxy matrix and cut into ultrathin slices via ultramicrotomy. Subsequent TEM imaging revealed a highly porous internal structure as depicted in **Figure 2D**.

The porosity of the microparticles and the role of mannitol to induce this porosity was further verified by comparing SEM images (**Figure 3**) before and after redispersion in water. These observations unambiguously proves the formation of a highly porous internal network structure within the TA/PVP microparticles after removal of mannitol. Image analysis of the TEM images on 20 individual particles revealed a pore volume of 36 ± 11 %.
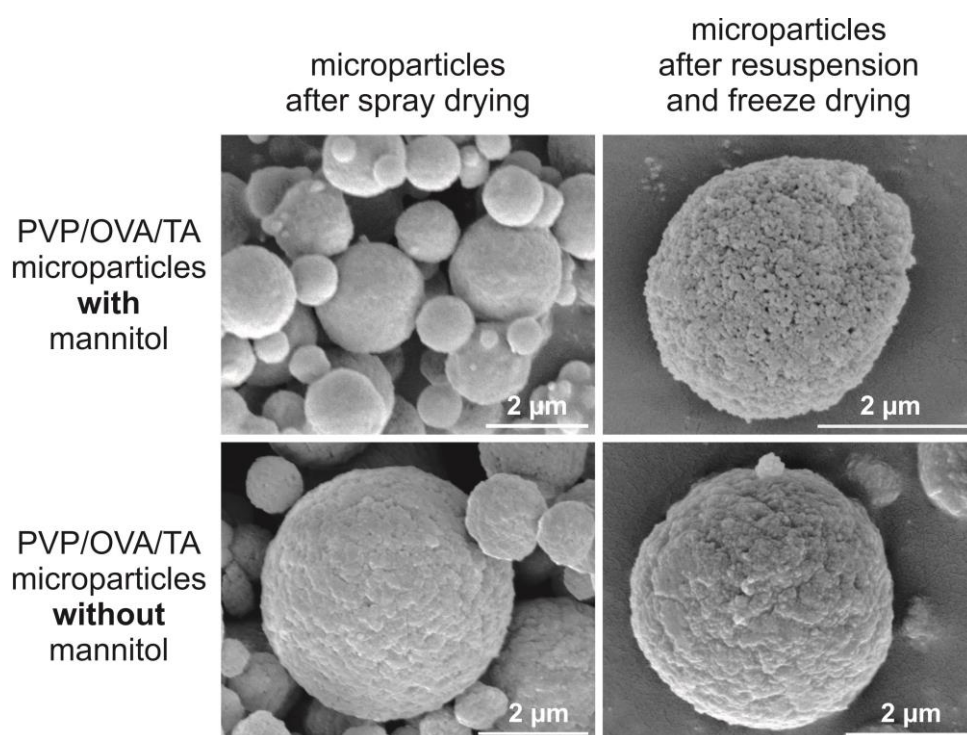

Figure 3. Scanning electron microscopy (SEM) images of microparticles spray dried with and without mannitol. The particles were images in native (i.e. after spray drying) state (left panels) and after resuspension in water, triple centrifugation washing to remove soluble compounds and finally freeze drying to preserve as much as possible the morphology of the particles (right panels).

In a next series of experiments we investigated to which extend such TA/PVP microparticles can encapsulate protein antigens. Therefore, ovalbumin (OVA; chicken egg albumin with a molecular weight of ~43 kDa) was used as model antigen. Ovalbumin is a relatively inert antigen containing both a MHCI and a MHCII peptide epitope recognized in the C57BL/6 mice strain. In addition, a large set of murine-based immunological tools are available to characterize the performance of OVA-based vaccine formulations. OVA was added to the aqueous mixture of TA, PVP and mannitol prior to spray

drying. As TA will also partly complex to OVA via a combination of hydrogen bonding and hydrophobic interactions,[38] we analyzed whether the sequence of mixing OVA , TA and PVP prior to spray drying (**Table 1**) has an influence on the extent to which OVA will be retained within the microparticles upon redispersion in aqueous medium (i.e. as 'encapsulation efficiency').

Table 1. Composition of the OVA formulations.

Sequence					ratio (wt.%)
1	mannitol	OVA	PVP	TA	40/1/5/5
2	mannitol	PVP	TA	OVA	40/5/5/1
3	mannitol	OVA	TA	PVP	40/1/5/5
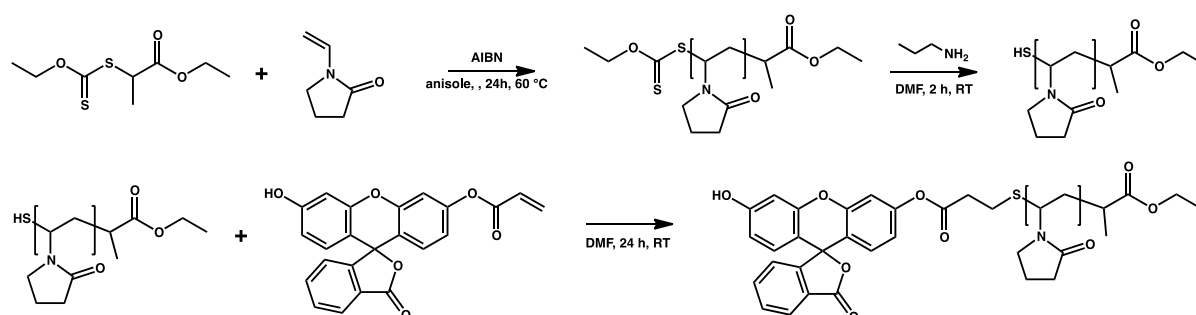
Scheme 3. Reaction scheme of the RAFT/MADIX polymerization of NVP and subsequent fluorescent labeling via thio-ene chemistry of the thiol end-group to the acrylate group of fluorescein acrylate.

To measure to which extend OVA remains entrapped within the TA/PVP matrix upon redispersion of the particles in aqueous medium (i.e. phosphate buffered saline (PBS)), we centrifuged the microparticles and determined the OVA concentration in the supernatant. Therefore, we used fluorescently labelled (i.e. Alexa Fluor488) OVA as the presence of TA would interfere with every available protein assay. Additionally, to provide full characterization of the particles also the release of TA and PVP in the supernatant was measured. Owing to its multitude of aromatic groups, TA can easily be detected by UV-VIS spectroscopy. Fluorescently labelled PVP was synthesized via RAFT/MADIX polymerization[39] followed by end group modification with fluorescein.

As depicted in **Scheme 3**, this labeling was performed by aminolysis of the xanthate group of the PVP, resulting from the chain transfer agent, into a thiol and subsequent Michael addition type thiol-ene conjugation with fluorescein-o-acrylate.[40] To assess whether the fluorescein group was indeed conjugated to the polymer, size exclusion chromatography (SEC) analysis was performed using a diode array detector (DAD). As shown in **Figure 4**, the UV-VIS absorption spectra recorded at the

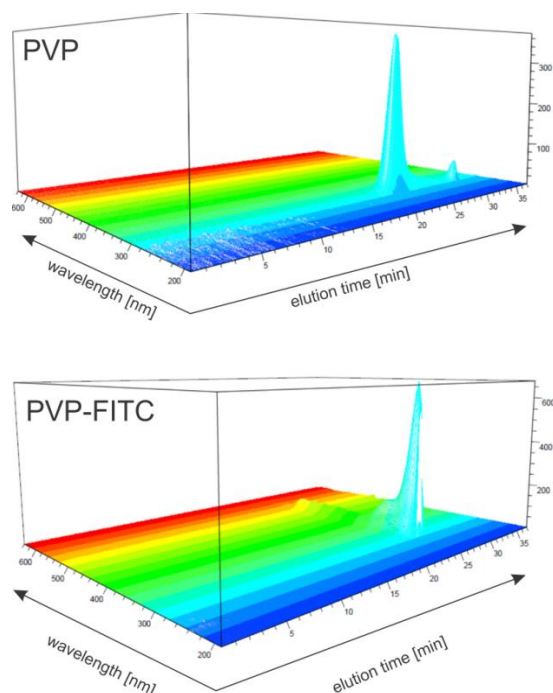retention times of PVP clearly reveal the co-elution of fluorescein with the PVP proving the covalent linkage.

Figure 4. SEC trace with DAD detector of PVP before and after conjugation with fluorescein-o-acrylate.

To measure the encapsulation efficiency of respectively the protein, TA and PVP, the microparticles were redispersed in phosphate buffered saline (PBS) followed by vigorous mixing and centrifugation. Next the supernatant was withdrawn and measured to determine the content of the respective components. **Figure 5** summarizes the encapsulation efficiency of the different formulations, expressed as the fraction (in %) of the respective components present in the feed mixture prior to spray drying, that is retained within the microparticles upon redispersion in PBS. These data show that PVP and TA remain largely entrapped within the microparticles upon redispersion in PBS, irrespective of the sequence in which the components are mixed, as in all cases only ~10 % of TA and PVP is released in the medium. However, the encapsulation efficiency of OVA strongly depends on the mixing sequence. On average 80 % of the OVA is retained within the microparticles when TA is added last. In the other two cases, a significantly lower amount of OVA (i.e. 20 – 30 %) remains entrapped within the microparticles upon redispersion in PBS. When TA is added last, the TA will complex simultaneously with OVA and PVP, allowing a better interaction of the OVA with TA compared to the situation where PVP and TA are mixed prior to addition of OVA. In this case, the strong interaction of PVP with TA likely hampers further complexation of TA with OVA. Why mixing TA with OVA prior to addition of PVP results in a low encapsulation efficiency is less clear. Possibly, TA-bound OVA becomes displaced when a large excess of a PVP is added, forming predominantly TA-

PVP complexes (as all three routes yield similar values for the entrapment of TA and PVP) and prevents stable entrapment of OVA into the microparticles upon spray drying.
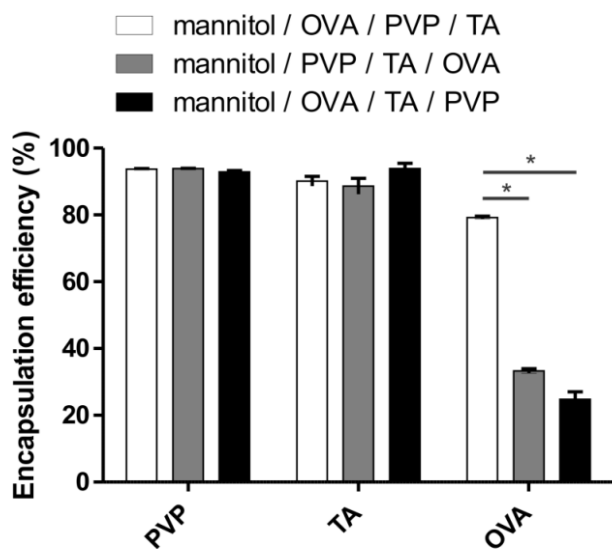

Figure 5. Encapsulation efficiency of PVP, TA and OVA within the porous microparticles upon redispersion in phosphate buffered saline. Three different mixing sequences of the components were evaluated. (*: $p < 0.05$).

We also found that the microparticles remain relatively stable during prolongued incubation at physiological conditions (i.e. PBS buffer (pH 7.4 and 0.15 M NaCl), 37 °C), with only a minor fraction of OVA and TA being released from the microparticles (**Figure 6**).
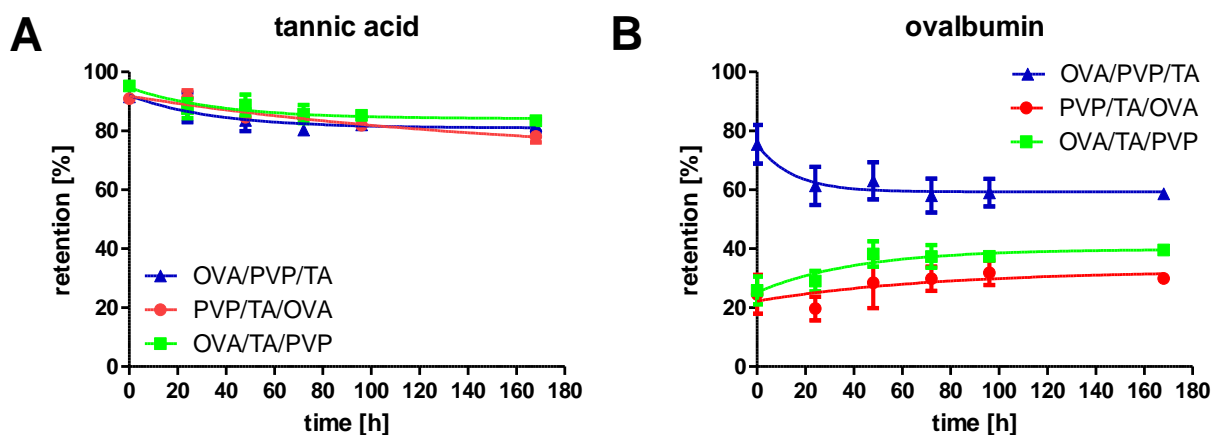

Figure 6. Retention of tannic acid (TA) and ovalbumin (OVA) as function of time within the porous microparticles upon redispersion in phosphate buffered saline.

3.3. *In vitro* evaluation

3.3.1. Cellular uptake

Subsequently, TA/PVP(OVA) microparticles were evaluated in a series of *in vitro* assays. First, we assessed whether these particles can be internalized by dendritic cells (DCs). Therefore DC2.4 cells were incubated with microparticles containing green fluorescently labelled OVA-Alexa Fluor488. Confocal microscopy was used to visualize particle uptake. To unambiguously discriminate between internalized particles and particles sticking to the cell wall we counterstained cell nuclei with Hoechst and the cell membrane with Alexa Fluor646 conjugated cholera toxin subunit B. By focusing the confocal plane on both the cell nuclei and cell membrane it is straightforward to consider particles as being internalized when they fall between the enclosure of the cell membrane. As shown in **Figure 7A** via flow cytometry and in **Figure 7B** via confocal microscopy, the microparticles are massively internalized by DCs.
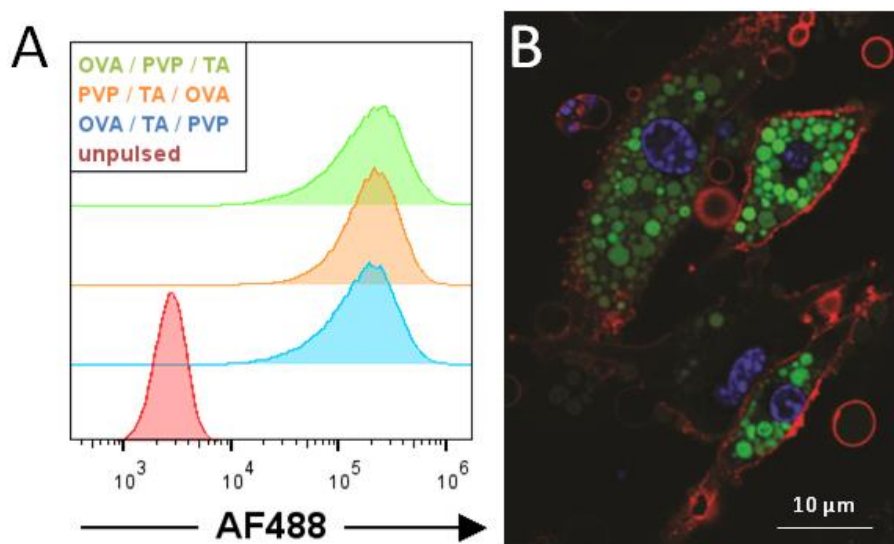

Figure 7. (A) Flow cytometry histograms of DC2.4 cells pulsed in vitro with microparticles (containing Alexa Fluor488-conjugated OVA). **(B)** Confocal microscopy image of DC2.4 cells pulsed with OVA/PVP/TA microparticles. Note that the other particles yielded similar images. Cell nuclei were stained blue with Hoechst, the cell membrane with AF647-conjugated cholera toxin subunit B and microparticles containing Alexa Fluor488-conjugated OVA (green fluorescence).

3.3.2. Cytotoxicity

Next, we assessed whether these particles and their components exhibit any cytotoxic effect (**Figure 8**). For this purpose, DC2.4 dendritic cells were incubated with different concentrations of microparticles and their respective individual constituents. Culture medium and DMSO were used as respectively negative and positive controls. Mannitol, OVA and PVP induced no cytotoxicity even at elevated concentrations as high as 1 mg/mL. TA does show cytotoxicity at 1 mg/mL and 0.1 mg/mL,

but not at 0.01 mg/mL. The microparticles on their turn only showed toxicity at 1 mg/mL concentrations. However, it has to be noted that at these elevated concentrations, the cells in the 96 well plate are fully covered with particles, thereby limiting diffusion of nutrients and mechanically damaging the cells. Obviously, the *in vivo* situation will be different, not involving the above mentioned constraints and thereby likely to be tolerant to relatively high particle concentrations.
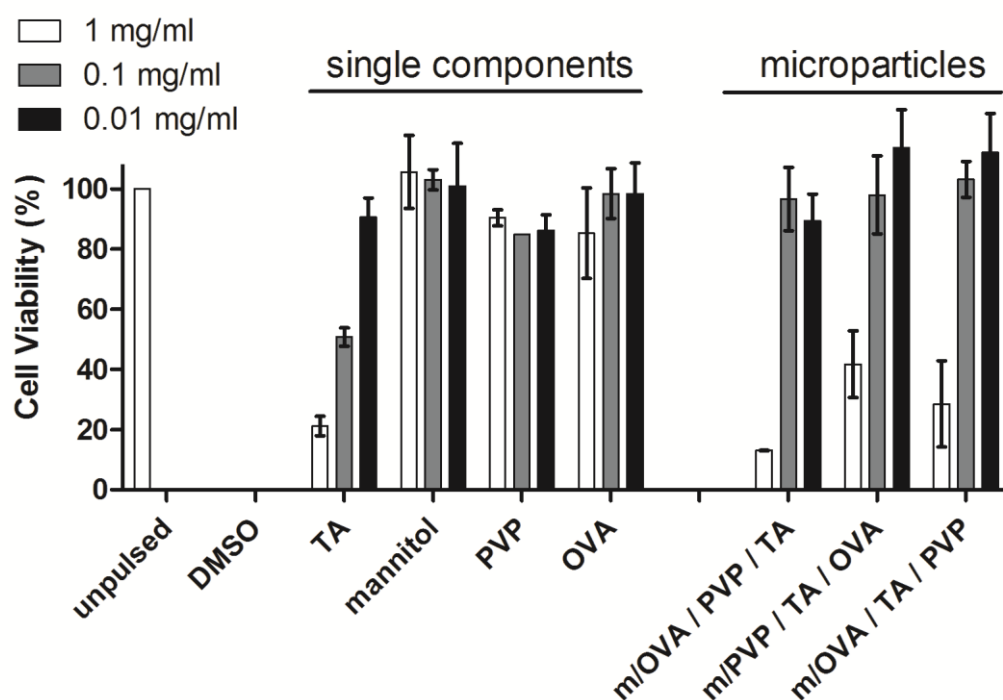

Figure 8. Cell viability measured by MTT assay performed on DC2.4 cells of the microparticles and their respective components. Pure cell culture medium and DMSO were used as negative and positive control, respectively. (n=6, technical replicates; *: $p < 0.05$).

3.3.3. Cross-presentation of encapsulated antigen

To assess whether encapsulation of OVA in TA/PVP microparticles via spray drying still allows OVA to be processed upon cellular uptake and, particularly, whether cross-presentation to CD8 T cells is promoted, we performed an *in vitro* CD8 T cell presentation assay. For this purpose, mouse bone marrow derived DCs were pulsed with different concentrations of either soluble or encapsulated OVA and subsequently co-cultured with OT-I cells. OT-I cells are CD8 T cells isolated from transgenic mice having a single T cell receptor recognizing the MHCI epitope of OVA(SIINFEKL). Prior to culturing them with DCs, OT-I cells are fluorescently labelled with CFSE, which is a membrane permeable dye that becomes metabolized into a non-membrane permeable variant by cytoplasmic enzymes. If OVA

is presented by DCs via MHCI, CFSE labelled OT-I cells will start to divide. Monitoring the decrease of the fluorescence from mother to daughter OT-I cells by flow cytometry offers a means to measure the quality of antigen cross presentation.

Figure 9A depicts the gating strategy applied to assess transgenic CD8 T cell proliferation. Cells were first gated on living cells, then on T cells and subsequently on CD8 T cells. The flow cytometry histograms in **Figure 9B** correspond to a DC to T cell ratio of 1:20, and clearly indicates that soluble OVA fails to induce OT-I proliferation at any of the tested OVA concentrations. The graph in **Figure 9C** shows that at all DC:T cell ratios addressed, only marginally response to soluble OVA was detectable. Additionally, we verified that empty (i.e. non-OVA containing) microparticles did not induce T cell proliferation by themselves (**Figure 10**). Contrary, encapsulated OVA strongly induced T cell proliferation with a clear dose-dependent trend being observed on the flow cytometry histograms for both antigen concentration and DC to T cell ratio. Indeed, OVA concentrations as low as 0.2 µg/mL induced T cell division only to a slight extend. Higher OVA concentrations such as 2 µg/mL induced strong T cell division for DC to T cell ratios of 1/20 and less. The quantification of T cell proliferation (i.e. percentage of divided OT-I cells) shown by the graphs in **Figure 9C** for different OVA concentrations and different DC:T cell ratios confirms the trends observed in the flow cytometry histograms, showing a dramatic increase in T cell proliferation when DCs were pulsed with encapsulated versus soluble OVA. Subtle differences are visible between the different types of microparticles with PVP/OVA/TA particles eliciting superior T cell proliferation at an OVA concentration of 2 µg/mL. However the same trend is not observed at 5 µg/mL. This again attributes to the importance of engineering soluble antigens into a particulate form to enhance the cross-presentation efficiency of exogenous antigen to CD8 T cells.
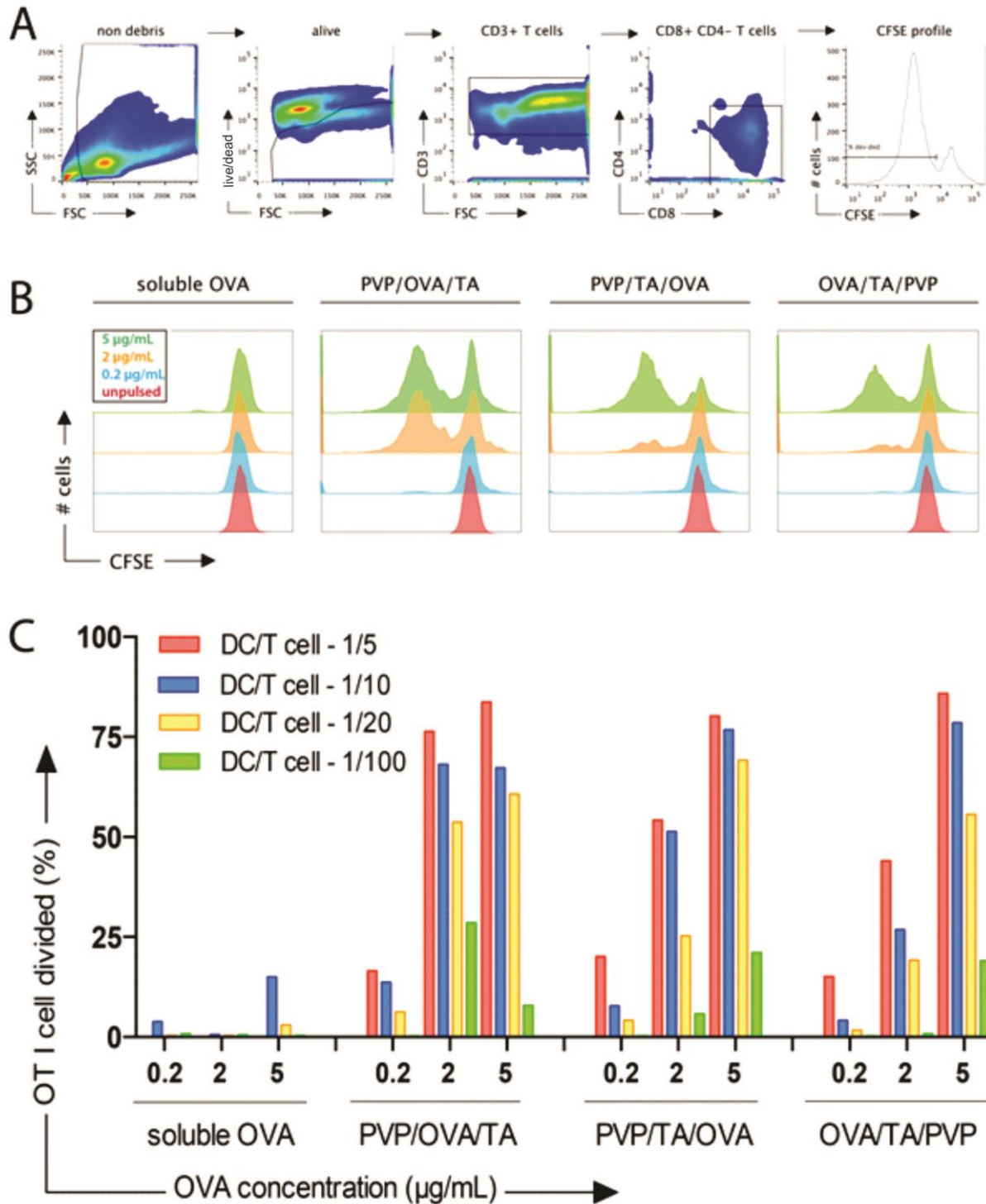
Figure 9. (A) Flow cytometry gating strategy to assess OT-I cell proliferation. **(B)** Flow cytometry histograms of OT-I proliferation in response to co-culturing with DCs pulsed with soluble OVA or encapsulated OVA at different OVA concentration. The OT-I cell to DC ratio 1:20. In **(C)** Quantitative representation of OT-I cells division as shown in the gating strategy in panel (A).
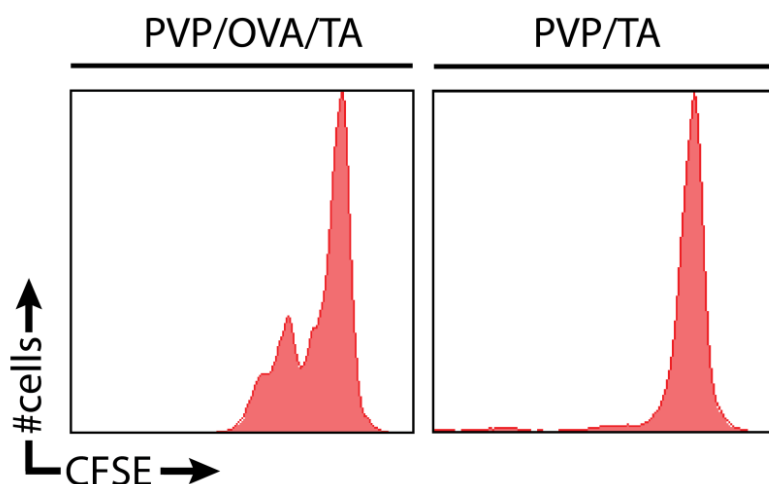
Figure 10. Flow cytometry histograms of OT-I proliferation in response to co-culturing with DCs pulsed with empty particles and OVA loaded particles (i.e. PVP/OVA/TA). The OT-I cell to DC ratio 1:20 and the OVA concentration was 2 μg/mL.

3.4. *In vivo* evaluation

Once confirmed *in vitro* that encapsulation of antigen in TA/PVP particles still allows antigen to be processed and presented by DCs to T cells, we aimed to assess the capability of our vaccine formulation strategy to enhance the antigen-specific cellular and humoral immune responses *in vivo*. As the PVP/OVA/TA particles exhibited the highest OVA encapsulation efficiency (thus providing a more defined system), and were most potent in stimulating CD8 T cell proliferation *in vitro*, we restricted the experimental set-up for the *in vivo* experiments to only one microparticle formulation, thereby also reducing the turnover of laboratory animals. Mice (in cohorts of 5) were immunized with either soluble OVA or encapsulated OVA following a prime-boost scheme with a 3 week time interval. To compare the performance of the hydrogen bonded microparticles with the electrostatic bond microparticles described earlier in this work, we evaluated both PVP/OVA/TA and DS/OVA/P$_L$ARG microparticles. Subsequently, the humoral immune response was quantified by measuring anti-OVA antibody titers in serum via enzyme-linked immunosorbent assay (ELISA), while the cellular immune response was quantified by measuring OVA-specific CD8 T cells in blood samples and the induction of INF-γ secreting CD4 and CD8 T cells in the spleen. **Figure 11A** summarizes the experimental set-up. As shown in **Figure 11B**, relative to soluble antigen, the IgG1 and IgG2c antibody titers for the polyelectrolyte microparticulate formulation were significantly enhanced after prime (**Figure 11B1 and B3**) and booster immunization (**Figure 11B2 and B3**). In case of the hydrogen bonded based microparticles, only IgG1 titers were significantly enhanced after prime and booster immunization. Only a very small booster effect is visible for the hydrogen bonded based microparticles, while in the case of the polyelectrolyte microparticle formulation the booster effect is

even absent for both antibody titers. The exact reason for this event remains unclear and needs to be investigated in future research. Tetramer staining on blood samples (**Figure 11C**) showed an significant increase in CTLs in the bloodstream for polyelectrolyte microparticles as well as for the hydrogen bonded microparticles compared to soluble OVA. Between the two different microparticles, the polyelectrolyte microparticles outperform the hydrogen bonded microparticles, especially after the booster immunization. ELISPOT (**Figure 11D**) analysis of the spleens showed that also the numbers of both IFN-γ secreting CD4 and CD8 T cells were significantly increased when mice were vaccinated with encapsulated (polyelectrolyte and hydrogen bonded microparticles) rather than soluble antigen, with primarily the CD8 T cell arm of the immune response being enhanced. When comparing the microparticles with each other, the number of IFN-γ secreting CD4 and CD8 T cells were significantly increased for the polyelectrolyte microparticles compared to the hydrogen bonded microparticles.

To investigate the underlying reason for lower induced immune responses for the hydrogen bonded PVP/OVA/TA microparticles, we compared the extend of OT-I CD8 T cell proliferation, when DCs were pulsed with antigen formulated in either hydrogen bonded PVP/OVA/TA microparticles versus electrostatic bound DS/OVA/P_LARG microparticles. Cytokine secretions (IFN-γ, IL-12, IL-13 and IL-17) measured in the supernatant of the DC-T cell co-cultures (**Figure 12**), was strongly increased in the microparticles group – both electrostatically and hydrogen bonded – relative to soluble OVA. As mentioned in Chapter 6, the cytokines IFN-γ, IL-13 and IL-17, are secreted by Th1, Th2 and Th17 cells respectively. During the induction of an adaptive immune response, IL-2 is produced by activated CD4 and CD8 T cells and is responsible for their proliferation. Overall, the electrostatic bonded DS/OVA/P_LARG microparticles exhibit superior performance in terms of antigen presentation.
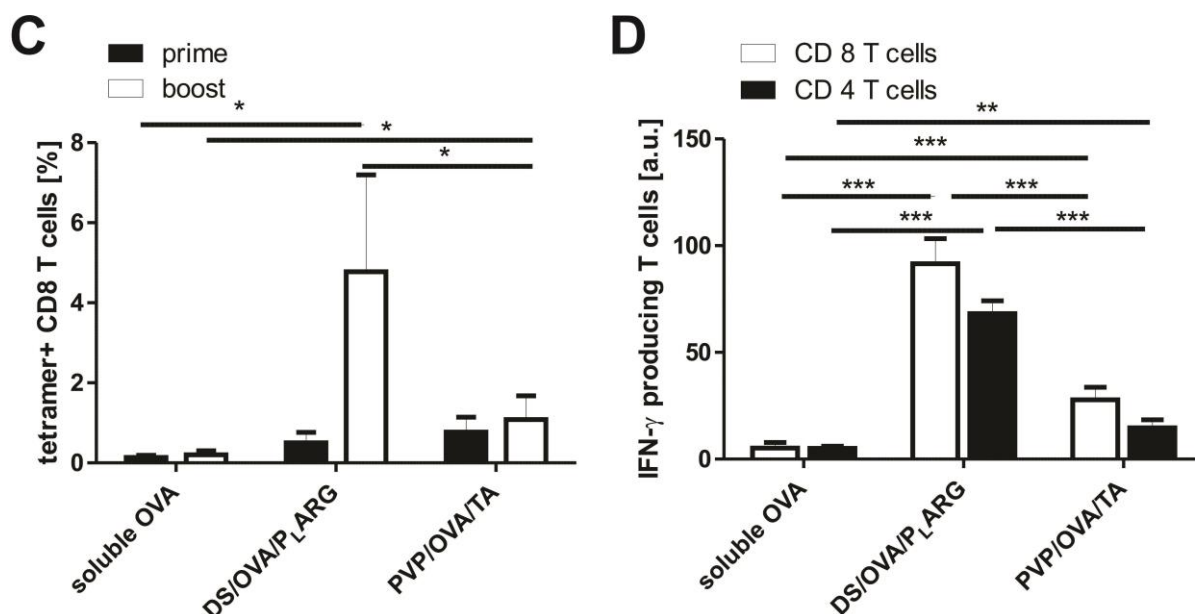
Figure 11. (A) Schematic representation of the experimental set-up of the immunization protocol and read out of the humoral and cellular immune response. **(B)** Antibody titers in serum. **(C)** Tetramer positive CD8 T cells in blood. **(D)** INF-γ secreting CD4 and CD8 T cells in the spleen. (n=5; *: $p < 0.05$))

To investigate whether enzymatic processing of the encapsulated antigen would be more efficient when encapsulated in electrostatic bound microparticles rather hydrogen bonded microparticles, we prepared particles loaded with DQ-OVA. DQ-OVA is a fluorogenic protease substrate, comprising ovalbumin that is strongly labeled, leading to fluorescence quenching. Upon proteolysis of DQ-OVA into dye-labeled fragments, the fluorescence quenching is alleviated and bright green fluorescence emerges. **Figure 13** depicts the increase in fluorescence intensity as function of time when pronase (a mixture of proteases) is added to soluble DQ-OVA and DQ-OVA formulated in hydrogen bonded or electrostatic bound microparticles. From these kinetics it is clear that antigen formulated in electrostatic bound DS/P$_L$ARG microparticles is processed to a much higher extend than in case of hydrogen bonded TA/PVP microparticles. Thus it is reasonable to assume that the encapsulated antigen is too strong complexed to the TA and/or that TA inactivates the enzymatic activity of the proteases.
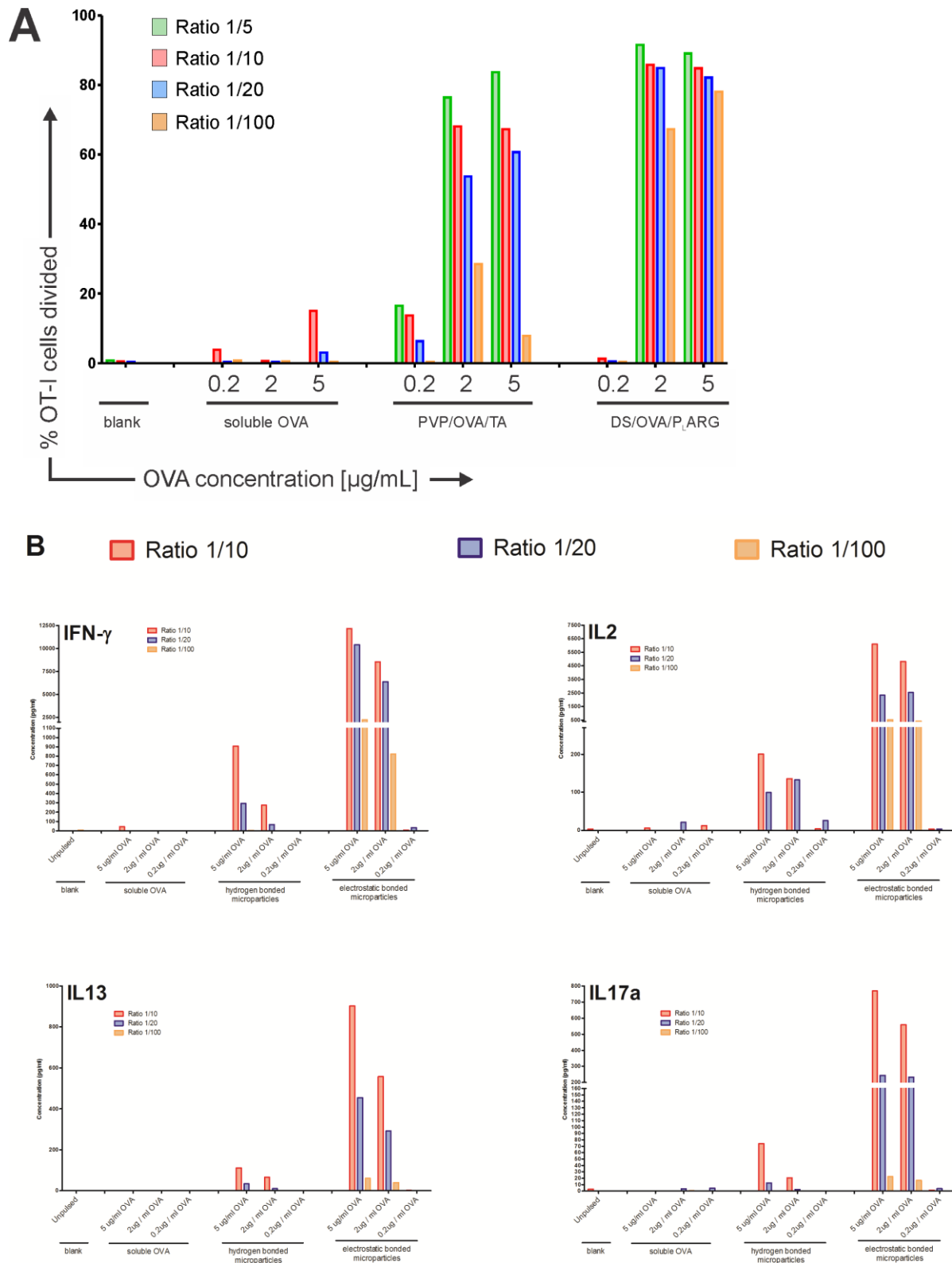
Figure 12. (A) Quantitative representation of OT-I cells division in response to co-culture of OT-I cells and DC that were pulsed with soluble OVA, PVP/OVA/TA or DS/OVA/P$_L$ARG microparticles. **(B)** Cytokine secretion measured by ELISA in the supernatant of the DC – T cell co-cultures.
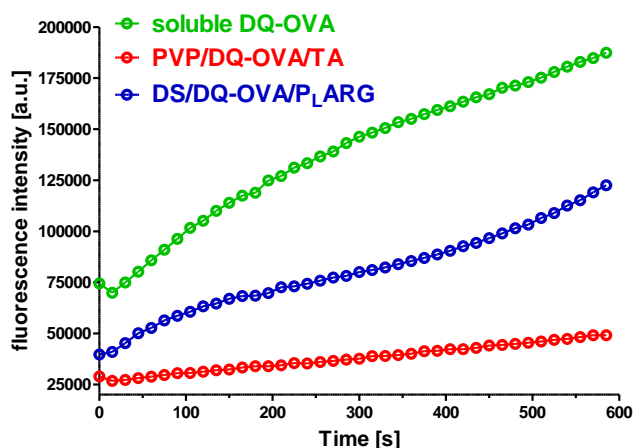
Figure 13. Enzymatic processing of DQ-OVA in soluble form or formulated in hydrogen bonded PVP/TA or electrostatic bound DS/P$_L$ARG microparticles.

4. CONCLUSION

In conclusion we have shown in this chapter that spray drying of TA and PVP with mannitol is a facile, efficient and cheap method to encapsulate co-spray dried vaccine protein antigens. Due to the strong hydrogen bond interaction between TA and PVP the particles retain their spherical morphology upon redispersion in aqueous medium, and stably entrap their payload. Importantly, mannitol acts as pore-forming component leading to a nanoporous internal structure of the microparticles. Furthermore, TA/PVP particles are non-cytotoxic, are efficiently phagocytosed by DCs *in vitro* and strongly promote cross-presentation to CD8 T cells *in vitro*. Immunization experiments in mice have shown that encapsulation of vaccine protein antigens promotes, relative to soluble antigen, the antigen-specific humoral and cellular immune response *in vivo*.

Compared to vaccine nano- and microparticle formulations that contain in addition to antigen also molecular adjuvants (i.e. molecular adjuvants such as Toll like receptor agonists (e.g. CpG and MPLA)) that strongly activate antigen presenting cells, the observed immune responses are still modest and is at the moment still outperformed by electrostatic bound polyelectrolyte microspheres. To address this issue, specially engineered components that exhibit less strong hydrogen bonding could offer a solution. Taken together, we believe that this type of delivery system has the potential to be further developed for (co)formulation of immune-stimulating cues, clinically relevant antigens against intracellular pathogens and for anticancer immune therapy. Additionally, as a dry powder formulation is produced, this formulation avoids the cold chain, thereby offering potential for the formulation of pandemic vaccines or vaccines intended for the developing world that both suffer from logistic issues under refrigerated conditions.

REFERENCES

1. Murthy, N.; Xu, M. C.; Schuck, S.; Kunisawa, J.; Shastri, N.; Frechet, J. M. J., A macromolecular delivery vehicle for protein-based vaccines: Acid-degradable protein-loaded microgels. Proc. Natl. Acad. Sci. U. S. A. 2003, 100, 4995-5000.

2. Luchini, A.; Geho, D. H.; Bishop, B.; Tran, D.; Xia, C.; Dufour, R. L.; Jones, C. D.; Espina, V.; Patanarut, A.; Zhou, W.; Ross, M. M.; Tessitore, A.; Petricoin, E. F., III; Liotta, L. A., Smart hydrogel particles: Biomarker harvesting: One-step affinity purification, size exclusion, and protection against degradation. Nano Lett. 2008, 8, 350-361.

3. Yoo, J. W.; Irvine, D. J.; Discher, D. E.; Mitragotri, S., Bio-inspired, bioengineered and biomimetic drug delivery carriers. Nat. Rev. Drug Discov. 2011, 10, 521-535.

4. De Koker, S.; Hoogenboom, R.; De Geest, B. G., Polymeric multilayer capsules for drug delivery. Chem. Soc. Rev. 2012, 41, 2867-2884.

5. Hubbell, J. A.; Thomas, S. N.; Swartz, M. A., Materials engineering for immunomodulation. Nature 2009, 462, 449-460.

6. Moon, J. J.; Huang, B.; Irvine, D. J., Engineering Nano- and Microparticles to Tune Immunity. Adv. Mater. 2012, 24, 3724-3746.

7. Rappuoli, R., From Pasteur to genomics: progress and challenges in infectious diseases. Nature Medicine 2004, 10, 1177-1185.

8. Kasturi, S. P.; Skountzou, I.; Albrecht, R. A.; Koutsonanos, D.; Hua, T.; Nakaya, H. I.; Ravindran, R.; Stewart, S.; Alam, M.; Kwissa, M.; Villinger, F.; Murthy, N.; Steel, J.; Jacob, J.; Hogan, R. J.; Garcia-Sastre, A.; Compans, R.; Pulendran, B., Programming the magnitude and persistence of antibody responses with innate immunity. Nature 2011, 470, 543-U136.

9. De Koker, S.; De Geest, B. G.; Singh, S. K.; De Rycke, R.; Naessens, T.; Van Kooyk, Y.; Demeester, J.; De Smedt, S. C.; Grooten, J., Polyelectrolyte Microcapsules as Antigen Delivery Vehicles To Dendritic Cells: Uptake, Processing, and Cross-Presentation of Encapsulated Antigens. Angew. Chem.-Int. Edit. 2009, 48, 8485-8489.

10. Moon, J. J.; Suh, H.; Bershteyn, A.; Stephan, M. T.; Liu, H.; Huang, B.; Sohail, M.; Luo, S.; Um, S. H.; Khant, H.; Goodwin, J. T.; Ramos, J.; Chiu, W.; Irvine, D. J., Interbilayer-crosslinked multilamellar vesicles as synthetic vaccines for potent humoral and cellular immune responses. Nature Materials 2011, 10, 243-251.

11. Moon, J. J.; Suh, H.; Li, A. V.; Ockenhouse, C. F.; Yadava, A.; Irvine, D. J., Enhancing humoral responses to a malaria antigen with nanoparticle vaccines that expand T-fh cells and promote germinal center induction. Proc. Natl. Acad. Sci. U. S. A. 2012, 109, 1080-1085.

12. Kwon, Y. J.; James, E.; Shastri, N.; Frechet, J. M. J., In vivo targeting of dendritic cells for activation of cellular immunity using vaccine carriers based on pH-responsive microparticles. Proc. Natl. Acad. Sci. U. S. A. 2005, 102, 18264-18268.

13. De Geest, B. G.; Willart, M. A.; Lambrecht, B. N.; Pollard, C.; Vervaet, C.; Remon, J. P.; Grooten, J.; De Koker, S., Surface-Engineered Polyelectrolyte Multilayer Capsules: Synthetic Vaccines Mimicking Microbial Structure and Function. Angew. Chem.-Int. Edit. 2012, 51, 3862-3866.

14. De Geest, B. G.; Willart, M. A.; Hammad, H.; Lambrecht, B. N.; Pollard, C.; Bogaert, P.; De Filette, M.; Saelens, X.; Vervaet, C.; Remon, J. P.; Grooten, J.; De Koker, S., Polymeric Multilayer Capsule-Mediated Vaccination Induces Protective Immunity Against Cancer and Viral Infection. ACS Nano 2012, 6, 2136-2149.

15. Reddy, S. T.; van der Vlies, A. J.; Simeoni, E.; Angeli, V.; Randolph, G. J.; O'Neill, C. P.; Lee, L. K.; Swartz, M. A.; Hubbell, J. A., Exploiting lymphatic transport and complement activation in nanoparticle vaccines. Nat. Biotechnol. 2007, 25, 1159-1164.

16. Dierendonck, M.; De Koker, S.; Cuvelier, C.; Grooten, J.; Vervaet, C.; Remon, J. P.; De Geest, B. G., Facile Two-Step Synthesis of Porous Antigen-Loaded Degradable Polyelectrolyte Microspheres. Angew. Chem.-Int. Edit. 2010, 49, 8620-8624.

17. Dierendonck, M.; De Koker, S.; De Rycke, R.; Bogaert, P.; Grooten, J.; Vervaet, C.; Remon, J. P.; De Geest, B. G., Single-Step Formation of Degradable Intracellular Biomolecule Microreactors. ACS Nano 2011, 5, 6886-6893.

18. Devriendt, B.; Baert, K.; Dierendonck, M.; Favoreel, H.; De Koker, S.; Remon, J. P.; De Geest, B. G.; Cox, E., One-step spray-dried polyelectrolyte microparticles enhance the antigen cross-presentation capacity of porcine dendritic cells. European Journal of Pharmaceutics and Biopharmaceutics 2013, 84, 421-429.

19. Caruso, F.; Caruso, R. A.; Mohwald, H., Nanoengineering of inorganic and hybrid hollow spheres by colloidal templating. Science 1998, 282, 1111-1114.

20. Decher, G., Fuzzy nanoassemblies: Toward layered polymeric multicomposites. Science 1997, 277, 1232-1237.

21. Donath, E.; Sukhorukov, G. B.; Caruso, F.; Davis, S. A.; Mohwald, H., Novel hollow polymer shells by colloid-templated assembly of polyelectrolytes. Angew. Chem.-Int. Edit. 1998, 37, 2202-2205.

22. Setia, S.; Mainzer, H.; Washington, M. L.; Coil, G.; Synder, R.; Weniger, B. G., Frequency and causes of vaccine wastage. Vaccine 2002, 20, 1148-1156.

23. Makkar, H. P. S.; Blummel, M.; Becker, K., Formation of complexes between polyvinyl pyrrolidones or polyethylene glycols and tannins, and their implication in gas-porduction and true digestibility in in-vitro techniques. British Journal of Nutrition   1995, 73, 897-913.

24. Erel-Unal, I.; Sukhishvili, S. A., Hydrogen-bonded multilayers of a neutral polymer and a polyphenol. Macromolecules 2008, 41, 3962-3970.

25. Kozlovskaya, V.; Zavgorodnya, O.; Chen, Y.; Ellis, K.; Tse, H. M.; Cui, W.; Thompson, J. A.; Kharlampieva, E., Ultrathin Polymeric Coatings Based on Hydrogen-Bonded Polyphenol for Protection of Pancreatic Islet Cells. Adv. Funct. Mater. 2012, 22, 3389-3398.

26. Kozlovskaya, V.; Kharlampieva, E.; Drachuk, I.; Cheng, D.; Tsukruk, V. V., Responsive microcapsule reactors based on hydrogen-bonded tannic acid layer-by-layer assemblies. Soft Matter 2010, 6, 3596-3608.

27. Sileika, T. S.; Barrett, D. G.; Zhang, R.; Lau, K. H. A.; Messersmith, P. B., Colorless Multifunctional Coatings Inspired by Polyphenols Found in Tea, Chocolate, and Wine. Angew. Chem.- Int. Edit. 2013, 52, 10766-10770.

28. Zhu, Z.; Gao, N.; Wang, H.; Sukhishvili, S. A., Temperature-triggered on-demand drug release enabled by hydrogen-bonded multilayers of block copolymer micelles. Journal of Controlled Release 2013, 171, 73-80.

29. Shukla, A.; Fang, J. C.; Puranam, S.; Jensen, F. R.; Hammond, P. T., Hemostatic Multilayer Coatings. Adv. Mater. 2012, 24, 492-+.

30. Kim, B.-S.; Lee, H.-i.; Min, Y.; Poon, Z.; Hammond, P. T., Hydrogen-bonded multilayer of pH-responsive polymeric micelles with tannic acid for surface drug delivery. Chem. Commun. 2009, 4194-4196.

31. Antunes, A. B. d. F.; Dierendonck, M.; Vancoillie, G.; Remon, J. P.; Hoogenboom, R.; De Geest, B. G., Hydrogen bonded polymeric multilayer films assembled below and above the cloud point temperature. Chem. Commun. 2013, 49, 9663-9665.

32. Ejima, H.; Richardson, J. J.; Liang, K.; Best, J. P.; van Koeverden, M. P.; Such, G. K.; Cui, J. W.; Caruso, F., One-Step Assembly of Coordination Complexes for Versatile Film and Particle Engineering. Science 2013, 341, 154-157.

33. Quinn, J. F.; Johnston, A. P. R.; Such, G. K.; Zelikin, A. N.; Caruso, F., Next generation, sequentially assembled ultrathin films: beyond electrostatics. Chem. Soc. Rev. 2007, 36, 707-718.

34.   Such, G. K.; Johnston, A. P. R.; Caruso, F., Engineered hydrogen-bonded polymer multilayers: from assembly to biomedical applications. Chem. Soc. Rev. 2011, 40, 19-29.

35.   Pound, G.; Eksteen, Z.; Pfukwa, R.; McKenzie, J. M.; Lange, R. F. M.; Klumperman, B., Unexpected reactions associated with the xanthate-mediated polymerization of N-vinylpyrrolidone. Journal of Polymer Science Part a-Polymer Chemistry 2008, 46, 6575-6593.

36.   De Koker, S.; De Geest, B. G.; Cuvelier, C.; Ferdinande, L.; Deckers, W.; Hennink, W. E.; De Smedt, S.; Mertens, N., In vivo cellular uptake, degradation, and biocompatibility of polyelectrolyte microcapsules. Adv. Funct. Mater. 2007, 17, 3754-3763.

37.   Gonnissen, Y.; Remon, J. P.; Vervaet, C., Development of directly compressible powders via co-spray drying. European Journal of Pharmaceutics and Biopharmaceutics 2007, 67, 220-226.

38.   Siebert, K. J.; Troukhanova, N. V.; Lynn, P. Y., Nature of polyphenol-protein interactions. Journal of Agricultural and Food Chemistry 1996, 44, 80-85.

39.   Perrier, S.; Takolpuckdee, P., Macromolecular design via reversible addition-fragmentation chain transfer (RAFT)/Xanthates (MADIX) polymerization. Journal of Polymer Science Part a-Polymer Chemistry 2005, 43, 5347-5393.

40.   Willcock, H.; O'Reilly, R. K., End group removal and modification of RAFT polymers. Polymer Chemistry 2010, 1, 149-157.

PART IV

SUMMARY AND GENERAL CONCLUSIONS

Summary and General Conclusions

Throughout the years, vaccines have become more and more important in preventing infectious diseases. According to the world health organization, vaccination saves every year 2 to 3 million lives. Eliciting potent cellular and humoral responses will be the key for the development of the next generation of vaccines against global killers like HIV, malaria and tuberculosis. Unfortunately, the currently licensed adjuvants fail in this task. By formulating vaccine antigens in particulate, rather than in soluble form, dramatically boosts the induction of cellular immunity, especially the generation of cytotoxic T cells (CTLs) that can recognize and eliminate infected or malignant cells. The underlying reason for this is that particulates (50 nm – 5 μm) are regarded by the immune system as being potentially pathogenic. Compared to soluble antigen, this leads to different routes of cellular uptake, processing and presentation to T cells. However, despite their high potential, microparticulate vaccine formulations did not yet reach the market. The reason for this can be attributed to the harsh conditions to which antigen is exposed during formulation, as well as the requirement of multiple batch operations with inherent difficulties for up scaling.

In this thesis a straightforward and scalable method to formulate vaccine antigens into microparticles is presented. This generic strategy is based on atomizing protein antigen mixed with oppositely interacting species and a pore-forming component into a hot air stream, leading to the production of solid microparticles. The latter can be redispersed in aqueous medium forming a stable microparticulate suspension. The rationale for designing porous particles was that this would facilitate inwards diffusion of intracellular proteases and thereby enhance antigen processing and presentation.

In **Chapter 1**, an introduction about the immune system was given. The crucial role of dendritic cells, the different pathways of cross-presentation as well as the failure of current vaccine strategies were discussed into detail.

Chapter 2 evaluates the applications of polymeric multilayer capsules (PMLC) as vaccine delivery systems. These PMLC are fabricated by layer-by-layer coating of interacting species onto a sacrificial template followed by the decomposition of this template, yielding hollow capsules. The route of

internalization and the intracellular localization of the capsules were described. Different triggers such as pH, enzymatic degradation and shift from oxidative and reductive environment were reviewed as release mechanisms of an encapsulated payload. Additionally, *in vitro* and *in vivo* interactions between PMLC and immune cells after pulmonary or subcutaneously delivery were addressed showing a high potential of PMLC for vaccine delivery purposes.

These PMLC have not reached the industrial market due to constraints regarding their multistep assembly procedure. Therefore in **CHAPTER 3**, procedures to simplify and automatize LbL assembly were discussed. Spray-based approaches were highlighted and in particular the spray drying process was described into detail. Finally, applications in pharmaceutical industry of spray drying were mentioned.

In **CHAPTER 4**, we reported on the design of porous polyelectrolyte microspheres by spray drying ovalbumin (OVA) as model antigen in combination with the oppositely charged polyelectrolytes dextran sulfate as polyanion and poly-L-arginine as polycation, together with calcium carbonate nanoparticles as a pore-forming component. The thus obtained solid microspheres showed an average size of 6 μm and a ζ-potential of -6.8 mV and remained stable upon resuspension into aqueous medium. Resuspending these solid microspheres in an EDTA solution leads to extraction of the $CaCO_3$ nanoparticles and yielded porous microspheres as evidenced by various microscopy techniques. These porous microspheres have a ζ-potential of -18 mV and show a similar size to the solid ones. By using confocal microscopy and green fluorescent ovalbumin, we could demonstrate that the antigen was retained within the polyelectrolyte framework and quantify an encapsulation efficiency of 94±1% and 85±1% for the solid and porous microspheres respectively. These are higher encapsulation efficiencies compared to a typical 50% encapsulation efficiency reported earlier for the hollow polyelectrolyte microcapsules. *In vitro* experiments with mouse bone marrow derived dendritic cells showed that the microspheres were efficiently internalized into acidic intracellular vesicles.

In **CHAPTER 5**, we used mannitol instead of $CaCO_3^{NP}$ as sacrificial component to co-spray dry with the polyelectrolytes. In the case of $CaCO_3^{NP}$ an additional step to remove the core template (i.e. dissolving in an EDTA solution) is needed, while mannitol is a biocompatible and highly water soluble pore-forming component and does not need to be removed from the formulation prior to use. These particles showed to be stable upon resuspension in aqueous medium, having a mean diameter of 7 μm and an encapsulation efficiency of 99 ± 1% for ovalbumin (i.e. model antigen). Furthermore,

XRPD revealed a change in the crystallographic state of mannitol after spray drying. Crude mannitol is crystalline, while mannitol after spray drying in combination with polyelectrolytes showed an decrease in crystallinity, rendering amorphous mannitol which favors protection of the encapsulated protein. By measuring the enzymatic catalytic activity of an enzyme, HRP, that was spray dried instead of OVA, we could prove that the biological activity was barely influenced by the spray drying process. Like the CaCO$_3$^{NP} microspheres, these mannitol based microspheres became internalized by dendritic cells into intracellular acidic and transmission electron microscopy showed the polyelectrolyte microspheres to be deformed intracellularly as function of time. Finally, we were able to demonstrate that the encapsulated OVA was still available for cross-presentation as a peptide-MHCI complex after internalization by DCs.

In **CHAPTER 6**, we explored the effect of formulation and process parameters on the microparticulate vaccine formulations. The relative amount of mannitol that was added before spray drying has an influence on particle recovery, particle integrity and encapsulation efficiency. Subsequently, the sequence of mixing mannitol, OVA, DS and P$_L$ARG before spray drying was investigated and was found to influence the ζ-potential and the spatial distribution of the antigen. Both positively and negatively loaded particles were efficiently internalized by DCs, did not show cytotoxicity and promote cross-presentation to CD8 T cells *in vitro*. *In vivo* experiments in mice showed that upon subcutaneous injection, the microparticles only induced a mild tissue response. Finally, relative to soluble OVA, OVA encapsulated in the microparticles enhanced serum antibody titers and splenic T cell responses.

In the field of polymeric self-assembly, hydrogen bonding, as an alternative to electrostatic assembly, is witnessing increased popularity. In **CHAPTER 7** we reported on the assembly of multilayer films of tannic acid and neutral poly(2-oxazolines) via hydrogen bonding. Using the temperature-responsive polymer poly(2-(n-propyl)-2-oxazoline), we were able to demonstrate that LbL assembly was possible both below and above the cloud point temperature of the polymer.

CHAPTER 8 further elaborates on hydrogen bonding as driving force for self-assembly and reports on the synthesis of antigen-loaded microparticles based on hydrogen-bonding between tannic acid and poly(N-vinylpyrrolidone). In a first step, the formulation of stable assemblies between the two components were assessed. Next TA and PVP were spray dried in combination with mannitol as a sacrificial component. After extraction of mannitol upon resuspension in aqueous medium, the microspheres remained stable and showed a mean diameter of 4 µm with a highly porous internal

structure. Since OVA can interact with TA, the sequence of mixing OVA, TA and PVP had an influence on the encapsulation efficiency. Independent on the mixing sequence, TA and PVP remained within the microparticles. On the other hand, the encapsulation efficiency of OVA was influenced by the mixing sequence. When TA was added last, the highest encapsulation efficiency (i.e. 80%) was obtained, likely due to the simultaneously complex formation between TA, OVA and PVP. When mixing first TA and PVP, complexes are already formed, which impedes further complexation when adding OVA. Also, we could demonstrate that the spray dried TA/PVP particles were efficiently taken up by DCs, did not show cytotoxicity and promote cross-presentation to CD8 T cells *in vitro*. Finally IgG1 and IgG2c antibody titers as well as tetramer positive CD8 T cells and IFN-γ producing CD4 and CD8 T cells were augmented in mice immunized with the spray dried particles compared to soluble antigen. Thus, the encapsulation of vaccine protein antigens in particular form elicits antigen-specific humoral and cellular immune response *in vivo* in contrast to soluble antigen. However the observed immune responses are still modest and the electrostatic bound DS/OVA/P$_L$ARG microparticles outperform the hydrogen bonded PVP/OVA/TA microparticles.

As a general conclusion, the vaccine formulation technology developed in this thesis allows to formulate vaccine antigens into microparticles in an easy and scalable way, with a minimum of batch steps and at a high encapsulation efficiency with minimal loss of biological activity. Importantly, a dry powder formulation avoids the cold chain transport and improves storage stability. Current limitations of the technology is the fact that the components used in the formulation still need to pass regulatory affairs. Additionally, particle size strongly influences the efficiency at which particles are internalized *in vivo* by antigen presenting cells, with submicron sized particles being much more efficient than larger ones. Therefore a major challenge remains the downsizing of the particles into the nanoscale which is extremely tough to realize with current spray drying technology.

Additionally proper evaluation with the current state-of-the art adjuvants has to be done, preferably using clinically relevant antigens. As the newer licensed vaccine adjuvants are mostly combination products and thus co-formulation with other immune-potentiating components, such as different Toll-like receptor agonists or saponins, there are opportunities for co-formulation of antigen and these adjuvants via our nanoporous micoparticle technology. In addition to mannitol, also other sugar compounds such as trehalose or sorbitol could be evaluated as stabilizing pore formers.

PART V

SAMENVATTING EN ALGEMEEN BESLUIT

SAMENVATTING EN ALGEMEEN

BESLUIT

In de loop van de jaren, hebben uitgebreide vaccinatiecampagnes een enorme impact gehad op het voorkomen en zelfs uitroeien van infectieuze ziektes. Volgens de Wereldgezondheidsorganisatie, redt vaccinatie jaarlijks 2 tot 3 miljoen levens. Het opwekken van krachtige cellulaire en humorale responsen wordt geacht de sleutel te zijn in de ontwikkeling van de volgende generatie vaccins tegen mondiale doodsoorzaken zoals HIV, malaria en tuberculose. Helaas falen de huidige adjuvantia in deze opdracht. Door vaccin antigenen te formuleren in de vorm van nano- of micropartikels, in plaats van in een oplosbare vorm, kan de cellulaire immuunrespons drastisch verhoogd worden, in het bijzonder het opwekken van cytotoxische T cellen. Deze cellen kunnen geïnfecteerde of verkankerde cellen herkennen en vernietigen. De onderliggende reden hiervoor is dat partikelvormig materiaal (50 nm -5 µm) door het immuunsysteem mogelijks als pathogeen wordt beschouwd. Wanneer dit wordt vergeleken met de antigenen in oplosbare vorm, leidt dit tot andere routes in cellulaire opname, het verwerken en presenteren aan T cellen. Niettegenstaande hun groot potentieel, hebben microparticulaire vaccinformulaties tot op heden de markt nog niet bereikt. De reden hiervoor is te wijten aan de vaak extreme condities waaraan een antigen wordt blootgesteld tijdens formulatie, evenals aan de meerdere tijdrovende processtappen die nodig zijn voor het aanmaken van nano- of micropartikels. Deze stappen gaan uiteraard gepaard met moeilijkheden bij het opschalen.

In deze doctoraatsthesis wordt een vereenvoudigde en schaalbare methode om vaccin antigenen in micropartikels te formuleren voorgesteld. Deze algemene strategie is gebaseerd op het vernevelen in een warme luchtstroom van een eiwitantigen in combinatie met tegengestelde interagerende polymeren samen met een porievormende component. Dit leidt tot de vorming van vaste micropartikels, die bij toevoeging van water een stabiele microparticulaire suspensie vormen. De achterliggende reden om poreuze partikels te ontwerpen was dat dit de inwaartse diffusie van intracellulaire proteasen zou vergemakkelijken en daardoor de antigenverwerking en presentatie verbeteren.

HOOFDSTUK 1 geeft een algemene inleiding over het immuunsysteem. De cruciale rol van dendritische cellen (DCs), de verschillende trajecten in kruispresentatie, evenals het falen van de huidige vaccin strategieën werden in detail besproken.

HOOFDSTUK 2 evalueert de toepassingen van polymeer microcapsules als vaccin toedieningssysteem. Deze polymeer microcapsules worden aangemaakt door het coaten op een tijdelijke kern van interagerende polymeren via de 'layer-by-layer' (LbL) techniek, gevolgd door het verwijderen van de desbetreffende tijdelijke kern, waardoor holle capsules bekomen worden. De cellulaire internaliseringsroute en de intracellulaire lokalisatie van de capsules werd beschreven. Verschillende triggers, zoals pH, enzymatische degradatie en verschuiving van een oxidatieve naar een reducerende omgeving werden besproken als mechanismen om de ingekapselde inhoud vrij te geven. Bovendien werden *in vitro* en *in vivo* interacties tussen PMLC en immuun cellen na pulmonaire of subcutane toediening behandeld. Hierbij werd aangetoond dat PMLC een groot potentieel als vaccinatie toedieningssysteem bezitten.

Deze polymeer microcapsules hebben het klinisch stadium nog niet bereikt wegens beperkingen omtrent hun aanmaakprocedure. Aangezien die bestaat uit meerdere processtappen werd er in **HOOFDSTUK 3** aandacht besteed aan procedures om de LbL aanmaak te vereenvoudigen en te automatiseren. De nadruk werd gelegd op methodes die gebaseerd zijn op sproeien en meer specifiek werd het sproeidroogproces in detail beschreven. Tenslotte werden toepassingen van sproeidrogen in de farmaceutische industrie vermeld.

In **HOOFDSTUK 4**, werden poreuze polyelektroliet microsferen geproduceerd door het sproeidrogen van ovalbumine (OVA) als modelantigen in combinatie met de tegengestelde geladen polyelektrolieten (dextraan sulfaat als polyanion en poly-L-arginine als polykation) en calciumcarbonaat nanopartikels ($CaCO_3^{NP}$) als porievormende component. De aldus verkregen vaste microsferen hadden een gemiddelde grootte van 6 μm en een zetapotentiaal van -6.8 mV. Tevens bleven ze stabiel na hersuspensie in waterig midden. Het hersuspenderen van deze vaste microsferen in een EDTA oplossing leidt tot de extractie van de calciumcarbonaat nanopartikels en leverde poreuze microsferen op zoals blijkt uit verscheidende microscopische technieken. Deze poreuze microsferen hadden een zetapotentiaal van -18 mV en een grootte vergelijkbaar aan de solide microsferen.

Met behulp van confocale microscopie en groen fluorescent ovalbumine, konden we aantonen dat het antigen werd vastgehouden binnen het polyelektroliet netwerk. Een inkapselingsefficiëntie van 94±1% en 85±1% werd respectievelijk voor de vaste en poreuze microsferen berekend. Deze inkapselingsefficiënties zijn hoger vergeleken met de holle polyelektroliet microcapsules. Voor deze laatste werd er tijdens vroeger onderzoek typisch een 50% inkapselingsefficiëntie vermeld. *In vitro*

experimenten met dendritische cellen afkomstig van muisbeenmerg toonden aan dat de microsferen efficiënt geïnternaliseerd werden in zure intracellulaire vesikels.

In **HOOFDSTUK 5** gebruikten we mannitol in plaats van $CaCO_3^{NP}$ als tijdelijke component om te co-sproeidrogen met de polyelektrolieten. In het geval van $CaCO_3^{NP}$ is een extra stap vereist om de tijdelijke kern te verwijderen, namelijk het oplossen in een EDTA oplossing. Mannitol daarentegen is een biocompatibele en een zeer goed water oplosbare porievormende component en hoeft voor gebruik niet uit de formulatie verwijderd worden. Deze partikels zijn stabiel na hersuspensie in waterig midden, hebben een gemiddelde diameter van 7 µm en een inkapselingsefficiëntie van 99 ± 1% voor ovalbumine (d.w.z. het modelantigen).

Bovendien toonde XRPD een verandering aan in de kristallografische staat van mannitol na sproeidrogen. Doorgaans is mannitol kristallijn, terwijl mannitol na sproeidrogen in combinatie met polyelektrolieten een daling in kristalliniteit vertoonde, en zo amorf mannitol opleverde. Dit is een gunstig effect voor de bescherming van het ingekapselde eiwit. Door de enzymatische katalytische activiteit van een enzym, HRP, – dat gesproeidroogd was in plaats van OVA– te meten konden we aantonen dat de biologische activiteit nauwelijks beïnvloed werd door het sproeidroogproces. Net zoals de $CaCO_3^{NP}$ microsferen, werden de microsferen die gebaseerd waren op mannitol geïnternaliseerd door dendritische cellen in de intracellulaire zure vesikels. Transmissie elektronen microscopie toonde aan dat de polyelektroliet microsferen intracellulair vervormd werden in functie van de tijd. Tenslotte konden we bewijzen dat het ingekapselde OVA nog steeds beschikbaar was voor kruispresentatie als een peptide:MHCI complex na internalisering door DCs.

In **HOOFDSTUK 6**, onderzochten we het effect van formulatie en procesparameters op de microparticulaire vaccin formulaties. De relatieve hoeveelheid mannitol die werd toegevoegd voor sproeidrogen beïnvloedde de opbrengst na sproeidrogen, de partikelintegriteit en de inkapselingsefficiëntie. Vervolgens werd de volgorde van toevoegen van mannitol, OVA, DS en P_LARG onderzocht en dit bleek een invloed te hebben op de ζ-potentiaal en de ruimtelijke distributie van het antigen. Zowel positief als negatief geladen partikels werden efficiënt opgenomen door dendritische cellen, vertoonden geringe celtoxiciteit en bevorderden kruispresentatie aan CD8 T cellen *in vitro*. Verder toonden *in vivo* experimenten in muizen aan dat een milde weefselreactie werd waargenomen na subcutane injectie van de micropartikels. Tenslotte, verhoogde OVA ingekapseld in micropartikels relatief gezien t.o.v. OVA in oplosbare vorm, serum antilichaam titers en T cel responsen van de milt.

Op het gebied van polymeer 'self-assembly', wint waterstofbrugbinding, als een alternatief voor elektrostatische aanmaak, aan populariteit. In **HOOFDSTUK 7**, werden films bestaande uit meervoudige lagen van tannine en neutrale poly(2-oxazolines) via waterstofbrugbinding geproduceerd. Door gebruik te maken van het temperatuurgevoelige polymeer poly(2-(n-propyl)-2-oxazoline) konden we aantonen dat 'layer-by-layer' techniek mogelijk was zowel onder als boven de fasetransitie temperatuur van het polymeer.

In **HOOFDSTUK 8** werd er verder ingegaan op waterstofbrugbinding als drijvende kracht voor polymeer 'self-assembly'. Antigenen ingekapseld in micropartikels die gebaseerd zijn op waterstofbrugbinding tussen tannine en poly(N-vinylpyrrolidone) (PVP) werden aangemaakt. In een eerste stap werd er nagegaan of er stabiele verbindingen tussen beide componenten werd bekomen. Daarna werden tannine en PVP gesproeidroogd in combinatie met mannitol als de porievormende component. Na hersuspensie in waterig midden, wat leidt tot de extractie van het mannitol bleven de microsferen stabiel. Een gemiddelde diameter van 4 µm werd gemeten en een zeer poreuze interne structuur werd waargenomen. Aangezien OVA kan interageren met tannine, had de volgorde van toevoegen van OVA, tannine en PVP een invloed op de inkapselingsefficiëntie. Tannine en PVP werden niet beïnvloed door de volgorde van toevoegen en bleven vastgehouden binnen de micropartikels. Anderzijds werd de inkapselingsefficiëntie van OVA wel beïnvloed door de volgorde van toevoegen. Wanneer tannine als laatste werd toegevoegd, werd de hoogste inkapselingsefficiëntie bekomen (d.w.z. 80%). Dit is waarschijnlijk te wijten aan de gelijktijdige complexvorming tussen tannine, OVA en PVP. Bovendien konden we ook aantonen dat de gesproeidroogde tannine/PVP partikels efficiënt werden opgenomen door dendritische cellen, geringe cytotoxiciteit vertoonden en kruispresentatie aan CD8 T cellen *in vitro* bevorderden. Tenslotte waren zowel IgG1 en IgG2c antilichaam titers als tetrameer positieve CD8 T cellen en IFN- γ producerende CD4 en CD8 T cellen verhoogd in muizen die geïmmuniseerd waren met de gesproeidroogde partikels ten opzichte van antigeen in oplossing. Dus, de inkapseling van vaccin eiwitantigenen in particulaire vorm verhoogde het opwekken van antigen-specifieke humorale en cellulaire immuun responsen *in vivo* in vergelijking met antigenen in oplosbare vorm. Toch zijn de waargenomen immuunresponsen maar matig en de elektrostatisch gebonden DS/OVA/P$_L$ARG micropartikels presteerden beter dan de waterstofbrug gebonden PVP/OVA/TA micropartikels

Samengevat, de vaccin formulatie technologie die in deze doctoraatsthesis werd ontwikkeld, laat toe om vaccin antigenen in micropartikels te formuleren op een gemakkelijke en schaalbare manier. Deze techniek vereist uiterst weinig processtappen en vertoont een hoge inkapselingsefficiëntie met een minimaal verlies aan biologische activiteit. Door het als droog poeder te formuleren, kan de

koude keten voor het transport vermeden worden en verbetert de stabiliteit bij het bewaren. Deze technologie heeft op dit moment als beperking dat de componenten in deze formulatie nog de regelgevende wetgeving moeten passeren. Bovendien beïnvloedt de deeltjesgrootte sterk de efficiëntie waarmee *in vivo* de partikels geïnternaliseerd worden door de antigen presenterende cellen. Partikels met een submicron grootte worden efficiënter opgenomen dan grotere partikels. Daardoor blijft het een grote uitdaging om de partikels te verkleinen tot op de nanoschaal. Dit is echter uitermate moeilijk te realiseren met de huidige sproeidroogtechnologie.

Verder dient de encapsulatie van de allernieuwste adjuvanten, met voorkeur voor klinisch relevante antigenen onderzocht te worden. Meer nog, de meest recent vergunde vaccin adjuvanten zijn vaak combinatieproducten en dus co-formulatie met immuun stimulerende componenten, zoals de verschillende Toll-like receptor agonisten of saponines, geven mogelijkheden om een antigen met deze adjuvanten via onze nanoporeuze micropartikel technologie te co-formuleren. Verder, kan naast mannitol andere suikercomponenten zoals trehalose of sorbitol geëvalueerd worden als stabiliserende poriënvormers.

178

CURRICULUM VITAE

PERSONALIA

Name	Dierendonck
First name	Marijke
Nationality	Belgian
Place and date of birth	Oostende, 27/06/1986
Address	Onderwijsstraat 18
	8430 Middelkerke
Email	marijke.dierendonck@gmail.com
Telephone	0494 94 98 80

LANGUAGE SKILLS

Native language	Dutch
Other languages	English, French, (German)

WORK EXPERIENCE

September 2010-present — PhD, Laboratory of Pharmaceutical Technology, Ghent university
- Guidance of students during practical courses: Artsenijbereidkunde (3rd bachelor) and Farmaceutische Technologie (2nd master)
- Guidance of thesis students (1st Master of Pharmacy and Master in industrial pharmacy)

July 2010, July 2009 — Pharmacist, Apotheek Claeys, Oostende

EDUCATION

September 2010-present — PhD, Laboratory of Pharmaceutical Technology, Ghent university

2009-2010 — Master in industrial pharmacy

2004-2009 — Pharmacist, Ghent University

PUBLICATIONS

Dierendonck, M.; De Koker, S.; Cuvelier, C.; Grooten, J.; Vervaet, C.; Remon, J.P.; De Geest, B.G. Facile two-step synthesis of porous antigen-loaded degradable polyelectrolyte microspheres. Angewandte Chemie International Edition, 2010, 49, 8620-8624

Dierendonck, M.; De Koker, S.; De Rycke, R.; Bogaert, P.; Grooten, J.; Vervaet, C.; Remon, J.P.; De Geest, B.G. Single-step formation of degradable intracellular biomolecule microreactors. ACS Nano, 2011, 5, 6886-6893

Dierendonck, M.; De Koker, S.; Vervaet, C.; Remon, J.P.; De Geest, B.G. Interaction between polymeric multilayer capsules and immune cells. Journal of Controlled Release, 2012, 161, 592-599

Antunes, ABDF, **Dierendonck, M.**; Vancoillie, G.; Remon, J.P.; Hoogenboom, R.; De Geest, B.G. Hydrogen bonded polymeric multilayer films assembled below and above the cloud point temperature. Chemical communications, 2013, 49, 9663-9665

Devriendt, B.; Baert, K.; **Dierendonck, M.**; Favoreel, H.; De Koker, S.; Remon, J.P.; De Geest, B.G.; Cox, E. One-step spray-dried polyelectrolyte microparticles enhance the antigen cross-presentation capacity of porcine dendritic cells. European Journal of Pharmaceutics and Biopharmaceutics, 2013, 84, 421-429

De Smet, R.; Demoor, T.; Verschuere, S.; Dullaers, M.; Ostroff, G.R.; Leclercq, G.; Allais, L.; Pilette, C.; **Dierendonck, M.**; De Geest, B.G.; Cuvelier, C.A. Beta-glucan microparticles are good candidates for mucosal antigen delivery in oral vaccination. Journal of Controlled release. 2013, 172, 671-678

Dierendonck, M.; De Koker, S.; De Rycke, R.; De Geest, B.G. Just spray it – LbL assembly enters a new age. Soft Matter, 2014, 10, 804-807

Dierendonck, M.; Fierens, K.; De Rycke, R.; Lybaert, L.; Maji, S.; Zhang, Z.; Zhang, Q.; Hoogenboom, R.; Lambrecht, B.N.; Grooten, J.; Remon, J.P.; De Koker, S.; De Geest, B.G. Nanoporous hydrogen bonded polymeric microparticles: Facile and economic production of cross presentation promoting vaccine cariers. Advanced Functional Materials, in press.

PRESENTATIONS ON CONFERENCES

Oral presentations

Dierendonck, M.; De Koker, S.; De Cock, L.J.; Vervaet, C.; Remon, J.P.; De Geest, B.G. Single-step vaccine formulation into polyelectrolyte microspheres via spray drying. 8th World Meeting on Pharmaceutics, Biopharmaceutics and Pharmaceutical Technology, March 19-22, 2012. Istanbul, Turkey.

Dierendonck, M.; De Koker, S.; De Cock, L.J.; Vervaet, C.; Remon, J.P.; De Geest, B.G. Single-step vaccine formulation into polyelectrolyte microspheres via spray drying. 16th Forum of Pharmaceutical sciences, May 7-8, 2012. Blankenberge, Belgium.

Dierendonck, M.; Fierens, K.; De Rycke, R.; Lybaert, L.; Maji, S.; Zhang, Z.; Zhang, Q.; Hoogenboom, R.; Lambrecht, B.N.; Grooten, J.; Remon, J.P.; De Koker, S.; De Geest, B.G. Nanoporous hydrogen bonded polymeric microparticles: Facile and economic production of cross presentation promoting vaccine cariers. Biopharmacy Meeting, December 18th , 2013. Ghent, Belgium.

Poster presentations

Dierendonck, M.; De Koker, S.; Vervaet, C.; Remon, J.P.; De Geest, B.G. Fabrication of encapsulated biomolecules within degradable polyelectrolyte microspheres using spray drying as a technique. 9th International Symposium on Frontiers in Biomedical Polymers, May 9-12, 2011. Funchal, Portugal.

Dierendonck, M.; De Koker, S.; Vervaet, C.; Remon, J.P.; De Geest, B.G. Spray drying as a facile method to formulate vaccine antigens into biodegradable polyelectrolyte microspheres. AAPS Annual Meeting and exposition, October 23-27, 2011. Washington DC, USA.

Dierendonck, M.; De Koker, S.; Vervaet, C.; Remon, J.P.; De Geest, B.G. Versatile and efficient microparticulate vaccine formulation via spray drying. Knowledge for growth, May 24th , 2012. Ghent, Belgium.

Dierendonck, M.; De Koker, S.; Remon, J.P.; Vervaet, C.; De Geest, B.G. Nanoporous polyelectrolyte complex microspheres for vaccine delivery. Biopharmacy Meeting, November 9th , 2012. Utrecht, The Netherlands.

Dierendonck, M.; De Koker, S.; De Geest, B.G. Nanoporous microparticles: A generic vaccine vaccine formulation platform. 13th European symposium on controlled drug delivery. April 16-18, 2014. Egmond aan Zee, The Netherlands.

Dierendonck, M.; De Koker, S.; De Geest, B.G. Nanoporous microparticles: A generic vaccine vaccine formulation platform. Knowledge for growth, May 8th, 2014, Ghent, Belgium.